Immune Mechanisms of Mesenchymal Stem Cell Therapy for Acute Graft versus Host Disease

By

Laura M. Tobin

B.Sc

A thesis submitted to

The National University of Ireland, Maynooth for the degree of

Doctor of Philosophy

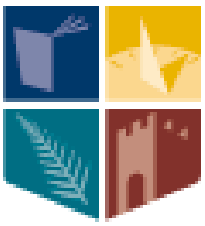

NUI MAYNOOTH

Ollscoil na hÉireann Má Nuad

Department of Biology

Institute of Immunology

National University of Ireland, Maynooth

February 2012

Research Supervisor: Dr. Bernard P. Mahon

DECLARATION OF AUTHORSHIP

I certify that the work presented herein is, to the best of my knowledge, original, resulting from research performed by me, except where acknowledged otherwise (Work carried out in Chapter 3 was done in collaboration with Dr. Jennifer Ryan and Dr. Karen English). This work has not been submitted in whole, or in part, for a degree at this or any other University.

_____ _____

Laura M. Tobin B. Sc Date

ABSTRACT

The aim of this work was to investigate the role of Mesenchymal stem cells (MSC) in the modulation of immune responses, focusing on suppression and induction of immune tolerance. To date, MSC therapy has proved beneficial for the treatment of inflammatory and autoimmune diseases, such as acute Graft versus Host Disease (aGvHD) and Crohn's disease. However, the exact mechanisms of therapeutic benefit remain unclear. The key goals of this study were to identify the role of MSC derived soluble and contact dependent factors and how these influence innate and adaptive immune responses; to develop a novel humanised mouse model of aGvHD; and to investigate the effect of MSC therapy for the prevention or treatment of aGvHD.

This study demonstrated that human MSC induced functional $CD4^+$ $CD25^+$ $FoxP3^+$ T regulatory cells from a purified population of human $CD4^+$ T cells *in vitro.* Induction was dependent on both soluble factors and direct cell contact. MSC derived TGFβ1 and prostaglandin E_2 were involved in this induction. Murine MSC suppressed dendritic cell (DC) maturation, antigen presentation and cytokine production, inducing DC with tolerogenic attributes *in vitro*. MSC modulation of DC function was also dependent on direct cell contact. Blocking studies revealed that the Notch signalling pathway was essential for this process.

A humanised mouse model of aGvHD based on delivery of human peripheral blood mononuclear cells (PBMC) to NOD-scid IL-2rγ^{null} (NSG) mice was developed to allow robust exploration of the role of MSC in cell therapy. MSC therapy resulted in the dramatic reduction of liver and gut pathology and significant increased survival of NSG mice with aGvHD. Protection was dependent on the timing of MSC therapy with conventional MSC proving effective only after delayed

administration. In contrast, IFNγ stimulated MSC were more potent and were effective when delivered concurrent with PBMC. The beneficial effect of MSC was not due to the induction of donor PBMC apoptosis, anergy or T regulatory cells in this model; but likely due to the inhibition of donor $CD4^+$ T cell proliferation and the significant reduction in systemic human TNFα.

These findings contribute to a broader understanding of immune regulation by MSC and provide a rational basis for ongoing and future clinical studies involving allogeneic human MSC as a cell therapy.

PUBLICATIONS

English, K., Ryan, J. M., Tobin, L., Murphy, J. M., Barry, F. P. & Mahon, B. P. 2009. Cell contact, prostaglandin E2 and transforming growth factor beta 1 play non-redundant roles in human Mesenchymal stem cell induction of $CD4^{+}CD25^{high}$forkhead box $P3^{+}$ regulatory T cells. *Clinical and Experimental Immunology*. 156:149-60.

Tobin, L. M., Cahill, E. F., English, K. & Mahon, B. P. Notch signalling is required for the induction of $CD4^{+}CD25^{+}FoxP3^{+}$ T regulatory cells and tolerogenic Dendritic cells by murine Mesenchymal Stem Cells. *In preparation.*

Tobin, L. M. & Mahon, B. P. Human Mesenchymal Stem Cells suppress donor $CD4^{+}$ T cell proliferation in a humanised mouse model of acute Graft versus Host Disease, prolonging survival. *In preparation*.

ABSTRACTS FOR CONFERENCE PROCEEDINGS

Cell contact, PGE_2 and TGFβ1 play a non redundant role in human Mesenchymal stem cell induction of $CD4^{+}CD25^{High}Foxp3^{+}$ regulatory T cells.

English, K., Ryan, J. M., **Tobin, L**., Murphy, J. M., Barry, F. P. & Mahon, B. P. *Irish Society of Immunology Annual Meeting*. 2008. RDS, Ballsbridge, Dublin.

Characterisation of Siglec expression by murine Mesenchymal Stem Cells.

Tobin, L. M., English, K., Johnston, J. & Mahon, B. P. *3rd UK Mesenchymal Stem Cell Meeting*. 2009. Sheffield, UK.

Allogeneic Mesenchymal Stem Cells protect against acute Graft versus Host Disease in a Humanised model: Dependence on time and dose.

Tobin, L. M. & Mahon, B. P. *Irish Society of Immunology Annual Meeting*. 2010. Science Gallery, Trinity College Dublin.

Allogeneic Mesenchymal Stem Cells protect against acute Graft versus Host Disease in a Humanised model through the reduction of $CD4^{+}$ T cell proliferation.

Tobin, L. M. & Mahon, B. P. *Irish Society of Immunology Annual Meeting*. 2011. National University of Ireland, Galway.

ABBREVIATIONS

AICD	Activation induced cell death
APC	Antigen presenting cell
BCR	B cell receptor
BMT	Bone marrow transplant
BSA	Bovine serum albumin
CD	Cluster of differentiation
ConA	Concanavalin A
CTL	Cytotoxic T Lymphocyte
CTLA4	Cytotoxic T Lymphocyte Antigen 4
DC	Dendritic cell
DMEM	Dulbecco's modified eagle media
DNA	Deoxyribonucleic acid
EBAO	Ethidium bromide acridine orange
EDTA	Ethylenediaminetetraacetic acid
ELISA	Enzyme linked immunosorbent assay
FACS	Fluorescence activated cell sorting
FCS	Fetal calf serum
FITC	Fluorescein Isothiocyanate
FoxP3	Forkhead box P3
GAPDH	Glyceraldehyde 3-phosphate dehydrogenase
GI	Gastrointestinal tract
GM-CSF	Granulocyte macrophage colony stimulating factor
GVHD	Graft versus host disease
GVL	Graft versus leukaemia
GVT	Graft versus tumour
HBSS	Hanks buffered saline solution

HGF	Hepatocyte growth factor
H & E	Haematoxylin and Eosin
HLA	Human leukocyte antigen
HO-1	Heme oxygenase-1
HRP	Horseradish peroxidase
HSCT	Haematopoietic stem cell transplantation
IFN	Interferon
IL	Interleukin
IDO	Indoleamine 2,3-dioxygenase
ICOS	Inducible costimulatory
LICOS	Inducible costimulatory Ligand
LPS	Lipopolysaccharide
M-CSF	Macrophage colony stimulating factor
MEM	Minimum essential medium
MFI	Mean fluorescent intensity
MHC	Major histocompatibility complex
MSC	Mesenchymal stem cell
NK	Natural Killer cell
NO	Nitric oxide
NSG	NOD-scid IL-2 receptor gamma knockout mouse
OVA	Ovalbumin
PBMC	Peripheral blood mononuclear cell
PBS	Phosphate buffered saline
PD	Programmed Death
PDL	Programmed Death Ligand
PE	Phycoerythrin
PGE2	Prostaglandin E2

PHA	Phytohaemagglutinin
RT	Room temperature
RT-PCR	Reverse transcriptase polymerase chain reaction
TCR	T cell receptor
TNF	Tumour necrosis factor
TGF	Transforming growth factor
T reg	T regulatory cell
VEGF	Vascular endothelial growth factor

ACKNOWLEDGEMENTS

Firstly, I would like to show my gratitude to my supervisor Dr. Bernard Mahon. Thank you for your support, guidance and encouragement throughout my time in the Cellular Immunology Lab. I owe a sincere thanks to Dr. Karen English, who when I started in the lab, all those years ago, taught me everything I needed to know to begin my research. I will be forever grateful for all your help and advice. I would like to acknowledge the Health Research Board for giving me the opportunity to take part in the Scholars in Immunology Programme. A special thanks to Dr. Shirley O'Dea (NUIM) and Dr. Ed Lavelle (TCD) for allowing me to carry out my first year rotations in their Labs.

To the girls, past and present, Emer, Heather, Cariosa and Deirdre. Where would I be today with you guys? You kept me going on those really tough days and we all know there were many. I will never forget the good times and all the laughs we have had over the past 4 years. Best of luck with your research and future careers.

To the most important people in my life, my parents, Mam and Dad, my sister Bid and my brother Steve, what can I say? Are words really enough? Everyday you gave me the encouragement and motivation to keep going and I am glad to say, we finally got there. I can truly say I would not be here today without you all, especially you Bid. I am eternally grateful for all your love and support.

Finally, but by no mean least, thank you to my fiancé Joey. We can finally say, "our" thesis is done! I really could not have finished this without you. It has been tough but it was all worth it in the end. I owe you big time!

1. INTRODUCTION

1.1 MESENCHYMAL STEM CELLS

Friedenstein was first to describe a rare fibroblast-like, non-hematopoietic cell population in the bone marrow that formed plastic adherent colonies *in vitro* and differentiated into osteocytes, adipocytes and chondrocytes (Friedenstein, 1966; Friedenstein, 1974). Based on this capacity to differentiate, Caplan coined the term "Mesenchymal Stem Cells" (MSC), to describe this population as potential agents for regenerative medicine (Caplan, 1991). Caplan and Prockop extended the concept of regenerative MSC by showing that MSC home to sites of injury and secrete large amounts of "trophic factors" that repair through recruitment and activation of other reparative cells or cytoprotective mechanisms (Caplan, 2006; Prockop, 2009). These findings positioned MSC as key modulators of localised tissue inflammation.

In the last decade, data from *in vitro* and *in vivo* models of inflammatory disease have indicated that MSC possess modulatory abilities that target the innate and adaptive immune systems (Ryan, 2005; Barry, 2005; Uccelli, 2008; Griffin, 2010). These findings suggested a role for MSC in the induction of immune tolerance and as potent therapeutic interventions. To this effect, there has been interest in the use of MSC as a cell therapy for inflammatory mediated diseases. The fact that MSC can directly suppress cells of the innate and adaptive immune systems, (Section 1.7.1 & 1.7.2), has led to the hypothesis that MSC induce immunological tolerance, through the secretion of cytokines and the induction of regulatory cells (Ryan, 2005; Caplan, 2006; English, 2008; Uccelli, 2008). This hypothesis of immunological tolerance induction by MSC will be explored in this thesis, at both an innate and adaptive immune level, using both human and murine derived MSC.

1.2 THE HISTORY OF IMMUNOLOGICAL TOLERANCE

It is reasonable to assume that the adaptive immune system of mammals has evolved for protection against an ever-changing population of microbial pathogens. The innate immune system senses danger and initiates a rapid immune response without evoking immunological memory (Hoffmann, 1999; Janeway, 1989). The adaptive immune system in contrast generates specific receptors capable of detecting a wide diversity of pathogens with fine specificity and with a capacity for long-lived immune memory (Burnet, 1957; Hozumi, 1976). Potentially harmful self-reactive lymphocytes are controlled by a mechanism known as "self tolerance" (Billingham, 1953), one of the key forms of immune regulation.

The idea of specific immunological tolerance was first proposed in the 1940's. Pioneering work carried out by Owen *et al.* described the phenomenon of red-cell chimerism (Owen, 1945). Dizygotic twin cattle share a prolonged exchange of blood for the duration of gestation. After birth, these twin cattle were found to share a stable mixture of each sibling's blood type throughout their lifetime. In order for this to occur, the exchange of red cell precursors and not just red blood cells alone must have taken place during their gestation stage, as the red cells were found to be native to each cow. The implication of this was that the recipient calf was tolerant to non-self or allogeneic red cell precursors from the sibling (Owen, 1945). Anderson and Billingham extended this idea of immune tolerance in dizygotic twin cattle by examining the transplantation of skin grafts between twin cattle. They found that dizygotic twin cattle could accept skin grafts from one another, but third party skin grafts were rejected (Anderson, 1951; Billingham, 1952). These findings showed that some level of immune tolerance between twin animals allowed successful transplantation.

Collectively, these findings led to the Nobel Prize winning experiment in tissue transplantation by Billingham, Brent and Medawar in 1953 (Billingham, 1953). They performed a series of experiments, using murine transplantation models where lymphoid cells taken from CBA mice (Black) were injected into an adult strain of mice at that time called strain A (White) (Fig 1.1). In this situation, the CBA cells were identified as foreign and were destroyed. Likewise, if the strain A mouse received CBA cells again, these too were destroyed. This led to the hypothesis that if it were possible to recreate the same circumstances as dizygotic twin cattle, (i.e. exposure in utero of CBA mice to strain A antigen) then tolerance would prevent rejection. To explore this, CBA cells were injected into neonatal strain A mice and surprisingly, these CBA cells were accepted resulting in the development of chimeric mice. Interestingly, adult strain A mice were found to accept any later skin tissue grafts from a CBA mouse, as if the graft were autologous (Billingham, 1953).

The induction of tolerance in this case was due to an alteration or acquired feature in the host and not an adaptation of the graft. Once tolerance was established, tolerance was systemic through the whole mouse. However, Billingham *et al.* found that tolerance could be destroyed through a mechanism known as adoptive transfer. In this situation, if a strain A mouse that had previously accepted a CBA skin graft, received strain A lymphoid cells from a mouse that had not been tolerised, these injected strain A cells would break the tolerant state and result in graft rejection. These findings indicated that a major aspect of tolerance was due to a central, rather than a peripheral, "editing" mechanism.

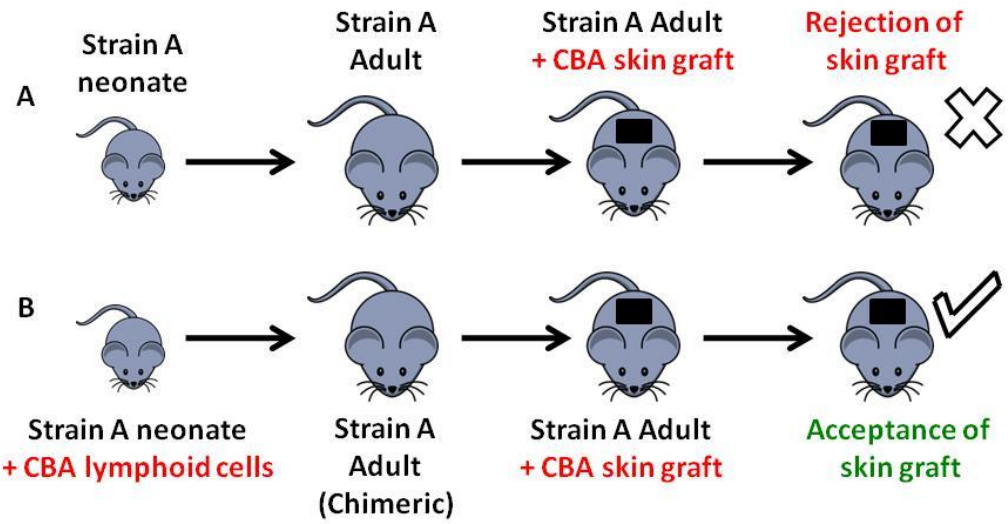

Fig 1.1 Billingham's discovery of tolerance in a tissue transplantation model. (A) Adult strain A mice received a skin graft from a CBA strain donor mouse. This CBA skin graft was rejected by the strain A mouse. (B) Neonatal strain A mice received CBA lymphoid cells, resulting in the development of a chimeric mouse. Interestingly, when this chimeric strain A mice received a CBA skin graft, these mice did not reject the graft.

1.3 CENTRAL TOLERANCE

Central tolerance is now understood in great detail. The central "editing" of the repertoire of lymphocytes occurs in the primary lymphoid organs: the bone marrow and thymus. Progenitor B cells undergo somatic diversification in the bone marrow, while progenitor T cells undergo the same mechanism in the thymus. Somatic diversification allows for the rearrangement of B cell receptor (BCR) or T cell receptor (TCR) genes, containing variable (V), diversity (D) and joining (J) gene segments for the generation of a diverse repertoire of lymphocytes each expressing a different specificity for a particular antigen receptor, a process known as V(D)J recombination (Cooper, 1965). This random rearrangement of V(D)J genes involves the recombination activating genes, RAG-1 and RAG-2 and (as the resulting sequence is not directly germ line encoded) inevitably this can lead to the generation of lymphocytes with high affinity for self antigen (Yu, 1999). In this case, a mechanism is required whereby self-reactive lymphocytes are deleted, while non-self reactive lymphocytes are permitted to leave the primary lymphoid organs and expand. This mechanism is central tolerance. However, these mechanisms are not perfect, as some self-reactive lymphocytes can escape central tolerance and enter the periphery. Therefore, in order to prevent the development of autoimmunity, a secondary mechanism exists in the periphery known as peripheral tolerance (Van Noort, 1993; Lohmann, 1996). This system of checkpoints and fail-safes are important for the maintenance of tolerance and keeping the risk of developing autoimmune disease at a minimum.

1.3.1 B CELL DEVELOPMENT AND CENTRAL TOLERANCE

The development of B cells from hematopoietic stem cells takes place in the bone marrow (Hardy, 2001). Pre and pro-B cells expressing rearranged B cell receptors (BCR) with low affinity to self, progress into development through positive selection. This results in the switching off of the RAG genes and the migration of immature B cells to the spleen and periphery (Buhl, 2000). Pro-B cells that are reactive to self-antigens are not permitted to progress into development and subsequently do not switch off the RAG genes. These autoreactive B cells are primed for programmed cell death primarily through apoptosis (Yu, 1999). Until 1993, it was thought that all self-reactive B cells were deleted in the bone marrow through apoptosis. However, Tiegs, Gay and Radic found that not all autoreactive B cells undergo apoptosis automatically. They identified a mechanism where autoreactive B cells can eliminate a self-reactive BCR and express a novel, non self-reactive, BCR through secondary V(D)J recombination. This process was coined receptor editing (Tiegs, 1993; Gay, 1993; Radic, 1993). The strength of the BCR signal when it encountered antigen determined whether antigen specific B cells were eliminated, edited or developed (Ehlich, 1994; Yu, 1999; Hardy, 2001). Although this mechanism of central tolerance in the bone marrow is successful, some self-reactive B cells do leave the bone marrow and enter the periphery. Along with the induction of apoptosis and receptor editing, two more factors limit autoreactive B cell responses in the periphery. First, B cell responses typically require T cell help (Parker, 1993) and so tolerance of the T cell compartment will limit autoreactive B cell expansion and secondly, the induction of peripheral tolerance (see below) can also eliminate these B cells to maintain immunological tolerance.

1.3.2 T CELL DEVELOPMENT AND CENTRAL TOLERANCE

T cells develop from hematopoietic progenitors in the bone marrow but then migrate to the thymus as $CD4^-$ $CD8^-$, double negative thymocytes, where they mature. Thymocytes from the bone marrow enter the thymus through high endothelial venules and migrate to the subcapsular region. Here these cells undergo V(D)J recombination, creating a repertoire of T cells expressing TCR with different antigen specificities (Miller, 1961; Cooper, 1965; Cantor, 1976). These developing T cells then migrate to the cortex, where they undergo a process of positive selection. Here these cells express both CD4 and CD8 markers and are known as double positive thymocytes (Cantor, 1976). T cells that receive a signal through MHC class I and a survival signal, retain CD8 expression, while losing CD4 expression (Cantor, 1976). While T cells that receive a signal through MHC II and a survival signal, retain CD4 expression and lose CD8 expression (Cantor, 1976). T cells that do not recognise self-MHC are eliminated by apoptosis, with surviving T cells migrating to the medulla, whereas those T cells weakly recognising self-MHC survive (positive selection). In the medulla, T cells that strongly recognise self-antigen presented on self-MHC by thymic antigen presenting cells, are eliminated by apoptosis-thus only non-reacting T cells are allowed to survive (negative selection) (Scollay, 1980; Egerton, 1990). The remaining T cells are naïve T cells, capable of recognising self-MHC and non-self antigen. These cells are permitted to leave the thymus and enter the periphery where they can encounter antigen specific for their TCR (Goldrath, 1999). However, similar to B cell development, some autoreactive T cells can escape central tolerance and enter in the periphery. In this case, any autoreactive T cells should be eliminated through the induction of peripheral tolerance.

An obvious problem with bone marrow/thymus selection mechanisms is that tissue specific proteins (e.g. pancreatic proteins) are unlikely to be expressed in the bone marrow/thymus. Over the last decade, it has come to light that many tissue specific proteins are in fact expressed by some stromal cells present in the medulla region of the thymus (Anderson, 2005; Kuroda, 2005). This situation allows for the negative selection of T cells that recognise self-antigens that are normally expressed by tissues outside the thymic medulla, and helped to explain an inexplicable autoimmune condition. In 1946, a severe autoimmune disease called autoimmune polyendocrinopathy candidiasis ectodermal dystrophy (APECED) was described in patients, presenting with chronic mucocutaneous candidiasis, hypoparathyroidism and type 1 diabetes (Leonard, 1946; Betterle, 1998). Although APECED manifested itself in 1946, it was not until 1997 that the underlying genetic defect that caused APECED was discovered (Nagamine, 1997; Gibson, 1998). Mutations in an autoimmune regulator gene, AIRE, were responsible for the development of APECED. AIRE gene expression is restricted to primary lymphoid organs, particularly the thymus (Gibson, 1998; Heino, 1999). In the thymus, AIRE is expressed by medullary epithelial cells, important cells in the negative selection of autoreactive T cells, (Kishimoto, 1997; Anderson, 2005). AIRE expression allows medullary epithelial cells to express peripheral tissue antigens, allowing for the deletion of autoreactive T cells specific for peripheral self-antigens before leaving the thymus (Klein, 2000). Mutations in the AIRE gene do not disrupt thymocyte development, as AIRE knockout mice have normal levels of thymocytes. However, these mice develop autoimmune disease (Kuroda, 2005). This suggested that mutations in AIRE affected thymic epithelial cells and their expression of peripheral tissue antigens. This mutation permits the development of naïve self-reactive

thymocytes, which are permitted to leave the thymus and enter the periphery (Klein, 2000).

1.4 PERIPHERAL TOLERANCE

A supplementary mechanism, peripheral tolerance, controls self-reactive T and B lymphocytes that may have escaped central tolerance and are circulating in the periphery. There are numerous ways in which the immune system deals with self reactive lymphocytes in the periphery; these are by induction of 1) deletion, 2) anergy, 3) ignorance and 4) suppression/regulation. Dendritic cells (DC), which are important innate cells involved in the induction of adaptive peripheral tolerance are located in the skin, airways, lymphoid tissues, other organs and blood (Steinman, 1974; Schuler, 1985; Holt, 1990). This distribution of DC strategically places these cells for optimal detection of both foreign but also self-tissue specific antigen for presentation to antigen specific $CD4^+$ T cells. The presentation of antigen (foreign or self) by DC to effector T cells shapes the type of immune response that will occur (Mosmann, 1986; Steinman, 2000).

The induction of self-tolerance in the periphery is achieved in numerous ways. Deletion involves the induction of apoptosis in self-reactive T and B lymphocytes (O'Shea, 2001; Abbas, 2003). The most common pathway for the deletion of self-reactive lymphocytes is activation-induced cell death (AICD) by the Fas/Fas ligand pathway (CD95/CD95L) (Fife, 2008), which results in the control of autoimmune disease development. Mice defective in Fas receptor genes (*lpr* mouse) or the Fas ligand (*gld* mouse) exhibit autoimmune lymphoproliferative and lupus like autoimmune syndrome (Roths, 1984). It has also been hypothesised that the

expression Fas ligand in immune privileged sites, such as the brain or the anterior chamber of the eye, can lead to apoptosis of Fas expressing activated T cells and inflammatory cells infiltrating these immune privileges sites (Griffith, 1995; Saas, 1997).

Anergy is defined as a state of lymphocyte unresponsiveness to specific antigen and is associated with a marked decreased in Interleukin (IL)-2 production and other effector functions (Schwartz, 1997). Anergic T cells persist in the periphery in an altered and unresponsive state, due to the absence of costimulation between antigen presenting cells such as DC and effector T cells (Steinman, 2000; Jonuleit, 2001). Costimulation typically involves (CD80 or CD86 but can also involve IL-1, IL-12, Tumour necrosis factor alpha (TNFα), and CD40). Typically, antigen presented to naive antigen specific T cells supports significant lymphocyte proliferation when supported by costimulation (Lanier, 1990). However, in the absence of costimulation, the induction of a classical form of anergy can occur (Glennie, 2005; Zappia, 2005). These anergic T cell are refractory to activation, even when their specific antigens are subsequently presented via APC expressing costimulatory molecules (Jenkins, 1987; Glennie, 2005; Zappia, 2005). Interestingly, this unresponsive state of classical anergy can be reversed through the addition of exogenous IL-2 and this has been used as a defining characteristic to measure anergy induction *ex vivo* (Glennie, 2005). The induction of anergic T and/or B cells provides a method of prolonged self-tolerance via a peripheral means.

The induction of suppressor or regulatory cells assists in the maintenance of peripheral tolerance through the active suppression of effector T cell populations. These regulatory cells, such as T regulatory (T reg) cells and suppressive DC contribute to the suppression of autoimmunity by preventing the activation of self-

reactive lymphocytes. This can occur directly through cell-cell contact-mediated suppression of self reactive conventional $CD4^+$ T cells by regulatory T cells, (infectious tolerance) (Jonuleit 2002; Kendal, 2011) or by killing effector cells or through the creation of an immunosuppressive environment via the release of regulatory cytokines (bystander suppression). The best-characterised T reg cell subsets coexpress CD4, the α-chain of the IL-2 receptor CD25 and the transcription factor forkhead box protein 3, FoxP3 (Jonuleit, 2003; Yamazaki, 2006). T reg cells can be further divided into natural T reg, which develop in the thymus and enter the periphery; and inducible T reg that are induced in the periphery from naïve T cells and aid in the maintenance of tolerance (Mills, 2004). Activated T reg can suppress effector T cell proliferation via an antigen non-specific mechanism, which is dependent on direct cell contact but independent of immunosuppressive cytokines (Thornton, 2000). However, both types of T reg can achieve suppression through the production of soluble factors, IL-10 and transforming growth factor beta (TGFβ) (Levings, 2002).

In bystander tolerance, T reg cells are activated through the recognition of specific antigen and secrete cytokines, such as IL-10 and TGFβ. This release of proinflammatory cytokines results in the suppression of effector T cells present in the local environment, irrespective of their antigen specificity (Jonuleit, 2002; Masteller, 2005). In the case of infectious tolerance, the presence of T reg cells stimulates the outgrowth of further T reg cell populations displaying a broader array of antigen specificities distinctly different from that of the original T reg population (Qin, 1993; Cobbold, 2009). The adoptive transfer of these T reg cells can prevent or treat type I diabetes *in vivo* even after the removal of the original T reg population (Tarbell, 2007).

Subpopulations of DC in the periphery can induce T reg from naïve $CD4^+$ T cells (Jonuleit, 2000; Yamazaki, 2003). These DC populations typically exhibit an immature phenotype with tolerogenic functions, including low levels of MHC molecule expression, decreased IL-12p70 and increased IL-10 production (Mahnke, 2002; Morelli, 2007). Tolerogenic DC can present antigen to antigen-specific T cells, but fail to deliver adequate costimulation for effector T cell proliferation (Morelli, 2007). A key factor involved in the induction of tolerogenic DC is IL-10, as the presence of this cytokine can reduce MHC II expression and IL-12 production (Bellinghausen, 2001; Mahnke, 2002). Tolerogenic DC expand $CD4^+$ $CD25^+$ T reg cells from $CD4^+$ $CD25^-$ precursors (Kretschmer, 2005). This results in the expansion of antigen-specific T reg, which contributes to the prevention of autoimmunity (Maldonado, 2010; Morelli, 2007).

1.5 THE B7 FAMILY OF MOLECULES INVOLVED IN IMMUNE TOLERANCE

Anergy occurs when $CD4^+$ T cells are stimulated in the absence of costimulation (Jonuleit, 2001) and the B7 family of surface molecules are important in this process (Collins, 2005). CD28, cytotoxic T lymphocyte antigen-4 (CTLA-4) and B7 family can provide both stimulatory and inhibitory signals involved in the activation of lymphocytes (Banchereau, 1998; Suzuki, 1999; McAdam, 2000; Nishimura, 1996; Salomon, 2001). For complete T and B cell activation, antigen recognition through TCR ligation requires an additional signal through B7 ligands. The CD28 receptor is expressed on naïve T cells and engagement of CD28 receptor with B7.1 (CD80) or B7.2 (CD86) on APC results in a potent costimulatory signal to

activate T cells (Banchereau, 1998). Signalling through CD28 induces the production of IL-2, upregulation of CD25 and the survival gene Bcl-X_L.

CTLA-4 (CD152) is similar in structure to CD28 and binds to the B7 ligands, CD80/86. However, CTLA-4 is not expressed on naïve T cells, but rather upregulated on T cells following their activation. CTLA-4 is a crucial negative regulatory of T cell activation and is important in the reduction of T cell responses and restoration of homeostasis after inflammation (Suzuki, 1999). This sliding threshold between CD28 and CTLA-4 is important for the regulation of immune activation and the prevention of autoimmunity (Allison, 1998).

To date, there have been several other proteins identified as new members of the CD28, CTLA-4 and B7 families. The inducible costimulatory (ICOS) (CD278) receptor which shares similarities to both CD28 and CTLA-4 (Carreno, 2002). ICOS is expressed on activated T cells, while its B7-like ligand LICOS (B7-H2), is expressed on APC (McAdam, 2000). While CD28 engagement induces IL-2 production, costimulation through ICOS enhances the production of IL-10 by T cells (McAdam, 2000).

The programmed death-1 marker (PD-1) is a member of the CD28 family and is a negative regulator of T and B cell activation. PD-1 receptor is expressed on activated T cells, while its ligands PDL-1 (B7.H1) and PDL-2 (B7.DC) are expressed on activated APC (Nishimura, 1996). Engagement of PD-1 by its ligands results in decreased interferon gamma (IFNγ), IL-10, IL-4 and IL-2 secretion and the reduction in adaptive immune responses (Freeman, 2000). The interplay between these receptors and ligands of the B7 family dictates the type of immune response

that will occur, costimulation or coinhibitory (Collins, 2005). This identifies these pathways as key players in the maintenance of immune tolerance.

1.5.1 The B7 Family of Molecules and the Induction of Regulatory Cells

Coinhibitory signals are important for the inhibition of T cell activation against self-antigens and induction of peripheral tolerance. Darrasse-Jeze *et al.* discussed a relationship between the numbers of T reg cells in the periphery with the number of DC present in lymphoid organs (Darrasse-Jeze, 2009). This study highlighted a feedback loop between DC and T reg cells, where altering the number of DC directly correlated to the number of T reg (Darrasse-Jeze, 2009). The induction of T reg cells by DC is not unidirectional, as $CD4^+CD25^+FoxP3^+$ T reg communicate with DC influencing their maturation state, inducing a more suppressive or tolerogenic DC expressing low levels of costimulatory molecules and suppressed IL-12 and TNFα production (Larmonier, 2007). The production of IL-10 and TGFβ by T reg is involved in the induction of tolerogenic DC (Cederbom, 2000; Larmonier, 2007).

$CD4^+$ $CD25^+$ T reg cells depend on mediators, such as IL-10 and TGFβ for their differentiation from effector T cells (Yamazaki, 2003). The balance between effector and regulatory $CD4^+$T cells involves the ICOS pathway. ICOS expressed by $CD4^+$T cells in target organs enhances IL-10 production, supporting T reg induction (Herman, 2004). Patients with deficient ICOS expression have $CD4^+$ T cells that are insensitive to tolerogenic signals from immature DC and have decreased levels of IL-10 (Tuettenberg, 2009).

The cross talk between DC and T reg cells involves the engagement of B7 on DC and CTLA-4 on T reg. CTLA-4 expressing T reg down regulated the expression of CD80 and CD86 on DC inducing a more suppressive DC phenotype (Wing, 2008). CTLA-$4^{-/-}$ T reg cells were less suppressive than CTLA-4^{+} T reg cells in coculture with DC *in vitro* (Tang, 2004). CTLA-4 upregulated indoleamine 2, 3-dioxygenase (IDO) production from both human and murine DC, which in turn promoted the induction of TGFβ producing T reg (Sharma, 2007; Grohmann, 2002). In the true sense of a feedback loop, this induction of IDO activated T reg cells increased the expression of PDL-1 on DC, which in turn increased the production of IL-10 by DC promoting a more tolerogenic environment (Munn, 2007).

$CD4^{+}CD25^{+}FoxP3^{+}$ T reg cells and the PD-1: PDL pathway are important for the termination of immune responses and the regulation of autoimmunity. The stimulation of naïve $CD4^{+}$ T cells with PDL-1-Ig in the presence of anti-CD3 and TGFβ induced the generation of $CD4^{+}$ $FoxP3^{+}$ T reg (Francisco, 2009). PDL-$1^{-/-}$ DC were also less effective in the generation of $CD4^{+}CD25^{+}FoxP3^{+}$ T reg from naïve $CD4^{+}$ T cells (Francisco, 2009). These data emphasised the importance of the PD-1 pathway in T reg cell induction. Interestingly, $CD4^{+}CD25^{+}FoxP3^{+}$ T reg express both PD-1 and PDL-1. DC express PDL-1 and upon encounter with naïve $CD4^{+}$ T cells, the expression of PD-1 is enhanced, leading to the induction of T reg cells. As T reg also express PDL-1, the encounter of naïve $CD4^{+}$ T cells (PD-1) and $CD4^{+}CD25^{+}FoxP3^{+}$ T reg (PDL-1) could result in the differentiation of naïve T cells into additional T reg (Francisco, 2010). The expression of PD-1 on DC could negatively regulate (hinder) DC function against bacterial infections (Yao, 2009). This suggested that PDL-1 expression by T reg cells could indirectly suppress T cell responses through the engagement of PD-1 on DC, modulating DC function and

immune responses. Ligation of the PD-1 pathway has proved important in diminishing effector T cell activation, while enhancing T reg cell induction.

Collectively, the above findings have highlighted the CTLA-4 and B7 family as key molecules for the regulation of adaptive immune tolerance, primarily through the induction of T reg cells and tolerogenic DC. These findings render these pathways as interesting targets for immunotherapeutic interventions for the treatment of T cell mediated diseases, especially in transplantation. The above data suggests that MSC induction of regulatory cells, DC or T cells, could involve signalling through the CTLA-4 and B7 family pathways.

1.6 Other Immune Molecules involved in Immune Regulation

1.6.1 Sialic-Acid Binding Immunoglobulin-Like Lectins

Siglecs are a family of type-1 sialic-acid binding, immunoglobulin-like, lectins that are involved in immune cell: cell interactions and regulate the function of cells in both the innate and adaptive immune systems through glycan recognition (Crocker, 2007). Siglecs are one of the best-characterised type-1 lectins to date. Siglecs play a role in modulating cellular functions through cell: cell interactions (Crocker, 2005). CD33-related Siglecs are mainly expressed by mature cells of the innate immune system, such as monocytes, DC or NK. At present it is known that humans express nine CD33-related Siglecs (CD33, Siglecs 5-11 and Siglec-14), while mice express only five (CD33, Siglec E, F, G, H) (McMillan, 2008). Each Siglec has specificity for one sialyated ligand/glycan, suggesting that each Siglec mediates a distinct function. However, more than one Siglec can be present on a cell

at any one time. CD33 related Siglecs have been shown to modulate leukocyte behaviour, including the inhibition of cellular proliferation, induction of apoptosis and the induction of pro-inflammatory cytokines (Vitale, 1999; Balaian, 2003; Lajaunias, 2005).

The maturation of DC results in changes in glycan expression, through a process known as glycosylation (Bax, 2007). This change in glycan expression on maturing DC can affect their recognition by Siglecs and galectins. CD33-related Siglecs relay an inhibitory signal, which inhibits activatory pathways (Falco, 1999). This suggests that signalling through Siglecs could play a role in maintaining immune tolerance. Siglec expression by MSC has not been shown to date. However, as CD33-related Siglecs are inhibitory, the possibility of MSC expressing Siglecs and these molecules interacting with DC is highly plausible. It was also feasible that MSC were acting as a type of aberrant APC (Rameshwar, 2008) and therefore MSC expression of Siglecs could be involved in such an adaptive response. Therefore, study of Siglec expression by MSC would inform the understanding of immune modulation by this proposed cell therapy.

1.6.2 NOTCH SIGNALLING PATHWAY

During development, cell: cell interactions are critical in deciding cell fates. Notch signalling is a well-conserved pathway involved in cell fate decisions during development, stem cell maintenance, cell proliferation, differentiation and apoptosis (Radtke, 2004; Fiuza, 2007). Notch signalling is evolutionarily conserved from *Drosphilia* to mammals (Artavanis-Tsakonas, 1999). There are four Notch genes (Notch 1, 2, 3 & 4) and five genes encoding Notch ligands (Jagged 1, 2 and Delta-like ligand 1, 3 & 4) in both human and mouse. Notch signalling is activated upon

direct cell: cell interaction between Notch receptors and membrane bound ligands, Jagged or Delta-like (Baron, 2002). During signalling, Notch receptors are presented to Notch ligands as a heterodimer. Upon receptor/ligand binding, the proteolytic cleavage of the receptor dimer occurs through γ-secretase activity, releasing the intracellular domain of the Notch receptor (NICD), which translocates to the nucleus. This cleavage of the receptor dimer is inhibited *in vitro* by γ-secretase inhibitors (GSI). Once, in the nucleus, NICD associates with transcription factors (CSL) and recruits coactivators to activate Notch target genes, such as Hes and Hey family genes (Vujovic, 2007).

Interactions between Notch receptors and ligands are crucial in the crosstalk between cells of the immune system and their surrounding microenvironment (Radtke, 2004). Both Notch receptors and ligands are expressed on DC and the presence of bacterial products, such as lipopolysaccharide (LPS) can up regulate the expression of Notch ligands on DC (Amsen, 2004). It has been demonstrated that the activation of both Notch 1 and Notch 2 receptors through ligand binding disrupts the differentiation of mature DC or macrophages, leading to the accumulation of immature myeloid DC (Cheng, 2003). Cheng *et al.* have shown that the Notch ligand Jagged-1, on bone marrow-derived stromal cells, stimulated the accumulation of DC precursors, while preventing their transition to terminally differentiated DC. The ligand Delta-like ligand-1 was found to promote the generation of fully differentiated DC (Cheng, 2007).

Various ligands demonstrate differential capacity for Notch receptor binding, which in turn regulate different T cell activation. Bone marrow derived DC, instruct T cell differentiation via Notch (Amsen, 2004; Morelli, 2007). Both Jagged-1 and Delta-like ligand-4 are involved in the differentiation of naïve $CD4^+$ T cells into

effector cells. Amsen *et al.* found that signalling through Delta-like ligand-4 or Jagged-1 promotes Th1 or Th2 responses respectively (Amsen, 2004). Delta-like ligand-1 and Jagged-1 induced partial or complete inhibition of T cell activation, respectively (Rutz, 2005). Notch signalling is involved in the induction of immunological tolerance. Hoyne *at al* demonstrated that murine DC over-expressing human Jagged-1 induced $CD4^+CD25^+FoxP3^+$ T reg that were capable of inhibiting both primary and secondary immune responses (Hoyne, 2000). Both murine and human naïve $CD4^+$ T cells have been differentiated into FoxP3 expressing T reg following stimulation in the presence of TGFβ1 (Fu, 2004; Rao, 2005). This induction of a FoxP3 expressing T reg population was dependent on Notch signalling (Fu, 2004; Rao, 2005; Samon, 2008). These findings showed that Notch signalling was required for TGF-β1 induced $FoxP3^+$ T reg cells (Samon, 2008). Collectively, these data, suggest that the crosstalk between innate and immune cells involves the Notch signalling pathway. This puts emphasises on the Notch signalling pathway and its involvement on MSC modulation of immune responses, especially through the induction of regulatory cells.

1.7 MSC AND IMMUNE REGULATION

MSC constitute 0.01-0.001% of bone marrow cells (Friedenstein, 1966). However, they have been found at low levels in virtually all organs and tissues, including liver, adipose tissue and synovium and within the pericyte population in the vasculature wall (da Silva Meirelles, 2006; Crisan, 2008). At present, no specific marker or combination of markers has been identified which specifically defines MSC. The International Society of Cellular Therapy (ISCT) proposed minimal

criteria to define multipotent MSC (Dominici, 2006). MSC should be adherent to plastic, express CD73, CD90 and CD105, but not CD11b or CD14, CD10 or CD79α, CD34, CD45 or HLA-DR. Finally MSC must be capable of differentiation into osteocytes, adipocytes and chondrocytes *in vitro* (Dominici, 2006). One of the major attractions of MSC lies in the fact that MSC possess a unique mechanism, which allows them to escape allogeneic deletion (Le Blanc, 2004). However, the exact mechanisms involved in MSC modulation of immunity *in vivo* are still unclear. Understanding the interactions between MSC and allogeneic immune cells *in vivo* will be critical for the use of MSC as a therapeutic agent.

1.7.1 MSC AND INNATE IMMUNITY

MSC interact with both innate and adaptive immune cells which requires both contact dependent and soluble factors (Fig 1.2 & Table 1.1). MSC affect DC differentiation and subsequent maturation. MSC produce several cytokines, such as macrophage colony stimulating factor (M-CSF), which are involved in DC differentiation from precursors (Djouad, 2007, Chen, 2006; Nauta, 2006). More importantly, MSC interrupt three key features of DC transition from an immature to a mature phenotype. Firstly, in the presence of MSC, the LPS driven upregulation of costimulatory molecules, MHC class II, CD40, CD80 and CD86 on DC is prevented (English, 2008; Jung, 2007). Secondly, MSC interfere with the ability of DC to present antigen (English, 2008). Finally, in the presence of MSC, the migratory capacity of DC towards CCL19 is affected, due to the down regulation of CCR7 and the upregulation of E-cadherin on DC, reducing the migration of DC to lymph node derived chemotactic signals (English, 2008). MSC modulation of DC function involves both cell: cell contact and soluble factor dependent mechanisms (Table 1.1). MSC secretion of IL-6 induces a semi-mature DC and partly inhibits the

differentiation of bone marrow progenitors into DC (Djouad, 2007). By blocking PGE_2 synthesis by MSC using indomethacin, DC differentiation and function is restored, suggesting PGE_2 involvement in MSC modulation of DC differentiation (Chen, 2007). Recently, the Notch signalling pathway, as a possible candidate for MSC mediated cell contact dependent mechanism has been hypothesised (Cheng, 2007, Zhang, 2009). The Notch ligand, Jagged-1, primarily expressed on bone marrow derived stromal cells, stimulates the accumulation of DC precursors, preventing their transition to a terminally differentiated DC (Cheng, 2007). Recently, Aldinucci *et al.* demonstrated that MSC required cell contact with human monocyte derived DC for the inhibition of DC function. DC cocultured with MSC are unable to form active immune synapses, retaining endocytic activity and podosome-like structure, typical of immature DC (Aldinucci, 2010). To date, the exact cell contact signal involved in this induction remains unclear. Collectively, these findings suggest that the Notch signalling pathway could play an important role in MSC modulation of DC function.

1.7.2 MSC AND ADAPTIVE IMMUNITY

The immunosuppressive activity of MSC extends to adaptive immunity, either indirectly through the modulation of cells of innate immunity as described above or directly through the modulation of B or T cells. MSC actively inhibit the function of B and T cell function through both soluble factors and cell contact factors (Schena, 2010; English, 2009). B cells contribute to the adaptive immune response through the production of antibody. The effect of MSC on B cell proliferation and differentiation remains contradictory and controversial. Data to date imply that MSC inhibit B cell proliferation by blocking the cell cycle at the G0/G1 phase in both human and murine studies (Corcione, 2006; Glennie, 2005). However, studies of

systemic lupus erythematosus contradict this; Traggiai *et al.* suggested that human MSC promote the differentiation and proliferation of B cell from patients with systemic lupus erythematosus (SLE) (Traggiai, 2008). In a more recent study, MSC inhibited the differentiation and proliferation of plasma cells to B cells in murine model of SLE. This inhibition was IFNγ dependent and involved PD-1/PDL pathway (Schena, 2010).

In vitro studies show that MSC abrogate T cell proliferation in response to alloantigens and mitogens (English, 2007). MSC inhibition of T cell proliferation is not MHC-restricted, as it occurs in the presence of autologous and allogenic MSC (Ryan, 2007; Ramasamy, 2007; English, 2008; Le Blanc, 2008) and in some cases this inhibition appears to be reversed by the addition of exogenous IL-2 (Di Nicola, 2002). Various immunosuppressive soluble factors have been implicated in MSC mediated T cell suppression, including IL-10, TGFβ1, PGE_2, HGF and nitric oxide (Di Nicola, 2002; Aggarwal, 2005; Sato, 2007; English, 2009). MSC do not constitutively express IDO, however, upon IFNγ stimulation the expression of IDO is induced (Meisel, 2004; Ryan, 2007). This observation suggests that MSC require proinflammatory cytokines for their activation and demonstrates an important function for soluble factors present in the local microenvironment of inflammation.

Not only do MSC suppress T cell proliferation, but they are involved in the induction of tolerance in the periphery through the generation of T regulatory cells *in vitro* and *in vivo* (Casiraghi, 2008; English, 2009; Kavanagh, 2010). Cell contact, PGE_2 and TGFβ1 play non-redundant roles in MSC induction of $CD4^+CD25^{high}FoxP3^+$ T reg cell *in vitro* (English, 2009). Importantly, $CD4^+CD25^{high}FoxP3^+$ T reg cells generated in the presence of MSC are fully functional T reg, capable of suppressing alloreactivity when repurified (English,

2009). IL-10 and an unidentified contact signal, induce secretion of HLA-G by human MSC to induce a T reg population (Selmani, 2008). Kavanagh *et al.* found that MSC induced $CD4^+$ $FoxP3^+$ T reg *in vivo* capable of mediated both local and systemic inflammation through the decrease of IL-4 and increase of IL-10 in a murine model of asthma (Kavanagh, 2010). Ge *et al.* also demonstrated the importance of MSC induction of $CD4^+CD25^+FoxP3^+$ T reg. Here, MSC induction of regulatory T cells was associated with IDO expression by MSC, to prevent kidney allograft rejection (Ge, 2010).

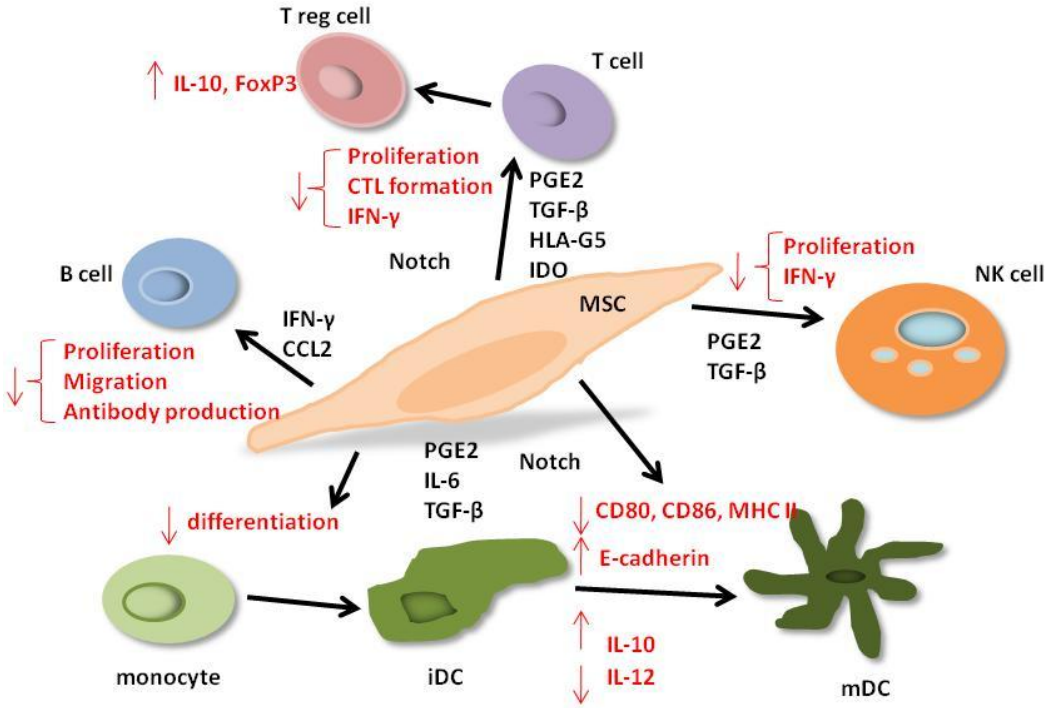

Fig 1.2 MSC modulation of immunity. MSC regulate critical aspects of innate and adaptive immune cells by suppressing their development or effector function through the release of soluble factors and contact dependent signals

Table 1.1 Soluble factors involved in MSC-mediated immune regulation

Soluble Factor	Reference
Transforming Growth Factor beta 1 (TGFβ1)	DiNicola, 2002, Tse, 2003, Ryan, 2007, English, 2007, English, 2009
Kynurenine	DiNicola, 2002, Ryan, 2007, English, 2007
Prostaglandin E2 (PGE_2)	Aggarwal, 2005, Ryan, 2007, English, 2007, English, 2009
Hepatocyte Growth Factor (HGF)	DiNicola, 2002
Interferon gamma (IFNγ)	Polchert, 2008, Krampera, 2005
Interleukin 1 beta (IL-1 β)	Groh, 2005
Tumour Necrosis Factor alpha (TNFα)	English, 2007, Beyth, 2005
Indoleamine 2,3-dioxygenase (IDO)	Krampera, 2005, Meisel, 2004, Ryan, 2007
Interleukin-6 (IL-6)	Djouad, 2007
Interleukin-10 (IL-10)	Jiang, 2005
Nitric Oxide (NO)	Sato, 2007
Heme oxygenase-1 (HO-1)	Cabannes, 2007
HLA-G5	Selmani, 2008

1.8 TRANSPLANTATION AND TRANSFUSION; PROTYPIC CELL THERAPIES

The major histocompatibility complex (MHC) or human leukocyte antigen system (HLA) in humans contains important polymorphic genes encoding proteins that present antigen to self-restricted T cells (Snell, 1948). The precise patterns of co-dominantly expressed MHC genes (the haplotype) are important in supporting the discrimination of self and non-self and the regulation of immune tolerance. The MHC haplotype is almost unique to each individual and therefore, allogeneic T cells (not tolerised through positive and negative selection against that haplotype) are powerfully activated by mismatched MHC molecules (Snell, 1948). For that reason, allogeneic T cells recognise any non-self MHC as foreign and may reject it.

In the case of transplantation, cells that express MHC molecules different to that of the recipient, are subject to recognition. This results in the rejection of the tissues displaying these foreign MHC antigens. This was a key finding discovered through a body of work carried out by Gorer, Snell, Daussett and others spanning the 1900s to the 1950s which built on the earlier studies of ABO blood groups and transfusion compatibility by Landsteiner (Landsteiner, 1900; Gorer, 1948; Snell, 1948; Daussett, 1958). Gorer found that human sera contained natural antibodies that could distinguish between red blood cells between three inbred strains of mice (Gorer, 1936). Following the immunisation of rabbits with inbred mouse sera, he identified three different blood group antigens, one of which was similar to that found in human blood. He called this mouse antigen, antigen II (Gorer, 1936). Gorer then went on to collaborate with Snell, who had discovered tumour transplantation resistance genes, which he called histocompatibility genes or H genes. They found that an H-2 locus encoded the strong or "major" histocompatibility antigens, which induced rapid transplant rejection when compared

to weaker or “minor” histocompatibility antigens (miHA) encoded at another locus (Gorer, 1948; Snell, 1948; Snell, 1951).

These findings focused interest on MHC genes and their role in human transplantation. In 1958, Daussett discovered the first human HLA antigen by screening patients that had received multiple blood transfusions. Daussett found that certain sera caused the clumping of leukocytes. He then found anti-sera that could detect an alloantigen present on human leukocytes, which he named MAC. This human antigen has been renamed HLA-A2 (Daussett, 1958). Ingeniously, at this time, Daussett hypothesised that this human antigen and any further antigens to be discovered would play very important roles in transplantation; in particularly bone marrow transplantation between MHC mismatched donors. The discovery of HLA genes by Gorer, Snell and Daussett (1936-1958), and the concept of immunological tolerance and tissue transplantation by Billingham, Medawar and Brent (1953), have contributed hugely to the area of transplantation between mismatched donors, both organ and bone marrow. This was revolutionised by the discovery of powerful immunosuppressants such as cyclosporine A and tacrolimus, which have permitted solid organ transplant even in the scenario of significant tissue mismatch (Messina, 2008).

1.8.1 ALLOGENEIC HAEMATOPOIETIC STEM CELL TRANSPLANTATION

Allogeneic haematopoietic stem cell transplantation (HSCT) is an important therapy, which has become widely used for the treatment of haematological malignancies and inherited blood disorders (Reddy, 2003). The number of allogeneic HSCT carried out is increasing, with more than 25,000 procedures performed (globally) annually (Ferrara, 2009). Patients receiving an allogeneic

HSCT (recipient/host) first undergo a conditioning regime that can include chemotherapy and/or radiation and/or T cell depleting antibodies (Shlomichik, 2007). This conditioning regime eradicates the recipient's own T and B cells leaving the recipient highly immunocompromised and ready for the engraftment of donor bone marrow. Donor T and B cells present in the graft reconstitute adaptive immune capacity in the recipient (Trenado, 2003). Donor T cells have an additional beneficial effect against any remaining leukaemic or tumour cells within the host, a phenomenon known as graft versus leukaemia (GvL) or graft versus tumour (GvT) (Horowitz, 1990; Trenado, 2003). However, donor T cells can also cause pathology involving the damage of host tissues called graft versus host disease (GvHD), which is primarily due to varying degrees of donor/host mismatch at both MHC and miHA (Korngold, 1978). In effect, GvHD represents a mirror image of transplant rejection, in that it is the donor allogeneic T cells that recognise the recipient host cells bearing recipient MHC antigen as "foreign".

1.8.2 THE IMMUNE RESPONSE IN GRAFT VERSUS HOST DISEASE

GvHD is a major complication following allogeneic HSCT, characterised by the induction of an intense cytokine storm particularly TNFα, leading to the activation of $CD4^+$ effector T cells which drive allogeneic reactivity. GvHD accounts for 15-30% of deaths that occur following allogeneic HSCT (Ferrara, 2009). In order for GvHD to occur, the donor graft must contain immune competent T cells, be transplanted into an immunodeficient recipient unable to mount a successful immune response against the graft and the recipient must express tissue antigens that are not present in the donor transplant: conditions now termed Billingham's triad (Billingham, 1966).

The development of GvHD occurs in three phases in humans. In phase I the preconditioning regimen prior to transplantation causes tissue/organ damage, especially of the gastrointestinal (GI) tract. Bacterial exposure (e.g. LPS) causes the release of inflammatory cytokines and chemokines from monocytes, especially TNFα and IL-1. In phase II these inflammatory cytokines activate endothelium to promote tissue inflammation, activate host APC (upregulation of MHC II and costimulation) and mobilise allogeneic effector cells to damaged organs. Here host APC expressing MHC II initiate the activation of the donor allogeneic $CD4^+$ T cells present in the graft, enhancing the secretion of inflammatory cytokines, which leads to further donor immune cell activation (Reddy, 2003). Finally in phase III, allogeneic donor $CD8^+$ CTL and NK cells destroy host cells directly; $CD4^+$ T cell drive tissue pathology and prime phagocytes to secrete further TNFα and IL-1 in a positive activation cycle, leading to the amplification of damage in multiple organs of the host (Reddy, 2003) (Fig 1.2).

There are two presentations of GvHD, acute (aGvHD) and chronic (cGvHD). By definition, aGvHD occurs within the first 100 days post transplantation, while cGvHD occurs after 100 days. However, this classification is unsatisfactory as there are presentations of GvHD that include symptoms of both acute and chronic (Martin, 1990; Sullivan, 1991). The frequency of GvHD development is directly linked to the degree of mismatch between the recipient and donor HLA antigens (Loiseau, 2007). Even when high levels of similarity are achieved between the recipient and donor bone marrow HLA haplotypes, 40% of patients develop systemic aGvHD, due to differences at minor HLA loci (Ferrara, 2009).

1.8.3 CLINICAL FEATURES OF AGVHD

Clinically, the target organs in aGvHD are the skin, GI tract and liver (Table 1.2). The skin is the most frequently affected organ, with 81% of patients affected, while aGvHD of the GI tract and liver can be seen in about 50% patients (Martin, 1990). Due to epithelial cell necrosis, the skin develops a maculopapular rash, which is visible on the palms of hands and soles of the feet in most patients (Ferrara, 2009). In severe cases, the skin can blister and ulcerate causing extensive pain and discomfort. Epithelial cell necrosis can also cause damage to the GI tract, which results in severe abdominal pain, presenting as diarrhoea (Martin, 1990). An increase in bloody diarrhoea can lead to anorexia, nausea and vomiting and result in extreme weight loss in patients (Ponec, 1999). Damage to the liver caused by aGvHD is difficult to distinguish from other causes of liver damage following HSCT, (e.g. drug toxicity) (Ferrara, 2009). However, liver damage in aGvHD typically presents as hyperbilirubinaemia and jaundice (Ferrara, 2009; Tolar, 2011).

The severity of aGvHD is characterised by the number of target organs involved and the extent of damage made to each organ. There are four grades of GvHD development; grade I (mild), grade II (moderate), grade III (severe) and grade IV (very severe). The more severe the GvHD development, the poorer patient prognosis can be (Ferrara, 2009). Patients presenting with grade III aGvHD have a 25% long-term survival rate, whereas grade IV patients have only a 5% long-term survival rate (Cahn, 2005); suggesting that reductions in the level of GvHD pathology might result in improved rates of survival.

Table 1.2 Symptoms of acute GvHD *(Martin, 1990; Ferrara, 2009)*

Affected Tissue	Symptoms
Skin (81% patients)	Macropapular skin rash (palms/soles)
GI Tract (54% patients)	Diarrhoea (bloody), nausea, weight loss (anorexia), abdominal pain
Liver (50% patients)	Hyperbilirubinaemia, Jaundice

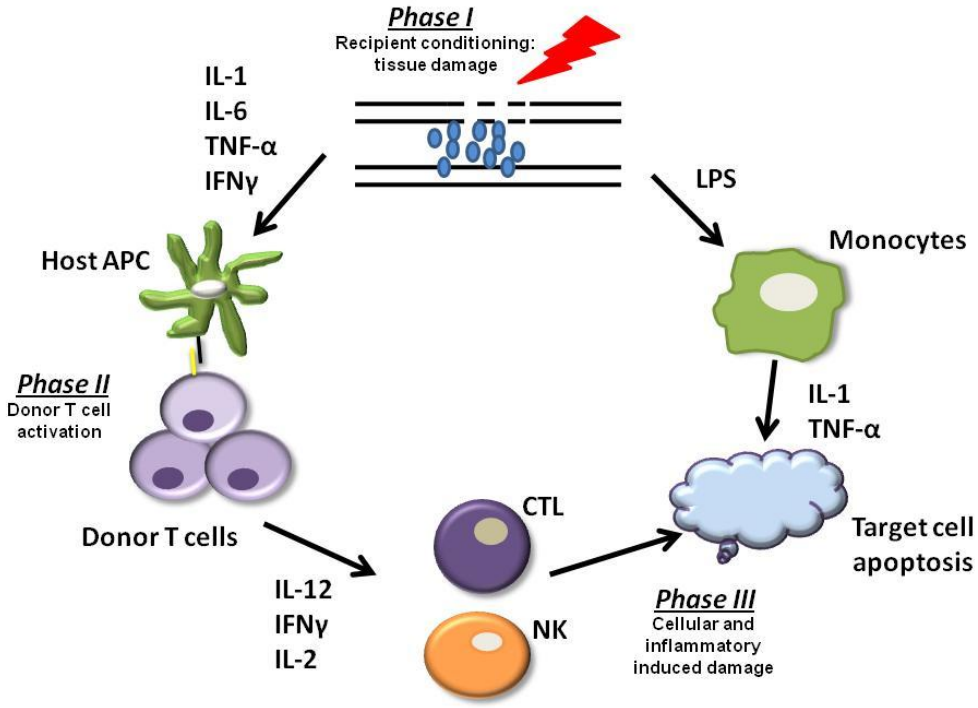

Fig 1.2 Development of Acute GvHD. Phase I; Preconditioning regime causes damage to the epithelial mucosa of the gastrointestinal tract, skin and liver, causing loss of barrier integrity and exposure of monocytes to LPS, gut bacteria and other damage related innate immune activators. This causes the release of inflammatory cytokines, TNFα and IL-1β, which in turn activate endothelium, host antigen presenting cells (APC) and monocytes. Phase II; Activated APC interact with donor T cells and stimulate their proliferation and differentiation. The release of IFNγ and IL-2 from donor T cells activates cytotoxic T lymphocytes (CTL) and natural killer (NK) cells. Phase III; The activation of effector cells and the release of inflammatory cytokines cause apoptosis and damage to target organs.

1.9 THERAPEUTIC PREVENTION OF AGVHD

1.9.1 FIRST LINE TREATMENT FOR AGVHD

Despite recent advances in the reduction of GvHD through altering the intensity of the preconditioning phase prior to transplantation (Levine, 2003), effective treatments for GvHD prevention are still lacking. Currently, the standard first line therapies for aGvHD are glucocorticosteroids such as methylprednisolone, in combination with immunosuppressive drugs, such as cyclosporine A or tacrolimus (Messina, 2008). Steroid therapies have improved the outcome and increased survival of patients with aGvHD (van Lint, 1998; van Lint, 2006; MacMillian, 2002). Steroids induce lysis of lymphocytes during interphase and promote anti-inflammatory responses, while immunosuppressive drugs keep patients in an immunocompromised state, dampening the activation of immune responses (Deeg, 2007). Different types and doses of steroids are used to treat patients with aGvHD and the grade and severity of aGvHD determines the response to steroid therapy (van Lint, 2006; MacMillian, 2002). A typical steroid regime for aGvHD therapy consists of methylprednisolone administered at 2 mg/kg per day for 7 to 14 days, followed by a gradual reduction in dose depending on patient response rates (Messina, 2008; Van Lint, 1998).

The major limitations to steroid therapy are the increased risk of infection, hyperglycaemia, osteoporosis and growth defects which may be life threatening (Deeg, 2007). However, it is important to note that steroid therapies have proved beneficial for very many patients to date (Van Lint, 2006; McDonald, 2006). Depending on the patient and the severity of aGvHD, the systemic exposure to steroid therapy can be tapered and the duration of therapy reduced (McDonald, 2006;

Cragg, 2000). Conversely, there are patients who do not successfully respond to steroid therapy (Deeg, 2007). In these cases, a second line of therapy is required.

1.9.2 SECOND LINE TREATMENT FOR AGVHD

In steroid refractory aGvHD, determining when to initiate secondary therapy is patient specific and depends on initial response to primary therapy. Typically, if the manifestations of aGvHD worsen in any organ over 3 days of primary treatment, if there are no clinical changes after 7 days, or if there is incomplete response after 14 days, then a secondary therapy is considered (Deeg, 2007). Polyclonal and monoclonal antibodies are the most widely used secondary therapies (Doney, 1985, Carpenter, 2002). The partial depletion or elimination of specific T cells from bone marrow prior to transplantation gives varied results (Chalandon, 2006; Ho, 2004). Anti-thymocyte globulin (ATG) has been in use for more than 3 decades (Doney, 1985). Administration of ATG reduces the frequency of GvHD in related-donor HSCT recipients without increasing relapse (Kroger, 2002). However, there are high levels of variability between recipients and the development of side effects, such as hypotension, thrombocytopenia and even anaphylactic reactions can occur in 80-90 % of patients, with long-term survival on ATG ranging from 5-32 % (MacMillian, 2002; Graziani, 2002). This has made the use of ATG in a clinical setting problematic.

Visilizumab is a humanised anti-CD3 antibody that selectively induces the apoptosis of activated T cells (Cole, 1999). In clinical trials, treatment with visilizumab improved aGvHD with the initial dose proving important for the overall outcome (Carpenter, 2002). However, complications with visilizumab therapy include the reactivation of latent Epstein Barr Virus (EBV) in patients with aGvHD

leading to post transplant lymphoproliferative disease (Carpenter, 2002). Alemtuzumab is a monoclonal antibody that binds to CD52, expressed by lymphocytes, monocytes and dendritic cells inducing apoptosis (Perez-Simon, 2002). In 2005, a phase clinical II trial found that the administration of alemtuzumab lowered the incidence of both acute and chronic GvHD (Perez-Simon, 2005). However, other studies reported complications with infection, such as cytomegalovirus and increased relapse rates, leading to subsequent graft failure (Perez-Simon, 2002; Delgado, 2006). An alternative strategy for the treatment of GvHD is the blockade of TNFα. Elevated levels of TNFα are indicative of more severe GvHD development (Holler, 1990; Kitko, 2008). Clinical trials to date have used two drugs: etanercept, which binds trimeric and membrane bound TNF, or infliximab, a monoclonal antibody that binds monomeric, trimeric soluble and transmembrane TNFα (Ehlers, 2005). A phase II clinical trial found that etanercept in combination with systemic steroid therapy supported complete resolution of aGvHD symptoms in 70% of patients, with 80% complete responses in GI tract and skin aGvHD (Levine, 2008). However, the well reported side effects of these drugs have proved problematic in the treatment of some patients (MacMillian, 2002; Graziani, 2002; Carpenter, 2002; Levine, 2008). Incomplete efficacy and adverse effects associated with the use of monoclonal and polyclonal antibodies, suggests the need for a more effective beneficial therapy for aGvHD. Therefore, current studies have focused on the idea of cell therapy for the treatment of inflammatory mediated diseases, including aGvHD.

1.10 CELL THERAPY FOR aGvHD

1.10.1 T REGULATORY CELLS AS A CELL THERAPY FOR aGvHD

GvHD is caused by the presence of donor T cells in the allograft; theoretically, the deletion of donor T lymphocytes prior to transplantation could solve this problem. However, a beneficial role for donor T cells in recipient haematopoietic reconstitution and the clearance of remaining leukaemic cells (GvL), have highlighted the importance of donor T cells for successfully transplantation (Horowitz, 1990). The most potent self-tolerance mechanism of adaptive immunity is carried out through the direct or indirect induction of T reg (Tang, 2008). It has been hypothesised that T reg induced tolerance could be used therapeutically in the induction of transplantation tolerance. Donor and recipient DC that have been rendered tolerogenic *in vitro* have been used to inhibit direct and indirect pathways of allorecognition, preventing graft rejection (Wakkach, 2003). Bone marrow derived DC can induce alloantigen specific $CD4^{+}CD25^{+}FoxP3^{+}$T reg *in vitro* that are capable of suppressing GvHD and autoimmunity (Wakkach, 2003; Tarbell, 2004; Yamazaki, 2006). Mouse studies have shown that bone marrow derived recipient DC generated *in vitro* with granulocyte macrophage colony stimulating factor (GM-CSF), IL-10, TGFβ1 and pulsed with LPS displayed tolerogenic properties that prevented the development of lethal GvHD following allogeneic bone marrow transplantation (Sato, 2003). A single dose of host derived tolerogenic DC downregulated donor T cell activation, while increasing the incidence of donor derived natural T reg cells. This therapy also retained GvL effects, which is important when considering tolerogenic DC as a possible therapeutic agent in GvHD (Sato, 2003). These findings emphasised a role for tolerogenic DC in the prevention of GvHD, primarily through the indirect induction of T reg cells.

Knowing that DC are capable of regulating T cell responses, especially through the induction of $CD4^+CD25^+Foxp3^+$ T reg has led to an examination of the effect of *ex vivo* expanded T reg cells as a direct tolerogenic therapy for GvHD. Early mouse models of GvHD in 2002 and 2003, found that when mice were irradiated and reconstituted with allogeneic donor bone marrow and T cells, the development of lethal aGvHD was seen, while the depletion of $CD25^+$ T cells accelerated GvHD development. However, if fresh donor type $CD4^+CD25^+$ T reg were administered at high ratios with effector T cells, the development of GvHD was significantly delayed (Cohen, 2002; Hoffmann, 2002; Taylor, 2002; Edinger, 2003). These findings suggested that $CD4^+CD25^+$ T reg might provide a cell therapy for the prevention of GvHD. As the numbers of T reg required for a beneficial effect *in vivo* were relatively high, this finding imposed a limitation for their use in a clinical setting. Therefore, the potential for *ex vivo* expanded T reg cells to inhibit GvHD was explored. *Ex vivo* expanded $CD4^+CD25^+$ T reg significantly inhibited GvHD development when expanded using host-type APC, rather than third-party APC (Trenado, 2002). It was also found that these *ex vivo* T reg cells survived longer *in vivo* (Trenado, 2002). More recently, Cao *et al.* showed that human $CD4^+CD25^+Foxp3^+$ T reg enriched from peripheral blood could be successfully expanded *ex vivo* to clinically relevant quantities in 2-3 weeks and that these cells maintained the expression of T reg cell markers, such as CD25, FoxP3, CD62L and CTLA-4 and displayed *in vitro* suppressive qualities (Cao, 2009). Following the induction of otherwise lethal xenogeneic GvHD, *ex vivo* expanded T reg cells significantly reduced GvHD symptoms and improved the survival of NOD-scid mice following co-transfer with human peripheral blood lymphocytes (Cao, 2009).

A correlation between $CD4^+CD25^+$ T reg cells and the occurrence and severity of both acute and chronic GvHD in 56 patients following allogeneic HSCT has also been examined (Li, 2010). Interestingly, these data found a significant reduction in the frequency of $CD4^+CD25^+$ T reg in peripheral blood of patients with either grades II-IV aGvHD or extensive cGvHD when compared to healthy donors. Furthermore, the reduction of T reg correlated with the severity of GvHD, with fewer T reg indicative of more severe GvHD. This was accompanied by a reduction in serum TGFβ (produced by T reg) and a significant increase in TNFα, a mediator of GvHD development (Li, 2010).

1.10.2 MESENCHYMAL STEM CELLS AS A CELL THERAPY FOR AGVHD

Currently, there are many potential applications for MSC in allogeneic stem cell transplantation, including the enhancement of HSC engraftment, the prevention and/or treatment of GvHD, Crohn's disease, Multiple sclerosis and Critical limb ischemia (Table 1.3). Initial studies using MSC as a cell therapy for the treatment of haematological malignancies have been promising. Lazarus *et al.* were the first to report that hMSC were applicable for clinical therapy and that autologous MSC, after myeloablative condition in cancer patients, could accelerate haematopoietic recovery (Lazarus, 1995). However, firm conclusions could not be made due to the haphazard nature of the study. Nevertheless, these studies gave circumstantial evidence that MSC could be expanded and administered to patients under good manufacturing practice (GMP). In 2002, Bartholomew *et al.* showed that bone marrow derived baboon MSC could prolong the survival of autologous, donor or third party skin graft in primates (Bartholomew, 2002). Since then, autologous and allogeneic *ex vivo* expanded MSC have been utilised in studies where bone marrow derived MSC were co-transplanted with HSC in patients with both haematological or

non-haematological disorders. Le Blanc *et al.* have used MSC transplantation in cases of repeat graft rejection/failure after HSC transplantation and in studies to enhance HSC engraftment (Le Blanc, 2007). In the case of all patients, MSC infusion resulted in rapid engraftment and 100% donor chimerism (Le Blanc, 2007).

One of the most impressive *in vivo* effects of infused MSC has been for the treatment of GvHD after allogeneic stem cell transplantation. Le Blanc *et al.* were the first to demonstrate a potential for MSC infusion for the treatment of GvHD (Le Blanc, 2004). A 9 yr old patient received a matched but unrelated donor HSC transplant for the treatment of leukaemia, after developing severe acute steroid refractory GvHD of the gut and liver. Haplo-identical MSC were generated and infused over two doses. The infusion of MSC was effective in treating the GvHD, showing no reactivity between the haplo-identical MSC and recipient lymphocytes (Le Blanc, 2004). Le Blanc's group has also shown that MSC, regardless of their source, i.e. HLA-identical sibling, haplo-identical or third party mismatched unrelated donors; demonstrate similar results in treating GvHD (Le Blanc, 2008). However, optimism for MSC as a cell therapy has become tempered by recent clinical trials carried out by Osiris Therapeutics. Prochymal ^{TM} cells, which are MSC-like cells, proved very safe and beneficial following their infusion into patients with aGvHD in a Phase II trial (Kebriaei, 2009). However, in a Phase III clinical, the treatment of steroid refractory aGvHD patients was deemed unsuccessful and failed to reach its primary endpoint (Martin, 2010; Allison, 2009). However, it is important to note here that Prochymal ^{TM} cells were beneficial for the treatment of aGvHD of the gut and liver but not aGvHD of the skin. The reason for this lack of improvement in treating aGvHD of the skin remains unclear. Why MSC therapy was found to be beneficial for the treatment of one aGvHD target organ (GI tract)

over another (skin) puts major emphasis on the need for more advantageous models for examining the exact mechanisms of MSC modulation.

Table 1.3 Ongoing clinical trials for which MSC and MSC like cells are currently being used to treat conditions

Condition**	Cell type	Sponsor	Description*
Acute Graft v Host Disease	Allogeneic MSC	University of Liege	Phase II
Ulcerative colitis	Umbilical cord MSC	Qingdao University	Phase I/II
Critical limb ischemia	Human adipose derived MSC	Fundacion Progreso y Salud Spain	Phase I/II
Multiple sclerosis	Autologous MSC	Royan Institute	Phase I/II
Parkinson's disease	Autologous MSC	Guangzhou General Hospital	Phase I/II
Aplastic anaemia	Allogeneic MSC	Guangzhou General Hospital	Phase I/II
Osteoarthritis	Allogeneic MSC	Stempeutics Research Pvt Ltd	Phase II
Type 2 Diabetes	Umbilical cord/placenta derived MSC	Shandong University	Phase I/II
Myocardial ischemia	Autologous MSC	University Hospital Toulouse; Nautes University Hospital	Phase I
Crohn's disease	MSC (Prochymal)	Osiris Therapeutics	Phase III

* Data based on http://clinicaltrials.gov as of 21.02.2012

** Multiple trials ongoing at different sites with different types of MSC; table is representative of the vast numbers of clinical trials ongoing.

1.11 ANIMAL MODELS OF ACUTE GVHD

Many non-human primates are used to model human disease. However, non-human primate models are associated with vigorous ethical constraints and can be very costly. To combat these problems, the use of mouse models offers a more feasible alternative to human observations, especially when hypothesis driven studies are needed. There are many mouse models available that model aGvHD development. Most involve the transplantation of donor lymphocytes into lethally irradiated hosts. The irradiation dose, the amount and type of donor lymphocytes transplanted into the host determine the severity of aGvHD development (Schroeder, 2011). MHC mismatched mouse models are the most straightforward tools for studying aGvHD (Table 1.4). In this situation, the model involves the transplantation of murine lymphocytes into a murine model (i.e. mouse in mouse). However, recent advances in the development of humanised mouse models have allowed more sophisticated and relevant studies to be performed.

Similar to human aGvHD, the pathology of aGvHD in murine models typically affects targets organs such as the lung, liver, skin and intestinal tract (both large and small). One of the key features of murine aGvHD pathology is weight loss. Extensive damage to the host's intestinal tract results in an increase in diarrhoea, reduced food intake, resulting in extreme weight loss. An increase in epithelial cell necrosis results in fibrosis in the lung, skin and liver, all visible following histological analysis. Similar to humans, a well-designed scoring system is involved in determining the severity (grade/score) of aGvHD pathology in all murine models.

1.11.1 MHC-MISMATCHED MOUSE MODELS

Differences in MHC haplotype are largely responsible for immune mediated rejection (Ferrara, 2009). Even in an MHC matched setting, differences in miHA can cause the rejection of transplanted cells or tissues (Korngold, 1978). The most common murine MHC-mismatched model for the study of aGvHD is C57BL/6 ($H2^b$) donor into BALB.c ($H2^d$) recipient. With this model, the mismatch is at MHC class I, MHC class II and miHA loci. Following conditioning irradiation, T cell depleted donor bone marrow cells and splenic T cells are administered to the recipient. In most MHC mismatched mouse models, the numbers of donor splenic T cells administered are important in determining the level of aGvHD that develops (Table 1.4). In this model, lethal aGvHD involving both $CD4^+$ and $CD8^+$ T cells typically occurs by day 10 to 21 when 0.5-2 x 10^6 splenic T cells are infused (van Leeuwen, 2002).

The C3H/HeJ ($H2^k$) donor into C57/Bl6 ($H2^b$) recipient is similar to the previous model, in that it is mismatched at MHC I, MHC II and miHA. However, typically more splenic T cells (25 x 10^6) are required for the development of lethal aGvHD between day 10 to 30 (Blazar, 1991). There are also congenic models of aGvHD that involve only one T cell type contributing to the phenotype. In this situation, the recipient mouse will have a limited defined mutation on their MHC background. One model illustrating this involves C57BL/6 ($H2^b$) donor into B6.C-$H2^{bm12}$ ($H2^b$ background with mutation at MHC II). In this case, the mismatch is on the MHC II background alone and following splenic T cell infusion, $CD4^+$ T cells drive aGvHD development between day 20 to 40 (Sprent, 1986).

1.11.2 HUMANISED MOUSE MODELS

One drawback to murine systems is that mouse models do not always reflect pathology of human diseases. Furthermore the effector cell is different (human v mouse) and these models are not well aligned for the study of human cell therapy products. The development of humanised mouse models has helped address these issues. The history of the development of the humanised mouse model is interesting and describes how research tools have progressed and advanced over the past decade (Table 1.5).

1.11.2.1 CB17-SCID HUMANISED MOUSE MODEL

The discovery of the *Prkdc*^{scid} mutation (protein kinase, DNA activated, catalytic polypeptide; severe combined immunodeficiency) mutation in CB17 mice was a milestone in the development of humanised mouse models of disease (Bosma, 1983). The absence of *Prkdc* expression results in the failure of the V(D)J rearrangement of lymphocyte antigen receptor genes which results in the absence of functionally mature T and B cells (Lieber, 1988). CB17 Prkdc^{scid} mice allow engrafting human PBMC. However, the engraftment of human cells was extremely low (0.01-0.1%) and was not sufficient for the study of the function of engrafted cells (Mosier, 1988). Some mice bearing the *scid* mutation developed functional T and B lymphocytes over time, a phenomenon known as "leakiness" (Bosma, 1988). This leakiness allowed for enhanced innate immune activity, resulting in increased numbers of NK cells, which hampered the engraftment of human PBMC in the CB17-scid mouse model (Christianson, 1996; Greiner, 1998). These findings led to the introduction of the *scid* mutation into mice of different backgrounds. In 1995, the introduction of the *scid* mutation onto the NOD background, displayed 5 to 10

fold higher human PBMC engraftment when compared with other mouse models (Hesselton, 1995). These findings allowed the NOD-scid mouse model to become the "gold standard" for human cell engraftment studies.

1.11.2.2 NOD-SCID HUMANISED MOUSE MODEL

Non-obese diabetic (NOD) mice have multiple immune defects, including defects in macrophage development and function, reduced complement activity and decreased NK activity (Kataoka, 1983; Baxter, 1993; Serreze, 1993). By introducing the *scid* mutation onto the NOD background, the NOD-scid model displayed defective lymphocyte development, similar to that of the CB17 mouse. However, unlike the CB17 mouse model, the NOD-scid mouse had reduced "leakiness" levels, as only 10% of 6 month old mice developed lymphocytes over time and the levels of engraftment were much higher than that found in the CB17 mouse model (Shultz, 1995; Hesselton, 1995). Despite the improvements with the NOD-scid model compared to previous humanised models, some limitations remained. The lifespan of the NOD-scid mouse was found to be around 8 months, due to the development of thymic lymphomas (Shultz, 1995). Although the engraftment of human cells was more than in the CB17 humanised model (0.01%-0.1%), the levels still remained relatively low at 1-10% engraftment (Hesselton, 1995). This may have been due to residual NK cell activity within the model (Shultz, 1995). In an effort to increase human cell engraftment, methods for blocking NK cell activity *in vivo* were pursued.

1.11.2.3 NOD-SCID β2M^{NULL} AND NOD RAG1^{NULL} PRF1^{NULL} HUMANISED MOUSE MODELS

In an attempt to increase human cell engraftment, the blockade of NK cell activity in vivo was examined. The NOD-scid β2m^{null} mouse, which lacked NK cell

activity, displayed increased human PBMC engraftment when compared to the NOD-scid mouse model. However, similar to the NOD-scid mouse, the development of thymic lymphomas occurred much earlier in the NOD-scid $\beta 2m^{null}$ mouse, which decreased their lifespan considerably (Christianson, 1997). In contrast, the NOD-$Rag1^{null}$ $Prf1^{null}$ mouse displayed defective NK cell activity. NK loss was due to lack of the Prf1 gene, which is important in the production of perforin (the killing mediator used by NK cells) (Shultz, 2000). Although NK cells were able to development, they were not functional. As expected, human cells engrafted well in the model, however, due to high levels of variability of engraftment between donors, this model was still unreliable and therefore, more reliable humanised mouse models were developed.

1.11.2.4 NOD-SCID IL-2Rγ^{NULL} HUMANISED MOUSE MODEL

The next generation of humanised mouse models focused on targeting mutations in the cytokine receptor common γ-chain. The NOD-scid mouse model was the best-humanised model to date, displaying increased lifespan, engraftment of human cells and reduced NK cell activity. In humans, a disease known as X linked SCID occurs due to mutations in the IL-2rγ chain gene, which contributes to IL-2, IL-4, IL-7, IL-9, IL-15 and IL-21 receptor signalling (Kovanen, 2004). Patients with X-linked SCID are characterised by the absence or marked reduction in T cells and NK cells (Sugamura, 1996). This IL-2rγ mutation was introduced onto the NOD-scid background. This allowed the development of a humanised mouse model, NOD-scid $IL2r\gamma^{null}$ mouse (NSG), with deficient T and NK cell activity that could readily engraft 6 fold higher levels of human PBMC (Pearson, 2008). The NSG mouse has an increased lifespan when compared to the NOD-scid mouse, which makes it ideal for long-term studies.

In 2005, Shultz *et al.* were among the first research groups to publish data that showed the development of a complete human immune system in NSG mice that were engrafted with human peripheral blood $CD34^+$ cells (Shultz, 2005). This finding highlighted the utility of this model in studying functional human immune diseases. This model allowed researchers to investigate how human immune cells work in the pathology of many human diseases and how human cell therapies might be deployed. For the purpose of this thesis, the NOD-scid IL2rγ^{null} humanised mouse model was used to investigate stem cell therapies for the treatment of aGvHD.

Table 1.4 MHC-mismatched mouse models of aGvHD

Donor strain	Recipient strain	Mismatch	Main T cell effector type	Outcome	References
C57/Bl6 ($H2^b$)	BALB.c ($H2^d$)	MHC I, MHC II, miHA	$CD4^+$ and $CD8^+$	Lethal aGvHD day 10-21	Van Leeuwen, 2002
C3H/HeJ ($H2^k$)	C57/Bl6 ($H2^b$)	MHC I, MHC II, miHA	$CD4^+$ and CD8	Lethal aGvHD day 10-30	Blazar, 1991
C57/Bl6 ($H2^b$)	B6C3F1 ($H2^{k/b}$)	MHC I, MHC II, miHA	$CD4^+$ and CD8	Lethal aGvHD	Fowler, 1996
C57/Bl6 ($H2^b$)	B6.C-$H2^{bm1}$ (Mutation on MHC I)	MHC I	$CD8^+$	Lethal aGvHD from $CD8^+$ T cells by day 30-80	Sprent, 1986
C57/Bl6 ($H2^b$)	B6.C-$H2^{bm12}$ (Mutation on MHC II)	MHC II	$CD4^+$	Lethal aGvHD from $CD4^+$ T cells by day 30-80	Sprent, 1986

Table 1.5 Xenogeneic/humanised mouse models for human cell engraftment

Mutant allele	Strain name	Strain classification	Phenotype	Advantages	Disadvantages	Ref
Prkdc^{scid}	CB17-scid	C.BKa lgh^{b}-Prkdc^{scid}/lcrSmn	-No mature T and B cells	-Lack mature T and B cells	-High level of innate immunity -NK cell activity -Leakiness -Very low engraftment levels	Bosma, 1983
Prkdc^{scid}	NOD-scid	NOD.CB17-Prkdc^{scid}	-No mature T and B cells -Decreased innate immunity	-Low level of innate immunity -Low NK cell activity -Increased engraftment	-Residual innate immunity -Residula NK cells -Deceased lifespan and lymphomas	Shultz, 1995
Prkdc^{scid} B2m$^{tm1Unc-J}$	NOD-scid B2m$^{-/-}$	NOD.Cg-Prkdc^{scid} B2mtm1Unc/J	-No mature T and B cells -No MHC class I expression	-Very low NK cell function -Increased engraftment	-Short lifespan and thymic lymphomas	Christianson, 1997
Rag1^{tm1Mom}	NOD-Rag1$^{-/-}$	NOD.129S7(B6)- Rag1 ^{tm1Mom}/J	-No mature T and B cells	-Low NK cell activity	-Residual innate immunity -Residual NK cell activity -Variable engraftment levels	Shultz, 2000
Prkdc^{scid} IL2rg^{tm1Wjl}	NOD/LtSz-scid IL2rg$^{-/-}$	NOD.Cg-Prkdc^{scid} IL2rg^{tm1Wjl}/SzJ	-No mature T and B cells -IL2Rγ-chain deficiency -Innate immune defects	-Long lifespan -Deficient innate immunity -No NK cell activity -High levels engraftment -Develops functional immune system -Complete absence of IL2g gene	-Lack appropriate MHC molecules for T cell selection in mouse thymus -Low and variable level of T cell dependent antibody responses	Shultz, 2005

1.12 AIMS & OBJECTIVES

This chapter has highlighted the many strands of enquiry that suggest a possible role for MSC in the modulation of immune responses through the induction of immune tolerance. The hypothesis is that MSC can be used to treat aGvHD and that a rational basis for this can be discovered. The goal is to build on previous work and identify both soluble and contact dependent factors involved in MSC immunomodulation and to investigate the effect of MSC in the prevention/treatment of aGvHD using a new humanised mouse model. The goals are addressed under the following aims:

i) To investigate the role of contact dependent signals and soluble factors involved in the induction of $CD4^+$ $CD25^+$ $FoxP3^+$ T regulatory cells by human MSC in v*itro* (Chapter 3)

ii) To identify a cell contact signal involved in the induction of tolerogenic DC by murine MSC *in vitro* (Chapter 4)

iii) To develop and optimise a humanised mouse model of aGvHD and determine if human MSC administered as a cell therapy are beneficial (Chapter 5)

iv) To define the possible mechanisms involved in MSC modulation of aGvHD development both *in vitro* and *in vivo* (Chapter 6)

Overall, this study sets out to achieve a greater understanding of MSC suppression of immunity. This knowledge will contribute to a broader understanding of immune regulation by MSC and provide a rational basis for ongoing and future clinical studies involving allogeneic human MSC as a cell therapy.

CHAPTER 2

MATERIALS & METHODS

2.1 METHODS

2.2 REGULATORY ISSUES

2.2.1 ETHICAL APPROVAL

All procedures involving animals or human material were carried out by licensed personnel. Ethical approval for all work was received from the ethics committee of NUI Maynooth.

2.2.2 COMPLIANCE WITH GMO AND SAFETY GUIDELINES

All GMO/GMM work was performed according to approved standard operation procedures and recording protocols approved by the Environmental Protection Agency (Ireland). Safe working practices were employed throughout this study as documented in the Biology Department of Safety manual NUI Maynooth.

2.2.3 ANIMAL STRAINS

The following mouse strains were used: BALB/c, C57BL/6 (Harlan, Bichester, Oxon, UK), FVB.Cg-Tg(GFPU)5Nagy/J, BALB/c-Tg(DO11.10)10Loh/J (Gift from Trinity College Dublin) and NOD.Cg-Prkdc^{scid}IL2^{tmlWjl}/Szj (Jackson Labs, Bar Harbour, Maine, USA). All mice were housed according to Dept. of Health (Ireland) guidelines and used with ethical approval. Sample sizes for animal experiments were determined by power statistic calculation.

2.3 ISOLATION OF CELLS

2.3.1 ISOLATION AND CULTURE OF ADULT MURINE MESENCHYMAL STEM CELLS (MMSC)

6-8 week old female BALB/c or C57BL/6 mice were sacrificed by cervical dislocation. Femurs and tibias were removed intact under aseptic conditions in a class II safety cabinet using a sterile dissection kit. Femurs and tibias were then separated using a sterile scissors. The ends of each bone were cut to expose the

marrow. Bone marrow was flushed into a sterile Petri dish from both the femur and tibia until the bones appeared white in colour and transparent. This entailed using a 27 gauge needle and Complete Isolation Media (CIM) (RPMI 1640 (Invitrogen-Gibco, Carlsbad, CA) supplemented with 10 % (v/v) foetal bovine serum (FBS) (Biosera, Essex, UK), 10 % (v/v) horse serum (Hyclone, Hertfordshire, UK), 100 U/ml penicillin (Invitrogen-Gibco), 100 µg/ml streptomycin and 2mM L-glutamine (Invitrogen-Gibco)) (Table 2.1) in a 5 ml syringe. Cell aggregates were disrupted using a 19 gauge needle and syringe. Cells were then centrifuged at 600 g for 5 min and resuspended in 5 ml CIM. Bone marrow cells were counted by ethidium bromide/acridine orange (EB/AO) viable staining (section 2.2) and seeded at a concentration of 6.0-6.5 × 10^7 cells in T75 flasks in 15ml of CIM or 2.0-2.5 × 10^7 cells in T25 flasks in 8 ml of CIM.

On day 1, non-adherent cells were removed by washing the flask with sterile PBS and fresh CIM was added. Adherent cells (passage 0) were washed with PBS and fresh CIM was added every 3-4 days for 4 weeks. At week 4, cells were washed with PBS and lifted by trypsinisation with 0.25 % (v/v) trypsin / 1 mM EDTA (Invitrogen-Gibco) for 2 minutes at 37°C. Trypsin was neutralised by addition of CIM and cells were centrifuged at 600 g for 5 min. Cells (passage 1) were counted and re-seeded at 5-6 × 10^6 cells in T75 flasks or 1-2 × 10^6 cells in T25 flasks in fresh CIM. Media were replaced every 3-4 days. This trypsinisation, wash, counting, and reculturing constituted a "passage" and that term will be used to describe the whole process hereon. One to two weeks later, the cells were passaged (passage 2) at a low seeding density of 50 cells/cm^2 in complete αMEM (CEM) (αMEM (Invitrogen-Gibco) supplemented with 10 % (v/v) foetal bovine serum (FBS), 10 % (v/v) horse serum, 100 U/ml penicillium, 100 µg/ml streptomycin and

2mM L-glutamine) (Table 2.1). cαMEM was replaced every 3-4 days. One to two weeks later, cells were passaged again (passage 3) and seeded at 50 cells/cm^2 or cryopreserved (section 2.6.3).

2.3.2 HUMAN MESENCHYMAL STEM CELLS (HMSC) ISOLATION AND CULTURE

Bone marrow stem cells were generated by collaborators in NUI Galway. Briefly, bone marrow aspirates were taken from the iliac crest of donor patients according to an approved clinical protocol (Murphy *et al.* 2002). Isolated human MSC were resuspended in complete DMEM (DMEM (Invitrogen-Gibco) supplemented with 10 % (v/v) foetal bovine serum (FBS), 200 U/ml penicillium and 200 µg/ml streptomycin (Table 2.1) and seeded at 1 × 10^6 cells in a T175 flask. cDMEM was replaced every 3-4 days. Once cells reached 70-90 % confluence, human MSC were washed with sterile PBS and trypsinised as normal with 0.25 % trypsin / 1 mM EDTA (Invitrogen-Gibco) and seeded at 50 cells/cm^2 or cryopreserved (section 2.6.3).

2.3.3 DENDRITIC CELL ISOLATION AND CULTURE

6-8 week old female BALB/c or C57BL/6 mice were sacrificed by cervical dislocation. Femurs and tibias were removed intact under aseptic conditions as described in section 2.3.1. Cells were then centrifuged at 600 g for 5 min and resuspended in 5 ml cRPMI. Bone marrow cells were counted and seeded at a concentration of 6 × 10^6 cells per 10cm tissue culture grade Petri dish (Falcon BD) in 10 ml cRPMI supplemented with 20 ng/ml Granulocyte Macrophage-Colony Stimulating Factor (GM-CSF) (PeproTech, Rocky Hill, NJ). On day 3, 10 ml of fresh cRPMI supplemented with 20 ng/ml GM-CSF was added to each dish. On day 6, 10 ml of cell suspension was removed from each dish and discarded. 10 ml of

fresh cRPMI supplemented with 20 ng/ml GM-CSF was added. After 8 days, cells were harvested by gentle aspiration and centrifuged at 600 g for 5 min. Cells were resuspended in cRPMI (Table 2.1) and counted. Cells were seeded at appropriate concentrations relevant to experimental assays.

2.3.4 MURINE SPLENOCYTE ISOLATION

Murine spleens were removed aseptically from mice into cRPMI supplemented with 10% (v/v) heat inactivated FBS, 100 U/ml penicillium, 100 µg/ml streptomycin and 2 mM L-glutamine (Table 2.1). Splenocytes were isolated by homogenising spleens through a 70 µm filter and were then suspended in 8 ml cRPMI containing 0.1 % v/v beta-mercaptoethanol (Invitrogen-Gibco). The homogenate was centrifuged at 300 g for 5 min and resuspended in 2 ml of red blood cell lysis buffer solution (BioLegend, San Diego, CA,) for 10 min at room temperature. 2 ml of medium was added to the suspension to neutralise the lysis solution which was then centrifuged at 600 g for 5 min. Supernatant was removed and the cells were then resuspended in fresh cRPMI and counted.

2.3.5 HUMAN PERIPHERAL BLOOD MONONUCLEAR CELL (PBMC) SEPARATION

Whole blood buffy coat packs, which contained red blood cells, white blood cells and platelets, were supplied by St. James's Hospital, Dublin. In parallel, freshly isolated blood was collected in heparin coated blood collection tubes (Sarstedt, Germany) from healthy donor volunteers in NUI Maynooth. PBMC were isolated from whole blood by density gradient centrifugation. The contents of buffy coat packs were diluted 1 in 4 with Hanks' Balanced Salt Solution (HBSS) (Invitrogen-Gibco) supplemented with 5 % (v/v) FBS (PAA) and 1 % HEPES (Invitrogen-Gibco), while fresh blood was diluted 1 in 2 with the same buffer. Buffy

coat packs were treated with 5 % (w/v) EDTA (Sigma-Aldrich) to prevent coagulation. 40 ml diluted blood was carefully layered on top of 10 ml lymphoprep (Axis-Shield, Oslo, Norway) in a 50 ml centrifugation tube (Sarstedt). Tubes were centrifuged at 400 g for 25 min with no brake and low acceleration. After centrifugation, the white buffy coat layer containing PBMC was removed into a new sterile 50 ml tube, leaving red blood cells and remaining plasma behind. PBMC were centrifuged at 800 g for 5 min with brake and acceleration at high settings. Supernantant was removed and the PBMC pellet was washed in 10 ml of HBSS and centrifuged at 600 g for 5 min a total of two times. The washed PBMC were resuspended in 10 ml of cRPMI (Table 2.1) and counted.

2.3.6 $CD4^+$ T CELL ISOLATION

Human/mouse $CD4^+$ T cells were isolated using MagCellect $CD4^+$ T cell isolation kit according to manufacturer's instructions (R & D Systems, Minneapolis, MN). Briefly, PBMC/splenocytes were resuspended in 1X MagCellect buffer to a cell density of 1.0×10^8 cells/ml. For every 1×10^7 cells processed, 10 µl of $CD4^+$ T cell biotinylated antibody cocktail was added and cells incubated for 15 min at 4 ˚C. After incubation, 12.5 µl of streptavidin ferrofluid per 1×10^7 cells was added and further incubated for 15 min at 4 ˚C. Following the incubations, the final volume of 3 ml was made by adding MagCellect buffer. The tubes were placed into a magnetic stand for 6 min at RT. The magnetically labelled cells migrated towards the magnet, leaving the desired $CD4^+$ T cells behind in suspension. This incubation was repeated for another 6 min to ensure a pure $CD4^+$ T cell population was obtained. The $CD4^+$ T cell suspension was centrifuged at 300 g for 5 min then resuspended in cRPMI and counted.

2.4 CELL VIABILITY & APOPTOSIS ASSESSMENT

2.4.1 MEASUREMENT OF CELL VIABILITY (FLUORESCENT MICROSCOPY)

A sample of cells was suspended in their specific growth media and diluted 1/10 in 2 % (w/v) ethidium bromide/acridine orange (EB/AO) (Sigma-Aldrich, Arklow, Ireland). 10 µl was pipetted onto a haemocytometer chamber and viable cells (green) were counted using a fluorescent light microscope.

2.4.2 APOPTOSIS *IN VITRO*

Apoptosis was detected by the binding of Annexin V/Propidium iodide (PI) staining. Cells were harvested, resuspended in PBS for washing and centrifuged at 300 g for 5 min. Cells were resuspended in 1 X binding buffer at a concentration of 1 x 10^6 cells/ml. 1 x 10^5 cells (100 µl) were transferred to a 5 ml tube. 5 µl of Annexin V-FITC (0.5 mg/ml) and 5 µl of propidium iodide (PI) (20 µg/ml) (BDBioscience) were added to each tube. Cells were gently vortexed and incubated for 15 min at room temperature in the dark. After 15 min, 400 µl of assay buffer (BDBioscience) was added to each tube and analysed by flow cytometry within 1 h.

2.5 CELL CHARACTERISATION BY FLOW CYTOMETRY

2.5.1 GENERAL FLOW CYTOMETRY

For analyses by flow cytometry, cells (MSC, DC or $CD4^+$ T cells) were harvested, washed in sterile PBS and resuspended in an appropriate volume of PBA (phosphate buffer saline solution (PBS) supplemented with 10 % (v/v) heat inactivated bovine serum albumin (BSA)) to yield approximately 1 x 10^5 cells/FACS tube (4 ml polypropelyene tubes) (Falcon, BD Biosciences). In directly labelled approaches, fluorochrome conjugated antibodies (Tables 2.4 & 2.5) or isotype

controls were incubated with cells for 15 min at 4 °C. After 15 min, cells were washed in 2 ml of PBA, vortexed and centrifuged at 250 g for 5 min. The supernatant was removed and cells resuspended in 200 μl PBA or 300 μl of cell fixative (PBS supplemented with 1 % (v/v) paraformaldehyde (PFA) (Sigma-Aldrich)).

A similar approach was used for indirect labelling. The primary biotinylated (eBioscience, San Diego, CA) (Table 2.4 & 2.5) antibody was incubated with cells as above. Secondary conjugated antibodies (eBioscience) were added to appropriate tubes and further incubated for 15 min at 4 °C. Cells were then washed with 2 ml PBA and vortexed before centrifugation at 250 g for 5 min. The supernatant was removed and cells resuspended in 200 μl PBA for immediate analysis or in 300 μl of cell fixative for storage at 4 °C overnight. Cells were analyzed by flow cytometry using a FACSCalibur cytometer using CellQuest software (BD Biosciences). A minimum of 1 x 10^5 cells were analysed for surface expression of markers and 10,000 events were acquired for each marker.

2.5.2 INTRACELLULAR FLOW CYTOMETRY FOR HUMAN FOXP3 EXPRESSION

FoxP3 expression was analysed intracellularly. Briefly, $CD4^+$ T cells or PBMC, recovered from coculture assays, were washed in PBA. $CD4^+$ T cells were labelled with CD4 PerCP or CD4 APC and CD25 PE or corresponding isotype control antibodies for 15 min at 4 °C. $CD4^+$ T cells or PBMC were washed and fixed with 2 % (v/v) PFA (Sigma-Aldrich). $CD4^+$ T cells or PBMC were then permeabilised using cold PBS and 0.2 % (v/v) Tween 20/PBS (Sigma-Aldrich). After permeabilisation, $CD4^+$ T cells or PBMC were incubated with FoxP3 FITC antibody or isotype control for 30 min at 4 °C. At the end of the incubation, $CD4^+$ T

cells or PBMC were washed with PBA and placed in 300 µl of cell fixative. Analysis was performed within 4 h of preparation using a FACSCalibur cytometer and CellQuest software (BD Biosciences).

2.6 CELL CULTURE

2.6.1 PROLIFERATION ASSAY

DC, $CD4^+$ T cells, splenocytes or PBMC were seeded in a 96-well tissue culture plate (1 x 10^6 cells/ml) in the presence or absence of MSC (1 x 10^5 cells/ml) in 200 µl final volume. In a mitogen driven proliferation assay, PBMC or splenocytes from one MHC donor or strain were stimulated with concanavalin A (ConA) or phytohaemagglutinin (PHA) (Sigma-Aldrich) at 5 µg/ml for 72 h. After 72 h, 100 µl of supernatant was carefully removed and stored at -20 °C for cytokine analysis. [^{3}H]-Thymidine (Amersham Biosciences, Buckinghamshire, England) at 0.5 µCi/ml was added for the final 6 h of culture and incubated at 37 °C 5 % CO_2. Cultures were harvested using an automatic cell harvester (Micro96 Harvester, Skatron Flow Laboratories, Oslo, Norway) onto glass fibre filter mats. The mats were dried and placed in plastic sample bags (Wallac– PerkinElmer, Waltham, MA, USA). 3 ml of β-scintillation fluid (Beta-Plate Scint, Wallac-PerkinElmer) was added to the bag containing the filter mat after which it was sealed and placed in a cassette. [^{3}H]-Thymidine incorporation was quantified by a β-scintillation counter (1450 Microbeta Liquid Scintillation Counter; Wallac-Perkin Elmer) and results were expressed in counts per minute (cpm).

2.6.2 MIXED LYMPHOCYTE REACTION (MLR): HUMAN AND MURINE

Freshly isolated PBMC or murine splenocytes were seeded at a density of 1 x 10^6/ml and added to a 96-well tissue culture plate in 200 µl final volume (1 x

10^5cells/well). PBMC from two HLA mismatched donors or splenocytes from two MHC mismatched strains were cocultured in a two-way MLR. The effect of MSC on lymphocyte proliferation was assessed by adding MSC to the MLR at a density of 1 x 10^5 cells/ml (1 x 10^4cells/well). The 96 well plate was incubated at 37 °C for 72 h after which 100 µl of supernatant was carefully removed and stored at -20 °C for cytokine analysis. [^{3}H]-Thymidine at 0.5 µCi/ml was added for the final 6 h of culture and incubated at 37 °C 5 % CO_2. Cell were harvested as stated in section 2.6.1.

2.6.3 CRYOPRESERVATION AND RECOVERY OF CELLS FROM LIQUID NITROGEN

Cells were suspended at 1 x 10^6/ml of freezing medium and temperature reduced 10 °C per minute overnight and stored in liquid Nitrogen within 24 h. Freezing medium consisted of cRPMI containing 20% (v/v) FCS supplemented with 10 % (v/v) Dimethyl Sulfoxide (DMSO) (Sigma-Aldrich). To recover cells, vials were quickly thawed at 37 °C. Just as the vial contents thawed, 8 ml of warmed medium was added and cells were centrifuged at 600 g for 5 min. Supernatant was discarded and the cells washed once more. The final pellet was resuspended in 2 ml of cRPMI and placed in T175 flask for culturing in cell specific media.

2.7 DIFFERENTIATION OF MSC

2.7.1 OSTEOGENIC

MSC were seeded at a density of 1 x 10^3cell/cm^2 in a 6-well tissue culture plate in 2 ml cDMEM (hMSC) or cα-MEM (mMSC). Once 70 % confluence was reached (typically 2-3 days), cells were incubated in osteogenic differentiation medium (Table 2.1). Fresh medium was added every 3-4 days for 21 days. At day

21, the medium was removed and the cells were washed in PBS and then fixed in 10 % (v/v) neutral buffered formalin for 20 min at room temperature. Formalin was removed and cells were washed in 2 ml of PBS. 1 ml of 1 % Alizarin Red (Table 2.2) was added to the fixed cells and allowed to stain for 20 min at RT. Excess stain was removed and the cells were washed with dH_2O. Finally, 1 ml of dH_2O was added to each well and cells were examined under the microscope for red deposits indicating the presence of osteocyte like cells (Pittenger, 1999).

2.7.2 ADIPOGENIC

MSC were seeded at a density of 1 x 10^3cell/cm^2 in a 6-well tissue culture plate (BD Falcon) in 2 ml cDMEM (hMSC) or cα-MEM (mMSC) as above and at 70 % confluence, cells were incubated in adipogenic differentiation medium (Table 2.1) with fresh medium added every 3-4 days for 21 days. At day 21, the medium was removed and the cells were washed in PBS and then fixed in 10 % neutral buffered formalin for 20 min at room temperature. Formalin was removed and cells were washed in 2 ml of PBS. 1ml of 0.5 % Oil Red O (Table 2.2) was added to the fixed cells and allowed to stain for 20 min. Excess stain was removed and the cells were washed with PBS. Finally, 1 ml of PBS was added to each well and cells were examined under the microscope for red fat globules indicating the presence of adipocyte like cells (Pittenger, 1999)

2.7.3 CHONDROGENIC

MSC were seeded at 2.5 x 10^5cells/pellet culture in 15 ml tube. MSC were centrifuged at 100 g for 5 min. Pellets were resuspended in complete human MSC media (control) or in complete chondrocyte media (Table 2.1). Tubes were placed in incubator at 37 ˚C, 5 % CO_2 in 15 ml tubes with caps loosened to allow for gaseous

exchange for 21 days. Media was changed every 2-3 days. On day 21, cell pellets were harvested by aspirating off all the media and washing pellets twice with PBS. Pellets were placed in 1 ml of trizol and stored at -20°C. Chondrocyte pellets were analysed for the expression of collagen II and aggrecan by RT-PCR (Table 2.7 & 2.8). Briefly, RNA was isolated from the pellets (section 2.9.1), reversed transcribed into cDNA (section 2.9.3) and the expression of chondrocyte markers were analysed by RT-PCR (section 2.9.4).

2.8 IMMUNOCHEMICAL TECHNIQUES

2.8.1 ENZYME LINKED IMMUNOSORBENT ASSAY (ELISA)

All ELISA were carried out according to manufacturer's instructions. Specific capture antibodies (human IFNγ & TNFα or murine IL-12p70 & IL-10) in PBS were added to 96 well microtitre plates (NUNC) and incubated overnight at room temperature. Plates were then washed 3 times in wash buffer (PBS supplememnted with 0.05 % v/v Tween 20) and then incubated in blocking solution (PBS supplemented with 1 % w/v BSA) for a minimum of 1 h. Plates were then washed and incubated with 100 µl/well of sample supernatant or corresponding cytokine standard for 2 h at room temperature. After washing, plates were incubated with specific detection antibodies for a further 2 h at room temperature. Plates were washed again and incubated with 100 µl/well of streptavidin horseradish peroxidase (HRP) (R & D Systems) conjugate diluted 1/200 in specific reagent diluent (Tris buffered solution (TBS) (Sigma-Aldrich) supplemented with BSA for 20 min. After washing, plates were incubated with 100 µl/well of tetramethylbenzidine (TMB) substrate (Sigma-Aldrich) for 20 min at room temperature out of direct light. The reaction was stopped after 20 min by adding 50 µl/well of 1 M H_2SO_4. The

absorbance (optical density (O.D)) of the samples and standards were measured at 450 nm for all ELISA using a plate reader (Labsystems, Helsinki, Finland). The cytokine concentration of each sample was determined by comparison to the standard curve of known cytokine concentrations.

2.8.2 MEASUREMENT OF CYTOKINES BY BEAD ARRAY ANALYSIS

Bead array technology is a method for quantifying multiple cytokines simultaneously in a single sample volume (25 µl). This technique is based on the same premise as enzyme-linked immunosorbent assay (ELISA). Bead array analysis uses fluorescence, instead of colorimetric intensity for quantification. Beads are internally labelled with varying intensities of fluorescent dye, corresponding to each specific cytokine, which allows for the differentiation of multiple analytes by flow cytometry. Analysis of cytokines from serum (human IFNγ & TNFα) was carried out using Flow Cytomix kits (BenderMedSystems) and analysed using a FACSCaliber flow cytometer (Becton Dickinson,). Standard curves and raw data were generated for each cytokine using FlowCytomix Pro 2.2 software (BenderMedSystems).

Cytokines were quantified as per manufacturer's instructions. Briefly, standards, samples or control (PBS) were added to 4 ml polypropylene FACS tubes (Falcon, BD Biosciences). Beads coated with primary antibodies for each individual cytokine were mixed together and added to each tube. Biotin-conjugated secondary antibodies were added to all tubes and allowed to incubated for 2 h at room temperature, protected from light. Following incubation, samples were washed with 1 ml of FACS buffer and centrifuged at 200 g for 5 min. After centrifugation, supernatant was carefully discarded and wash step was repeated. Streptavidin-PE

was added to the tubes and allowed to incubate fro 1 h at room temperature and protected from light. Following this incubation, samples were washed twice more and then sample tube was resuspended in 500 µl of assay buffer. Cytokines were quantified from samples based on fluorescence intensity and comparison to the standard samples.

2.9 MOLECULAR TECHNIQUES

2.9.1 RNA ISOLATION

Total RNA was extracted using trizol® reagent (Invitrogen) according to the manufacturer's instructions. Briefly, 1 x 10^6 cells were lysed in 1ml trizol at room temperature for 5 min. 100 µl of RNA-grade 1-Bromo-3-chloropropane (Sigma-Aldrich) was added to the cells, mixed vigorously and incubated at room temperature for 5 min. Samples were centrifuged at 12,000 g for 15 min at 4 °C. Two distinct layers resulted with RNA remaining in the clear, aqueous upper layer. 350-400 µl of RNA was carefully removed, ensuring the lower white DNA layer was not disturbed, and precipitated with 500 µl isopropanol (Riedel-deHaen). The samples were incubated at room temperature for 10 min and followed by centrifugation for 10 min at 4 °C. The resulting RNA pellet was washed with 1 ml 75 % (v/v) ethanol and centrifuged at 7,500 g for 5 min at 4 ^{o}C. The ethanol was aspirated and the RNA pellet was allowed to briefly air dry prior to resuspension in 30 µl RNase-free water (Promega, Southhampton, UK). The purity and concentration of RNA was determined using a spectrophotometer (Nanodrop 2000, ThermoScientific, Wilmington, DE, USA) which calculated the ratio of absorbance at 260 nm to 280 nm. A ratio between 1.8 and 2.0 indicated sufficient purity of the RNA. Samples outside this range were discarded.

2.9.2 DNase Treatment of RNA

Genomic DNA was removed from RNA samples by treatment with DNase I (Invitrogen, Paisley, UK). 1 µl of DNase (Amplification grade) was added to 500 ng of RNA and incubated for 15 min at room temperature. 1 µl of 25mM EDTA (Promega), to inactivate the DNase, was added to the mixture and incubated at 65°C for 10 min.

2.9.3 cDNA Synthesis

Following DNase treatment of RNA, total RNA was reverse transcribed using 25 Units Superscript II (Invitrogen). Each reaction contained a 1 x GoTaq reaction buffer (Promega), 2.5 mM $MgCl_2$ (Promega), 10 mM dNTP mix (Promega), 50 U/ml of ribonuclease inhibitor (Invitrogen) and 20 µg/ml Oligo (dT) $_{12\text{-}18}$ primer (Invitrogen) diluted in nuclease-free water (Promega). The conditions for cDNA synthesis were as follows: 25 ^{o}C for 10 min, 42 ^{o}C for 60 min, 95 ^{o}C for 5 min and 4 ^{o}C for 10 min. Quantification of cDNA was performed by measuring the absorbance value of the sample 260 nm. Samples were stored -20 ^{o}C until required.

2.9.4 Reverse Transcription-Polymerase Chain Reaction (RT-PCR)

PCR was used to determine the presence of specific DNA sequences (or mRNA following reverse transcription) using primers summarised in Table 2.6 and 2.7. Expression of the housekeeping gene, Glyceraldehyde 3-phosphate dehydrogenase (GAPDH) was used as a positive control. PCR reactions contained 2.5 mM $MgCl_2$ (Promega), 25 mM dNTP (Promega), 1 x GoTaq reaction buffer (Promega), 40 U/ml Taq polymerase (Promega) and 0.4 pM of the appropriate primer (NCBI:BLAST). The reaction mastermix was adjusted to a final volume of

24 µl with nuclease-free water. The PCR conditions were as follows: denaturation at 95 °C for 45 sec (10 min for first cycle), annealing for 45 sec (optimal annealing temperatures are summarised in Table 2.7 and 2.8 and extension for 1 min at 72°C. DNA products were resolved on a 1.3 % w/v agarose gel and detected by binding of gel red (Biotium, Hayward, CA).

2.9.5 REAL TIME-POLYMERASE CHAIN REACTION (QRT-PCR)

cDNA was analysed for the quantification of mRNA expression. Briefly, cDNA (500 ng) were amplified in the presence of SYBR® Green PCR mastermix (Qiagen). Accumulation of gene-specific products were measured continuously by means of fluorescence detection over 35 cycles. Each cycle consisted of: denaturation at 95 °C for 15 min, annealing at 95 °C for 30 sec, optimum temperature (Table 2.7 & 2.8) for 30 sec, 72 °C for 30 sec, extension at 72 °C for 10 min and then 4 °C forever. Standard curves for FoxP3 and TGF-β1 expression were generated by amplifying 10-fold serial dilutions of known quantities of FoxP3 or TGF-β1 standard generated previously in the laboratory. The expression of Notch, ICOS, LICOS, PD-1 and PDL-1 were quantified in relation to the housekeeper GAPDH. Quantification of target gene expression was obtained using sequence detector software (DNA Opticon ™). The resultant target mRNA concentration was expressed as fg product/500ng cDNA.

2.9.6 SILENCING OF RNA (SIRNA)

MSC were seeded at 4×10^4/ well in 24 well plates in duplicate until approximately 60% confluent. siRNA for murine Jagged-1 was pre-designed (Silencer® Select siRNA, Applied Biosystems, Warrington, UK) and diluted in RNase free water (supplied with kit) to different concentrations, as per

manufacturer's instructions. Lipofectamine (Invitrogen, Paisley, UK) was used as a transfection reagent for all siRNA experiments, as per manufacturer's instructions. MSC with or without siRNA were cultured in Opti-Mem®I media (Gibco-Invitrogen, Paisley, UK). After 24 h, MSC RNA was isolated (Section 2.9.1) and transcribed into cDNA (Section 2.9.3). Murine Jagged-1 expression on MSC was examined by RT-PCR (Section 2.9.4) (Table 2.8).

2.10 MSC FUNCTIONAL ASSAYS IN VITRO

2.10.1 *IN VITRO* MATURATION OF DC AND COCULTURE WITH MSC

Immature DC were harvested on day 8 and matured in the presence of lipopolysaccharide (LPS) (Sigma-Aldrich) at 100 ng/ml for 24 or 48 h in the presence or absence of mMSC. The seeding densities used were, 1 x 10^5 MSC: 3 x 10^5 DC in 24 well plate for 24 h RT-PCR analysis or 3 x 10^5 MSC: 1 x 10^6 DC in 6 well plate for 48 h flow cytometry analysis. For transwell experiments, MSC were seeded in the bottom of the well (6 well or 24 well) and DC were placed in the transwell inserts (0.4μM) (Nunc). The expression of regulatory molecules (ICOS, LICOS, PD-1, PDL-1 & CTLA4), notch receptors (Notch 1 & 2), Notch ligands (Jagged 1, 2 & Delta like ligand 1) and notch target gene (Hes 1) on DC were analysed by RT-PCR after 24 h (Table 2.8). After 48 h, maturation markers (MHCII and CD86), CD11c and corresponding isotype controls were analysed by flow cytometry on DC (Table 2.4). For the neutralisation study, mouse anti-Jagged 1 (8 μg/ml & 5 μg/ml) or corresponding control antibody was added to the co-cultures and the expression of maturation markers were analysed by flow cytometry (Table 2.4). In some experiments, the Notch inhibitor, γ-secretase inhibitor (GSI) (Calbiochem, Merck, Germany) reconstituted in DMSO (Sigma-Aldrich), at 1 μM

was added to DC: MSC cocultures for 48 h and the expression of maturation markers were analysed by flow cytometry. Supernatants from coculture were analysed for the presence of IL-10 and IL-12p70 by ELISA (section 2.8.1)

2.10.2 Antigen Presentation Assay (Eα: I-A^B detection)

Immature DC were isolated from C57/Bl6 mice and harvested on day 8 of culture by gentle aspiration. DC at 3 x 10^5/well were incubated with 10 µg/ml I-Eα peptide 52-68 (ASFEAQGALANIAVDKA) (Anaspec, San Jose, CA) for 48 h in the presence or absence of MSC (1 x 10^5/well) in a 24 well plate. As a control, DC were cultured with MSC alone or MSC and diluted DMSO (vehicle for Eα peptide) for 48 h in 24 well plate. Peptide binding was detected using the biotin-conjugated anti-I-A^b: Eα complex specific antibody, Y-Ae (eBioscience). Binding of biotin-conjugated antibody was detected by FITC conjugated extravadin (Sigma-Aldrich) and analysed by flow cytometry.

2.10.3 Ovalbumin (OVA) Specific Antigen Proliferation Assay

Immature DC from C57/Bl6 mice were isolated and harvested on day 8 of culture by gentle aspiration. DC at 1 x 10^6/well of a 6 well tissue culture plate were pulsed with 20 µg/ml OVA (Sigma-Aldrich) in the presence or absence of MSC (3 x 10^5/well) for 24 h. After 24 h, DC were harvested by gentle aspiration and centrifuged at 300 g for 5 min. DC were further cultured with 4 x 10^5/ml naïve OVA-specific I-Ad restricted $CD4^+$ DO11.10 T cells isolated from the spleens of DO11.10 mice. Cells were cultured for 72 h and a proliferation assay performed as stated in section 2.6.1.

2.10.4 STIMULATION OF MURINE MSC WITH INFLAMMATORY CYTOKINES

Murine MSC at 3 x 10^5/well of a 6 well tissue culture plate were allowed to adhere overnight. mMSC were stimulated with prolactin (PeproTech, London, UK), IFNγ (R&D Systems), LPS (Sigma-Aldrich) or TNFα (R&D Systems) at 50 ng/ml for 24 h. The expression of Notch receptors (Notch 1 & 2), Notch ligands (Jagged 1, 2 & Delta like ligand 1) and regulatory molecules (PD-1, PDL-1, ICOS, LICOS and CTLA4) were analysed by RT-PCR (Table 2.8).

2.10.5 *IN VITRO* COCULTURE OF HUMAN PBMC/$CD4^+$ T CELL AND MSC

Whole PBMC or freshly isolated $CD4^+$ T cells (1×10^6/well) were cocultured with hMSC (3×10^5/well) for 24 or 72h in 6 well plates (Nunc) or in transwell plates (0.4μM) (Nunc). Neutralisation or antagonist studies were performed using anti-TGFβ1 at 4 μg/ml (R & D Systems) or indomethacin at 40 μM (Sigma-Aldrich) (Table 2.5). The expression of forkhead box P3 (FoxP3) and transforming growth factor beta 1 (TGFβ1) were analysed by qRT-PCR (Table 2.7) after 24 h. The expression of CD4, CD25 and FoxP3 were analysed by flow cytometry (Table 2.5) 72 h after co-culture.

2.10.6 COMPLEMENT INDUCED KILLING *IN VITRO*

Human MSC were cultured at 2 x 10^5/well of a 24 well tissue culture plate overnight in complete medium to allow cells to adhere. Human lung epithelial cells (A549) or mouse splenocyte control cells were cultured at 2 x 10^5/well of a 24 well tissue culture plate in serum free media (RPMI supplemented with 1 % v/v ITS and 1 % v/v penicillium streptomycin). Medium was removed from human MSC and replaced with serum free medium. Cells were then exposed to either human or

mouse complement at 1/16 dilution of final volume for 4 h. Cells were then washed out of the complement solution after 4 h, and dying/apoptotic cells were detected using by flow cytometry as described in section 2.4.2. Times and concentrations were arrived at after prior optimisation experiments.

2.10.7 Assessment of Human MSC Induced Apoptosis of PBMC

Human PBMC at 1 x 10^6/well were cocultured with MSC at 3 x 10^5/well of a 6 well for 24 h in cRPMI. The analysis of MSC induced apoptosis was analysed by flow cytometry. As a positive control, a chemotherapy drug, cisplatin (Sigma-Aldrich) at 500 µg/ml was added to some wells. After 24 h, all human PBMC were recovered from culture by gentle aspiration from adherent MSC and apoptotic cells were detected using FITC Annexin V apoptosis detection kit as described in section 2.4.2.

2.10.8 Assessment of Human MSC Induced $CD4^+$ T cell Anergy

Murine DC were isolated using the protocol outline in section 2.3.4 from BALB/c mice. Human $CD4^+$ T cells were isolated from human PBMC as stated in section 2.3.6 & 2.3.7. Murine DC (1.5 x 10^5/ml) were cocultured with human $CD4^+$ T cells (1 x 10^6/ml) and stimulated with poly IC (20 µg/ml) in the presence or absence of human MSC (1 x 10^5/ml) for 5 days in cRPMI supplemented with 0.1% v/v beta-mercaptoethanol. After 5 days, human $CD4^+$ T cell were repurified from cocultures using MagCellect CD4 isolation kit and allowed to rest for 24 h in cRPMI. Following the rest period, a proliferation assay was performed. Repurified human $CD4^+$ T cells (1 x 10^6/ml) were cocultured with irradiated BALB.c DC (1 x 10^5/ml) in a 96 well plate and restimulated with polyIC (20 µg/ml) in the presence or absence of recombinant human interleukin 2 (rhIL-2) (100 U/ml) for 72 h. After 72

h, 100 µl of supernatant was carefully removed and stored at -20 °C for cytokine analysis. ^{3}H]-Thymidine (Amersham Biosciences, Buckinghamshire, England) at 0.5 µCi/ml was added for the final 6 h of culture and incubated at 37 °C 5 % CO_2. Cultures were harvested using an automatic cell harvester as stated in section 2.6.1.

2.11 HUMANISED MOUSE MODEL OF AGVHD

2.11.1 ACUTE GRAFT VERSUS HOST DISEASE HUMANISED MOUSE MODEL

A humanised mouse model was developed and optimised from a protocol described by Pearson *et al.* (Pearson, 2008). NOD.Cg-Prkdc^{scid}IL2^{tmlWjl}/Szj (NOD-Scid IL-2rγ^{null}) (NSG) were exposed to a conditioning dose of 2.4 Gray (Gy) of whole body gamma irradiation. Freshly isolated human PBMC were administered by intravenous injection to the tail vein using a 27 gauge needle and a 1 ml syringe between 4 h but no longer than 24 h following irradiation. Before infusion, PBMC were washed three times with sterile PBS. PBMC in varying amounts ranging from 2 x 10^5 to 4 x 10^7 cells per mouse were administered on day 0. This allowed for the identification of the optimum amount of PBMC required for consistent acute graft versus host disease (aGvHD) development between 10 and 20 days. The optimum dose for PBMC for aGvHD development was found to be 6.3 x 10^5 g^{-1}. aGvHD development was determined by examining features including weight loss exceeding 15 % total body weight, ruffled fur, hunched posture. Animals were returned to their cages where they were monitored closely for the first hour and at regular intervals thereafter for any signs of distress or ill health. Animals were weighed daily and weigh loss was documented accordingly. Any animals which displayed greater than 15 % total body weight loss were sacrificed humanely.

2.11.2 PATHOLOGICAL SCORING SYSTEM FOR ACUTE GRAFT VERSUS HOST DISEASE

The development of aGvHD was assessed using a series of pathological features. Weight loss greater than 15 % total body weight were consider to have aGvHD and were sacrificed. Other pathological features taken into consideration were; posture (hunching), activity, fur texture and diarrhoea. Any animals scoring a cumulative score of 8 for the pathological features were considered to have aGvHD and were sacrificed humanely. The scoring system used were; posture: 0; normal, no hunching; 0.5; slight hunching that straightens when walking; 1.0; animal stays hunched when walking; 1.5; animal does not straighten out; 2.0; animal tends to stand on rear toes. Activity: 0; normal, very mobile and hard to catch; 0.5; slower than normal and little easier to catch; 1.0; no activity, but will move when touched; 1.5; no activity, very little movement when touched; 2.0; no activity at all, not even when touched. Fur: 0; normal, no fur pathology; 0.5; ridging on the side of belly and neck; 1.0; ridging across and side of belly and neck; 1.5; fur is matted and ruffled; 2.0; badly matted on belly and top. Diarrhoea: 0; normal; 0.5 mild change in bowel movement; 1.0; moderate change in bowel movement; 1.5; severe change in bowel movement; 2.0; extensive diarrhoea.

2.11.3 INTRAVENOUS TRANSFER OF HUMAN MSC AND PBMC

Before infusion, human PBMC or MSC were washed three times with sterile PBS. PBMC were administered to mice at 6.3×10^5 g^{-1} and MSC were administered at 4.4×10^4 g^{-1}. PBMC or MSC were delivered to the tail vein using a 27 gauge needle and a 1 ml syringe. Each mouse received a total of 0.2 ml. PBMC were

given on day 0 while MSC were given on day 0, 7 or 14. Following i.v injection, animals were returned to their cages where they were monitored as above.

2.11.4 ISOLATION OF LUNG OR LIVER CELLS FROM HUMANISED MOUSE MODEL

Lungs or livers were removed aseptically from NOD-Scid IL-2rγ^{null} and transferred to a 15 ml tube containing complete RPMI (cRPMI). Using a sterile forceps, the organs were transferred to a Petri dish and sectioned using a sterile scalpel. The small lung or liver pieces were then digested in 10 ml of collagenase from *Clostridium histolyticum* (300 U/ml) (Sigma-Aldrich) and DNase I (10 mg/ml) (Roche Diagnostics, Germany) digestion solution at 30°C under constant horizontal shaking at 300 rpm. After 1 h of digestion, the homogenates were passed through a 40 µm filter into a 50 ml tube using a sterile plunger and 10 ml of cRPMI. The digested tissue samples were then centrifuged at 300 g for 5 min. The supernatants were discarded and the pellets resuspended in 3 ml of lysis buffer and incubated at room temperature for 5 min. After 5 min, the cells were centrifuged for 5 min at 300 g and resuspended in PBS for FACS analsyis.

2.11.5 DETECTION OF HUMAN CELLS *IN VIVO* BY FLOW CYTOMETRY

PBMC at a concentration of 6.3 x 10^5 g^{-1} were delivered to the tail vein of mice on day 0. After 15 days, animals were sacrificed and splenocytes were harvested (section 2.3.5). Splenocytes were analysed b y flow cytometry for expression of murine and human CD4, CD8 and CD45 or corresponding isotype controls. Facs analyses was performed within 4 h of preparation using a FACSCalibur cytometer and CellQuest software (BD Biosciences).

2.11.6 CFSE STAINING OF CELLS

Freshly isolated human PBMC were washed twice in PBS and resuspended at 5 x 10^7/ml in warm PBS. Carboxyfluorescein succinimidyl ester (CFSE) was prepared at 5 mM stock was by dissolving the supplied powder in 18 µl of DMSO (Invitrogen). PBMC at 2 x 10^7 were labelled with various concentrations of diluted CFSE, 2.5 µM, 5 µM or 10 µM. Cells were incubated for 10 min at room temperature in the dark. After 10 min, 2 ml of cold PBS was added and PBMC centrifuged at 600 g for 5 min then washed twice in PBS. CFSE labelled PBMC were then used in further experiments.

2.11.7 *IN VITRO* PROLIFERATION USING CFSE STAINED PBMC

Human PBMC were stained with various concentrations of CFSE as described in section 2.11.6. CFSE labelled PBMC (4 x 10^6/ml) were cultured in the presence or absence of recombinant human IL-2 (rhIL-2) at 100 U/ml (R & D Systems) and PHA at 5 µg/ml (Sigma-Aldrich) in a 6 well tissue culture plate pre-coated with human anti-CD3 at 2.0 µg/ml (eBioscience). To determine the effect of MSC on CFSE labelled PBMC proliferation, MSC were added to wells at 4 x 10^5/ml. After 5 days, PBMC were harvested and the level of CFSE labelled cell proliferation was analysed by flow cytometry, with a minimum of 100,000 cells acquired. A decrease in CFSE staining was indicative of PBMC proliferation.

2.11.8 DETECTION OF CFSE LABELLED PBMC *IN VIVO*

PBMC were labelled with 10 µM CFSE as described in section 2.11.6. CFSE labelled PBMC were washed twice with PBS and administered at 6.3 x 10^5 g^{-1} to irradiated NOD-Scid IL2rγ^{null} mice on day 0. After 5 days and 12 days, the lung,

liver and spleen were harvested from each mouse. Splenocytes were isolated following protocol described in section 2.3.5, with lung and liver cells isolated as described in section 2.11.4. A single cell suspension of 1 x 10^6 cells/ml were counterstained with anti-human CD4 APC for 15 min at 4 °C. Cells were centrifuged at 300 g for 5 min and resuspended in 300 µl of cell fixative. Cells were analysed for CFSE staining (FL-1) and the expression of human CD4 (FL-4) by flow cytometry with a minimum of 100,000 cells acquired.

2.11.9 DETECTION OF APOPTOTIC CELLS *IN VIVO*

PBMC at a concentration of 6.3 x $10^5 g^{-1}$ were delivered via the tail vein of 2.4 Gy irradiated NOD-Scid IL2rγ^{null} mice on day 0. "Licensed" MSC at 4.4 x 10^4 g^{-1} were administered i.v on day 0 or unlicensed MSC at 4.4 x 10^4 g^{-1} were administered on day 7. On day 12, 8 µg (100 µl) of FAM-FLIVO™ green dye (FL-1) was injected per mouse and left to circulate for 1 h. After 1 h, the lung and liver were harvested and cells were isolated as described in section 2.11.4. Cells were counterstained with anti-human CD4 APC (FL-4) and analysed by flow cytometry with a minimum of 10,000 cells acquired. To optimise the FLIVO dye, BALB/c mice were lethally irradiated with 12 Gy gamma irradiation. After 24 h, 8 µg (100 µl) of FAM-FLIVO™ green dye (FL-1) was injected per mouse and left to circulate for 1 h. After 1 h, the lung and liver were harvested. Cells were analysed for the expression of FLIVO™ green dye (FL-1).

2.12 HISTOLOGY

2.12.1 TISSUE PREPARATION

Livers, lungs and GI tract were removed from experimental mice and fixed in 10% (v/v) formalin (Sigma-Aldrich). Tissues were processed for histology using an automated processor (Shandon Pathcentre, Runcorn, UK), which immerses the tissues in fixatives and sequential dehydration solutions, including ethanol (70%, 80%, 95% x 2, 100% x 3) and xylene (x 2) (BDH AnalaR® Laboratory Supplies Poole, UK). Tissues samples were then embedded in paraffin wax using the Shandon Histocenter 2 (Shandon) and left to set overnight at 4 °C. 4µm sections were cut using a microtome (Shandon Finesse 325, Thermo-Shandon, Waltham, MA, USA). Sections were placed in cold water containing ethanol followed by transfer to a hot water bath (42 °C) to smooth out any folding in the sections. Sections were placed on microscope slides (Thermo Scientific), air-dried overnight at RT before staining with H &E (Section 2.12.2) and blindly scored using the system detailed in section 2.12.3.

2.12.2 HAEMATOXYLIN/EOSIN STAINING

Prior to staining, 5 µm tissues section slides were incubated at 56 °C for a minimum of 1 h to aid clearance of wax. Slide sections were immersed in two changes of xylene for 10 min each, following by re-hydration in three decreasing concentrations of ethanol (100% x 2, 95% (v/v) and 80%) for 5 min each. Sections were then placed in two changes of water to rinse off excess xylene and immersed in Haematoxylin (Sigma-Aldrich) solution for 3 min. Slides were washed in water for 2 min and placed in 1 % acid alcohol for 20 seconds, followed by a further wash step in water. Slides were then counterstained in Eosin Y (Sigma-Aldrich) for 3 min and

washed again in water (Table 2.3). Finally, slides were put through a series of dehydration steps in ethanol (80%, 95% and 100%) for 5 min each. Slides were then mounted with DPX mountant (BDH) and examined under a light microscope.

2.12.3 HISTOLOGICAL SCORING

Following H & E staining, slides were coded without reference to prior treatment and examined in a blind fashion. A semi-quantitative scoring system was used to assess abnormalities in the lung, liver and GI tract (Hill, 1997; Grass, 1999; Polchert, 2008). The scoring was carried out as follows:

Lung: 0; normal; 0.5; rare scattered areas of mononuclear cells; 1.0; minimal or focal areas of cellular infiltrate; 2.0; mild and more diffuse cellular infiltration; 3.0; moderate amount of mononuclear cell infiltration; 4.0; extensive mononuclear cell infiltration. ***Liver***: 0; normal; 1.0; rare collections of mononuclear cells in the parenchyma; 2.0; endothelialitis present in at least one vessel, with an increase in mononuclear cell infiltration; 3.0; endothelialitis present in more than one vessel, with a further increase in mononuclear cell infiltration; 4.0; endothelialitis present in virtually all vessels, with extensive mononuclear cell infiltration. ***GI tract***: 0; normal; 1.0; mild necrotic cells with minor cell infiltration; 2.0; diffuse, but mild villous blunting, necrotic cells and increase in cell infiltration; 3.0; diffuse, but moderate villous blunting, necrotic cells and further increase in cell infiltration; 4.0; diffuse but severe villous blunting, necrotic cells and extensive cell infiltration.

2.13 STATISTICAL METHODS

The students paired t test was used when statistical analysis was required between two experimental groups. One way ANOVA was used to test for statistical

significance of differences when multiple experimental groups were compared. Kaplan Meier curves (log rank test) were used to compare survival between treatment groups. Power analysis was carried out to determine the number of animals that would yield a significant difference in the in vivo studies. Statistical methods (Power analysis (SISA)) were used to determine the minimum number of animals per treatment group to obtain a power in the study. SISA software is online at http://home.clara.net/sisa/power.htm.

Table 2.1 Summary of media for cultured cells

Medium Name	Description	Supplier
Murine MSC isolation medium (CIM)	RPMI 1640	Invitrogen-Gibco
	100 U/ml penicillin	Invitrogen-Gibco
	100 µg/ml streptomycin	Invitrogen-Gibco
	2 mM L-glutamine	Invitrogen-Gibco
	10 % (v/v) horse serum	Hyclone
	10 % (v/v) heat inactivated, low-endotoxin foetal calf serum (FCS)	Biosera
Murine MSC expansion medium(cαMEM)	Minimum Essential Medium alpha (MEM	Invitrogen-Gibc
	10 % (v/v) heat inactivated low endotoxin FCS	Biosera
	10 % (v/v) horse serum	Hyclone
	100 U/ml penicillin	Invitrogen-Gibco
	100 µg/ml streptomycin	Invitrogen-Gibco
	2 mM L-glutamine	Invitrogen-Gibco
Human and murine osteoblast differentiation medium	Dulbecco's Modified Eagle's Media (DMEM) containing 100 mg/ml glucose (human) or Minimum Essential Medium alpha (MEM) (murine)	Invitrogen-Gibco
	1 mM dexamethasone,	Sigma-Aldrich
	20 mM β-glycerolphosphate,	Sigma-Aldrich
	50 µM L-ascorbic acid-2-phosphate,	Sigma-Aldrich
	50 ng/ml L-thyroxine sodium pentahydrate	Sigma-Aldrich

Table 2.1 Summary of media for cultured cells continued

Medium Name	Description	Supplier
Chondrogenic medium	Dulbecco's Modified Eagle's Media (DMEM) containing 100 mg/ml glucose	Invitrogen-Gibco-
	100 nM dexamethasone	Sigma-Aldrich
	50 µg/ml ascorbic-acid-2-phosphate	Sigma-Aldrich
	40 µg/ml proline	Sigma-Aldrich
	1 mM sodium pyruvate	Sigma-Aldrich
	1 % v/v ITS + supplement	BD Biosciences
	10 ng/ml TGF-β3	TS:beta
Human and murine adipocyte differentiation medium	Dulbecco's Modified Eagle's Media (DMEM) containing 100 mg/ml glucose (human) or Minimum Essential Medium alpha (MEM) (murine)	Invitrogen-Gibco
	5.0 µg/ml insulin in 0.1N acetic acid	Sigma-Aldrich
	50 µM indomethacin	Sigma-Aldrich
	1 µM dexamethasone	Sigma-Aldrich
	0.5 µM IBM x in MeOH	Sigma-Aldrich
Serum free medium	RPMI 1640	Invitrogen-Gibco
	100 U/ml penicillin	Invitrogen-Gibco
	100 µg/ml streptomycin	Invitrogen-Gibco
	1 % v/v ITS + supplement	BD Biosciences

Table 2.1 Summary of media for cultured cells continued

Media	Culture media	Supplier
Murine Dendritic Cell Medium	RPMI 1640	Invitrogen-Gibco
	100 U/ml penicillin	Invitrogen-Gibco
	100μg/ml streptomycin	Invitrogen-Gibco
	2mM L-glutamine	Invitrogen-Gibco
	10% (v/v) heat inactivated low-endotoxin FCS	Biosera
	20 ng/ml recombinant murine GM-CSF	PeproTech
Murine/Human $CD4^+$ T Cell or Murine Splenocyte Medium (cRPMI)	RPMI 1640	Invitrogen-Gibco
	100 U/ml penicillin	Invitrogen-Gibco
	100 μg/ml streptomycin	Invitrogen-Gibco
	2mM L-glutamine	Invitrogen-Gibco
	10% (v/v) heat inactivated low-endotoxin FCS	Biosera
	0.01% (v/v) beta mercaptoethanol	Invitrogen-Gibco
Human MSC culture Medium (cDMEM)	Dulbecco's Modified Eagle's Media (DMEM) containing 100 mg/ml glucose	Invitrogen-Gibco
	10% (v/v) FCS	PAA
	200 U/ml penicillin	Invitrogen-Gibco
	200 μg/ml streptomycin	Invitrogen-Gibco

Table 2.2 Reagents used to detect human and murine MSC Differentiation.

Reagent	Components	Concentration	Supplier
MSC Osteoblast Differentiation	Alizarin Red S stain	1 % (w/v)	Sigma-Aldrich
	dH_2O	100 ml	
	pH adjusted to between 4.1-4.3 using 0.1% v/v ammonium hydroxide		Sigma-Aldrich
MSC Adipocyte Differentiation	Oil Red O	0.5 % (w/v)	Sigma-Aldrich
	Isopropanol	30 ml	Sigma-Aldrich
	Working solution: 0.5% w/v Oil Red O stock		
	PBS	20 ml	Sigma-Aldrich

Table 2.3 Histological staining solutions

Reagent	Components	Concentration	Supplier
Harris Hematoxylin	Hematoxylin	Neat	Sigma-Aldrich
Eosin	Eosin Y	1 % (w/v)	Sigma-Aldrich
	Potassium dichromate	1.6 % (w/v)	Sigma-Aldich
	dH_2O	100 ml	
Acid alcohol	Hydrochloric acid	1 % (v/v)	WVR
	2-propanol	69.3 % (v/v)	WVR
	dH_20	29.7 % (v/v)	

Table 2.4 Antibodies directed against murine markers

Antibody	Conjugate	Concentration	Clone	Source
CD3e	FITC	5 µg/ml	145.2C11	eBioscience
CD4	FITC	5 µg/ml	GK1.5	eBioscience
CD8	FITC	5 µg/ml	53-6.7	eBioscience
CD11b	Biotin	5 µg/ml	M1/70	eBioscience
CD34	Biotin	5 µg/ml	RAM34	eBioscience
CD40	PE	2 µg/ml	1C10	eBioscience
CD44	Biotin	2 µg/ml	IM7	eBioscience
CD45	Biotin	5 µg/ml	30-F11	eBioscience
CD80	PE	2 µg/ml	16.10A1	eBioscience
CD86	PE	5 µg/ml	GL1	eBioscience
CD90	FITC	5 µg/ml	LT84EC	eBioscience
CD105	Biotin	5 µg/ml	MJ7/18	eBioscience
CD106	FITC	5 µg/ml	429	eBioscience
CD117	FITC	5 µg/ml	2B8	eBioscience
MHC class I	FITC	5 µg/ml	28-14-8	eBioscience
MHC class II	PE	1 µg/ml	NIMR-4	eBioscience

Sca-1	PE	5 µg/ml	D7	eBioscience
YA-e	Biotin	5 µg/ml	EBioY-Ae	eBioscience

Table 2.5 Antibodies directed against human markers

Antibody	Conjugate	Concentration	Clone	Source
CD3	FITC	5 µg/ml	HIT3a	eBioscience
CD4	APC/PE/PerCp	5 µg/ml	SK3/OKT4	eBioscience
CD8	FITC	2.5 µg/ml	RPA-T8	eBioscience
CD25	PE	1.25 µg/ml	BC96	eBioscience
CD29	FITC	2.5 µg/ml	TS2/16	eBioscience
CD34	FITC	5 µg/ml	4H11	eBioscience
CD40	PE	5 µg/ml	5C3	eBioscience
CD44	FITC	5 µg/ml	IM7	eBioscience
CD45	FITC	5 µg/ml	H30	eBioscience
CD54	FITC	5 µg/ml	HA58	eBioscience
CD80	PE	5 µg/ml	2D10.4	eBioscience
CD86	PE	5 µg/ml	IT2.2	eBioscience
CD90	FITC	5 µg/ml	eBio5E10	eBioscience
CD105	FITC	5 µg/ml	SN6	eBioscience
CD106	PE	5 µg/ml	STA	eBioscience
CD117	PE	2.5 µg/ml	YB5.B8	eBioscience
CD154	FITC	2.5 µg/ml	24.31	eBioscience
HLA-ABC	FITC	10 µg/ml	W6/32	eBioscience
HLA-DR	PE	0.075 µg/ml	L243	eBioscience
FoxP3	FITC	5 µg/ml	PCH101	eBioscience

Table 2.6 Neutralisation Antibodies and Antagonists

Antibody/Antagonist	Concentration	Supplier
anti-human TGFβ1	4 µg/ml	eBioscience
Indomethacin	40 µM	Sigma-Aldrich

Table 2.7 Summary of primer sequences: Human

Primer	Forward 5'-3'	Reverse 3'-5'	Product size (bp)	Anneal temp (°C)	$MgCl_2$ Conc (mM)
GAPDH	GGTGAAGGTCGGAGTCAACG	AAAGTTGTCATGGATGACC	540	55	2.5
Collagen II	GCCCAAGAGGTGCCCCTGGAATA	CCTGAGAAAGAGGAGTGGACATA	703	57	2.5
Aggrecan	TGAGGAGGGCTGGAACAAGTACC	GGAGGTGGTAATTGCAGGGAAC	350	55	2.5
TGF-β1	CAGATCCTGTCCAAGCTG	TCGGAGCTCTGATGTGTT	270	54	2.5
FoxP3	AGGTGGCAGGATGGTTTCT	AACAGCACATTCCCAGAGTTC	223	57	2.5

Table 2.8 Summary of primer sequences: Murine

Primer	Forward 5'-3'	Reverse 3'-5'	Product size (bp)	Anneal temp (°C)	$MgCl_2$ Conc (mM)
IL-10	AGGTGCGTTCCTC	AAAGCCAACCAA	241	55	2.5
IL-4	TCAACCCCCAGCTAGTTGTC	CCTTCTCCTGTGACCTCGTT	124	57	2.5
E-cadherin	GGCTGGACCGAGAGAGTT	CTGCTTGGCCTCAAAATC	350	58	1.5
GAPDH	GGTGAAGGTCGGAGTCAACG	AAAGTTGTCATGGATGACC	540	55	2.5
CCR7	AGTCTTCCAGCTGCCCTACA	CAGCCCAAGTCCTTGAAGAG	219	55	2.5
Notch-1	GTCGCTGGATACAAGTGCAA	TGTGGGACAGACACAGGAAA	150	55	2.5
Notch-2	CGTGTGAGAATGCTGCTGTT	TTGTGGCAGACACCATTGTT	148	60	2.5
Jagged-1	AGTCTTCCCCTTGTGCCTTT	CACTTGGCCCCATCAAGTAT	154	55	2.5
Jagged-2	AGGCACCTACTGCCATGAAA	CGTTGGGATTGATGTCACAG	143	55	2.5
Delta like ligand-1	CAACAAGAAGGCGGACTTTC	CACTTGGTGTCACGTTTGCT	150	57	2.5
Hes-1	GCCTTGGCTCACTCCGCGTT	TCTGCCACCCCTAGTCCCGC	304	60	2.5
ICOS	AATGGGCAAACATTCTCCTG	AGTGCTAGGGCTGACTTCCA	285	58	2.5
LICOS	GGACTCCATGAAGCAGGGTA	TCAGAGGTGCTGATGACAGG	180	60	2.5
PD-1	TGGGCAGCTGTATGATCTGC	TTCACCTGCAGCTTGTCCAA	149	55	2.5
PDL-1	AAAGTCAATGCCCCATACCG	TTCTCTTCCCACTCACGGGT	151	55	2.5
CTLA-4	CAGGTGACCCAACCTTCAGT	CAGTCCTTGGATGGTGAGGT	243	58	2.5

Siglec E	CCCAGTTCATGG ATTCTGGT	TTCAGGGAGC AGTCATTCCT	150	62	2.5
Siglec F	TGCCTCTGCCTC ATCTTTTT	CAACGCATTG TTGGATGAAG	144	58	2.5
Siglec G	CGGATGGAGAG AGGATTTGA	AAGGTCCAGG AAAACAAGCA	149	60	2.5
Siglec H	GGTTCCATGAA GGGGAAAAT	AACCGTTGTC ACCCTTTTGT	150	55	2.5
Aggrecan	GTTGGTTACTTC GCCTCCAG	GTCCTCCAAG CTCTGTGACC	103	55	2.5

CHAPTER 3

HUMAN MSC SUPPRESS INNATE AND ADAPTIVE IMMUNITY

3.1 INTRODUCTION

MSC display potent immunosuppressive qualities (Barry, 2003; Pittenger, 1999), which makes MSC a promising tool for cellular immunotherapy (Heng, 2009). Unlike other stem cells types, MSC do not aggressively activate innate or adaptive immune responses, allowing for their acceptance into an allogeneic host without rejection. At the commencement of this work, MSC modulation of innate responses was known to include the inhibition of dendritic cell (DC) maturation (English, 2008), and the prevention of natural killer (NK) cell activation (Spaggiari, 2006). MSC had been described as being involved in the modulation of adaptive immune cells, including the skewing of T cell phenotypes (Ryan, 2007) and the inhibition of B cell proliferation (Corcione, 2006). More recently, the inhibition of complement activation through factor H has been described (Tu, 2010).

Modulation of allogeneic responses by MSC involves multiple factors; cell: cell contact and the release of soluble factors play non-redundant roles in MSC immunomodulation (Djouad, 2003; Krampera, 2003). For example, IL-6 along with a contact dependent signal are required for MSC modulation of DC maturation (Djouad, 2007; English, 2008). MSC derived transforming growth factor beta (TGF-β), prostaglandin E2 (PGE_2) (English, 2007; Ryan, 2007), suppress T cell proliferation in conjunction with a cell contact signal. In this chapter, the goals were:

(1) to define the phenotype of human MSC (hMSC) used in this study by evaluating surface marker expression, differentiation capacity and immunosuppressive ability *in vitro*. (2) To analyse the influence of innate immune mechanisms, in particular complement activation, on the survival of hMSC *in vitro*.

(3) To investigate the mechanism(s) involved in hMSC suppression of adaptive immunity

(4) To investigate the role of hMSC-derived soluble factors on T reg cell induction in vitro.

(5) To examine the functional capacity of hMSC-derived T reg cells to suppress immune responses *in vitro.*

3.2 CHARACTERISATION OF ADULT HUMAN MSC BY FLOW CYTOMETRY

There are no specific surface markers that uniquely identify hMSC, therefore a range of markers were used to validate the hMSC isolation techniques employed. The ISCT have proposed specific criteria for the characterisation of multipotent MSC (Horwitz, 2005; Dominici, 2006). For this study, human bone marrow derived MSC were isolated and expanded from an aspirate of bone marrow taken from the iliac crest of donor patients from a collaborating laboratory in NUI Galway (as described by Barry & Murphy, 2004).

Candidate populations of hMSC, received from NUIG at passage 1, were grown in DMEM medium for up to eight passages. hMSC cultured at passage 1 were adherent to plastic of tissue culture flasks and were spindle shaped/fibroblast-like in morphology (Fig 3.1). However, morphology is a subjective criterion and therefore the expression of specific surface markers (eg, stem cell antigen-1 (Sca-1) and CD44) and the lack of expression of other surface markers (CD45 and CD11b) are typically used for the identification of MSC (Peister, 2004). hMSC isolated in this chapter were characterised by flow cytometry. hMSC batches displayed

consistent expression of specific surface marker proteins typical of adult hMSC; HLA-ABC, Thy 1.1 (CD90), CD106, CD29, CD44, CD54 and CD105 (Fig 3.2). hMSC did not express HLA-DR, CD45, CD11b, the haematopoietic cell markers CD34, CD117 or the costimulatory markers CD40 or CD86 (Fig 3.2). The stability of typical hMSC marker expression was examined from passages 3-8 (Fig. 3.2). The hMSC batches used here had no evidence of haematopoietic stem cell contamination, which provided some confidence, that a pure population of hMSC was present.

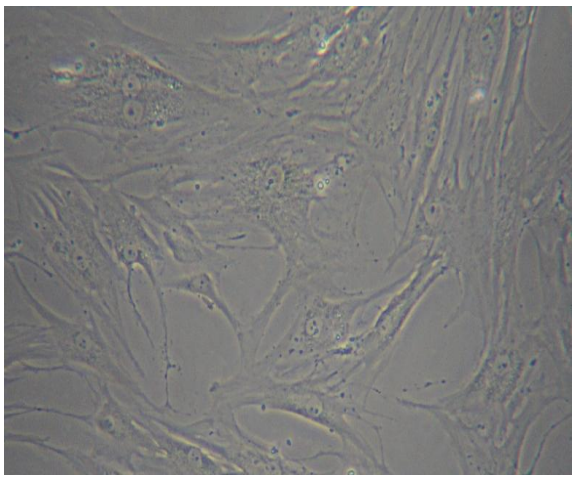

Fig 3.1 Adult Human Bone Marrow-Derived Mesenchymal Stem cells (hMSC) have a morphology similar to fibroblasts. hMSC were isolated and cultured in DMEM media until 80-90% confluent. The appearance of spindle shaped cells was characteristic of a homogenous population of hMSC. This population is representative of hMSC at passage 5, however, each passage from 3-8 was found to have similar morphology. Magnification × 100, phase contrast light microscopy.

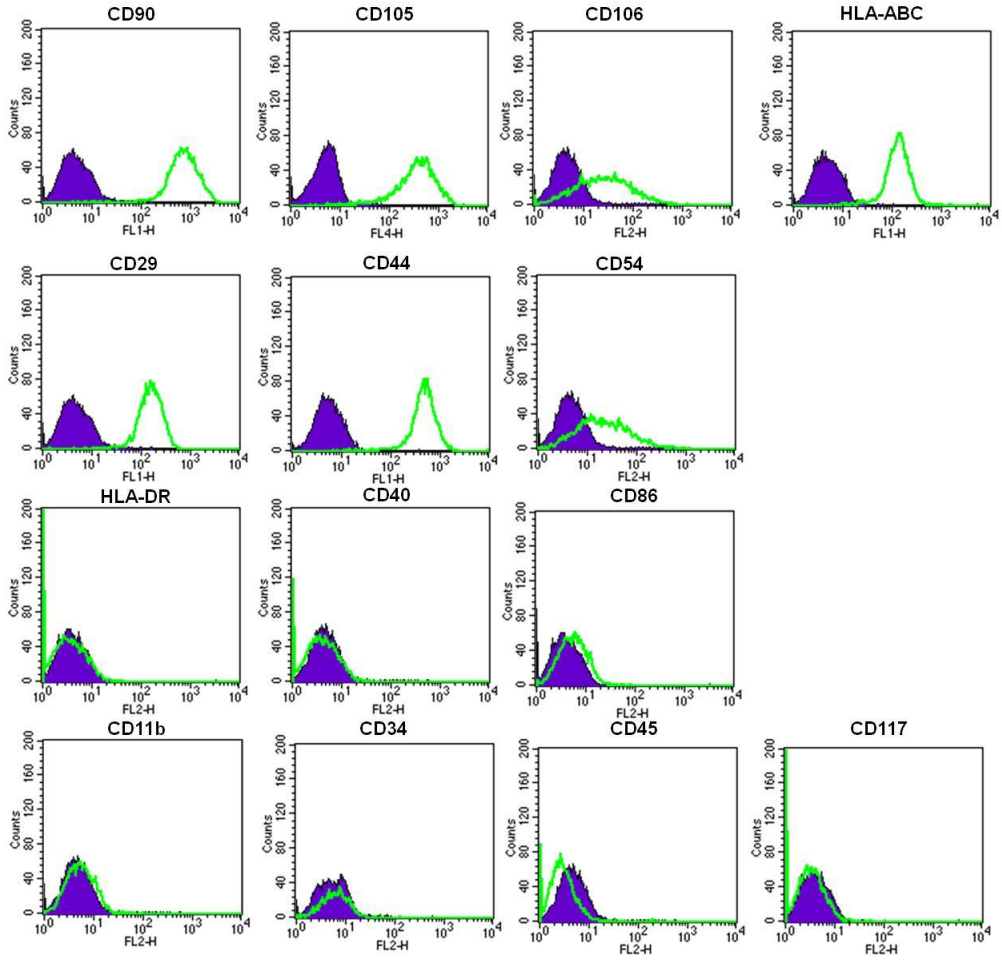

Fig 3.2 Characterisation of surface marker protein expression by human MSC. MSC were characterised for the expression of specific surface protein by flow cytometry. MSC typically expressed HLA-ABC, CD90, CD105, CD106 and CD44. MSC did not express HLA-DR, haematopoietic markers CD34, CD117 or costimulatory markers CD40 and CD86. Isotype controls are represented by purple filled plots while cell specific markers by open green plots. Data are representative of hMSC marker expression at passage 5, however, it was examined at each passage from 3-8.

3.3 DIFFERENTIATION CAPACITY OF MSC

The "stemness" of hMSC was determined through their capacity to differentiate into a number of mesodermal cell lineages. hMSC isolated as described above were cultured in specific differentiation media (Table 2.2) to stimulate the differentiation of hMSC into adipocytes, osteocytes or chondrocytes. Adipocytes were visualised by staining with Oil Red O, which stains lipid vacuoles red (Fig 3.3 A). Osteoblasts were stained using Alizarin Red S, which when combined with calcium ions, forms a red product (Fig 3.3 B). Chondrocyte differentiation was determined through the expression of collagen II and aggrecan by semi-quantitative RT-PCR (Fig 3.3 C). Control cells (hMSC not cultured in differentiation media) were stained with the corresponding dyes or analysed for equivalent mRNA expression (Fig 3.3). hMSC used in this study differentiated along each pathway and maintained their multilineage potential through each subsequent generation for batches of hMSC used in this study from passage 3 to 8 (Fig. 3.3).

3.4 ALLOGENEIC MSC SUPPRESS PROLIFERATION IN A MIXED LYMPHOCYTE REACTION (MLR)

The ability of MSC to modulate immune responses was previously examined and confirmed by others (Ryan, 2007, English, 2008; DiNicola, 2002). However, it was important to confirm this characteristic on the hMSC used here, prior to their use in further *in vitro* studies. The immunosuppressive capacity of hMSC was investigated in two ways. Firstly, the ability of hMSC to modulate a mitogen driven lymphocyte proliferation was studied. This involved human PBMC from a single donor that were stimulated with Concanavalin A (ConA) in the presence or absence

of allogeneic hMSC. The level of proliferation was measured using ^{3}H thymidine incorporation. hMSC significantly inhibited the mitogen driven proliferation of PBMC *in vitro* ($p<0.0001$) (Fig 3.4 A).

Secondly, the ability of hMSC to suppress alloreactivity was examined using a two-way mixed lymphocyte reaction (MLR). PBMC from two MHC-mismatched donors were cocultured in the presence or absence of hMSC allogeneic to both PBMC populations. In the presence of hMSC, PBMC proliferation was significantly reduced ($p<0.05$), when compared to the coculture of allogeneic PBMC without hMSC (Fig 3.4 B). These data indicated that the hMSC populations (passage 3 to 8) used here were capable of suppressing both mitogen driven and alloantigen driven proliferation and the batches selected were characteristic of those used previously by others.

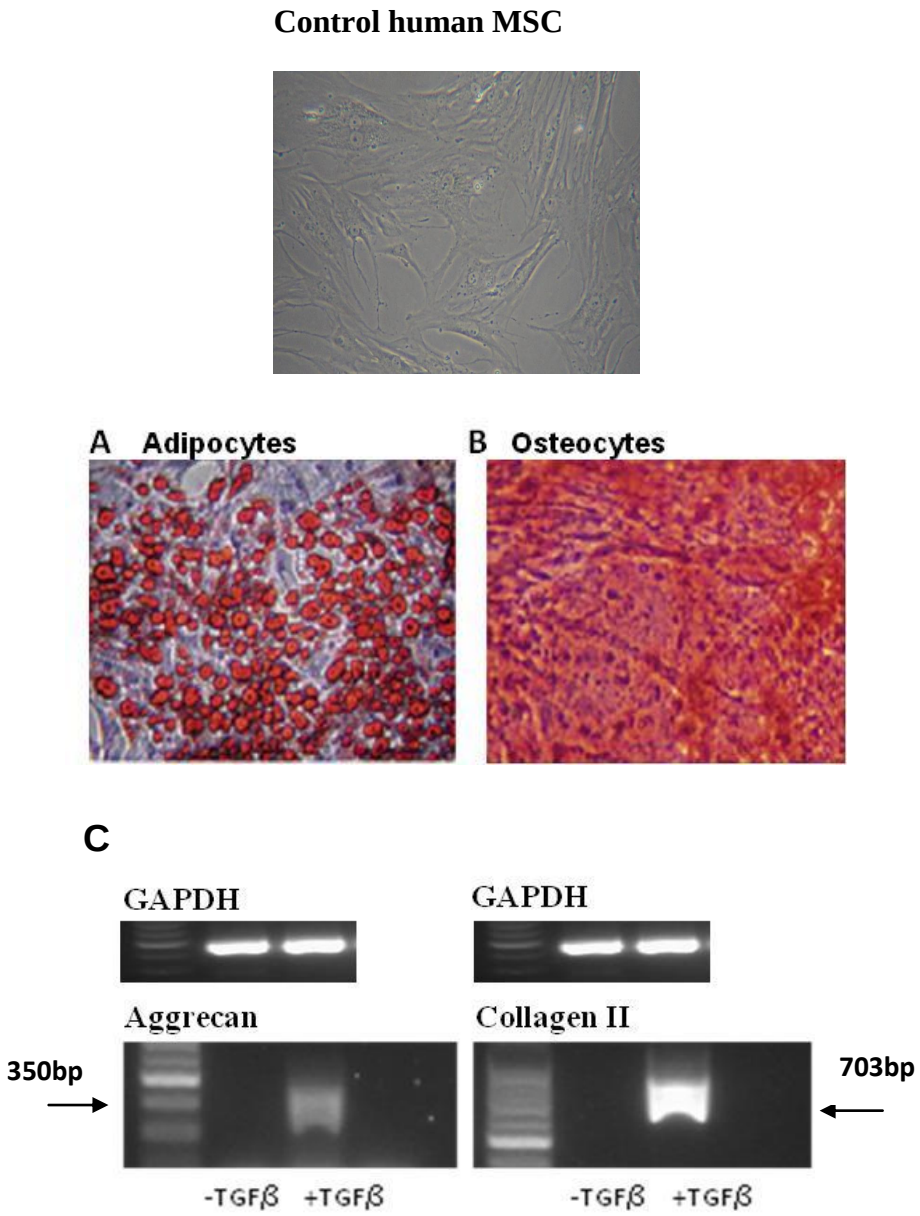

Fig 3.3 Differentiation capacity of hMSC. hMSC were cultured in specific differentiation media for 21 days for the characterisation of (A) adipocytes, (B) osteocytes and (C) chondrocytes. (A) hMSC were differentiated into adipocytes and stained using oil red O. (B) hMSC were differentiated into osteocytes and visualised by alizarin red S staining. Magnification × 100 using Phase contrast light microscopy. (C) hMSC were differentiated (+TGFβ3) into chondrocytes and compared to controls (-TGFβ3) for the expression of aggrecan and collagen II by semi-quantitative RT-PCR. Data are representative of hMSC differentiation capacity from passage 5. Similar data were obtained from hMSC between passages 3 to 8.

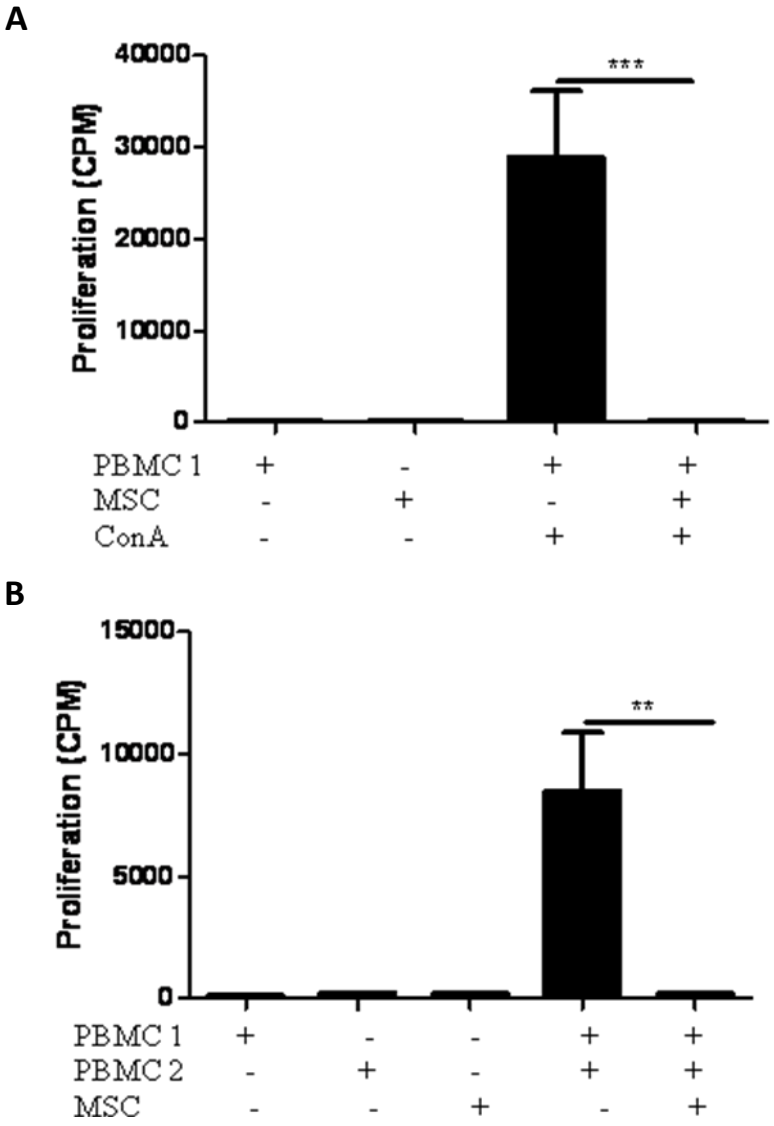

Fig 3.4 Allogeneic MSC inhibit mitogen and alloantigen driven proliferation. hMSC were examined for their capacity to inhibit (A) mitogen driven (ConA) and (B) alloantigen driven proliferation of PBMC. (A) hMSC (1 x 10^5/ml) were cocultured with MHC mismatched donor PBMC (1 x 10^6/ml). (B) hMSC were cocultured with two MHC mismatched donor PBMC in a two way mixed lymphocyte reaction. Proliferation was assessed by ^{3}H Thymidine incorporation. hMSC significantly inhibited both (A) mitogen driven proliferation ($p<0.0001$) and (B) alloantigen driven proliferation ($p<0.05$). Results are representative of three independent experiments performed in triplicate. Statistical analysis was carried out using the student paired t test. Similar data were obtained for hMSC from passage 3 to 8.

3.5 MURINE COMPLEMENT DID NOT AFFECT THE SURVIVAL OF HUMAN MSC *IN VITRO*

For use in cell therapy, hMSC must possess potent immunosuppressive abilities that span both the innate and adaptive immune system. The complement system is a vital component of innate immunity that plays a role in hyperacute and acute transplant rejection (Baldwin, 1995). As later work would require use of hMSC in murine models, it was necessary to determine whether suppression extended to the action of complement. In this study, the effect of human and murine complement on the survival of hMSC *in vitro* was investigated. The induction of hMSC apoptosis after exposure to complement was examined by flow cytometry using a well-optimised apoptosis kit (BDBioscience).

Human lung epithelial cells, (A549, control cells), murine splenocytes (control cells) or hMSC were cultured in the presence or absence of murine (mC') or human complement (hC') for 4 h. The complement concentration (1/16 batch dilution) was arrived at after a series of optimisation experiments. After 4 h, the induction of apoptosis was analysed by flow cytometry through annexin V (FL-1) and propidium iodide (PI) staining (FL-2) (Table 3.1) (Fig 3.5). As expected, murine complement induced the apoptosis of human A549 cells *in vitro* (11% cells), while human complement had no effect (4% cells) (Fig 3.5 A). Unsurprisingly, human complement induced the apoptosis of murine splenocytes (69% cells), with murine complement having no effect on the survival of murine splenocytes (3% cells) after 4 h (Fig 3.5 B) (Table 3.1).

After identifying that human complement induced destruction of murine cells and murine complement lysed human cells *in vitro* (Fig 3.5 A & B), hMSC were

cultured in the presence of human or murine complement for 4 h. Murine (0.6% cells) or human (0.6% cells) complement had no effect on hMSC survival *in vitro* (Fig 3.5 C) (Table 3.1). These data suggested that hMSC are resistant to the lytic effects of the alternative complement pathway and indicated another mechanism by which MSC suppress innate immune responses. These data were important to note for future animal and clinical studies as it suggested that the use of xenogeneic or humanised mouse models would be viable for studying MSC as a cell therapy (Chapter 6).

TABLE 3.1 HUMAN MSC ARE NOT SUSCEPTIBLE TO MURINE OR HUMAN COMPLEMENT KILLING

	% Cells lysed (MFI)		
Target Cell Type	**No Complement**	**Human Complement**	**Murine Complement**
Human A549	6.3 (490)	4.0 (391)	11.0 (384)
Murine Splenocytes	7.0 (1416)	69.0 (2633)	3.0 (1244)
Human MSC	0.6 (119)	0.6 (111)	0.6 (128)

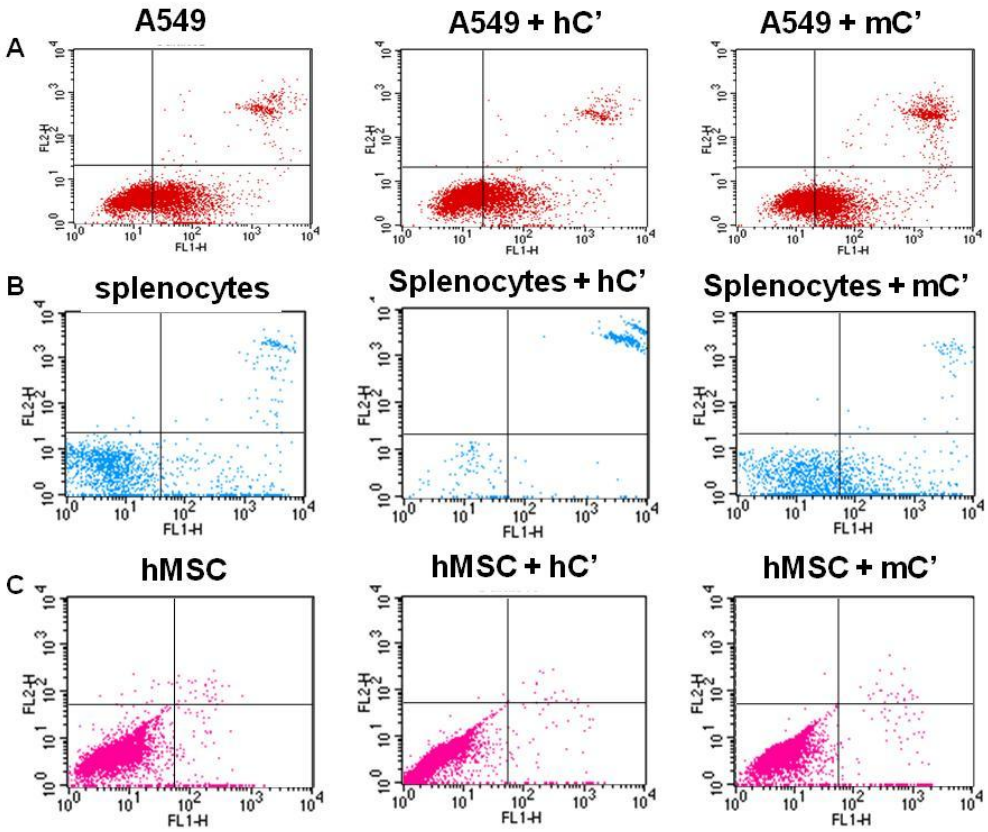

Fig 3.5 Murine complement did not kill human MSC *in vitro*. (A) Human A549 (3 x 10^5/well), (B) murine splenocytes (1 x10^6/well) or (C) hMSC (3 x 10^5/well) were exposed to human (hC') or murine complement (mC') (1/ 16 dilution) for 4 h. After 4 h, cells were harvested and analysed for cell apoptosis using annexin V (FL-1) and PI (FL-2) staining by flow cytometry. (A) Murine complement induced cell apoptosis of human A549 cells. (B) Human complement induced cell apoptosis of murine splenocytes. (C) hMSC survival was not affected by the presence of human or murine complement. Data are representative of three studies.

3.6 ALLOGENEIC HMSC INDUCE T CELLS WITH A REGULATORY PHENOTYPE

The study above showed that hMSC suppressed innate immunity; however, the remaining focus of this chapter concerns adaptive immunity and the effect of MSC on lymphocytes. MSC modulate many aspects of adaptive immunity (Chapter 1.7.2). There are multiple cell types in a population of PBMC used in an MLR, therefore it is difficult to determine which of the multiple suppressive effector functions hMSC are modulating in this system. In this chapter, the ability of allogeneic hMSC induction of T cells with a regulatory phenotype from a purified population of human $CD4^+$ T cells was investigated. The expression of the T cell regulatory transcription factor, forkhead box P3 (FoxP3) and CD25 were examined as typical markers of T reg-like populations.

Human $CD4^+$ T cells purified by magnetic bead separation, as described in section 2.3.7, were cultured in the presence or absence of hMSC for 24 h and the expression of FoxP3 examined by qRT-PCR (Fig 3.6 A & B). hMSC induced significantly more $CD4^+$ T cells that expressed FoxP3 ($p<0.02$) when compared to $CD4^+$ cells that did not encounter hMSC (Fig 3.6 B). The expression of FoxP3 and CD25, at the protein level was examined. Purified human $CD4^+$ T cells were cultured in the presence or absence of hMSC for 72 h. After 72 h, $CD4^+$ T cells were pulled back from coculture by gentle aspiration from adherent hMSC and examined for the expression of FoxP3 and CD25 by intracellular flow cytometry. Fewer $CD4^+$ T cells expressed FoxP3 (7.93% cells) (Fig 3.7 A) and CD25 (0.4% cells) (Fig 3.7 B) when cultured in the absence of hMSC. In contrast, there was a consistent increase in the $FoxP3^+$ $CD25^+$ $CD4^+$ T cells after coculture with hMSC (9.27% FoxP3 and 1.3% CD25) (Fig 3.7 A & B). These data indicated that hMSC induce a $CD4^+CD25^+FoxP3^+$ T population typical of T reg cells.

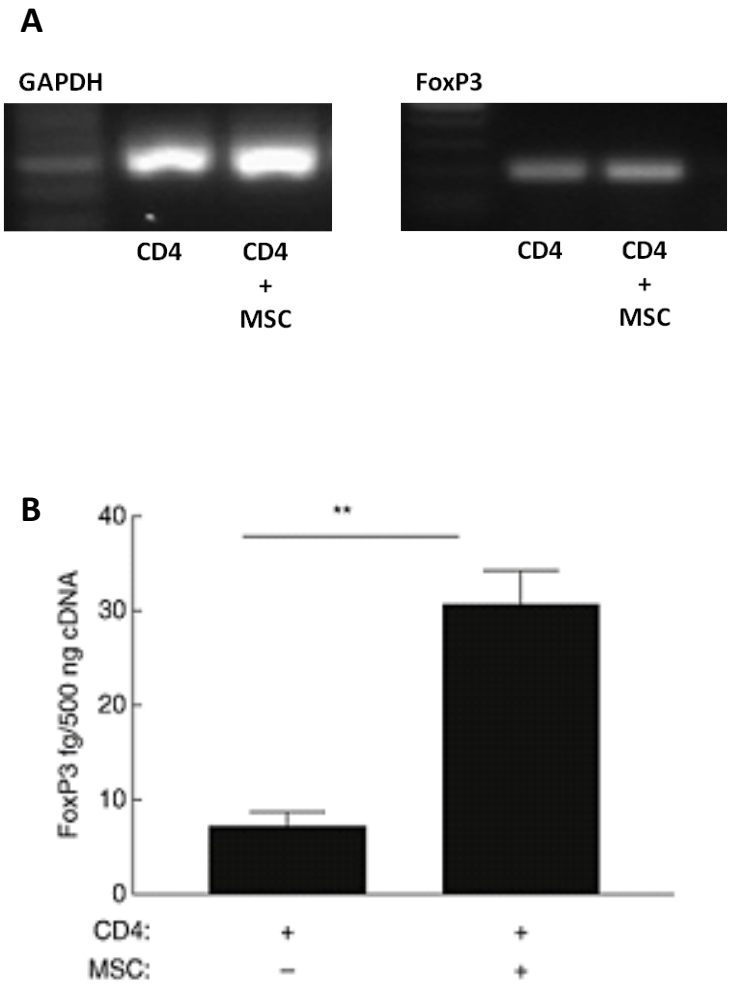

Fig 3.6 hMSC induced increased expression of FoxP3 in purified $CD4^+$ T cells. $CD4^+$ T cells (3 x 10^5/well) were cultured in the presence or absence of hMSC (1 x 10^5/well) in a 24 well plate for 24 h. After 24 h, purified $CD4^+$ T cells were pulled by from culture by gentle aspiration and examined for the expression of a house keeper, glyceraldehyde-3-phosphate-dehydrogenase (GAPDH) and FoxP3 by (A) semi quantitative RT-PCR and (B) Quantitative real time PCR for FoxP3 mRNA. (B) $CD4^+$ T cells expressed low levels of FoxP3 in the absence of hMSC but the level of FoxP3 was significantly increased when $CD4^+$ T cells were cocultured with hMSC ($p<0.02$). Results are representative of three independent experiments with qRT-PCR expressed as mean fg/500ng cDNA ± SE each performed in duplicate. Statistical analysis was carried out using the student paired t test.

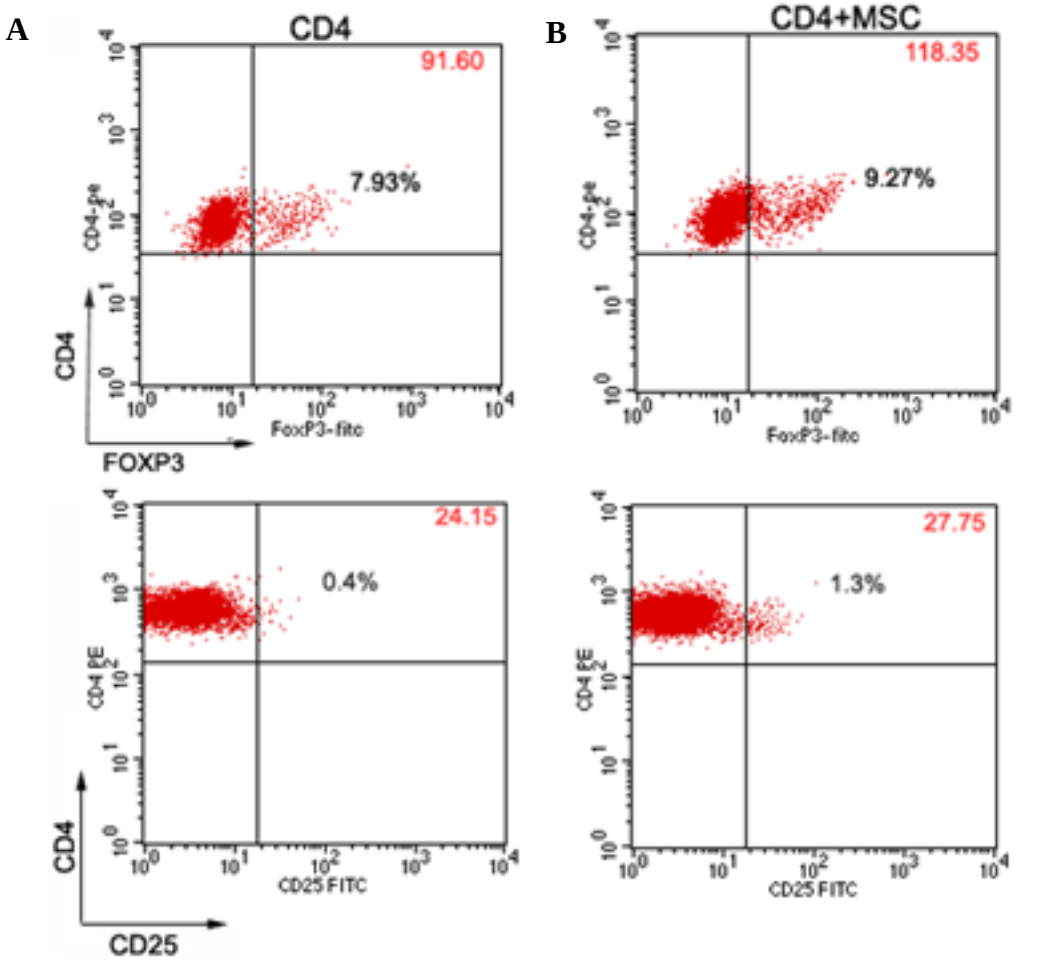

Fig 3.7 hMSC induced a T cell population expressing FoxP3 and CD25. $CD4^+$ T cells (1 x 10^6/well) were cultured in the presence or absence of hMSC (3 x 10^5/well) in a 6 well plate for 72 h. The expression of FoxP3 and CD25 was examined by intracellular flow cytometry. (A) $CD4^+$ T cells alone expressed low levels of both FoxP3 and CD25. (B) Upon coculture with hMSC, both FoxP3 and CD25 expression were up regulated on $CD4^+$ T cells. The percentages of double positive cells are in the upper right quadrant (%), with the mean fluorescent intensity (MFI). Data are representative of three independent experiments. (The collaboration with Dr. Jennifer Ryan and Dr. Karen English in this experiment is gratefully acknowledged).

3.7 ALLOGENEIC MSC INDUCTION OF FOXP3 AND CD25 EXPRESSION BY HUMAN CD4$^+$ T CELLS IS IN PART CONTACT DEPENDENT

Conflicting evidence exists whether cell contact contributes to the immunomodulatory function of MSC (Di Nicole, 2002, Djouad, 2003; Krampera, 2003). To investigate the role of cell contact in hMSC immune modulation, transwell experiments were carried out. hMSC were cultured in direct cell contact with CD4$^+$ T cells. Alternatively, contact was blocked through a transwell system, where hMSC were adherent to the bottom of a 24 well tissue culture plate and CD4$^+$ T cells were separated by a 0.4µm membrane transwell insert (contact prohibited). After 24 h of culture, CD4$^+$ T cells were pulled back from culture by gentle aspiration and examined for the expression of FoxP3 by qRT-PCR (Fig 3.8). When hMSC were separated from CD4$^+$ T cells in the transwell system, the induction of FoxP3 was significantly decreased among CD4$^+$ T cell population, when compared to CD4$^+$ T cells that had direct contact with hMSC (Fig 3.8). This suggested that cell contact between CD4$^+$ T cells and hMSC was involved in FoxP3 induction.

FoxP3 and CD25 protein levels were analysed by combined intra/extracellular flow cytometry. hMSC and CD4$^+$ T cells were cocultured with cell contact permitted and cell contact prohibited (transwell) for 72 h . Expression of FoxP3 and CD25 was investigated using flow cytometry. In the transwell system, allogeneic hMSC did not induce FoxP3$^+$ CD25$^+$ expression in purified CD4$^+$ T cells (2.86% FoxP3 and 0.19% CD25), when compared to cultures where contact was permitted (8.54% FoxP3 and 1.3% CD25) (Fig 3.9). This reiterated the finding by qRT-PCR, suggesting that direct cell contact was required for the induction of FoxP3 expression.

Next, the requirement for cell contact in a multi-cell system was examined. Unseparated allogeneic whole PBMC were cultured in the presence or absence of hMSC in a transwell system similar to above (contact permitted or prohibited). After 72 h, PBMC were recovered by gentle aspiration and the expression of FoxP3 and CD25 were analysed by flow cytometry. The expression of FoxP3 and CD25 by PBMC was increased when cell contact between PBMC and hMSC was permitted (1.46% FoxP3 and 1.68% CD25) (direct contact) or prohibited (1.33% FoxP3 and 2.33% CD25) (transwell) (Fig 3.10). This indicated that in the presence of other immune cells, cell contact was not required for allogeneic hMSC to induce a $FoxP3^+$ $CD25^+$ regulatory-like T cells. These data give some explanation into the contradictory data described by others. It also suggests that other cells can supplement the contact signal derived from hMSC *in vitro*.

3.8 ALLOGENEIC MSC INDUCE THE SECRETION OF IMMUNOSUPPRESSIVE CYTOKINES BY $CD4^+$ T CELLS

The pattern of cytokine secretion contributes to the characterisation of a T reg cell population. One of the key cytokines secreted by T reg cells is transforming growth factor beta-1 (TGFβ1). Therefore, the expression of TGFβ1 was examined on $CD4^+$ T cells following their coculture with hMSC. Purified $CD4^+$ T cells and hMSC were cocultured for 24 h *in vitro*. The expression of TGFβ1 on $CD4^+$ T cells cultured in the presence or absence of hMSC was examined by qRT-PCR. TGF-β1 mRNA expression was significantly higher in $CD4^+$ T cells which were previously cultured with hMSC (Fig 3.11 A & B). This was confirmed at a protein level, purified $CD4^+$ T cells and hMSC were cocultured for 48 h and the production of

TGFβ1 by $CD4^+$ T cells was examined by bead array analysis. The secretion of TGFβ1 by $CD4^+$ T cells following their coculture with hMSC was significantly higher than that of $CD4^+$ T cells alone (Fig 3.11 C). These data demonstrated that hMSC were capable of induced $CD4^+$ T cells that secreted immunosuppressive cytokines, typical of a regulatory population.

3.9 SOLUBLE FACTORS PLAY NON REDUNDANT ROLES IN MSC INDUCTION OF HUMAN $CD4^+$ $CD25^+$ $FOXP3^+$ T REG-LIKE CELLS

Modulation of allogeneic responses by MSC requires multiple factors. Cell-cell contact and the release of soluble factors play non-redundant roles in MSC immunomodulation, as demonstrated in Fig 3.8, 3.9 and 3.10. Previous studies have shown that Prostaglandin E2 (PGE_2) and TGFβ1 production contribute to the induction of FoxP3 T reg cells (Baratelli, 2005; Fu, 2004). Ryan *et al.* have shown that PGE_2 secreted by MSC was required for modulation of alloantigen driven proliferation in an MLR, while TGFβ1 was up regulated in MSC licensed by IFN-γ (Ryan, 2007).

The influence of prostaglandins and TGFβ1 on hMSC immunomodulation was examined. The production of prostaglandins was ablated using the cyclooxygenase antagonist indomethacin , while TGFβ1 production was neutralised through the addition of a human anti-TGFβ1 antibody. FoxP3 mRNA expression by $CD4^+$ T cells cocultured with hMSC in the presence or absence of neutralising antibody or chemical antagonist was examined by qRT-PCR (Fig 3.12 A), while both FoxP3 and CD25 expression was analysed by intra/extracellular flow cytometry (Fig 3.12 B). The presence of indomethacin or anti-TGFβ alone in cocultures

resulted in the decreased expression of FoxP3 mRNA on $CD4^+$ T cells (Fig 3.12 A). While a combination of indomethacin and anti-TGFβ1 led to a further reduction of FoxP3 mRNA expression on $CD4^+$ T cells to near background levels (Fig 3.12 A).

Similar to the data seen in figure 3.7, hMSC increased the expression of both FoxP3 (6.66%) and CD25 (2.8%) on $CD4^+$ T cells when analysed by flow cytometry. However, following the neutralisation of TGFβ1 or antagonism of prostaglandin production, the expression of FoxP3 (6.07%) and CD25 (0.89%) was decreased on $CD4^+$ T cells after coculture with hMSC (Fig 3.12 B). These data indicated that both prostaglandins and TGFβ1 play non-redundant roles in hMSC induction of $CD4^+$ $CD25^+$ $FoxP3^+$ T reg-like cells. In effect, both cell contact and the subsequent release of soluble factors are required for MSC immunomodulation. The transwell system demonstrated that cell contact was required in the absence of other immune cells, with soluble factors alone insufficient for the induction $CD4^+$ $CD25^+$ $FoxP3^+$ T reg-like population. The neutralisation or antagonism experiments, where cell contact was permitted demonstrated that both prostaglandins and TGFβ1 are the soluble effector molecules involved in hMSC induction of $CD4^+$ $CD25^+$ $FoxP3^+$ T reg-like cells.

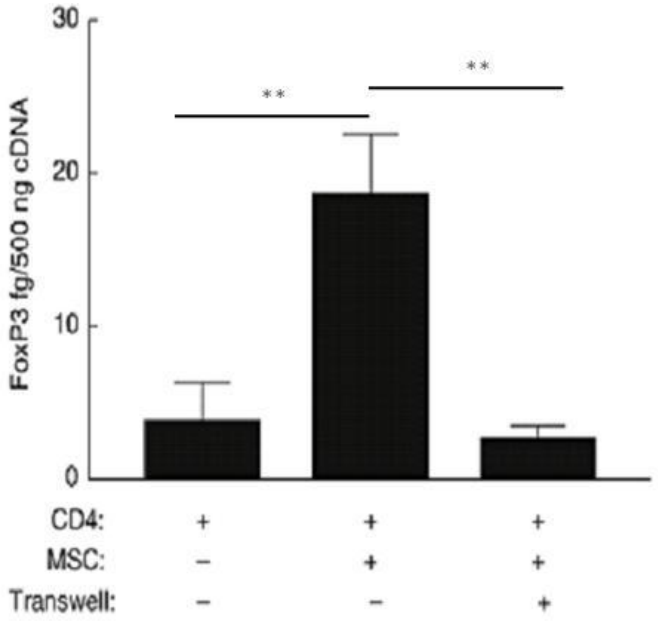

Fig 3.8 Direct cell contact is required for the induction FoxP3 in purified CD4$^+$ T cells. Purified CD4$^+$ T cell (3 x 10^5/well) were cultured in the presence or absence of hMSC (1 x 10^5/well) in a 24 well plate for 24 h. Cell contact was prohibited using a transwell system. The expression of FoxP3 was determined by qRT-PCR. The induction of FoxP3 was significantly less on purified CD4$^+$ T cells when direct cell contact with hMSC was prohibited (transwell) ($p<0.05$). This indicated that direct cell contact was required for FoxP3 induction on CD4$^+$ T cells by hMSC. Statistical analysis was carried out using the student paired t test. Data are representative of three experiments. (The collaboration with Dr. Jennifer Ryan and Dr. Karen English in this experiment is gratefully acknowledged).

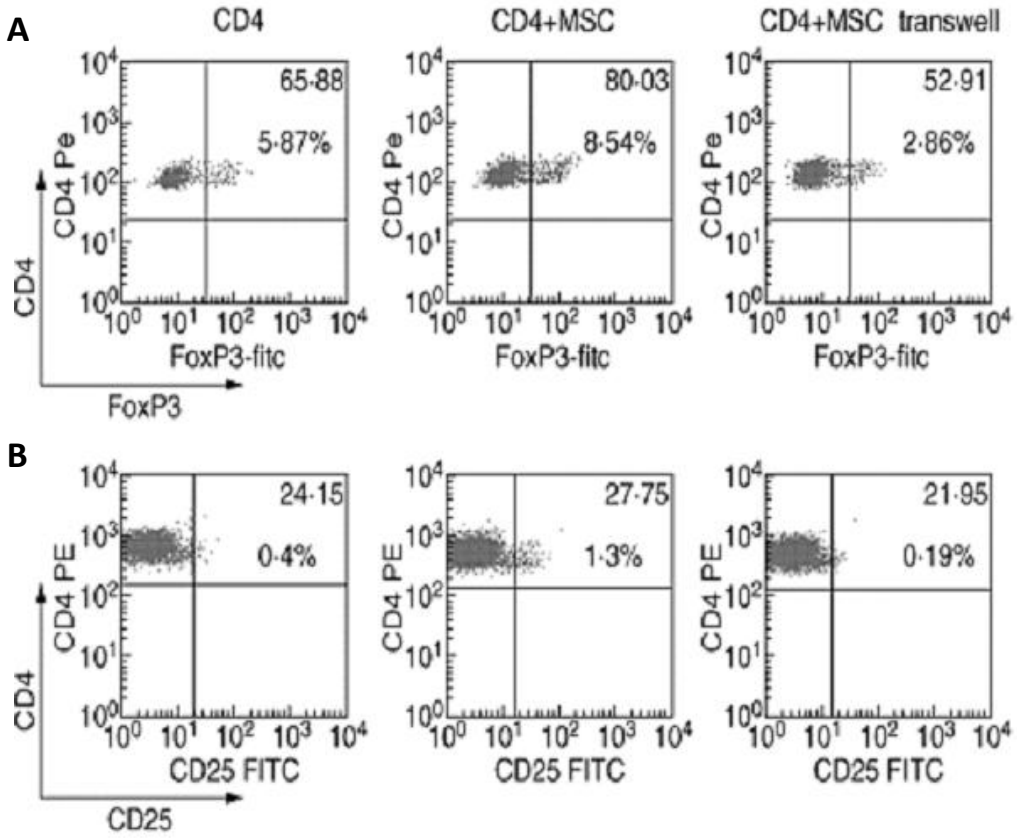

Fig 3.9 Direct cell contact is required for the induction of FoxP3 and CD25 expression on purified CD4$^+$ T cells by allogeneic hMSC. Purified CD4$^+$ T cell (1 x 10^6/well) were cultured in the presence or absence of hMSC (3 x 10^5/well) in a 6 well plate for 72 h. Cell contact was prohibited using a transwell system. Expression of (A) FoxP3 and (B) CD25 were determined by intra/extracellular flow cytometry. FoxP3$^+$ CD25$^+$ expression was increased in cultures when CD4$^+$ T cell and hMSC cell contact was permitted. hMSC did not induce FoxP3$^+$ CD25$^+$ expression on purified CD4$^+$ T cells in cocultures where contact was prohibited (transwell). Cell contact is required for FoxP3$^+$ CD25$^+$ T reg-like cell induction by allogeneic hMSC. Data are representative of three experiments. The percentages of double positive cells (%) and the mean fluorescent intensity are represented in the quadrant. (The collaboration with Dr. Jennifer Ryan and Dr. Karen English in this experiment is gratefully acknowledged).

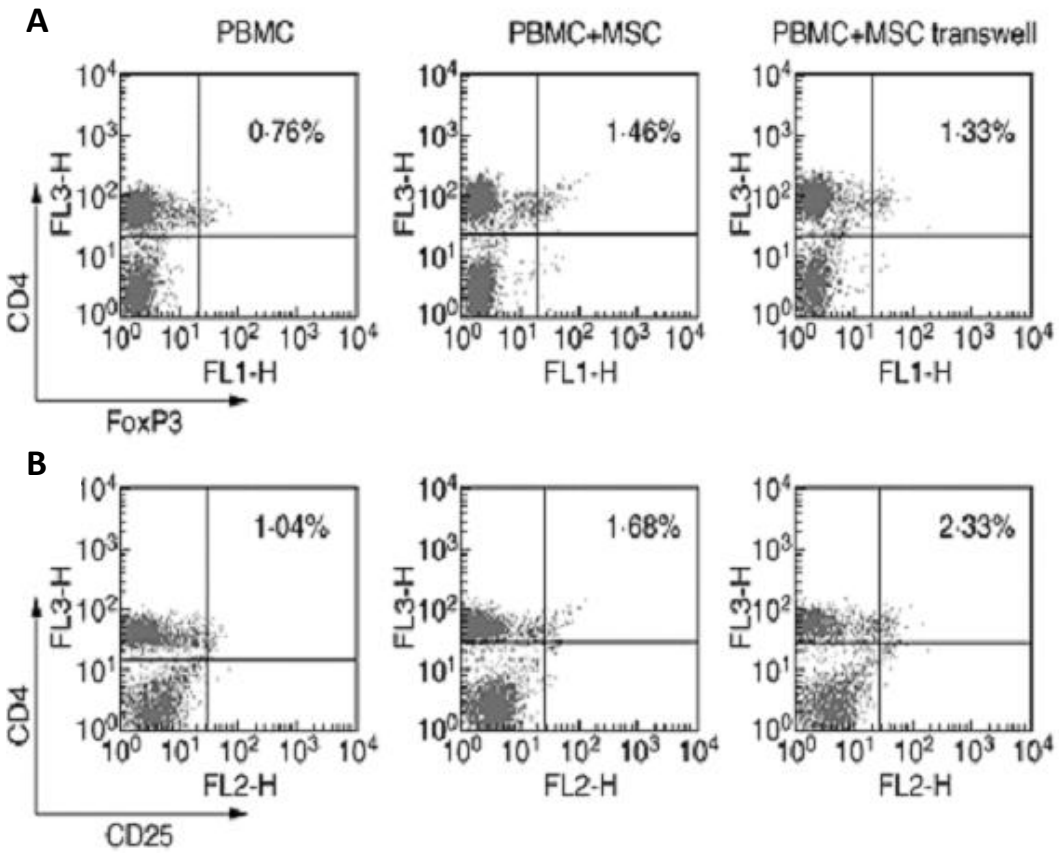

Fig 3.10 Cell contact is not required for the induction of FoxP3 and CD25 expression in a multi-cell system. PBMC (1 x 10^6/well) were cultured in the presence or absence of MSC (3 x 10^5/well) in a transwell system for 72 h. The expression of (A) Foxp3 and (B) CD25 were determined by intra/extracellular flow cytometry. FoxP3 and CD25 expression were increased on PBMC that had direct cell contact with hMSC. Unlike purified $CD4^+$ T cells (Fig 3.8), when cell contact was prohibited between hMSC and PBMC, the expression of FoxP3 and CD25 was not decreased. In the presence of other immune cells, cell contact is not required for allogeneic hMSC induction of $FoxP3^+$ and $CD25^+$ T reg-like cells. Data are representative of three experiments. The percentages of double positive cells are in the upper right quadrant (%). (The collaboration with Dr. Jennifer Ryan and Dr. Karen English in this experiment is gratefully acknowledged).

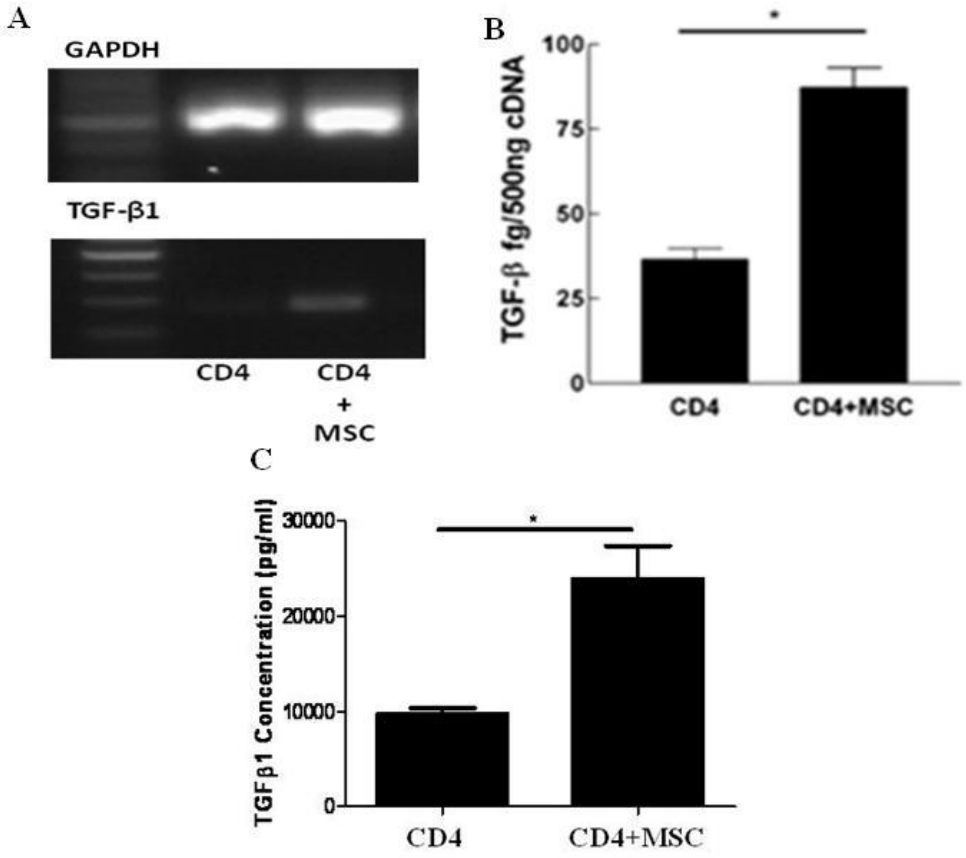

Fig 3.11 Purified $CD4^+$ $CD25^+$ $FoxP3^+$ T cells induced by allogeneic hMSC express Transforming growth factor beta 1 (TGFβ1). $CD4^+$ T cells (1 x 10^6/ml) and hMSC (3 x 10^5/ml) were coculture for 24 h for mRNA analysis and 48 h for cytokine analysis**.** (A) RT-PCR detection of TGFβ1 mRNA and (B) TGFβ1 mRNA by qRT-PCR on $CD4^+$ T cells was examined. The expression of TGFβ1 was significantly higher in $CD4^+$ T cells which were previously cultured in the presence of hMSC ($p<0.001$). (C) The secretion of TGFβ1, an important immunosuppressive cytokine was detected by bead array analysis. Significantly more TGFβ1 was secreted when $CD4^+$ T cells were cocultured with hMSC ($p<0.05$). These data indicated the induction of an immunosuppressive phenotype and environment. Statistical analysis was carried out using the student paired t test. Data are representative of three experiments, performed in triplicate.

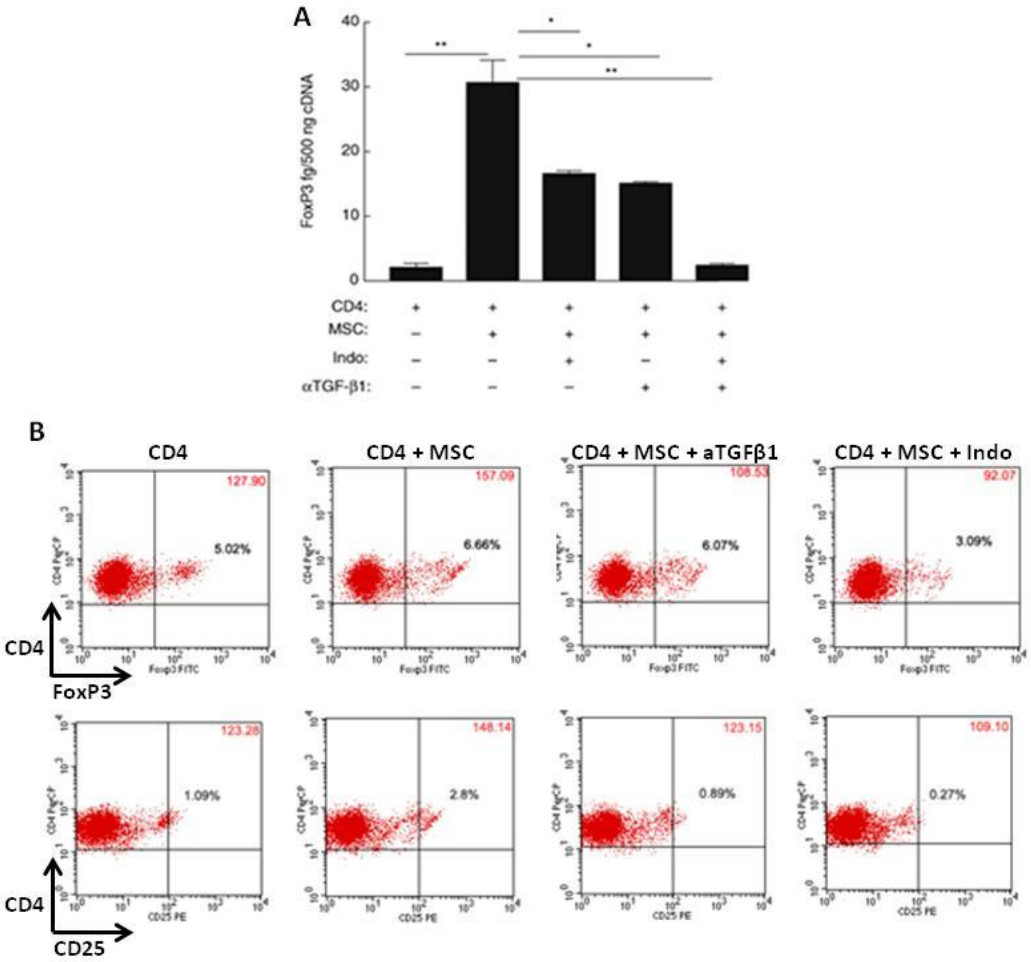

Fig 3.12 Prostaglandins and TGFβ1 play non-redundant roles in MSC induction of CD4$^+$ CD25$^+$ FoxP3$^+$ T cells. Purified CD4$^+$ T cells (1 x10^6/ml) were cultured in the presence or absence of hMSC (3 x10^5/ml) for (A) 24 h or (B) 72 h. The production of prostaglandins was ablated using the cyclooxygenase antagonist indomethacin (indo) (40 µM) and TGFβ1 was neutralised with anti-TGFβ1 (4 µg/ml). (A) FoxP3 mRNA expression was analysed by qRT-PCR after 24 h, while (B) FoxP3 and CD25 protein expression were analysed by intracellular flow cytometry after 72 h. The presence of indomethacin or anti-TGFβ1 in cultures resulted in the (A) decreased expression of FoxP3 mRNA and (B) decreased FoxP3 and CD25 expression by flow cytometry on CD4$^+$ T cells following coculture with hMSC. Data are representative of three experiments. The percentages of double positive cells (%) and mean fluorescent intensity (MFI) are represented in the quadrant. Statistical analysis was carried out using the student paired t test. (The collaboration with Dr. Jennifer Ryan and Dr. Karen English in this experiment is gratefully acknowledged).

3.10 $CD4^+$ $CD25^+$ T CELLS INDUCED BY ALLOGENEIC MSC ARE CONVENTIONAL T REG CELLS

Purified $CD4^+$ $CD25^+$ T cells that encountered hMSC secreted TGFβ1, (Fig 3.10) supporting hypothesis that hMSC-derived signals condition the local tissue environment to promote the induction of T reg cells. The release of immunosuppressive cytokines alone or the expression of CD25 and FoxP3, are not however sufficient in determining whether the $CD4^+$ $CD25^+$ T cells induced by hMSC are conventional T reg cells. To investigate whether hMSC generate functional T reg cells, $CD4^+$ $CD25^+$ T cells induced by coculture with hMSC were repurified and examined for their suppressive activity in an MLR.

Purified $CD4^+$ T cells and allogeneic hMSC were cocultured for 72 h. After 72 h, $CD4^+$ T cells were repurified (isolated) using a CD25 microbead isolation kit, to obtain a $CD4^+$ $CD25^+$ T cell population. These repurified $CD4^+$ $CD25^+$ T cells were then cocultured with PBMC from two MHC mismatched donors in an MLR. The repurified $CD4^+$ $CD25^+$ T cells were found to significantly reduce alloantigen driven proliferation (Fig 3.13). This indicated that the T cell populations induced by allogeneic hMSC could reasonably be described as conventional T reg cells with a functional suppressor function.

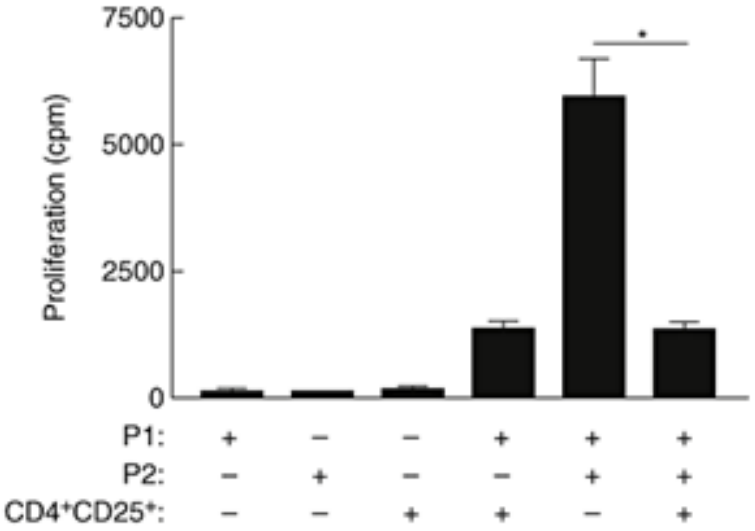

Fig 3.13 Purified CD4$^+$ CD25$^+$ FoxP3$^+$ T cells induced by allogeneic MSC suppress alloresponses. CD4$^+$ CD25$^+$ T cells induced by coculture with MSC were repurified by microbead separation and cocultured with PBMC from two MHC mismatched donors in 96 well plates in an MLR. Repurified CD4$^+$ CD25$^+$ T cells significantly reduced allodriven proliferation in an MLR ($p<0.05$). [^{3}H]-Thymidine incorporation was expressed as counts per minute (cpm). Statistical analysis was carried out using the student paired t test. Data represent triplicates repeated three times. (The collaboration with Dr. Jennifer Ryan and Dr. Karen English in this experiment is gratefully acknowledged).

3.11 SUMMARY

The aim of this chapter was to determine how hMSC suppress innate and adaptive immune responses *in vitro*. First, the effect of complement activation on hMSC survival was analysed. Second, the role for cell contact and the release of soluble factors by hMSC in the induction of a T reg population were investigated. Finally, the induction of functional T reg-like cells by hMSC was examined *in vitro*. hMSC were not destroyed by human or murine complement *in vitro*. These data suggested that, in the case of hMSC therapy in a xenogeneic murine model or in allogeneic human clinical studies, the alternative complement pathway activation might not confound hMSC action. These data will be important when considering hMSC as a cell therapy, as complement is a vital component of innate immunity and involved in hyper-acute transplant rejection. The induction of a T reg-like cell by hMSC was investigated *in vitro*. Allogeneic hMSC cocultured with purified $CD4^+$ T cells resulted in a significant increase in FoxP3. Direct cell contact and hMSC-derived soluble factors, such as TGFβ1 and prostaglandins played non-redundant roles in the induction of $CD4^+$ $CD25^+$ $FoxP3^+$ T reg-like cell. These hMSC induced $CD4^+$ $CD25^+$ $FoxP3^+$ T reg cells in turn, suppressed alloantigen driven proliferation.

The experiments described in this chapter have provided novel insight into hMSC immunomodulation and identifying the mechanisms used by hMSC in the induction of functional T reg cells. TGFβ1 and prostaglandins production were two key soluble factors involved in hMSC mediated modulation. However, this chapter did not identify the possible contact candidates required for the induction of regulatory immune cells. The identification of a contact signal required for successful immunomodulation by MSC would be important in contributing to the rational use of MSC as an immunomodulatory cell therapy in the future.

CHAPTER 4

IDENTIFYING CONTACT DEPENDENT SIGNALS INVOLVED IN MESENCHYMAL STEM CELL MODULATION OF DENDRITIC CELL FUNCTIONS

4.1 INTRODUCTION

In Chapter 3, hMSC induction of T reg cells from purified populations of $CD4^+$ T cells was shown to involve both soluble factors and cell contact dependent signals. Although the identity of the contact signals were not addressed in that chapter, possible candidates have been suggested by others (Djouad, 2007; Zhang, 2009). Theoretically, MSC might influence $CD4^+$ T cells in two ways, through direct cell contact or indirectly via contact with DC. The identity of the direct cell contact signal between murine MSC (mMSC) and $CD4^+$ T cells was pursued by another member of the group and was not explored here. However, the ability of mMSC to interfere with DC maturation, antigen presentation and induction of regulatory/ tolerogenic DC was examined in this chapter.

DC are the most potent antigen presenting cell (APC), involved in antigen uptake, and processing for presentation to naïve $CD4^+$ T cells (Banchereau, 2000). For the purpose of this study, murine bone marrow derived DC were used, as the use of human DC was not possible due to limited availability of DC and $CD4^+$ T cells from the same HLA background. The aims of this chapter were:

a) To determine if mMSC modulate DC function *in vitro*, by interfering with DC maturation, antigen presentation or the release of IL-10 and IL-12p70.
b) To investigate and identify the potential cell contact signals contributing to mMSC interaction with DC.

Potential mMSC ligands were analysed for their role in DC maturation and/or antigen presentation. Following this, likely candidates were neutralised or blocked

in coculture studies between mMSC and DC and their precise roles in DC maturation and/or antigen presentation were determined.

4.2 CHARACTERISATION OF ADULT MURINE MSC

In order to examine the DC MSC interaction it was necessary to switch to murine systems. This was due to the limitations on DC isolation, batch size/reproducibility and the need for $CD4^+$ T cells from the same donor. Therefore, mMSC were used and required similar characterisation as carried out in Chapter 3. mMSC were isolated from the femurs and tibiae of BALB/c or C57 BL/6 female mice, using plastic adherence and selective media, as described in section 2.3.1. At each passage, mMSC were examined microscopically for changes in appearance. A homogenous population of mMSC was evident from passage 3 to 8 with fibroblastic, spindle-shaped morphology (Fig 4.1). There was no evidence of spontaneous differentiation in these cultures. Batches of mMSC were characterised by flow cytometry after every passage analogous to work in chapter 3. The expression of Sca-1 and CD44 and the lack of expression of CD45 and CD11b were used to characterise a population of mMSC (Peister, 2004; Horwitz, 2005). mMSC isolated by other groups typically express variable levels of Sca-1, CD106 and CD44, with no expression of CD11b, CD34, CD45, CD48, CD117 or CD135 (Baddoo, 2003). Isolated cells at passage 3 expressed MHC class I, Sca-1 and CD44,but not the haematopoietic markers CD45, CD11b, CD34, MHC class II or the haematopoietic progenitor cell marker CD117 (Fig 4.2). Subsequent culturing of mMSC to passage 8 resulted in increased expression of MHC class I, Sca-1, CD44 and CD106. Cells expressing CD45, CD11b, CD34, CD117 or MHC class II were not observed at any passage between 3 and 8 (Fig 4.3).

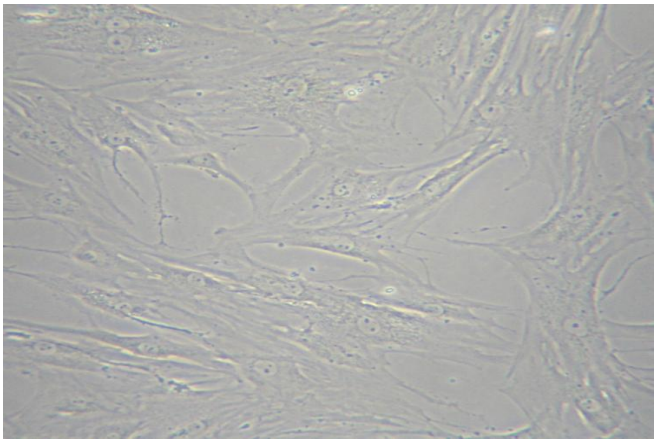

Fig 4.1 mMSC have a fibroblastic morphology. mMSC were isolated from BALB/c or C57 BL/6 mice. mMSC were adherent to plastic and cultured to 80-90% confluency. Morphology was examined using phase contrast microscopy from passage 3-8. Image above represents typical cells from passage 5. Original magnification × 100.

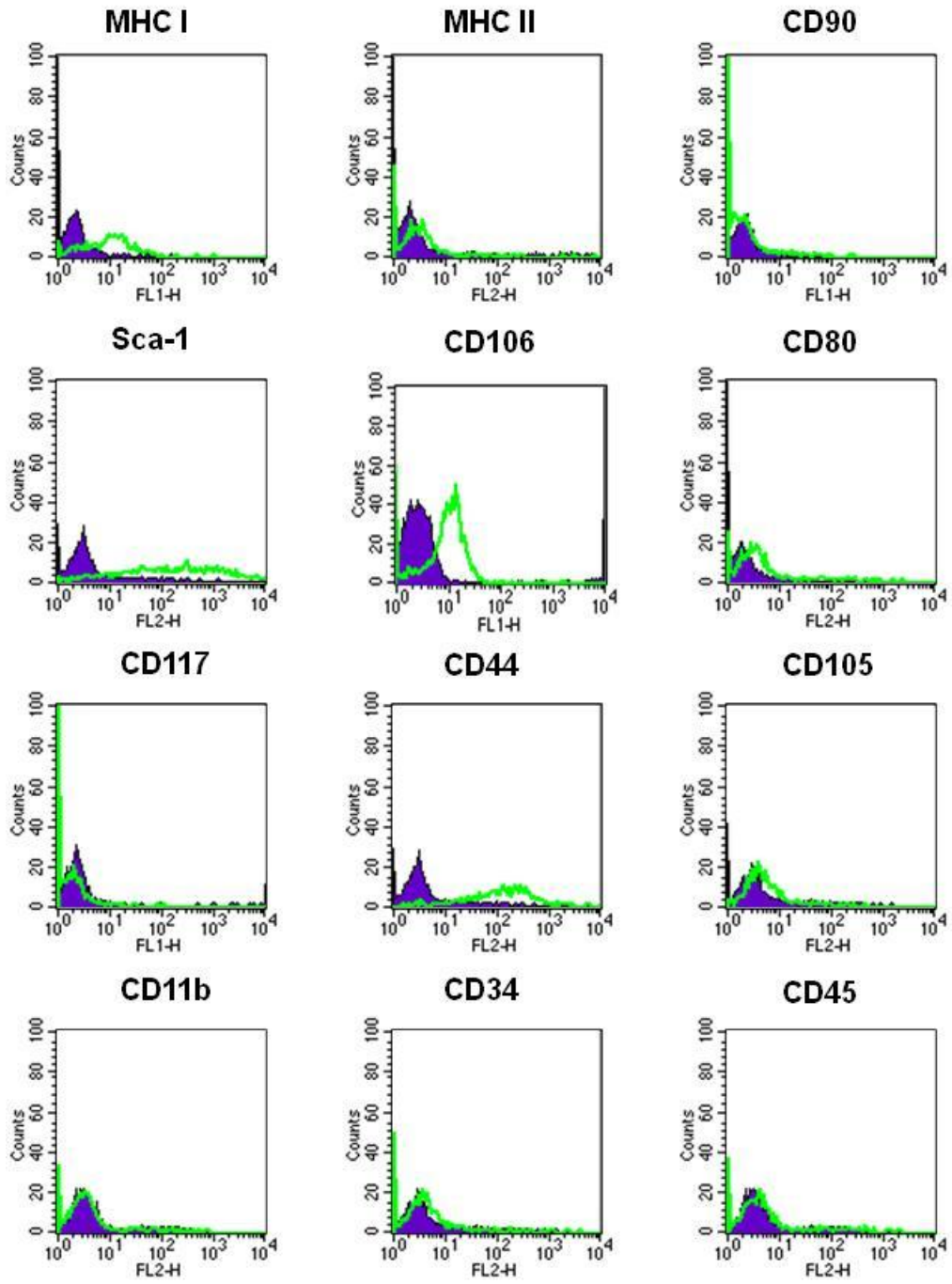

Fig 4.2 Surface marker expression by mMSC. mMSC isolated by adherence to plastic from BALB/c or C57 BL/6 mice expressed MHC class I, Sca-1, CD106 and CD44, but not MHC II, CD117, CD34, CD11b, CD45 or CD80 at passage 3. Cultured MSC were characterised by flow cytometry for expression of a panel of markers (open histogram-green) and corresponding isotype controls (closed histogram-purple). A minimum of 10,000 events were acquired for each marker.

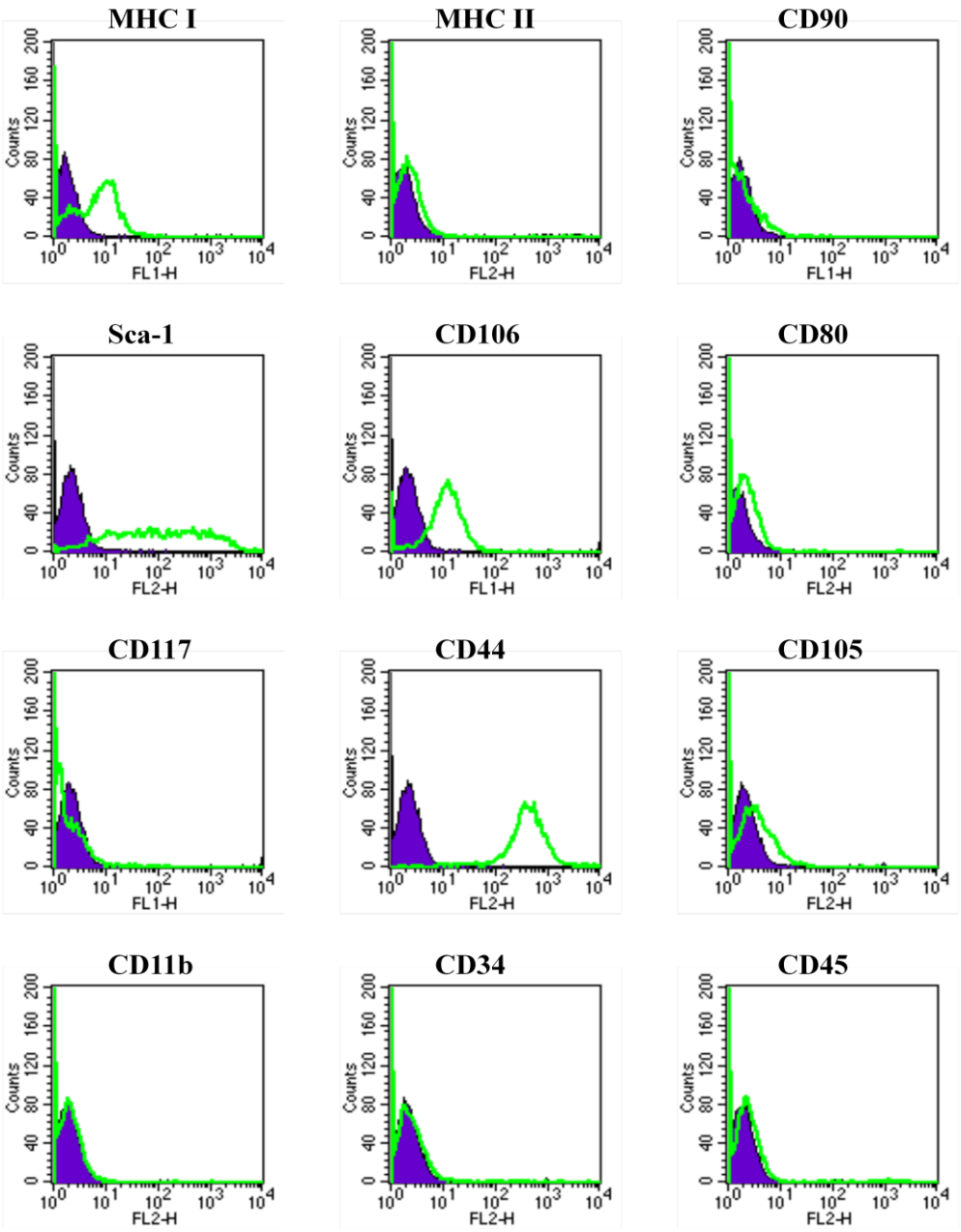

Fig 4.3 mMSC surface marker expression at later passages. MSC isolated by adherence to plastic from BALB/c or C57 BL/6 mice expressed MHC class I, Sca-1, CD106 and CD44, but not CD117, CD34, CD11b, CD45 or CD90 at passage 8**.** MSC were characterised by flow cytometry for expression of a panel of markers (open histogram-green) and corresponding isotype controls (closed histogram-purple). A minimum of 10,000 events were acquired for each marker.

4.3 mMSC Show Trilineage Differentiation Capacity

The capacities of the mMSC used in this study to differentiate to osteoblasts, adipocytes or chondrocytes were examined. mMSC were cultured in the presence or absence of differentiation factors as described in Table 2.1. mMSC were then stained with reagents to identify differentiated cells (Section 2.7 & Table 2.2). Osteoblasts were detected using Alizarin Red S (Fig 4.4 B), adipocytes by staining with Oil Red O (Fig 4.4 D) and chondrocytes were assessed by the expression of Aggrecan, a proteoglycan found in the extracellular matrix of cartilage by RT-PCR (Fig 4.4 E). mMSC maintained their tri-lineage differentiation capacity through passage 3 to 8 (Fig 4.4). These data confirmed the multilineage potential associated with mMSC. Together with the data from figure 4.2 and 4.3, this suggested that the cells used in this study were typical mMSC according to the ISCT criteria (Horwitz, 2005).

4.4 mMSC Suppress Allogeneic Proliferation

The ability of MSC to suppress lymphocyte proliferation is important when characterising the validity of a population of MSC, according to ISCT regulations. Previous members of the Mahon group examined MSC suppression of lymphocyte proliferation (Ryan, 2007; English, 2008). However, it was important to verify this characteristic for each new batch of mMSC isolated. Therefore, the immunosuppressive ability of mMSC isolated for the purpose of the studies herein was first analysed using mitogen driven proliferation assay. Splenocytes from C57BL/6 (H-2^b) mice were cultured in the presence or absence of allogeneic BALB/c (H-2^d) mMSC or in the presence of a mitogen concanavalin A (ConA). As expected, mitogen stimulation induced a significant increase in splenocyte

proliferation, whereas the presence of allogeneic mMSC significantly inhibited proliferation ($p<0.0001$) (Fig 4.5 A). This result indicated that allogeneic mMSC were capable of potent immunosuppression of lymphocyte proliferation.

mMSC possess the ability to suppress alloreactivity (Djouad, 2003). To verify this, mMSC were included in a two-way mixed lymphocyte reaction (MLR). Splenocytes from C57BL/6 ($H\text{-}2^b$) (D1) and FV/BN ($H\text{-}2^q$) (D2) mice were cocultured in the presence or absence of (third party) allogeneic BALB/c ($H\text{-}2^d$) mMSC (Fig 4.5 B). Coculture of allogeneic splenocytes resulted in proliferation, however, this was significantly suppressed in the presence of mMSC ($p<0.0182$) (Fig 4.5 B). mMSC are slow growing cells and do not proliferate in the time course of this experiment. These data indicated that the mMSC populations isolated were capable of suppressing both mitogen driven and alloantigen driven proliferation.

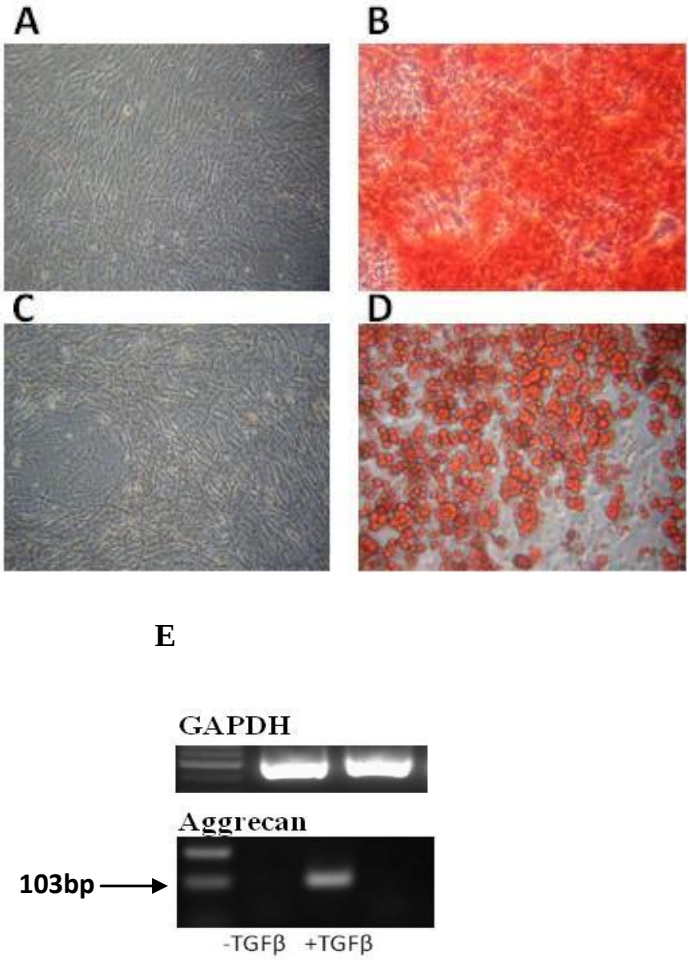

Fig 4.4 mMSC differentiated along the osteogenic, adipogenic and chondrogenic lineages. mMSC were seeded at a density of 1 x 10^3cells/cm^2 and cultured in (A & C) complete αMEM media, (B) osteogenic induction media or (D) adipogenic induction media for 21 days. (B) Osteogenesis was assessed using Alizarin Red S. (D) Adipogenesis was visualised by staining cells with Oil Red O. Magnification x 100 using phase contrast microscopy. (E) Chondrogenic differentiation was determined by RT-PCR for the expression of the proteoglycan aggrecan. mMSC expressed Aggrecan following 21 days of culture in differentiation complete αMEM media containing TGFβ3. mMSC did not spontaneously differentiate into osteocytes, adipocytes or chondrocytess when cultured for 21 days in complete αMEM media without differentiation components. The above data represent passage 5. Collectively, these data are representative of the differentiation capacity of mMSC from passage 3 to 8.

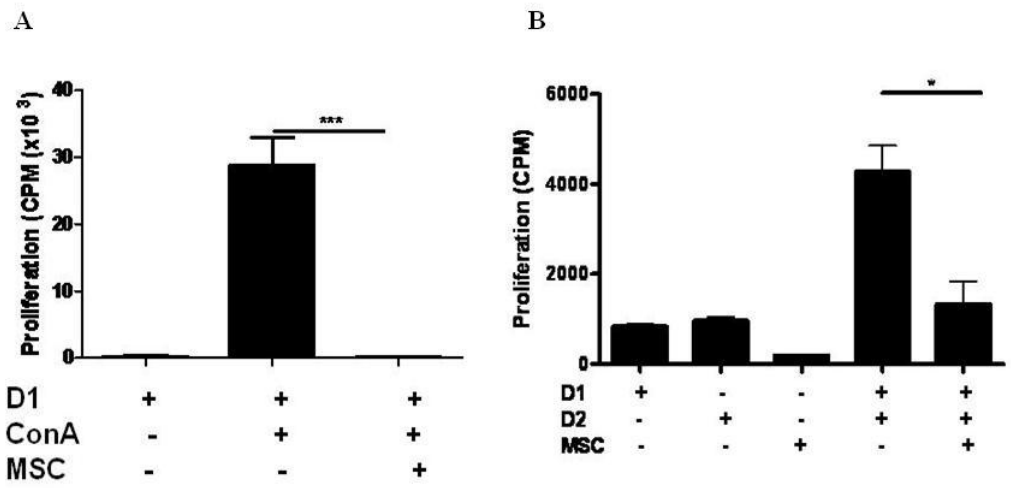

Fig 4.5 Allogeneic mMSC inhibit mitogen driven and alloantigen driven proliferation. BALB/c ($H2^d$) mMSC (passage 5) were examined for their capacity to inhibit (A) mitogen driven (ConA) proliferation of C57BL/6 ($H2^b$) splenocytes and (B) alloantigen driven proliferation of MHC-mismatched donor mice (C57BL/6 ($H2^b$)) (D1) and FV/BN ($H2^q$) (D2)) splenocytes. mMSC (1 x 10^5/ml) and splenocytes (1 x 10^6/ml) were cocultured for 72 h. [^{3}H]-Thymidine at 0.5 µCi/ml was added for the final 6 h of culture. Cells were harvested using an automated cell harvester. (A) mMSC significantly inhibited mitogen driven lymphocyte proliferation ($p<0.0001$). (B) mMSC significantly suppressed allo-driven proliferation ($p<0.0182$). Statistical analysis was carried out using the student paired t test. Results are representative of three independent experiments for each passage of mMSC from 3 to 8.

4.5 MURINE MSC PREVENT LPS DRIVEN DC MATURATION

The transition from immature to mature DC is characterised by a number of changes, including the increased secretion of IL-12 and the increased expression of MHC class II and costimulatory molecules. Bone marrow derived DC were stimulated with LPS in the presence or absence of allogeneic mMSC for 48 h. After 48 h, the expression of MHC class II and the costimulatory molecule CD86 were analysed on DC by flow cytometry (Fig 4.6 A). Supernatants from these cultures were collected at 48 h and cytokine secretion was analysed by ELISA (Fig 4.6 B).

Maturation of DC with LPS for 48 h resulted in an increase in maturation marker expression, both MHC class II (3405 MFI) and CD86 (1222 MFI) by flow cytometry (Fig 4.6 A). However, mMSC coculture prevented the increase in MHC class II (2636 MFI) and CD86 (815 MFI) expression (Fig 4.6 A). DC that had been stimulated with LPS for 48 h secreted elevated levels of IL-12p70 and lower levels of IL-10 (Fig 4.6 B) as has been previously reported (English, 2008). Following coculture with mMSC, DC secreted significantly less IL-12p70 ($p<0.0001$) and significantly more IL-10 ($p<0.0001$) (Fig 4.6 B). mMSC did not secrete IL-12p70 suggesting that this was a direct influence on DC. However, mMSC secrete low levels of IL-10 and this could contribute to the elevated levels of IL-10 present in coculture supernatant (Fig 4.6 B). These data suggested that mMSC disrupt the maturation of DC, preventing the upregulation of MHC class II and CD86 expression, in conjunction with a decrease in IL12-p70 production and an increase in IL-10 production. These data are consistent with a hypothesis suggesting that mMSC keep DC in a semi-mature or tolerogenic state.

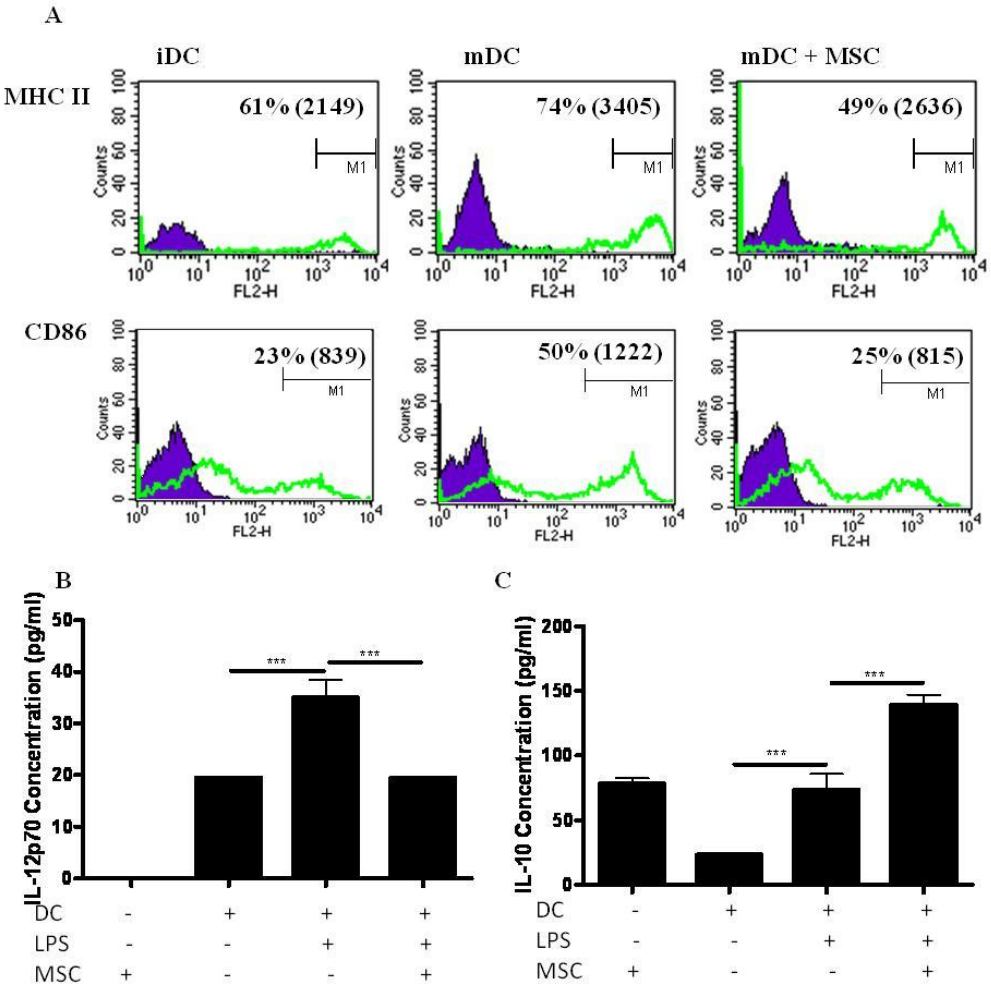

Fig 4.6 mMSC prevent LPS driven DC maturation. Immature DC (iDC) were stimulated with LPS (100 ng/ml) (mDC) and cultured in the presence or absence of mMSC for 48 h. DC were analysed by flow cytometry for the expression of maturation markers, (A) MHC class II and CD86 or by ELISA of culture supernatant for (B) IL-12p70 or (C) IL-10. (A) mDC were separated from adherent mMSC by gentle aspiration after 48 h for flow cytometry. Percentage positive and mean fluorescence intensity (MFI) represented on histogram. Isotypes are shown as closed histograms (purple), while specific marker expressions are represented as open histograms (green). Data are representative of three independent experiments. Supernatants were collected after 48 h for cytokine analysis by ELISA. (B) mMSC significantly ($p<0.0001$) decreased the production of IL-12p70 by DC, while (C) significantly ($p<0.0001$) increasing the production of IL-10. Statistical analysis was carried out using the student paired t test. Data are representative of three experiments each performed in triplicate.

4.6 mMSC INDUCE A TOLEROGENIC DC

Presentation of antigen in the presence of costimulation by DC is critical for the activation of naïve $CD4^+$ T cells. In the event of antigen presentation in the absence of costimulation, clonal T cell anergy or apoptosis can occur (Schwartz, 1989). Tolerogenic DC are said to be resistant to maturation, with low levels of MHC II and costimulatory molecule expression, low production of IL-12p70, high production of IL-10, impaired T cell activation and increased ability to generate alloantigen specific T reg cells (Morelli, 2007). To examine this and in a bid to strengthen the data above, the effect of mMSC on antigen presentation by DC was analysed by flow cytometry, measured by the display of I-Eα peptide. The YAe antibody used recognises the I-Eα peptide but only when displayed by the $I\text{-}A^b$ MHC class II molecule of C57/BL6 DC. C57/BL6 DC express $I\text{-}A^b$ but not I-E and cannot constitutively express the I-Eα: $I\text{-}A^b$ MHC class II trimeric complex (Murphy, 1992).

DC isolated from C57BL/6 bone marrow were pulsed with I-Eα peptide for 48 h. Antigen displayed by DC was recognised through the addition of fluorescently labelled YAe antibody and analysis by flow cytometry (Fig 4.7 A). DC pulsed with the I-Eα peptide were capable of displaying specific I-Eα antigen (90%). However, following coculture with mMSC, DC were unable to display the antigen at high levels (42%) (Fig 4.7 A), suggesting that mMSC prevented or impaired the presentation of alloantigen by DC.

mMSC cocultured with DC prevented the increase of maturation markers, MHC class II and CD86, keeping the DC in a semi-mature state (Fig 4.6 A). However, in order to describe these DC as tolerogenic, they must be less capable of supporting T cell proliferation. It was therefore necessary to demonstrate that DC

encounter with mMSC resulted in the induction of a DC population impaired for that function. The approach to demonstrate such a "tolerogenic function" involved a two-step design. First, DC were pulsed with antigen, ovalbumin (OVA), in the presence or absence of mMSC. The DC were then repurified and cocultured with OVA antigen specific $CD4^+$ T cells isolated from DO11.10 mice. If the DC population were tolerogenic, the hypothesis was that T cell proliferation would be impaired. To examine this hypothesis, C57BL/6 mMSC were cocultured with BALB/c DC pulsed with OVA for 48 h. Then, DC were repurified from adherent mMSC by gentle aspiration and placed into fresh culture with DO11.10 isolated $CD4^+$ T cells, which carry a transgenic T cell receptor specific for OVA peptide 323-339, for a further 72 h. As expected, OVA pulsed DC were capable of supporting DO11.10 $CD4^+$ T cell proliferation (Fig 4.7 B). However, DC pulsed with OVA in the presence of mMSC were subsequently unable to stimulate $CD4^+$ T cell proliferation (Fig 4.7 B). This was a striking finding given that each T cell in this population was specific for the antigen employed. A fully functional mMSC was required for the induction of a tolerogenic DC, as OVA pulsed DC in presence of formalin fixed MSC (fMSC) retained the capacity to support $CD4^+$ T cell proliferation (Fig 4.7 B). Thus it is reasonable to conclude that mMSC induced a genuinely tolerogenic DC population that was unable to classically support the proliferation of antigen specific $CD4^+$ T cells *in vitro*.

A YAe Detection

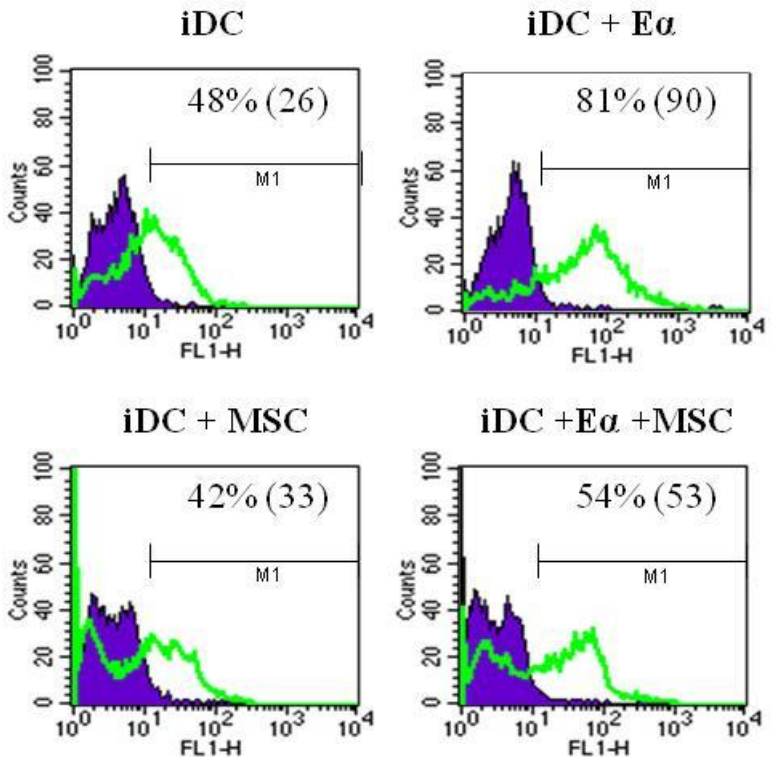

B

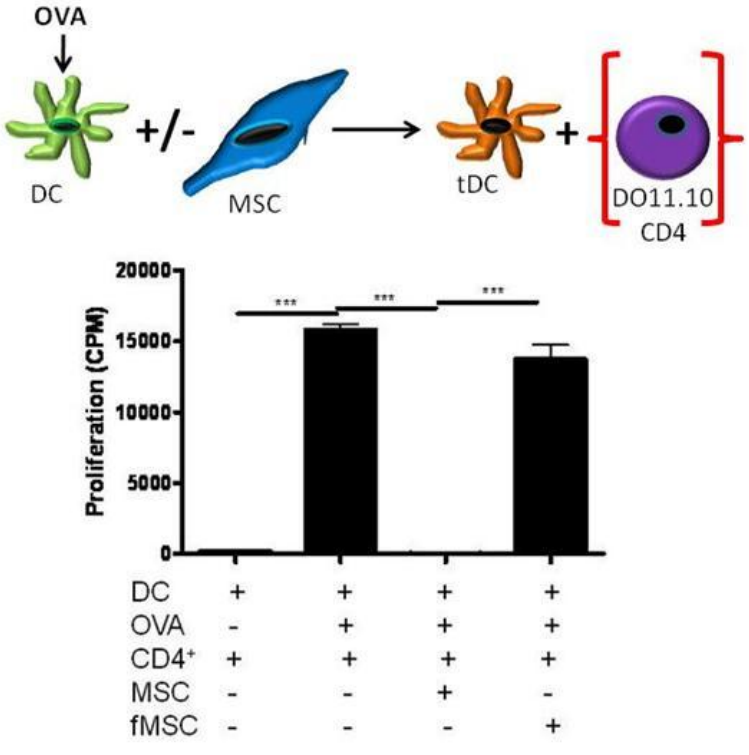

Fig 4.7 mMSC interfere with antigen presentation by DC, inducing a tolerogenic DC. (A) iDC alone or iDC pulsed with Eα peptide (10 μg/ml) in the presence or absence of mMSC were labelled with biotinylated YAe antibody, followed by streptavidin-FITC and analysed by flow cytometry. mMSC reduced the presentation of I-Eα peptide by iDC. (B) iDC that were previously pulsed with OVA in the presence or absence of mMSC or formalin fixed mMSC (fMSC) for 48 h were repurified and cocultured with OVA specific DO11.10 $CD4^+$ T cells for 72 h. Proliferation through ^3H Thymidine incorporation was measured. DC pulsed with OVA supported proliferation of DO11.10 $CD4^+$ T cells ($p<0.0001$). DC pulsed with OVA in the presence of mMSC significantly reduced ($p<0.0001$) the proliferation of DO11.10 $CD4^+$ T cells *in vitro*. Fully functional mMSC were required for the induction of a tolerogenic DC, as fixed mMSC (fMSC) did not interfere with the presentation of antigen by DC. Statistical analysis was carried out using the student paired t test. Data are representative of three experiments performed in triplicate.

4.7 DIRECT CELL: CELL CONTACT BETWEEN MSC AND DC IS REQUIRED FOR THE INDUCTION OF A "SEMI-MATURE" DC *IN VITRO*

The need for direct cell: cell contact between MSC and immune cells has remained unclear to date. Many groups suggest that MSC require direct cell contact with its target cell while others suggest otherwise (Beyth, 2005; Jiang, 2005; Nauta, 2006; Djouad, 2007). Therefore, the need for direct cell contact between mMSC and DC for maturation inhibition was examined. A similar approach to that carried out in Chapter 3 was employed. Using a transwell system, the direct cell contact between mMSC and DC was prohibited. Similar to data shown in Figure 4.6 A, when direct cell contact between mMSC and DC was permitted, mMSC successfully prevented the maturation of DC inducing a semi-mature population, as indicated by low levels of MHC class II (1083 MFI) and CD86 (815 MFI) expression (Fig 4.8). However, when direct cell contact was prohibited using the transwell system, mMSC no longer prevented DC maturation as an increase in maturation marker expression was observed(MHC II (1663 MFI)and CD86 (1320 MFI)), indicating successful DC maturation (Fig 4.8). This finding showed that in order for mMSC to induce a semi-mature DC population direct cell contact between the two cell populations was required. This finding encouraged the investigation into identifying possible cell contact molecules involved in this immune modulation by mMSC on DC maturation.

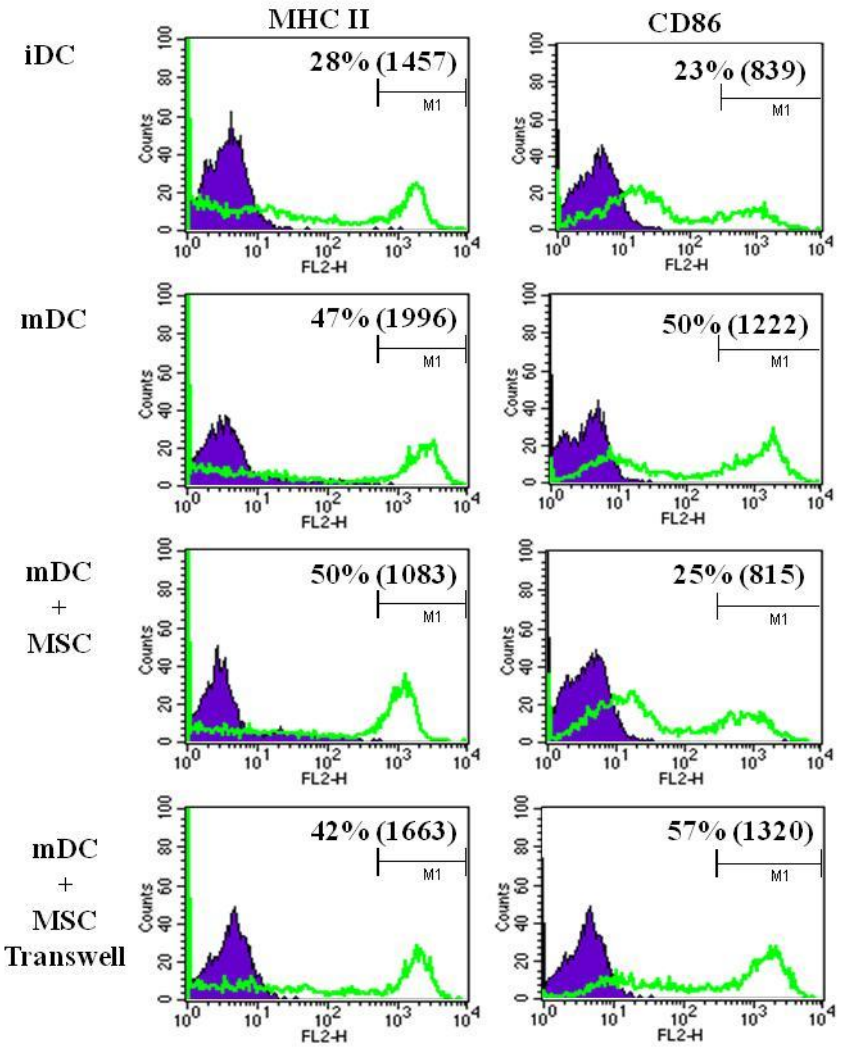

Fig 4.8 Direct cell contact between mMSC and DC is required for the induction of a semi-mature DC population. DC (1 x 10^6/well) matured with LPS (100 ng/ml) (mDC) displayed increased MHC class II and CD86 expression after 48 h by flow cytometry. DC matured in the presence of mMSC (3 x 10^5/well) had decreased levels of MHC class II and CD86 expression, indicating a semi-mature phenotype. When direct cell contact was prohibited in a transwell system, mMSC were unable to interfere with the maturation of DC and no longer induced a semi-mature phenotype. Percentage of cells and mean fluorescence intensity (MFI) is indicated in each histogram. Data are representative of three experiments.

4.8 EXAMINATION OF CANDIDATE CONTACT SIGNALS: CD33-RELATED SIGLEC EXPRESSION BY MURINE MSC

After identifying the need for direct cell contact between mMSC and DC, the following sections investigated the roles of possible contact molecules involved in mMSC modulation of DC maturation. Siglecs were the first candidate investigated. Siglecs are a family of type-1 sialic-acid binding immunoglobulin-like lectins that are involved in immune cell: cell interactions and regulate the function of cells in both the innate and adaptive immune systems through glycan recognition (Crocker, 2007) (Chapter 1.6.1). CD33-related Siglecs also play a role in the regulation of cellular proliferation and differentiation during immune responses (Crocker, 2003). Therefore, Siglecs were a credible candidate signal used by mMSC in immune modulation.

To determine if mMSC expressed Siglecs, a semi-quantitative molecular approach to measure the CD33-related Siglecs E, F, G and H was followed (Fig 4.9). Tissues known to express Siglec E and H (splenocytes), F (bone marrow) or G (bone marrow & splenocytes) were used as positive controls to optimise the conditions required for RT-PCR. The optimum annealing temperatures for the detection of Siglec expression were Siglec E 62°C; Siglec H, 58°C; Siglec F, 60°C; and Siglec G, 60°C. All further RT-PCR analyses were carried out using these optimised temperature conditions.

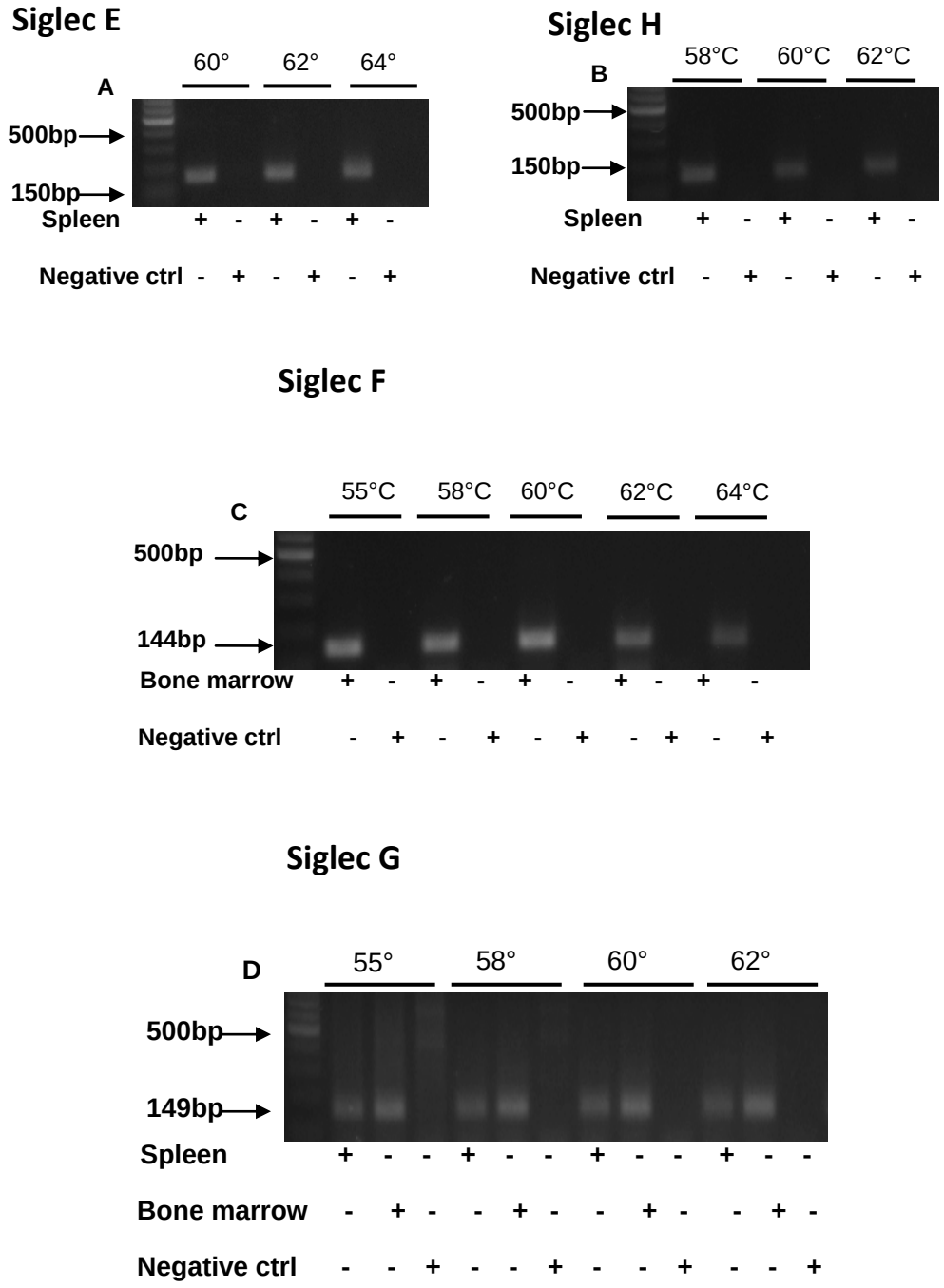

Fig 4.9 Optimisation of Siglec primers. Primers for (A) Siglec E, (B) Siglec H, (C) Siglec F and (D) Siglec G were optimised for RT-PCR using temperature gradients ranging from 55°C to 64°C. (A) Siglec E optimal temperature was 62°C, (B) Siglec H optimal temperature was 58°C, (C) Siglec F optimal temperature was 60°C and (D) Siglec G optimal temperature was 60°C. Spleen derived cells were used as a positive control for (A) Siglec E, (B) Siglec H and Siglec G (D). Bone marrow cells were used as a positive control for both (C) Siglec F and (D) Siglec G.

4.9 CD33-Related Siglecs Are Not Expressed By Murine MSC

The expression of CD33-related Siglecs on unstimulated or stimulated mMSC was examined. IFNγ or prolactin were chosen as stimulants as prolactin induces (chondrogenic) differentiation of bone marrow derived MSC (Ogueta, 2002), whereas IFNγ induces increased immunosuppressive activity by MSC both *in vitro* and *in vivo* (English, 2007; Ryan, 2007; Polchert, 2008). After stimulation with or without prolactin or IFNγ for 24 h, the expression of CD33-related Siglecs on mMSC or unstimulated mMSC were analysed by RT-PCR. mRNA for CD33-related Siglecs were not detectable on unstimulated or stimulated mMSC after 24 h (Fig 4.10). Reagents for murine Siglecs are not well developed but the expressions of Siglec E and H were also analysed by flow cytometry after stimulation with or without prolactin or IFNγ for 24 h. Stimulated and unstimulated mMSC did not express Siglec H or Siglec E by flow cytometry (Fig 4.11). Thus, mMSC did not appear to express the CD33 family of Siglecs, suggesting that mMSC expression of Siglecs is not the contact dependent signal.

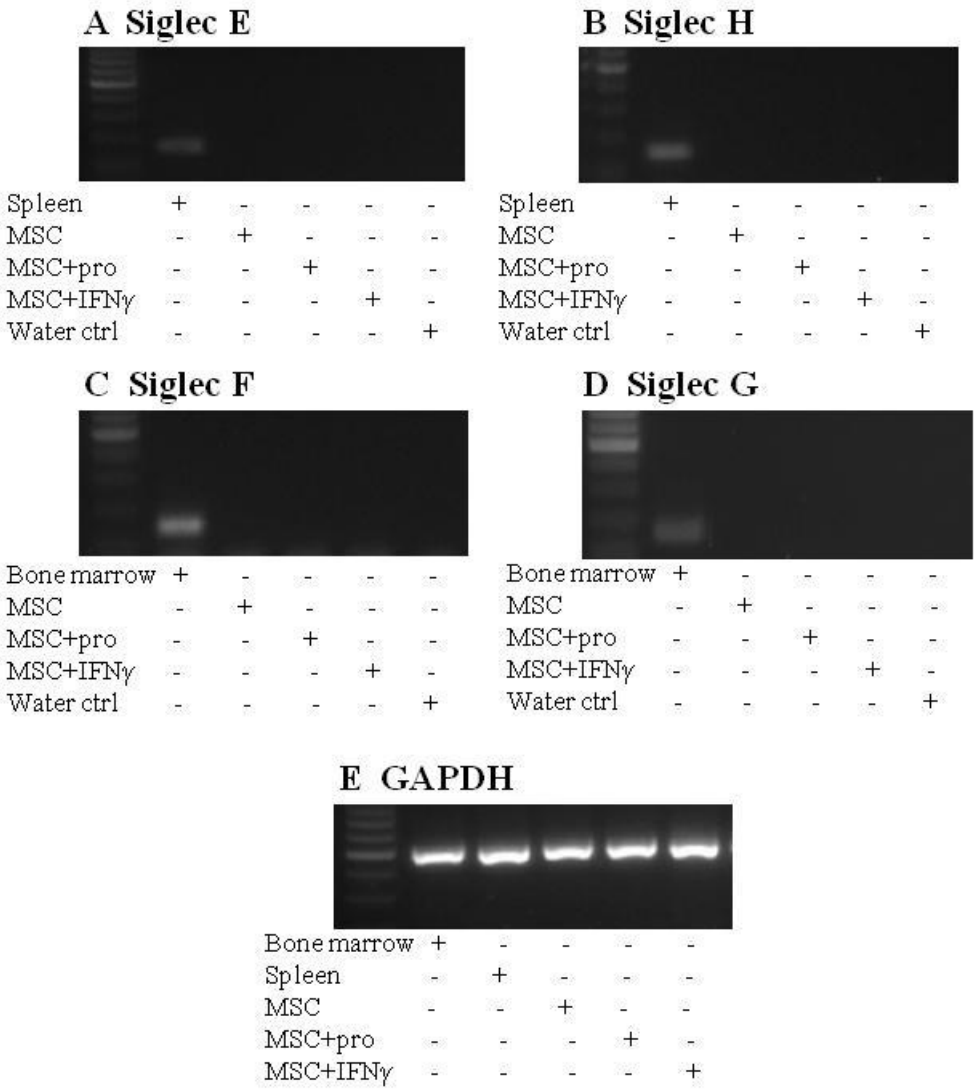

Fig 4.10 CD33-related Siglecs are not expressed by mMSC. Optimised primers were used to determine the expression of (A) Siglec E (62°C), (B) Siglec H (58°C), (C) Siglec F (60°C) and (D) Siglec G (60°C) on mMSC and mMSC stimulated with prolactin (50 ng/ml) or IFNγ (50 ng/ml) after 24 h. RT-PCR analysis showed that CD33-related Siglecs are not expressed by MSC. Housekeeper gene expression, (E) GAPDH, used as a positive control for cDNA synthesis.

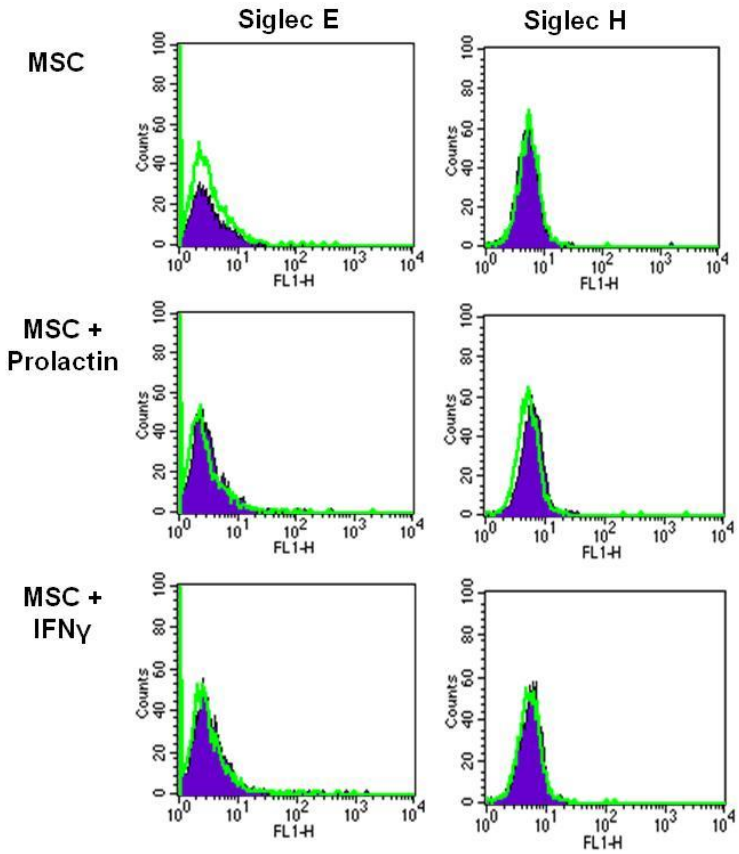

Fig 4.11 MSC do not express Siglec E or H. Siglec E and H expression were analysed by flow cytometry on (A) mMSC alone or mMSC stimulated with (B) prolactin (50 ng/ml) or (C) IFNγ (50 ng/ml) for 24 h. Unstimulated mMSC and stimulated mMSC did not express Siglec E or H. Isotype controls are represented by filled purple histograms, while cell specific markers by open green histograms. Data are representative of three experiments.

4.10 REGULATORY MOLECULE EXPRESSION BY MMSC AND BONE MARROW DERIVED DC

As mMSC did not appear to express CD33 related Siglecs, the expression of other regulatory molecules were examined. In the first instance, the B7 family of receptors and ligands: CTLA-4, ICOS and PD-1, were examined as these are involved in the activation, regulation and inhibition of immune cell responses (Amarnath, 2010; Alegre, 2001; Herman, 2004; Latchman, 2001; Nishimura, 2001). The expression of B7 family receptors and ligands were examined on both mMSC and DC by RT-PCR.

mMSC were stimulated with prolactin, TNFα or IFNγ for 24 h and the expression of CTLA-4, ICOS, LICOS, PD-1 and PDL-1 on mMSC were determined by RT-PCR and qRT-PCR (Fig 4.12 A & B). Unstimulated mMSC did not express CTLA-4, ICOS or PD-1 receptors, but appeared to express the ligands LICOS and PDL-1 (Fig 4.12 A). Upon further investigation by qRT-PCR, mMSC did not express LICOS or PDL-1 (Fig 4.12 A). However, stimulation of mMSC with IFNγ resulted in the up regulation of PDL-1 expression (Fig 4.12 A & B).

Bone marrow derived DC were isolated from C57BL/6 mice and matured in the presence of LPS for 24 h. The expression of ICOS, LICOS, PD-1 and PDL-1 was analysed by qRT-PCR (Fig 4.13 A & B). Immature DC (iDC) and mature DC (mDC) expressed similar levels of LICOS and PDL-1, while ICOS and PD-1 receptor expression was increased following maturation with LPS (Fig 4.13 B). The data herein suggested that the B7 family receptors and ligands were possible candidates for cell contact dependent immune cell modulation by mMSC and DC.

A

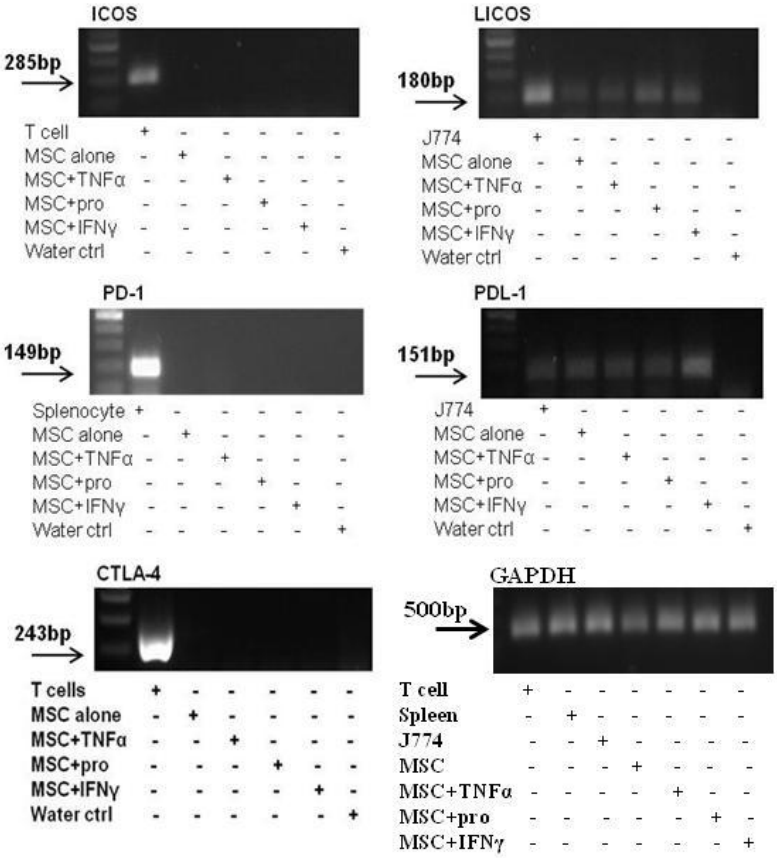

B

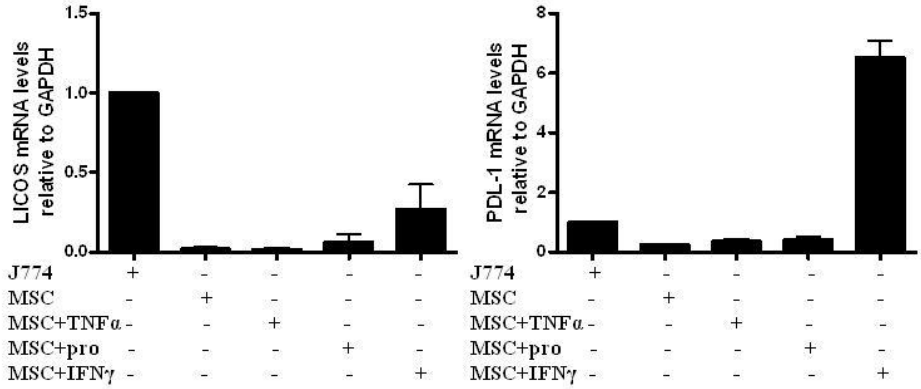

Fig 4.12 mMSC express LICOS and PDL-1. mMSC were stimulated with TNFα (50 ng/ml), prolactin (50 ng/ml) or IFNγ (50 ng/ml) for 24 h. (A) The expression of regulatory molecules, CTLA-4, ICOS, LICOS, PD-1 and PDL-1 were analysed by RT-PCR. mMSC did not express CTLA-4, ICOS and PD-1 receptors, but did express LICOS and PDL-1. (B) The expression of LICOS and PDL-1 were analysed by qRT-PCR on unstimulated and stimulated mMSC. IFNγ stimulation increased the expression of LICOS and PDL-1 on mMSC.

A

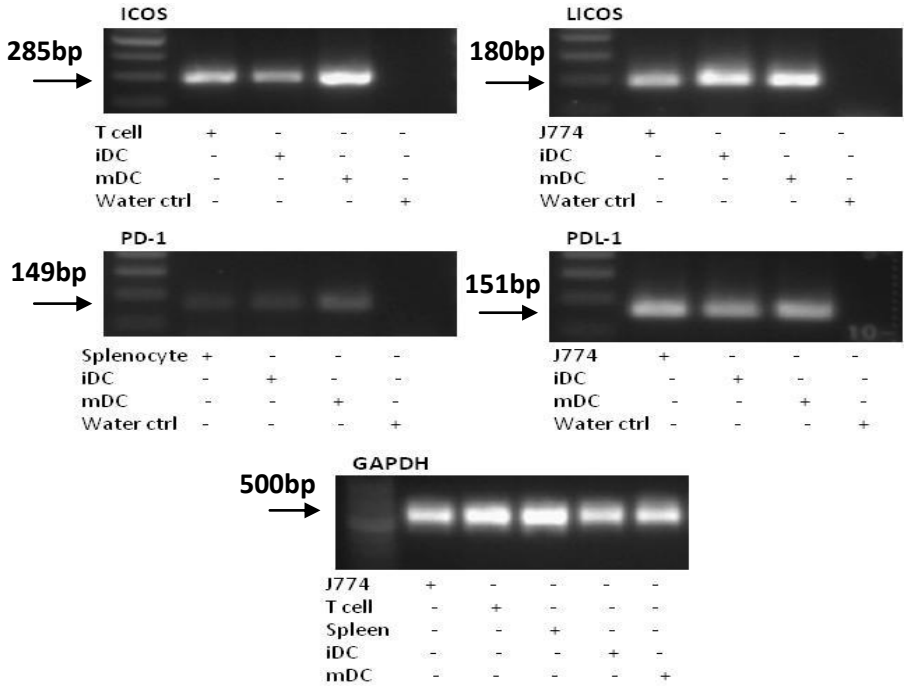

B

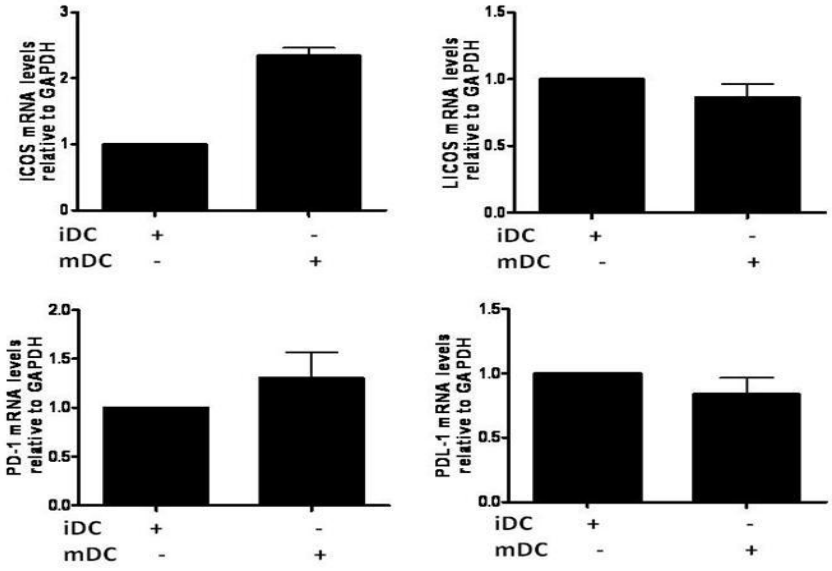

Fig 4.13 DC express ICOS, LICOS, PD-1 and PDL-1. Bone marrow derived DC were isolated and matured in the absence (iDC) or presence (mDC) of LPS at 100 ng/ml for 24 h. The expression of ICOS, LICOS, PD-1 and PDL-1 was analysed by (A) RT-PCR and (B) qRT-PCR. Both immature (iDC) and mature DC (mDC) expressed similar levels of LICOS and PDL-1, while maturation increases the expression of ICOS and PD-1 receptors.

4.11 NOTCH EXPRESSION BY MMSC

Notch signalling is involved in cell fate decisions during development, stem cell maintenance, cell proliferation, differentiation and apoptosis (Radtke, 2004; Fiuza, 2007) (Chapter 1.6.2), and Notch-ligand interaction has a role in other immune modulatory situations (Fiuza, 2007). Therefore, the Notch signalling pathway was investigated as a possible candidate for the cell contact signal used by mMSC. The expression of Notch receptors, Notch 1 and 2 and the Notch ligand, Jagged 1, 2 and Delta-like ligand 1 were analysed on mMSC alone or mMSC stimulated with TNFα, prolactin, LPS or IFNγ for 24 h by RT-PCR (Fig 4.14) (Table 4.1). Primers were previously optimised in the laboratory, prior to analysis using known positive controls for expression. The expression of Notch 1, Notch 2, Jagged 1 and Delta-like ligand-1 were observed on mMSC, while Jagged 2 was not expressed by mMSC (Fig 4.14 A). Stimulation of mMSC by prolactin, TNFα or LPS decreased the expression of Notch 1 when compared to unstimulated mMSC ($P<0.05$). Stimulation of mMSC with prolactin, IFNγ or LPS resulted in a decrease of Notch 2 expression when compared to mMSC alone. While IFNγ stimulation of mMSC decreased Jagged 1 expression when compared to mMSC alone (Fig 4.14 B).

The expression of Notch receptors and ligands by unstimulated mMSC was characterised at the protein level by flow cytometry (Fig 4.15). mMSC expressed Notch 1, Notch 2, Jagged 1 and Delta-like ligand-1, but not Jagged 2 similar to that found by RT-PCR (Fig 4.15). The expression of both Notch receptors and ligands on stimulated or unstimulated mMSC suggested that Notch signalling could possibly be the contact dependent signal involved in modulation of immunity by MSC.

A

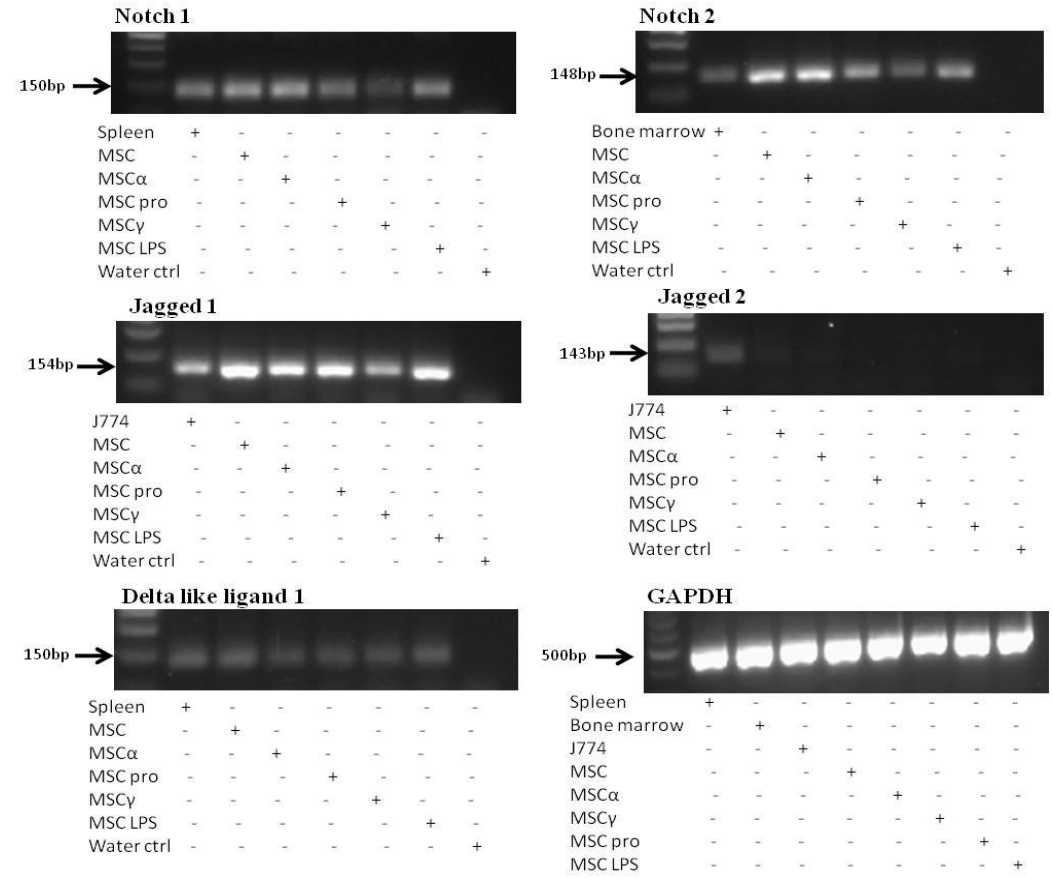
Notch 1
150bp
Spleen + - - - - - - -
MSC - + - - - - - -
MSCα - - + - - - - -
MSC pro - - - + - - - -
MSCγ - - - - + - - -
MSC LPS - - - - - + - -
Water ctrl - - - - - - + -
Notch 2
148bp
Bone marrow + - - - - - - -
MSC - + - - - - - -
MSCα - - + - - - - -
MSC pro - - - + - - - -
MSCγ - - - - + - - -
MSC LPS - - - - - + - -
Water ctrl - - - - - - + -
Jagged 1
154bp
J774 + - - - - - - -
MSC - + - - - - - -
MSCα - - + - - - - -
MSC pro - - - + - - - -
MSCγ - - - - + - - -
MSC LPS - - - - - + - -
Water ctrl - - - - - - + -
Jagged 2
143bp
J774 + - - - - - - -
MSC - + - - - - - -
MSCα - - + - - - - -
MSC pro - - - + - - - -
MSCγ - - - - + - - -
MSC LPS - - - - - + - -
Water ctrl - - - - - - + -
Delta like ligand 1
150bp
Spleen + - - - - - - -
MSC - + - - - - - -
MSCα - - + - - - - -
MSC pro - - - + - - - -
MSCγ - - - - + - - -
MSC LPS - - - - - + - -
Water ctrl - - - - - - + -
GAPDH
500bp
Spleen + - - - - - - - -
Bone marrow - + - - - - - - -
J774 - - + - - - - - -
MSC - - - + - - - - -
MSCα - - - - + - - - -
MSCγ - - - - - + - - -
MSC pro - - - - - - + - -
MSC LPS - - - - - - - + -

B

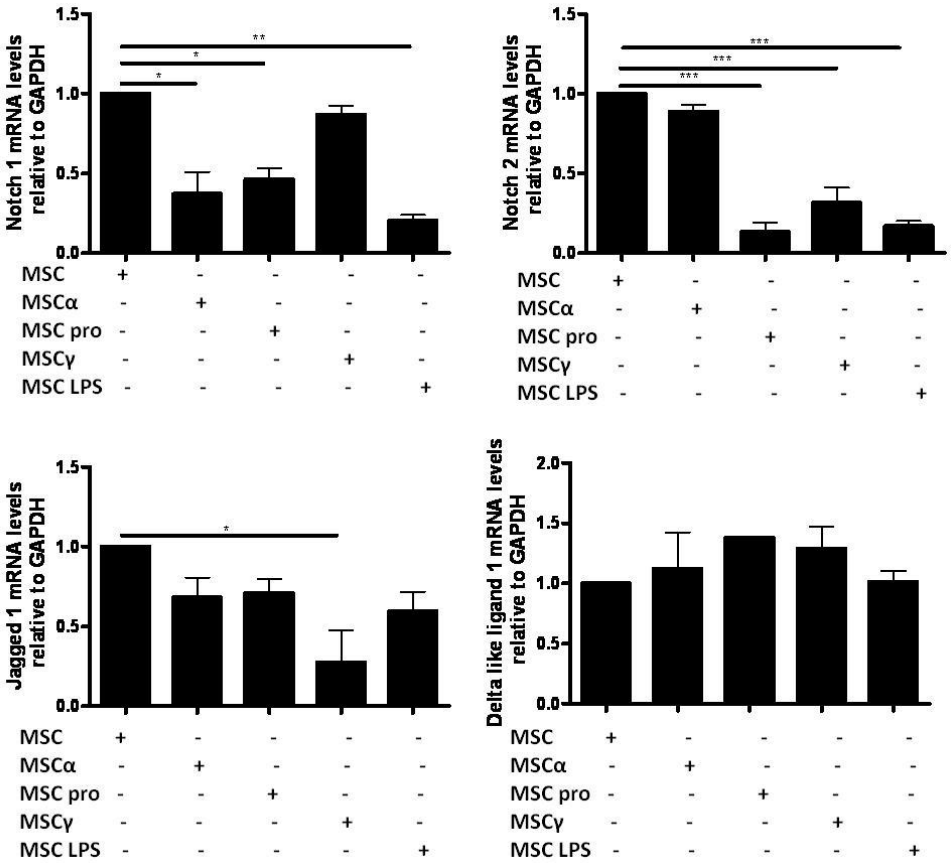

Fig 4.14 MSC expressed Notch receptors and ligands. mMSC were unstimulated or stimulated with TNFα, prolactin, IFNγ or LPS at 50 ng/ml for 24 h. Expression of Notch receptors and ligands were analysed by (A) RT-PCR and (B) qRT-pCR. (A) mMSC expressed Notch 1, Notch 2, Jagged 1 and Delta-like ligand 1. mMSC did not express Jagged 2. (B) Stimulation of mMSC by prolactin, TNFα or LPS decreased the expression of Notch 1 ($p<0.05$). Stimulation of mMSC with prolactin, IFNγ or LPS resulted in a decrease of Notch 2 ($p<0.05$). While IFNγ stimulation of mMSC decreased Jagged 1 expression ($p<0.05$). Statistical analysis was carried out using the students paired t test.

Table 4.1 Expression of Notch receptor and ligands by mMSC Summary

Treatment of Cells	Notch 1	Notch 2	Jagged 1	Jagged 2	Delta-like ligand 1
MSC	+	+	+	-	+
MSC+ TNFα	+	+	+	-	+
MSC+ Prolactin	+	+	+	-	+
MSC+ IFNγ	+	+	+	-	+
MSC + LPS	+	+	+	-	+

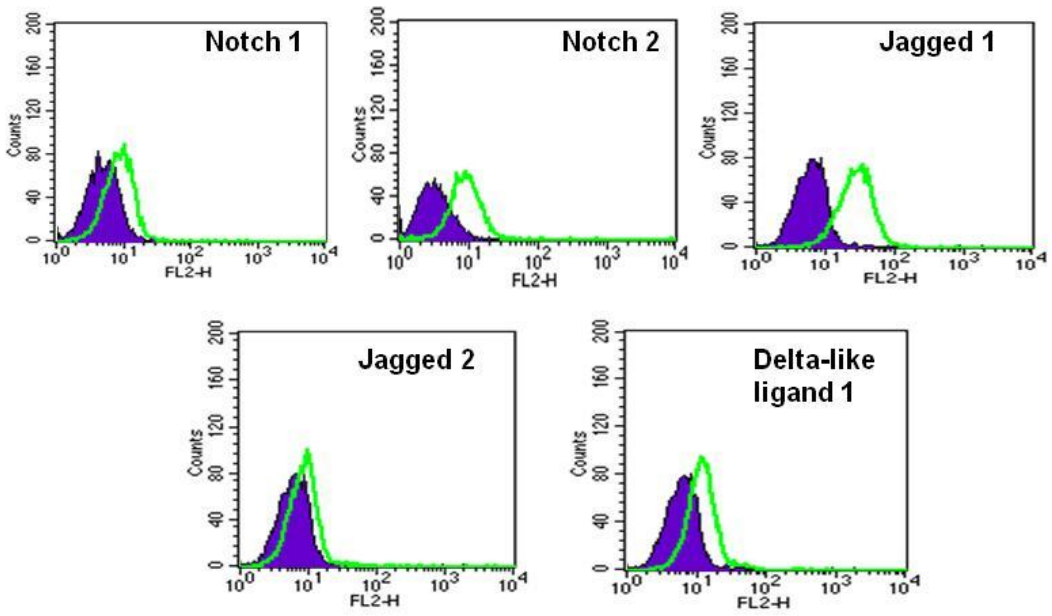

Fig 4.15 Notch expression by MSC. Expression of Notch 1, Notch 2, Jagged 1, Jagged 2 and Delta-like ligand 1 by mMSC alone were analysed by flow cytometry. mMSC expressed Notch 1, Notch 2, Jagged 1 and Delta-like ligand 1. mMSC did not express Jagged 2. Isotypes are represented as closed histograms (purple), while specific marker expressions are represented as open histograms (green).

4.12 EXPRESSION OF NOTCH BY MURINE DC

The expression of Notch by immature DC (iDC) and LPS matured DC (mDC) were analysed by qRT-PCR and flow cytometry. iDC were generated by culturing bone marrow cells with GM-CSF for 8 days and matured with LPS for a further 48 h. The expression of Notch 1, Notch 2, Jagged 1, Jagged 2 and Delta-like ligand 1 on iDC and mDC were examined by RT-PCR and followed on a quantitative level by qRT-PCR (Fig 4.16 A & B) (Table 4.2). iDC expressed Notch 1 and Jagged 2 which decreased upon maturated with LPS (Fig 4.16 A & B). iDC expressed low levels of Notch 2, which increased following LPS maturation (Fig 4.16 A & B). The expression of Jagged 1 and Delta-like ligand 1 were increased on DC following maturation by LPS (Fig 4.16 A & B). These data found that DC were capable of Notch receptor and ligand expression at an RNA level.

The expression of Notch receptors and ligands were analysed on DC matured in the presence of LPS for 48 h by flow cytometry (Fig 4.17). Data corresponded to mRNA analysis, Notch 1 and Jagged 2 expression on DC was decreased after stimulation with LPS (Fig 4.17), while Notch 2, Jagged 1 and Delta-like ligand 1 expression were increased following maturation with LPS (Fig 4.17). As the expression of specific Notch receptors and ligands were present on both DC and mMSC, this suggested that Notch signalling could be a possible candidate for mMSC: DC cell-cell interaction.

A

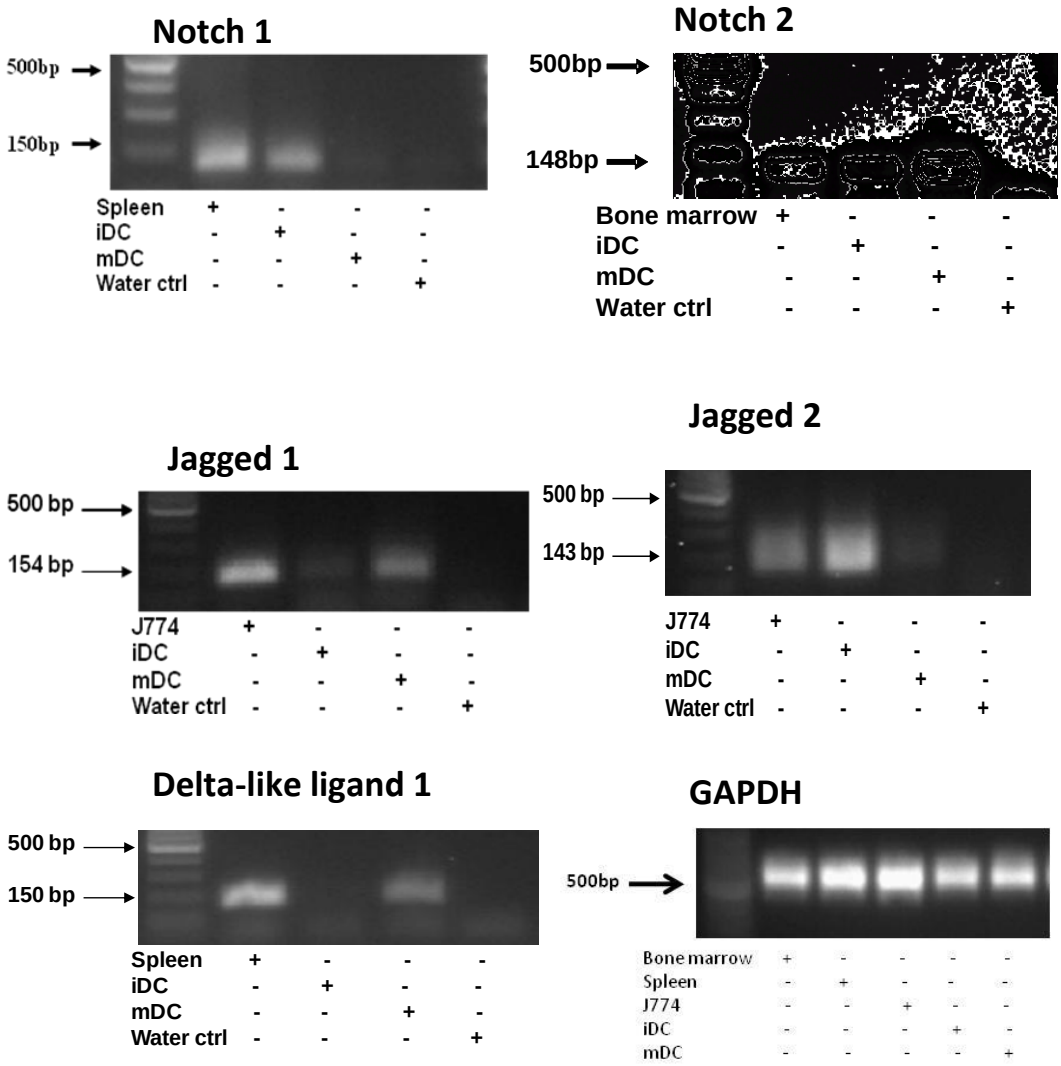
Notch 1
500bp
150bp
Spleen + - - -
iDC - + - -
mDC - - + -
Water ctrl - - - +
Notch 2
500bp
148bp
Bone marrow + - - -
iDC - + - -
mDC - - + -
Water ctrl - - - +
Jagged 1
500 bp
154 bp
J774 + - - -
iDC - + - -
mDC - - + -
Water ctrl - - - +
Jagged 2
500 bp
143 bp
J774 + - - -
iDC - + - -
mDC - - + -
Water ctrl - - - +
Delta-like ligand 1
500 bp
150 bp
Spleen + - - -
iDC - + - -
mDC - - + -
Water ctrl - - - +
GAPDH
500bp
Bone marrow + - - - -
Spleen - + - - -
J774 - - + - -
iDC - - - + -
mDC - - - - +

B

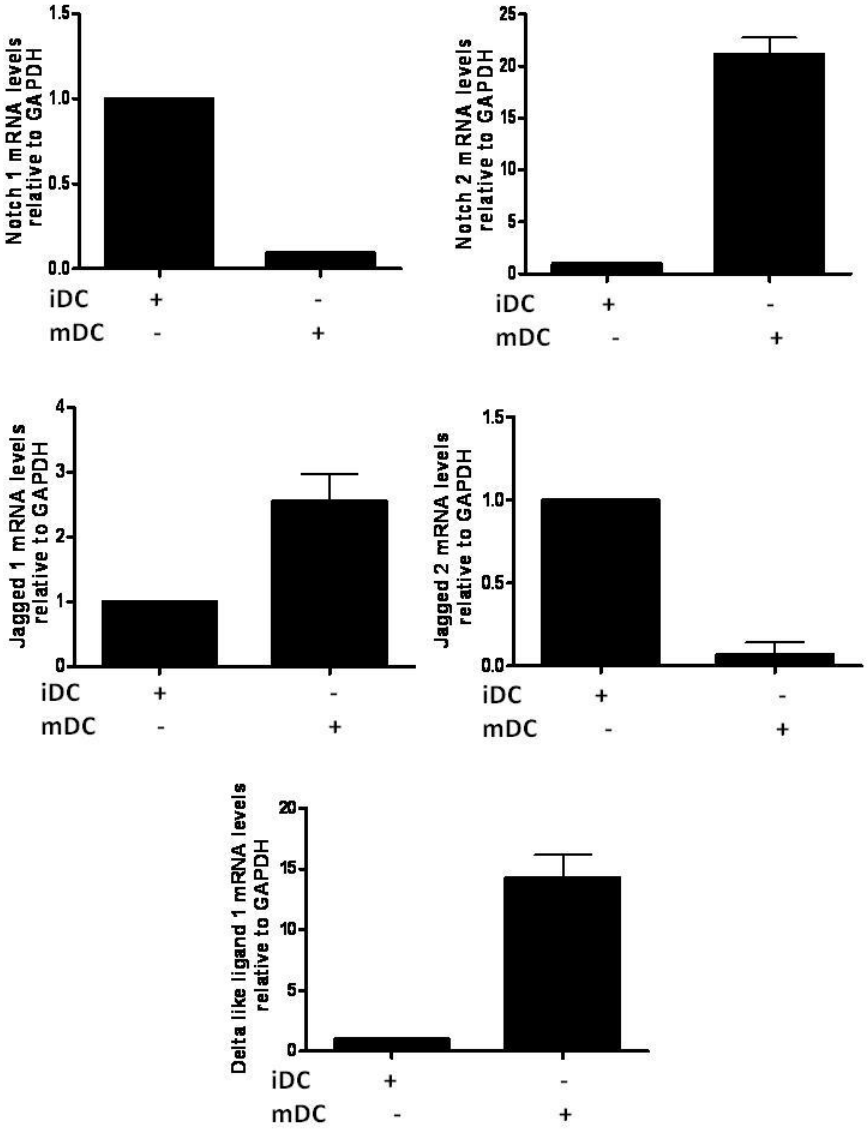

Fig 4.16 Notch expression by dendritic cells. iDC were matured with 100 ng/ml LPS for 24 h. Expression of Notch receptors, Notch 1, Notch 2 and Notch ligands Jagged 1, Jagged 2 and Delta-like ligand 1 were analysed by (A) RT-PCR and (B) qRT-PCR. Maturation by LPS reduced the expression of Notch 1 and Jagged 2 on DC. Notch 2, Jagged 1 and Delta-like ligand 1 expression were increased on DC following maturation by LPS. Data are representative of three independent experiments.

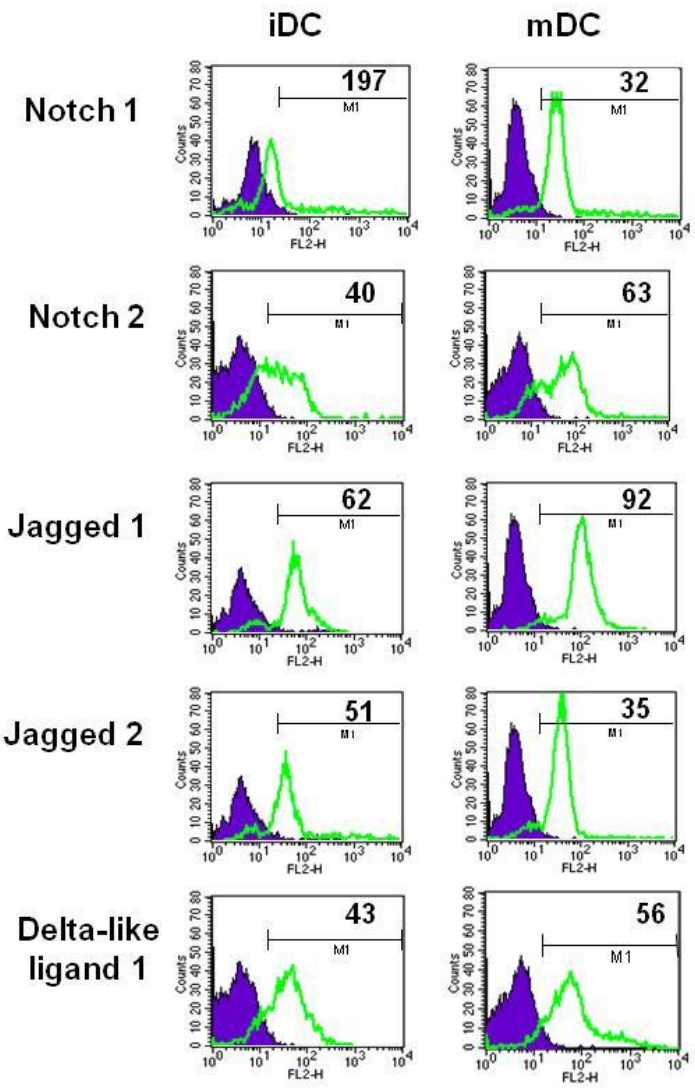

Fig 4.17 Notch expression on dendritic cells by flow cytometry. DC were matured with LPS (100 ng/ml) for 48 h and the expression of Notch receptors and ligands were analysed by flow cytometry. Notch 1 and Jagged 2 expression was decreased on DC following stimulation with LPS. Notch 2, Jagged 1 and Delta-like ligand 1 expression was increased on DC after maturation with LPS for 48 h. Data are representative of three experiments.

Table 4.2 Summary of Notch expression by DC

Cells	Notch 1	Notch 2	Jagged 1	Jagged 2	Delta-like ligand 1
Immature DC (iDC)	++	+	+	++	+
Mature DC (mDC)	+	++	++	+	++

4.13 mMSC CONTACT WITH DC ACTIVATES NOTCH SIGNALLING

The next step in identifying a possible cell contact signal involved in mMSC modulation of DC maturation was to look at the Notch signalling pathway functionally. To investigate whether the Notch signalling pathway was involved in mMSC suppression of DC maturation, the activation of Notch target genes, such as HES1 was examined. mMSC cocultured with LPS stimulated DC (mDC) induced the expression of the Notch target gene, HES1 (Fig. 4.18 A). However, the expression of HES1 was reduced when Notch signalling was blocked using a gamma secretase inhibitor, GSI (Fig 4.18 A). These data suggested that Notch signalling was involved in mMSC-DC maturation interaction. Therefore, further studies using the Notch inhibitor, GSI, were carried out.

mDC were cocultured with mMSC in the presence or absence of GSI or DMSO (vehicle control). After coculture, the expression of the maturation markers, MHC class II and CD86 were analysed by flow cytometry (Fig 4.18 B & C). As expected, DC showed increased expression of both MHC class II (3405 MFI) and CD86 (319 MFI) when matured with LPS. However, in the presence of mMSC, the expression of MHC class II (2636 MFI) and CD86 (285 MFI) were reduced, characteristic of a semi-mature DC phenotype (Fig 4.18 B & C). The addition of Notch inhibitor, GSI to the coculture restored the expression of MHC class II (3081 MFI) and CD86 (319 MFI) to levels similar to mDC. Vehicle control, DMSO, in coculture experiments had no effect (Fig 4.18 B & C).

mMSC prevented the production of IL-12p70 by mDC but increased IL-10 in coculture (Fig 4.6 B). The effect of blocking Notch signalling (by GSI) on the production of IL-12p70 and IL-10 by DC in coculture with mMSC was analysed by

ELISA (Fig 4.19). After 48 h, coculture supernatant was harvested and analysed for IL-12p70 and IL-10 production. Although blocking Notch signalling *in vitro* in coculture experiments restored the maturation of DC, the production of IL-12p70 was not altered. However, blocking Notch in cocultures between mMSC and DC appeared to increase IL-10 production. These data suggested that mMSC suppress DC maturation through Notch. However, the modulation of cytokine signalling seems to be independent of Notch signalling and may well be through MSC derived IL-10.

A HES1

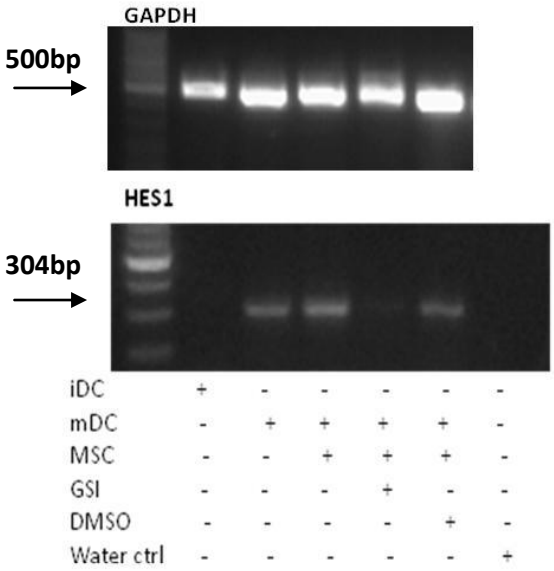

B MHC class II

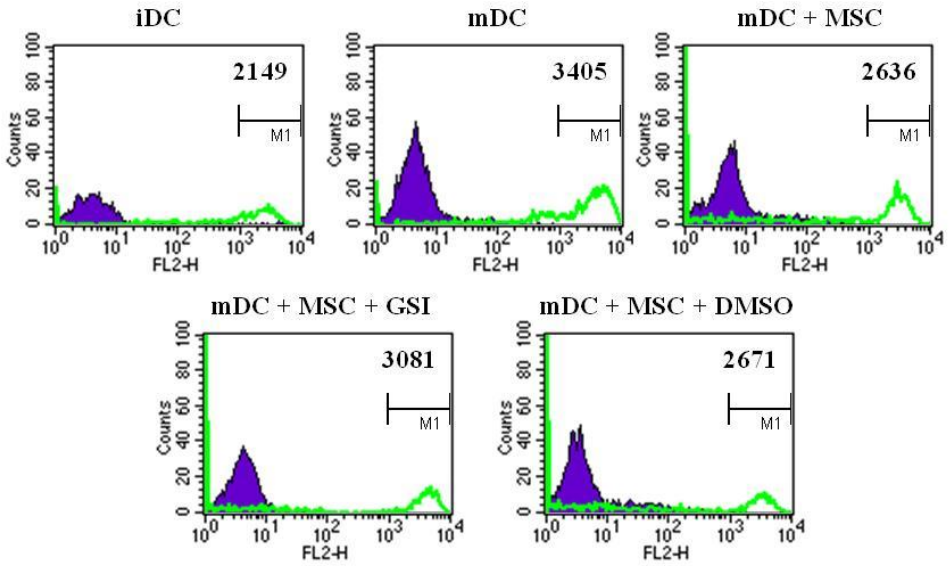

C CD86

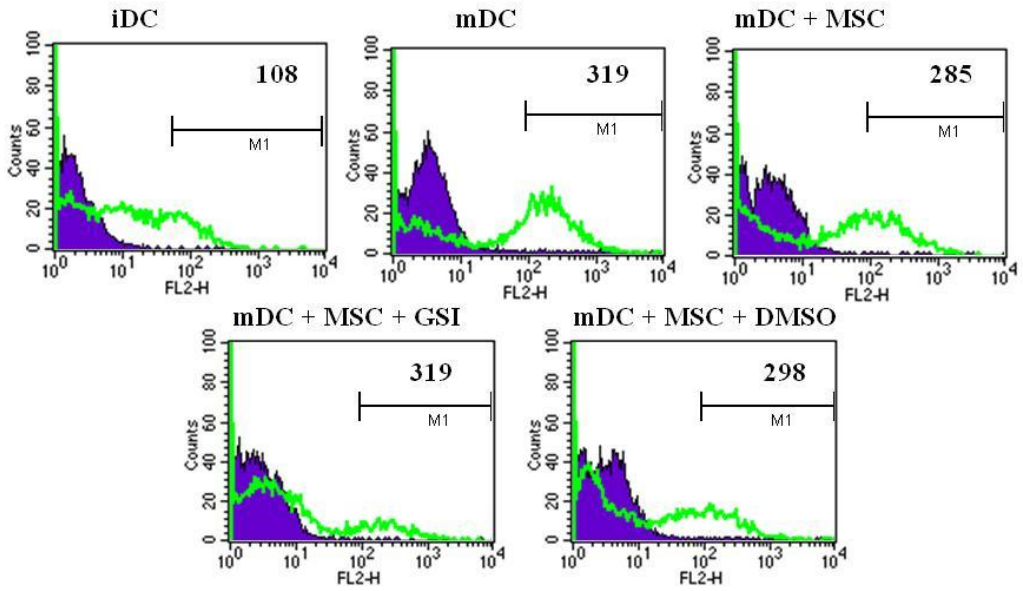

Fig 4.18 Notch signalling is involved in MSC inhibition of DC maturation. DC were matured with LPS (100 ng/ml) in the presence or absence of mMSC for 24 or 48 h. Notch signalling was blocked through the addition of GSI (1 µM) to MSC: DC cocultures. After 24 h, (A) DC were analysed for the expression of Notch target gene HES1 by RT-PCR. HES1 expression was down regulated on DC when Notch signalling was blocked using GSI. After 48 h, DC were harvested and analysed for the expression of (B) MHC class II and (C) CD86 by flow cytometry. Blocking Notch signalling using GSI inhibited mMSC modulation of DC maturation. Vehicle control for GSI, DMSO, had no effect on DC maturation. Isotypes are represented as closed histograms (purple), while specific marker expressions are represented as open histograms (green). Mean fluorescence intensity (MFI) are represented on histogram (upper right). Data are representative of three independent studies.

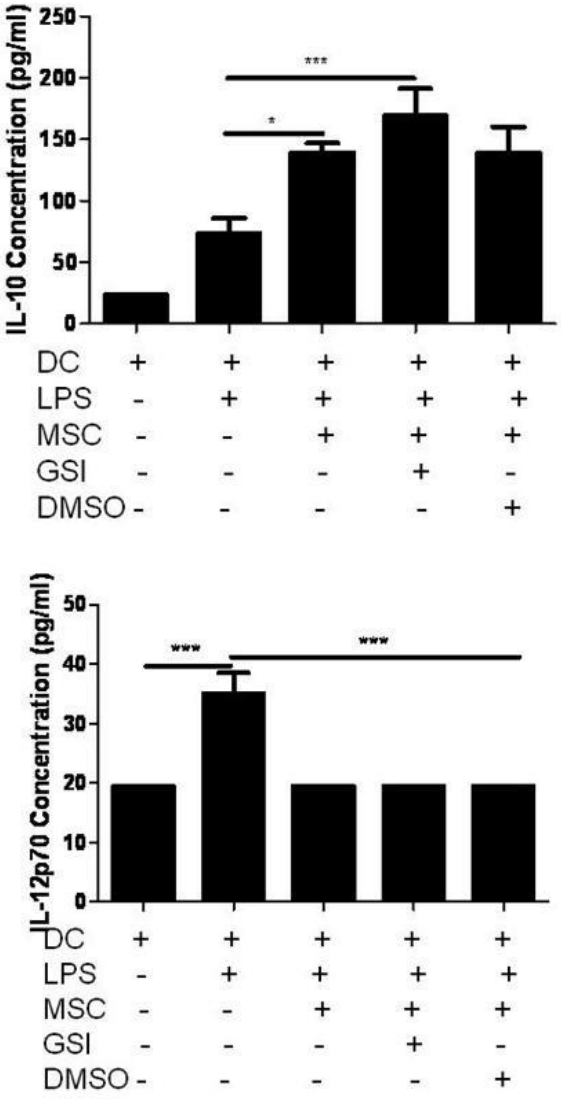

Fig 4.19 Blocking Notch signalling between MSC and DC had no effect on cytokine production. mMSC and DC were cocultured in the presence of LPS for 48 h. Notch signalling was blocked through the addition of GSI. Supernatants were harvested after 48 h of coculture and analysed for the presence of IL-10 and IL-12p70 by ELISA. mMSC significantly ($p<0.05$) decreased IL-12p70 production and significantly ($p<0.05$) increased the production of IL-10 by DC. Blocking Notch signalling through the addition of GSI had no effect on cytokine production when compared to DC cocultured with mMSC. Statistical analysis was carried out using the students paired t test. Data are representative of three independent experiments performed in triplicate.

4.14 NOTCH SIGNALLING IS REQUIRED FOR MSC SUPPRESSION OF ANTIGEN PRESENTATION BY DC

mMSC interfere with the presentation of I-Eα peptide by C57 BL/6 isolated DC (Fig 4.7 A). However, to investigate whether Notch signalling was required for antigen presentation by DC, the Notch γ-secretase inhibitor, GSI, was used in coculture experiments. DC isolated from C57/BL6 bone marrow were pulsed with I-Eα peptide and cocultured with mMSC in the presence or absence of GSI or DMSO for 48 h. In the presence of mMSC, DC pulsed with I-Eα peptide were unable to display the antigen (Fig 4.20) (47%), in line with the result shown previously (Fig 4.7 A). However, when Notch signalling was blocked using GSI, mMSC could no longer prevent DC from displaying I-Eα antigen (Fig 4.20), as the percentage of cells presenting I-Eα was similar to that of DC alone pulsed with I-Eα antigen (75%). These data confirmed that not only was Notch signalling involved in mMSC inhibition of DC maturation, but it was required for the inhibition of antigen presentation by DC when mMSC were present.

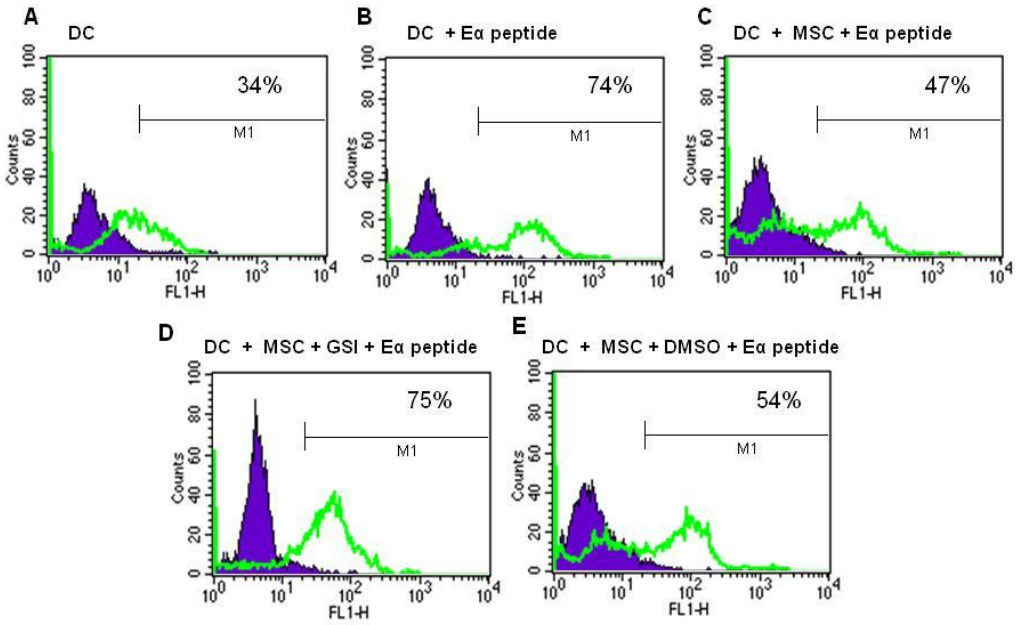

Fig 4.20 Notch is involved in MSC suppression of DC antigen presentation. DC alone or DC pulsed with I-Eα peptide (10 μg/ml) in the presence or absence of MSC, GSI or DMSO were cultured for 48 h. The number of DC presenting the I-Eα peptide was measured by YAe expression, by flow cytometry. (B) DC pulsed with I-Eα peptide expressed higher levels of YAe when compared with (A) DC alone. However, (C) when mMSC were present, DC were unable to present antigen. By blocking Notch signalling using GSI, (D) DC antigen presentation was restored, indicating that Notch signalling was involved in mMSC interference of DC antigen presentation. (E) GSI vehicle control had no effect on antigen presentation. Percentage of cells within the marked region are represented in the histogram. Isotype shown in purple YAe expression in green. Data are representative of three experiments.

4.15 NOTCH IS REQUIRED FOR MMSC INDUCTION OF TOLEROGENIC DC

In order to examine the possible role of Notch signalling in the induction of a tolerogenic DC by mMSC, the experiment described in section 4.6 (Fig 4.7 B) was repeated with GSI present in the cocultures. DC were pulsed with OVA in the presence or absence of mMSC. DC were the harvested by gentle aspiration from adherent mMSC and placed in a proliferation assay with OVA specific DO11.10 $CD4^+$ T cells. DC pulsed with OVA were capable of supporting DO11.10 $CD4^+$ T cell proliferation (Fig 4.21). However, DC pulsed with OVA in the presence of mMSC were unable to stimulate $CD4^+$ T cell proliferation (Fig 4.21).

To investigate if Notch signalling was essential for this induction of a functional tolerogenic DC by mMSC, GSI or inhibitor vehicle control DMSO were also included in coculture experiments. Following coculture with mMSC and GSI, OVA pulsed DC were repurified and placed in coculture with DO11.10 $CD4^+$ T cells. Interestingly, by blocking Notch signalling through the addition of GSI, mMSC were no longer able to induce a functional tolerogenic DC, as indicated by a significant increased in $CD4^+$ T cell proliferation ($p<0.0001$) (Fig 4.21). These data confirmed that Notch signalling was required for the induction of a functional tolerogenic DC population by mMSC *in vitro*.

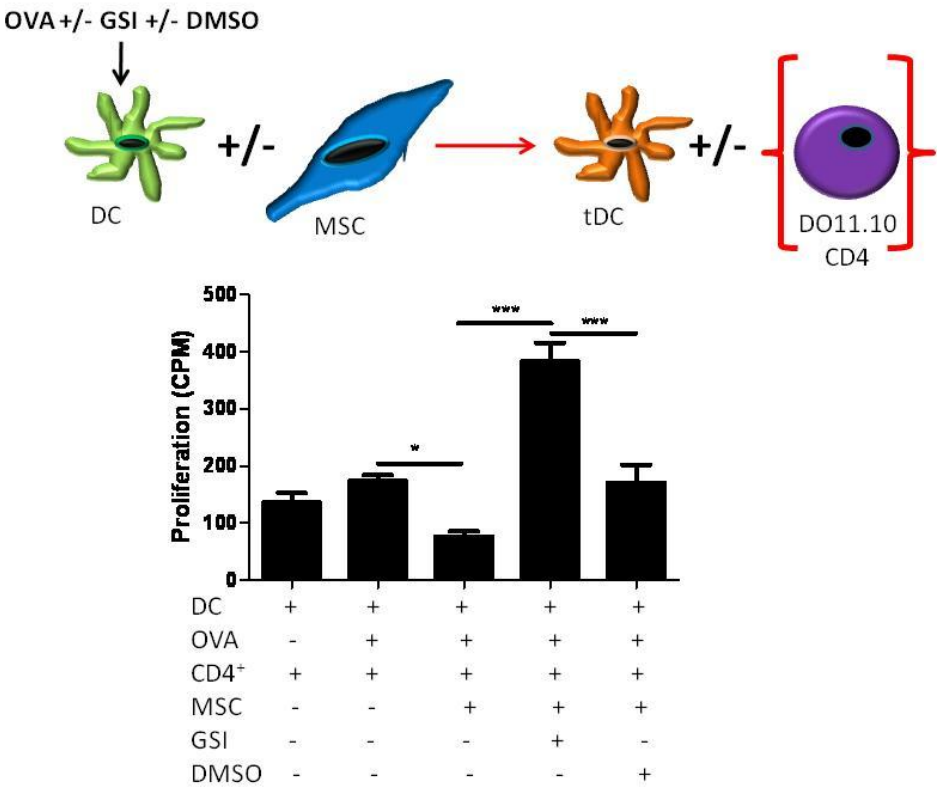

Fig 4.21 Notch is required for the induction of a functional tolerogenic DC by MSC. DC pulsed with OVA in the presence or absence of mMSC, GSI (1 µM) or DMSO for 24 h were harvested and washed twice before further culturing with DO11.10 $CD4^+$ T cells for 72 h. After 72 h, proliferation through ^3H Thymidine incorporation was measured. DC pulsed with OVA supported the proliferation of DO11.10 $CD4^+$ T cells. DC that had been cultured in the presence of mMSC were significantly less able to support proliferation of DO11.10 $CD4^+$ T cells ($P<0.05$). However, DC cultured in the presence of mMSC and GSI did not inhibit the proliferation of DO11.10 $CD4^+$ T cells, as indicated by a significant increase on $CD4^+$ T cell proliferation ($p<0.0001$). This indicated a requirement for Notch signalling in the induction of a tolerogenic DC by mMSC. Statistical analysis was carried out using the students paired t test.

4.16 ATTEMPTS TO EXPLORE JAGGED 1 IN DC MATURATION

mMSC express the Notch ligand Jagged 1. Recently, Cheng *et al.* found that Notch ligand Jagged 1 stimulated the accumulation of DC precursors, while preventing their transition to terminally differentiated DC (Cheng, 2007). These data suggested that Jagged 1 ligand could be the possible ligand involved in cell contact between mMSC and DC. The neutralisation of Jagged 1 expression by mMSC was examined.

DC were matured with LPS in the presence of absence of mMSC. In some treatment groups, the neutralisation of Jagged 1 was carried out through the addition of anti-mouse Jagged 1 antibody. The expression of maturation marker, MHC class II and costimulatory marker, CD86 were analysed by flow cytometry (Fig 4.22 A & B respectively). DC cocultured with mMSC had reduced levels of maturation marker expression a semi-mature DC phenotype. Following the neutralisation of Jagged 1 (5 μg/ml) in coculture between mMSC and DC, the levels of maturation marker expression on DC increased marginally to similar levels seen by mature DC, suggesting that the ligand Jagged 1 could possibly be involved in DC: MSC interactions (Fig 4.22 A & B). However, on closer inspection, the control antibody for anti-Jagged 1 was found to have an effect on DC maturation marker expression. These data suggested that this antibody was not sufficient in the neutralisation of Jagged 1 and that a more specific technique was required for knock down of Jagged 1 expression on mMSC. Therefore, the idea of silencing Jagged 1 expression by siRNA was investigated.

Expression of murine Jagged 1 RNA was silenced using a pre-designed siRNA pre-select kit. mMSC were cultured in 24 well plates to about 60%

confluency. Different amounts of siRNA in the presence of Lipofectamine 2000, a transfection reagent, were added to wells in duplicate for 24 or 48 h. siRNA ranging from 10 nmol to 25 nmol were used. After siRNA/mMSC culture for 24 h and 48 h, Jagged 1 expression was analysed on mMSC by RT-PCR (Fig 4.22 C & D). Jagged 1 siRNA at 15 nmol was optimal for complete Jagged 1 knockdown after 24 h (Fig 4.22 C). However, after 48 h, the expression of Jagged 1 had returned to normal expression on mMSC (Fig 4.22 D). To identify if Jagged 1 is the ligand involved in mMSC modulation of DC maturation or inhibition of antigen presentation, Jagged 1 expression would require complete knock down for a minimum of 48 h for coculture experiments. These data found that both the neutralisation and silencing of Jagged 1 expression by mMSC were insufficient tools for identifying the ligand as a specific contact candidate. In order to investigate a role for Jagged 1 on mMSC as a possible contact candidate, a more specific knock down technique would need to be employed.

A MHC class II

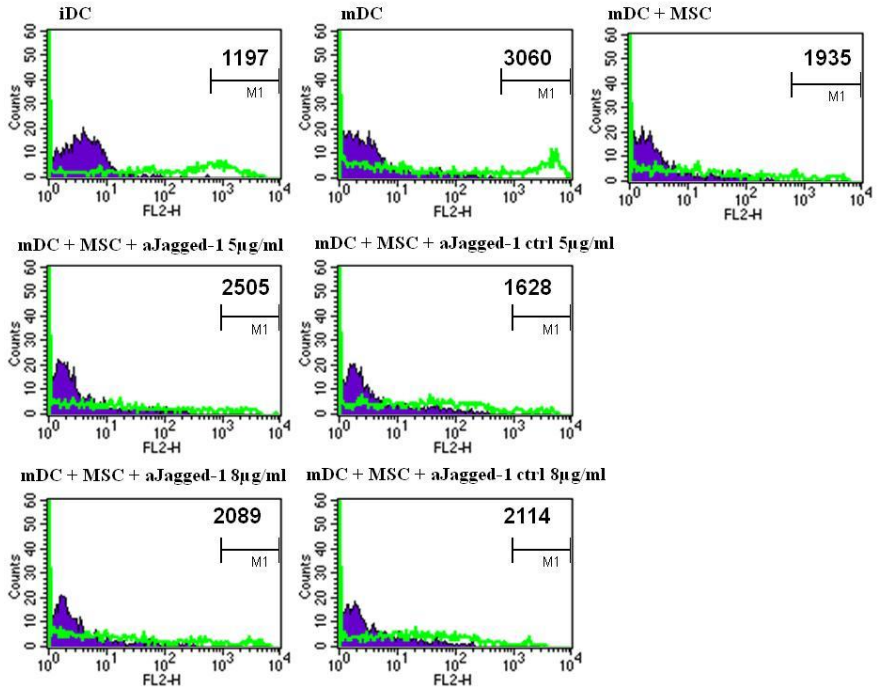

B CD86

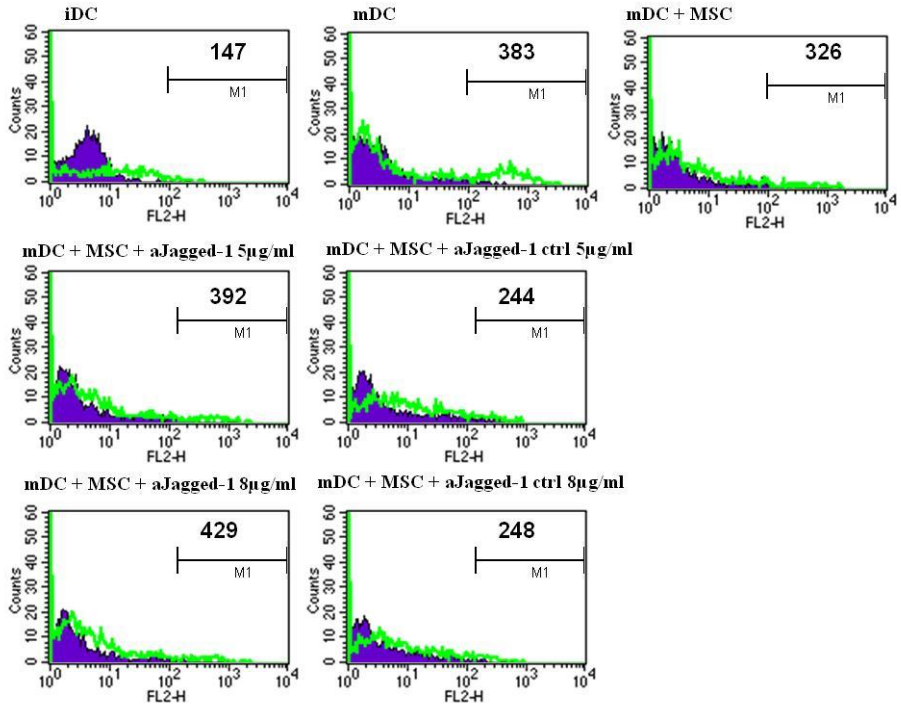

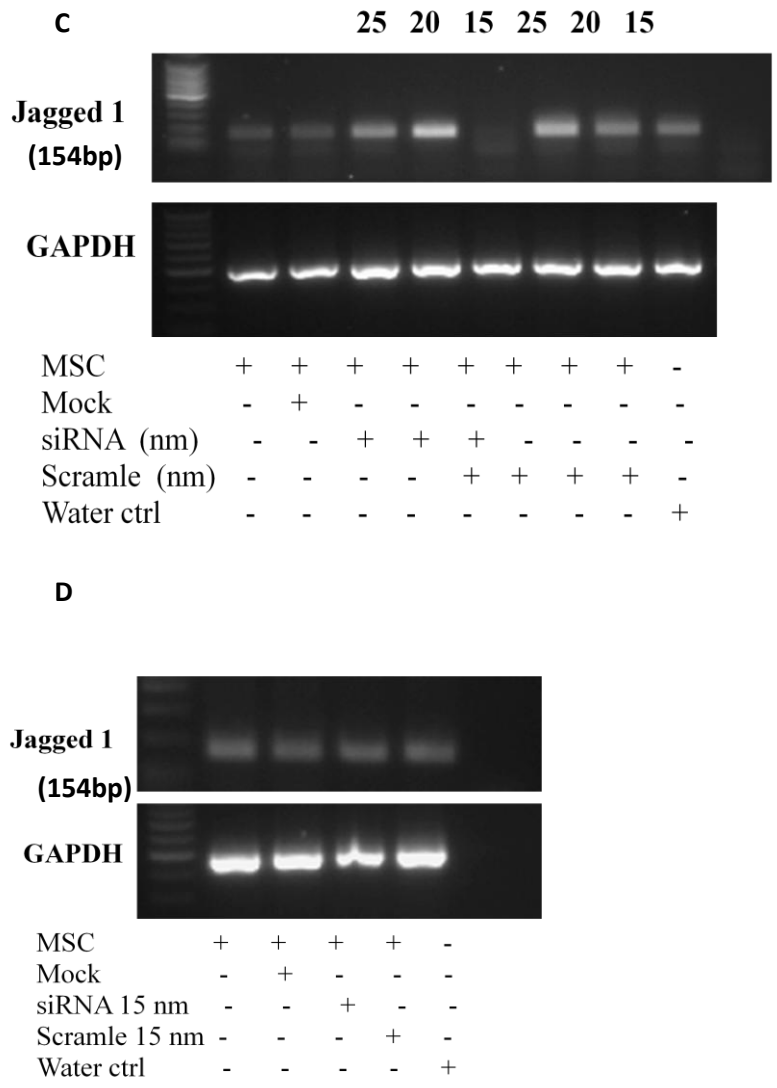

Fig 4.22 Neutralising Jagged 1 in coculture studies did not affect DC maturation. DC were matured with LPS in the presence or absence of mMSC for 48 h. Murine Jagged 1 was neutralised using an anti-mouse Jagged 1 antibody or corresponding control (8 µg/ml or 5 µg/ml). The expression of DC maturation markers (A) MHC class II and (B) CD86 were examined by flow cytometry after 48 h. Jagged 1 was not involved in mMSC: DC maturation. siRNA in the presence of Lipofectamine 2000, a transfection reagent, were added to mMSC at 60% confluency in duplicate. siRNA ranging from 15 nmol to 25 nmol were used for (C) 24 or (D) 48 h, then the expression of Jagged 1 was analysed by RT-PCR. (C) siRNA at 15 nmol silenced Jagged 1 expression for 24 h. After 48 h, (D) the expression of Jagged 1 had returned to that of MSC alone. Housekeeper gene expression, (D) GAPDH, used as a positive control for cDNA synthesis.

4.17 SUMMARY

The aims of the experiments described in this chapter were to identify the contact dependent signal required for MSC mediated immunosuppression. In this Chapter, mMSC were found to suppress DC maturation and DC antigen presentation. mMSC induced a semi-mature/tolerogenic DC. This was shown when OVA pulsed DC cocultured in the presence of mMSC were unable to induce the proliferation of D011.10 $CD4^+$ T cells.

To identify possible contact signals between mMSC and DC, a number of possible candidates were analysed. Siglecs are known to regulate the function of cells in both the innate and adaptive immune systems through glycan recognition (Crocker, 2007). This encouraged the investigation of CD33-related Siglec expression by mMSC. However, after CD33-related Siglecs were shown not to be expressed by mMSC. Therefore, further investigation into Siglecs, as a contact signal between MSC and DC was discontinued.

The B7 family of molecules provide signals that are critical for both stimulating and inhibiting T cell activation (McAdam, 1998). The expression of specific B7 family receptors and ligands were analysed on mMSC and DC by qRT-PCR. mMSC did not express ICOSor PD-1 receptors or ligands. While, DC expressed both ICOS and PD-1 receptors and ligands. This suggested that the B7 family of receptors were not involved in the cell contact between mMSC and DC.

Previous work identified Notch signalling to be involved in DC maturation (Cheng, 2003). Therefore, a role for the Notch signalling pathway in mMSC modulation of DC maturation and antigen presentation was investigated. mMSC and DC expressed Notch receptors and ligands as analysed by qRT-PCR and flow

cytometry. mMSC prevented the upregulation of maturation marker expression by DC, increasing the secretion of IL-10 and decreasing the production of IL-12p70. mMSC inhibited the presentation of antigen by DC, inducing a tolerogenic DC *in vitro*. Using a γ-secretase inhibitor (GSI) to block Notch signalling, mMSC were no longer able to interfere with DC maturation, antigen presentation or the induction of a function tolerogenic DC. These data highlighted a role for Notch signalling between mMSC and DC.

Identifying a role for a specific Notch ligand was difficult, as there are only a limited number of neutralisation reagents available for Notch signalling. An anti mouse Jagged 1 neutralising antibody was not adequate to deliver convincing data regarding the identity of the Notch ligand and although mMSC were successfully silenced for Jagged 1, knock down in expression was not durable. By 48 h, the expression of Jagged 1 on mMSC had returned to normal. A more permanent knock down of Jagged 1 on MSC is required. Taken together, these data showed that mMSC induce tolerogenic DC and provided evidence for a role of Notch signalling in the contact dependent component of MSC mediated immune modulation of DC function.

CHAPTER 5

DEVELOPMENT OF A HUMANISED MOUSE MODEL OF ACUTE GRAFT VERSUS HOST DISEASE

5.1 INTRODUCTION

The ability of MSC to suppress immune responses *in vitro* and some of the associated mechanisms through which this occurs, were identified in Chapters 3 and 4. However, the relevance of MSC immune modulation requires an examination of *in vivo* efficacy. Furthermore, the *in vivo* efficacy of MSC therapy needs demonstration in systems appropriate and relevant to human disease. Allogeneic HSC transplantation (HSCT) is the therapy of choice for high-risk haematological malignant and certain non-malignant or autoimmune disorders (Chapter 1.8.1). The major confounding complication following HSCT is the development of GvHD

The rationale for the use of MSC as a cell-based therapy for aGvHD is based on the poor success rates with steroid therapy and observations that MSC have immunosuppressive qualities (Le Blanc, 2004; Polchert, 2008; English, 2010). In 2004, Le Blanc *et al.* described the successful treatment of a patient with steroid resistant grade IV aGvHD using allogeneic MSC (Le Blanc, 2004). However, the mechanism by which MSC therapy was beneficial was unclear. More recently, Osiris Therapeutics reported that Prochymal (an MSC like product) was successful in treating 76% of patients with steroid refractory liver GvHD in a phase III trial; however, no beneficial effects were seen for the topical manifestations of GvHD and overall the therapy did not achieve the efficacy endpoints required (Martin, 2010). These data show that next generation modified MSC may be a future therapy, but also highlight that there is little understanding of how MSC mediate their beneficial effects in a clinical setting. The development of more appropriate animal models to understand how MSC modulate GvHD would contribute greatly in developing novel MSC and second generation MSC based therapies, which would allow questions of dose and timing to be resolved and even allow standardisation of human products.

The objectives of this chapter were: a) to establish a consistent and reproducible humanised mouse model of aGvHD and b) to determine if human MSC therapy could alleviate or prevent disease progression in this model. The strategy adopted was to use a xenogeneic human in mouse model, where human PBMC were delivered to immunodeficient mice to provoke aGvHD, combined with the use of human MSC as a therapy. These objectives were broken down into a number of specific approaches:

1) Optimisation of a humanised mouse model to provide a consistent aGvHD like disease.

2) Determination if allogeneic human MSC were effective as a therapy for aGvHD treatment/prevention. This included study of the timing of MSC treatment for a beneficial effect.

3) An *in vitro* and *in vivo* examination of the "licensing" effect found by our group and Polchert *et al.*, whereby MSC "licensed" with IFNγ prior to administration proved to be more beneficial as a therapy (Ryan, 2007; Polchert, 2008).

5.2 Development of a Humanised Mouse Model of Acute Graft versus Host Disease

Humanised mice are promising models in which to study human hematopoiesis and immunity. Recently, new murine models suitable for HSC engraftment have been developed (Chapter 1.11). Among the more promising are the so-called humanised models that include the NOD-Scid IL2 receptor gamma null mice (NOD-Scid IL2rγ^{null}) (NSG) created by Pearson *et al.* (Pearson, 2008). One benefit of the NSG mouse is that human PBMC delivered by intravenous injection

(i.v.) allows for the study of human immune function, as the transferred lymphocytes are functionally mature and go directly into circulation (Pearson, 2008).

Using the protocol created by Pearson *et al.* as a guideline and starting point, a humanised mouse model of aGvHD was developed (Fig 5.1). After conditioning by low dose total body irradiation of 2.4 Gray (Gy), 2 x 10^7 human PBMC were administered via the tail vein and the development of aGVHD examined. As suggested by Pearson *et al.* and the recommendation of the local ethics committee, the development of aGvHD was defined as total body weight loss greater than 15% of original starting weight with a series of clinical manifestations including posture (hunching), reduced activity, fur texture (ruffling) and diarrhoea. These parameters were amalgamated into a pathological score (Chapter 2.11.2) and mice that scored 2.0 for each parameter mentioned above (a cumulative score of 8.0) or had an excess of 15% weight loss were considered to have severe aGvHD and were sacrificed humanely.

Optimisation studies were carried out using small numbers of NSG mice. Whilst this was far from ideal, it was dictated by small litter sizes and was necessary to conserve valuable mice for more informative studies. Preliminary experiments using the above protocol found that NSG mice (n=3) that received human PBMC (2 x 10^7) all developed aGvHD like symptoms, including >15% weight loss (Fig 5.2 A), hunched posture, reduced activity and ruffled fur (Fig 5.2 C). NSG mice that received PBS (vehicle control) displayed no aGvHD symptoms and remained healthy (Fig 5.2). However, further preliminary studies found that the development of pathology was inconsistent at this PBMC dose. This inconsistency was evident when comparing data from repeat experiments (Fig 5.2 & Fig 5.3). In the latter studies, PBMC administration did not lead to aGVHD development, as NSG mice

(n=3) that received PBMC had no significant weight loss (Fig 5.3 A), developed little or no signs of aGvHD (Fig 5.3 C), with the majority of mice surviving for more than 28 days (Fig 5.3 B). These inconsistencies suggested that further optimisation was required and that the model described by Pearson *et al.* would require refinement.

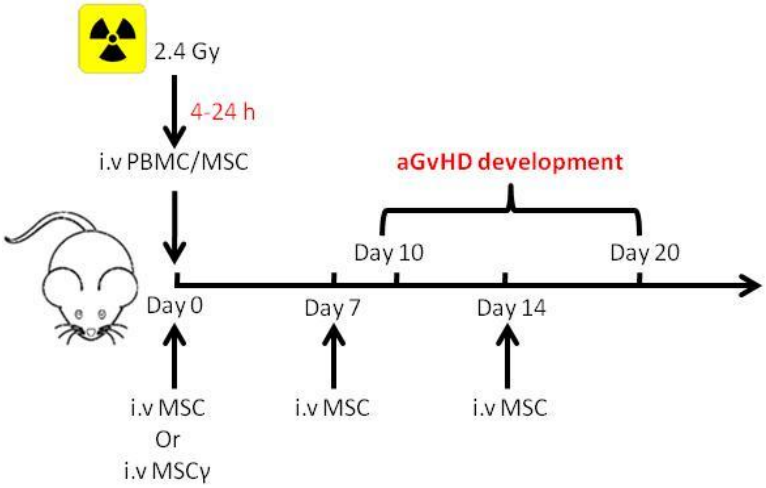

Fig 5.1 Development of a humanised mouse model of acute graft versus host disease. NOD-Scid IL2rγ^{null} (NSG) mice were irradiated receiving 2.4 Gy, after 4 h, freshly isolated PBMC (2 x 10^7/mouse) were administered intravenously in 200 µl (i.v.) via the tail vein. In later experiments, hMSC were given i.v. on day 0, 7 or 14, with prestimulated hMSC given i.v. on day 0. aGvHD development was monitored daily by recording weight loss, fur texture, posture, activity and diarrhoea.

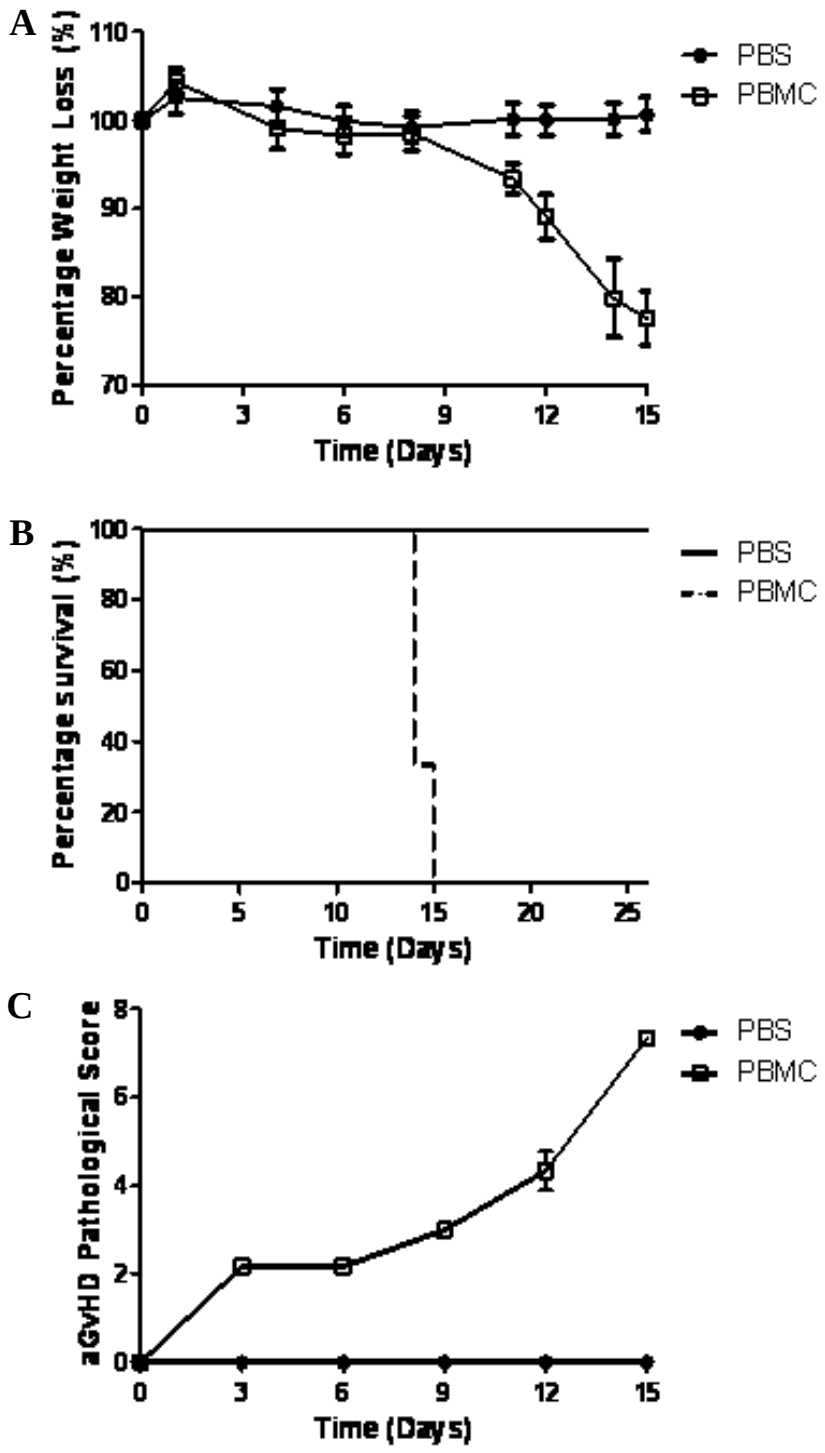

Fig 5.2 aGvHD development in a humanised mouse model. Human PBMC at 2 x 10^7 were given i.v. via the tail vein to low dose irradiated NSG mice. aGvHD development measured daily by (A) weight loss, (B) Survival or (C) Pathological Score (hunched posture, ruffled fur, reduced activity or diarrhoea). aGvHD development occurred between day 10 and 15 (n=3).

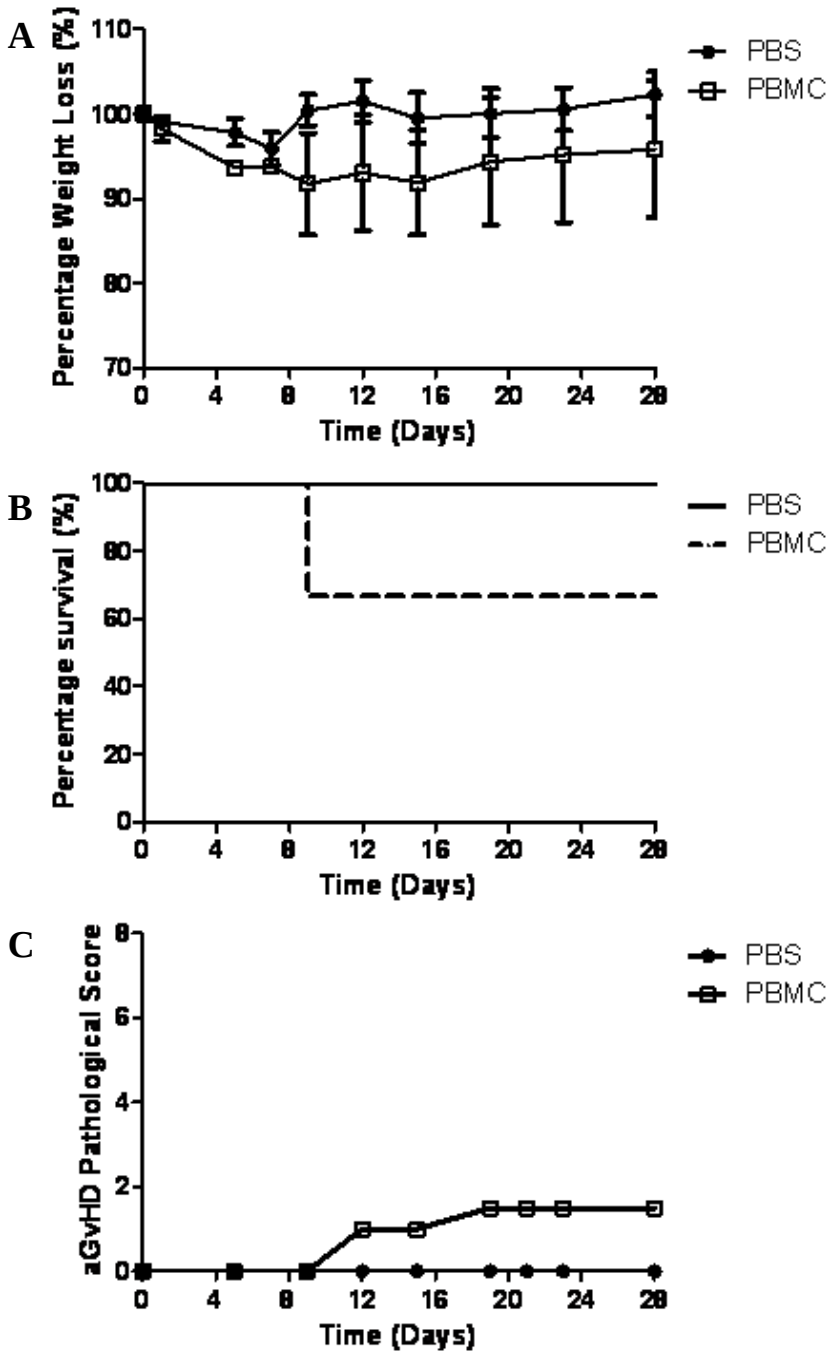

Fig 5.3 aGvHD development was not consistent between experiments. Human PBMC at 2 x 10^7 were given i.v. via the tail vein of low dose irradiated NSG mice. aGvHD development, measured by (A) weight loss (B) Survival or (C) Pathological Score (including hunched posture, ruffled fur, reduced activity and diarrhoea) were measured daily. However, PBMC administration at 2 x 10^7 per mouse did not consistently lead to aGvHD development between day 10 and 15, as after 20 days (B) 66% of mice had survived (n=3).

5.3 HUMAN PBMC READILY ENGRAFT IN NOD-SCID IL2RγNULL MICE

To further understand the model, it was important to determine if freshly isolated human PBMC could engraft in NSG mice. Using the protocol described in section 5.2 and in section 2.11.1, PBMC (2 x 10^7/mouse) were administered to low dose irradiated mice, and at day 12 NSG mice were sacrificed and spleens were harvested. Splenocytes were examined for the expression of mouse and human CD4, CD8 or CD45 by flow cytometry. As NSG mice lack mature lymphocytes, it was not surprising that splenocytes isolated from NSG mice that received PBS did not possess detectable cells that expressed any mouse or human T cell markers (Fig 5.4 A & B respectively). This indicated that the NSG mouse model was not "leaky" with rare occurrence of murine lymphocytes and that human reagents did not cross react with non-target mouse cells. Following human PBMC transfusion, cells expressing human CD4, CD8 or CD45 were detected (Fig 5.4 C). The key finding of this experiment was that human cells engrafted in the model and were not eliminated. Human PBMC remained detectable for at least 12 days post transfusion, a period when aGvHD pathology was developing.

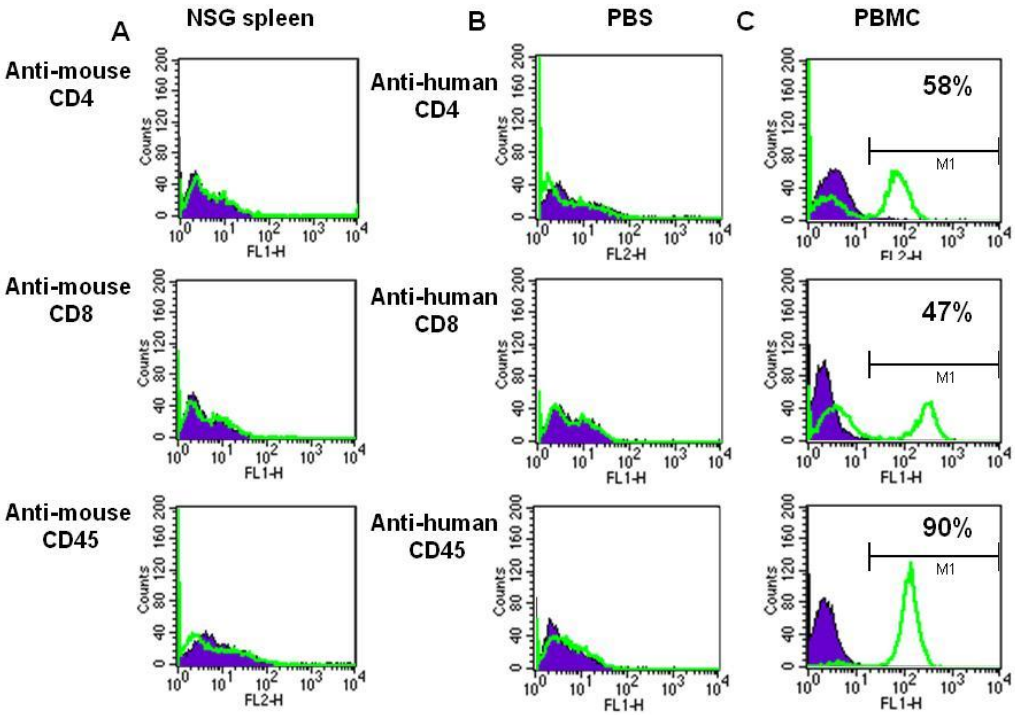

Fig 5.4 Human PBMC engraftment in NOD-Scid IL2rγ^{null} mice. Using flow cytometry, NSG mice that received PBS or human PBMC were examined for murine and human T cell markers on day 12 post transfusion. Murine CD4^{+}, CD8^{+} or CD45^{+} cells were not detected in the spleen of PBS or PBMC treated mice. Human CD4^{+}, CD8^{+} and CD45^{+} cells were detected among the splenocytes of NSG mice that received human PBMC. Data are representative of three spleens per treat group.

5.4 THE DOSE OF PBMC IS CRITICAL FOR CONSISTENT AGVHD DEVELOPMENT

Pearson *et al.* suggested 2 x 10^7 PBMC were required for consistent aGvHD development in a humanised mouse model (Pearson, 2008). However, using the above protocol (Fig 5.1), PBMC at 2 x 10^7 per mouse yielded inconsistent aGvHD development (Fig. 5.2 & 5.3). Therefore, the number of PBMC required for consistent development of aGvHD was examined. PBMC isolated from buffy coat preparations (Chapter 2.3.6) were administered i.v. at varying doses per mouse (Fig 5.5 & 5.6). PBMC (2 x 10^5, 2 x 10^6, 2 x 10^7, 3 x 10^7 or 4 x 10^7 per mouse) were administered following low dose total body irradiation of 2.4 Gy. The percentage weight loss (Fig 5.5 A & 5.6 A), percentage survival (Fig 5.5 B & 5.6 B) and pathological parameters (Fig 5.5 C & 5.6 C) were recorded daily. PBMC at 2 x 10^7 per mouse induced aGvHD development in 40% of mice by day 15 (n=5), with 60% of mice surviving for more than 30 days (Fig 5.5 B). PBMC administered at 2 x 10^5 or 2 x 10^6 (n=5) did not induce aGvHD development, with 100% mice surviving for more than 30 days (Fig 5.5 B). This suggested that, although Pearson *et al.* recommended 2 x 10^7 PBMC for aGvHD development in this model, a higher dose of PBMC was required for consistent aGvHD pathology. Lower doses of PBMC were not successful in inducing aGvHD.

Upon increasing the dose of PBMC per mouse, a more consistent outcome was observed (Fig 5.6). PBMC given i.v. at 2 or 3 x 10^7 per mouse (n=3) induced aGvHD by day 15 (Fig 5.6). Interestingly, only 2 of 3 mice given PBMC at 4 x 10^7 developed aGvHD by day 15 (n=3). This was difficult to explain and no experimental observation was noted indicating a reason. It may be that the sample size was too low; however, it may be that at high doses, physiological effects of

large cell numbers may lead to deletion or PBMC apoptosis. Alternatively, PBMC cell clumping may impair the ability of PBMC to function *in vivo*. It should be noted that in these dose-ranging studies, small numbers of mice were used without repetition. This limitation was to preserve the numbers of valuable experimental animals and these studies were not used to test a hypothesis but rather to optimise a protocol.

The above data indicated the need for a higher dose of PBMC for more consistent aGvHD development in this model. However, protocols with more consistency were still required as some repeat experiments using 3×10^7 PBMC per mouse did not result in aGvHD development or resulted in aGvHD development by day 10, which was too severe to treat using MSC as a cell therapy (data not shown). Differences in PBMC delivery rate, source, T-cell dose and initial mouse weight were unavoidable in our experimental set up. Some of these differences were potentially involved in the development of aGvHD. Therefore, attempts were made to limit variation in set up and in further studies PBMC were isolated freshly from whole blood sampled on the day of administration and the source of PBMC were confined to a panel of four selected healthy donors.

The optimal dose of PBMC required for aGvHD pathology was now determined by taking into account the initial starting weight of NSG mice. Using the initial starting weight and the number of PBMC administered, the amount of freshly isolated PBMC required for aGvHD pathology was calculated per gram of mouse body weight. By reanalysing earlier data, it was calculated that 6.3×10^5 PBMC g^{-1} (23 g mouse) were required for aGvHD development by day 12-15 post i.v. injection. This protocol was found to be reproducible and consistent in additional experiments, as all NSG mice (n=5) that were given 6.3×10^5 PBMC g^{-1} developed

aGvHD had more than 15% weight loss, displayed pathological symptoms of aGvHD and were sacrificed by day 14 (Fig 5.7). This protocol was therefore adopted as the optimised aGvHD model for subsequent studies.

5.5 INITIAL MSC EFFICACY STUDIES AGAINST AGVHD IN A HUMANISED MOUSE MODEL

Human MSC (hMSC) used as a therapy were characterised as described in chapter 3, section 3.2 to 3.5. hMSC expressed typical surface markers, MHC class I, Sca-1 and CD90, retained tri-lineage differentiation capacity into osteocytes, adipocytes and chondrocytes and were capable of suppressing both allogeneic and mitogen driven proliferation *in vitro*. Prior to optimisation of the humanised mouse aGvHD model, initial studies were performed with hMSC as a therapy when given on day 7. In this case, PBMC at 2×10^7 and varying doses of hMSC at 2×10^6, 0.4×10^6 or 0.08×10^6 were given per mouse. The percentage weight loss, survival and aGvHD pathological scoring are represented in Fig 5.8. In some instances, hMSC appeared to influence aGvHD development, as NSG mice that received hMSC (2×10^6, 0.4×10^6) as a therapy on day 7 developed the signs of aGvHD, weight loss, ruffled fur, reduced activity and hunched posture (Fig 5.8 A & C). However, NSG mice that received PBMC did not develop any significant signs of aGvHD and all mice survived (Fig 5.8 A, B & C). As the humanised model was highly variable at this point, no firm conclusions were made, but it did inform the choice in determining the exact number of PBMC (6.3×10^5 g^{-1}) and hMSC (4.4×10^4 g^{-1}) per gram of body weight in later studies.

Following the optimisation of the humanised model (Fig 5.7), hMSC as a cell therapy was examined again. However, previous work from our lab (Kavanagh,

2011) and other groups (Li, 2008) were taken into consideration when deciding on a dose for hMSC treatment. We found that hMSC therapy of between 0.5 x 10^6 and 2 x 10^6 cells per mouse proved beneficial in reducing pathology in many mouse inflammatory models, including aGvHD and allergen driven asthma (Li, 2008; Kavanagh, 2011). Therefore, hMSC given at 1 x 10^6 cells per mouse (23g mouse) or more precisely the equivalent of 4.4 x 10^4 cells per gram (as calculated in section 5.4) on day 7 were used here. hMSC therapy was found to have a beneficial influence on aGvHD development, as by day 12 NSG mice that received PBMC alone developed aGvHD, while NSG mice treated with hMSC showed little or no signs of aGvHD (Fig 5.9). This hMSC dose was therefore selected for all future studies.

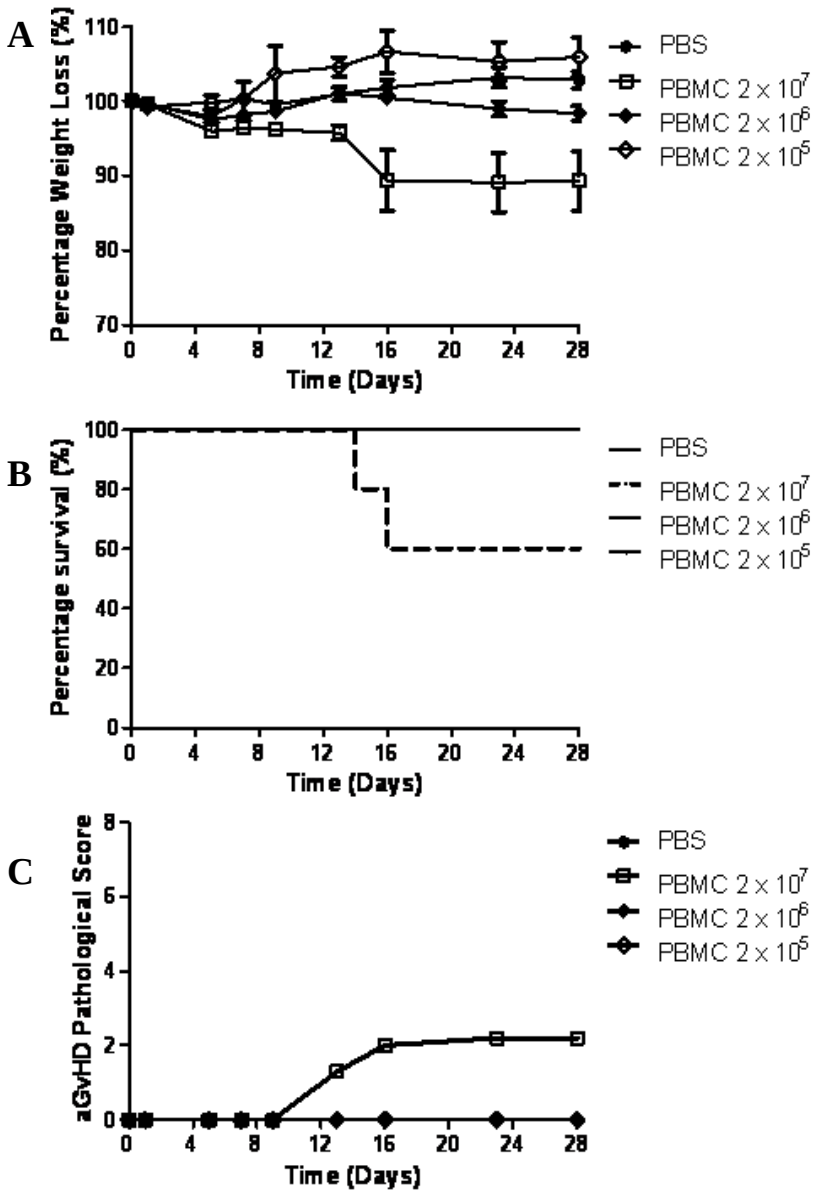

Fig 5.5 Optimisation of PBMC dose-initial studies. NSG mice received 2.4 Gy irradiation. After 4 h, PBMC at 2 x 10^7, 2 x 10^6 or 2 x 10^5/mouse were injected i.v. into the tail vein. Mice were monitored daily for the development of aGvHD. (A) Percentage weight loss (B) percentage survival and (C) pathological signs of aGvHD development were recorded. PBMC at 2 x 10^7 per mouse did not induce consistent aGvHD development (n = 5 mice per group).

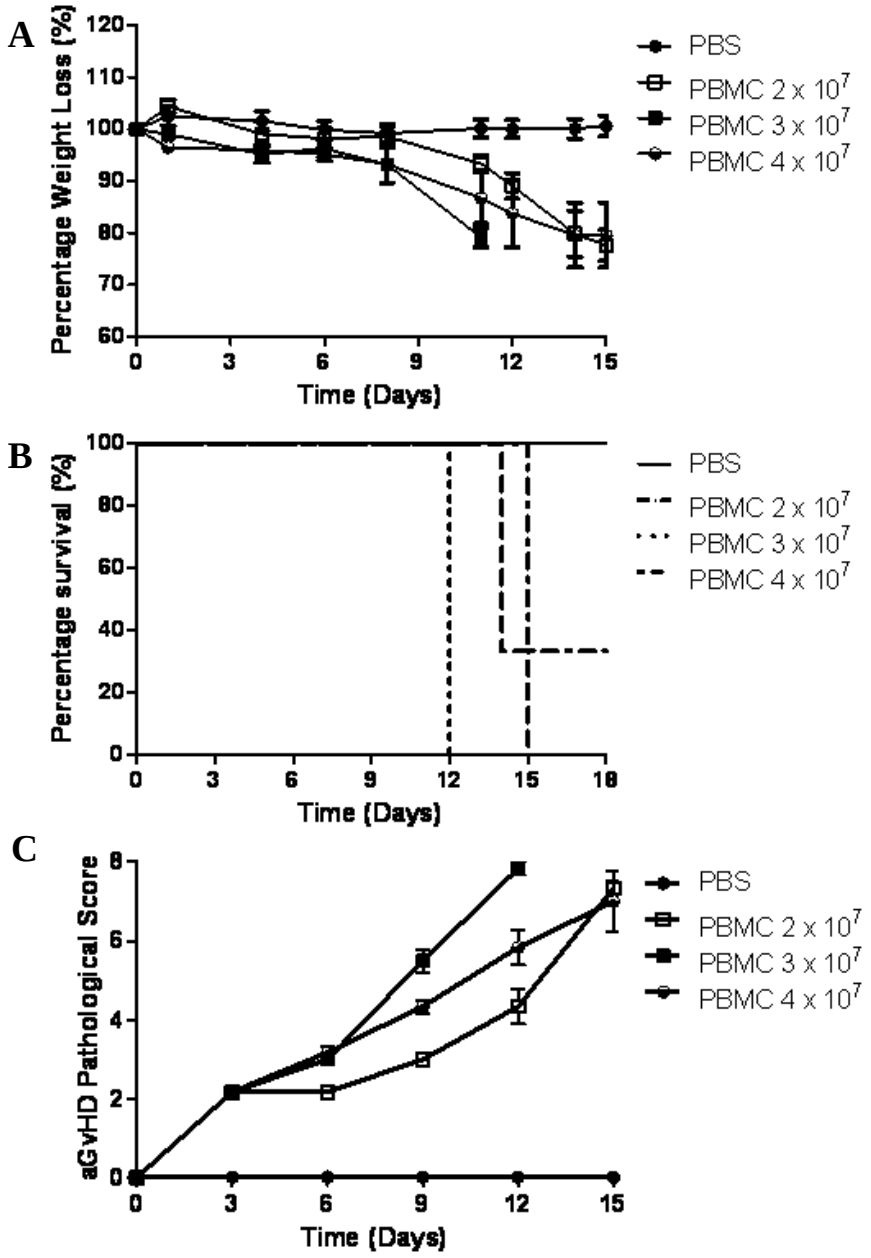

Fig 5.6 Optimisation of PBMC dose-follow on studies. NSG mice received 2.4 Gy irradiation. After 4 h, PBMC at 2 x 10^7, 3 x 10^7 or 4 x 10^7/mouse were i.v. injected into the tail vein. Mice were monitored daily for the development of aGvHD. (A) Percentage weight loss, (B) survival and (C) pathological signs of aGvHD development were recorded. 3 x 10^7 and 2 x 10^7 PBMC/mouse induced aGvHD development in 100% of mice by day 12 and 15 respectively (n = 3 mice per group).

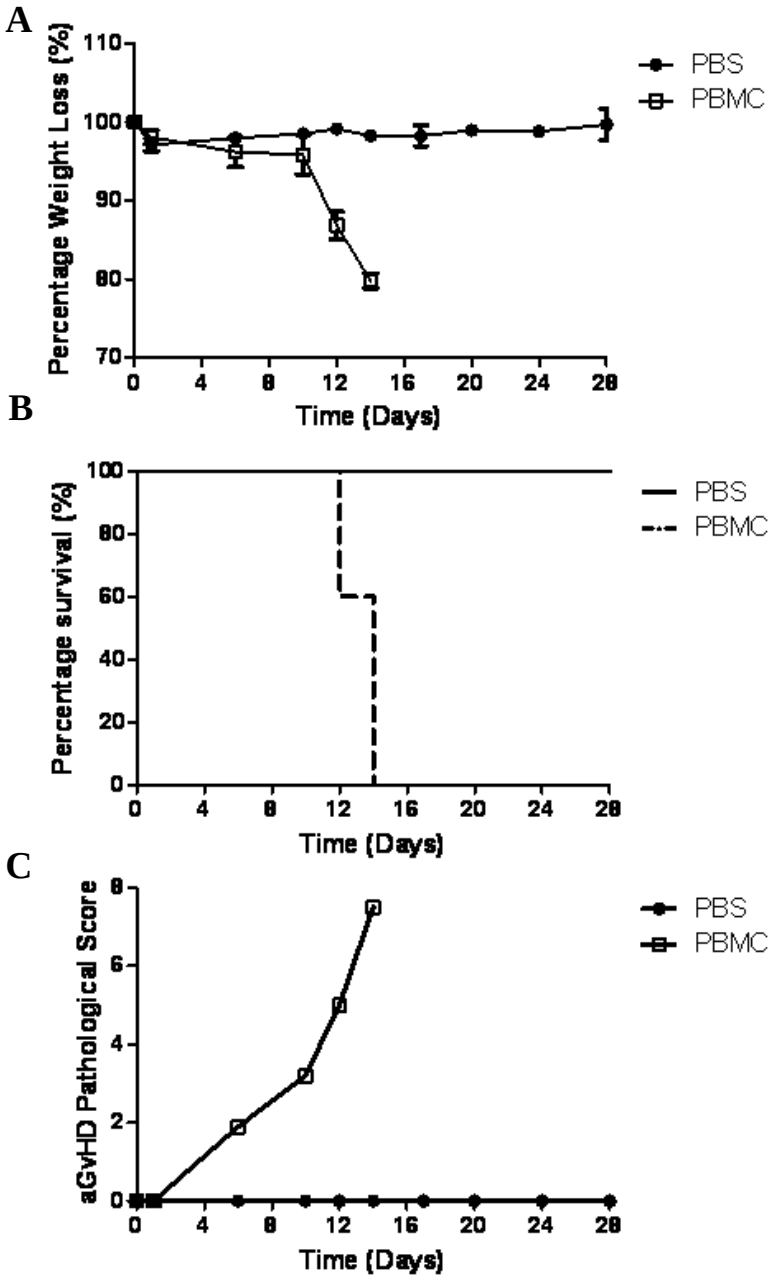

Fig 5.7 Optimisation of PBMC dose-optimised model. NSG mice received 2.4 Gy gamma irradiation. After 4 h, PBMC at 6.3 x 10^5 g^{-1} were i.v. injected into the tail vein. NSG mice were monitored daily for the development of aGvHD. aGvHD development indicative of (A) >15% weight loss, recorded by day 14. (B) Percentage survival and (C) pathological signs of aGvHD development reached a cumulative score of eight by day 14. 6.3 x 10^5 g^{-1} PBMC induced consistent aGvHD development (100%) by day 14. (n = 5 mice per group).

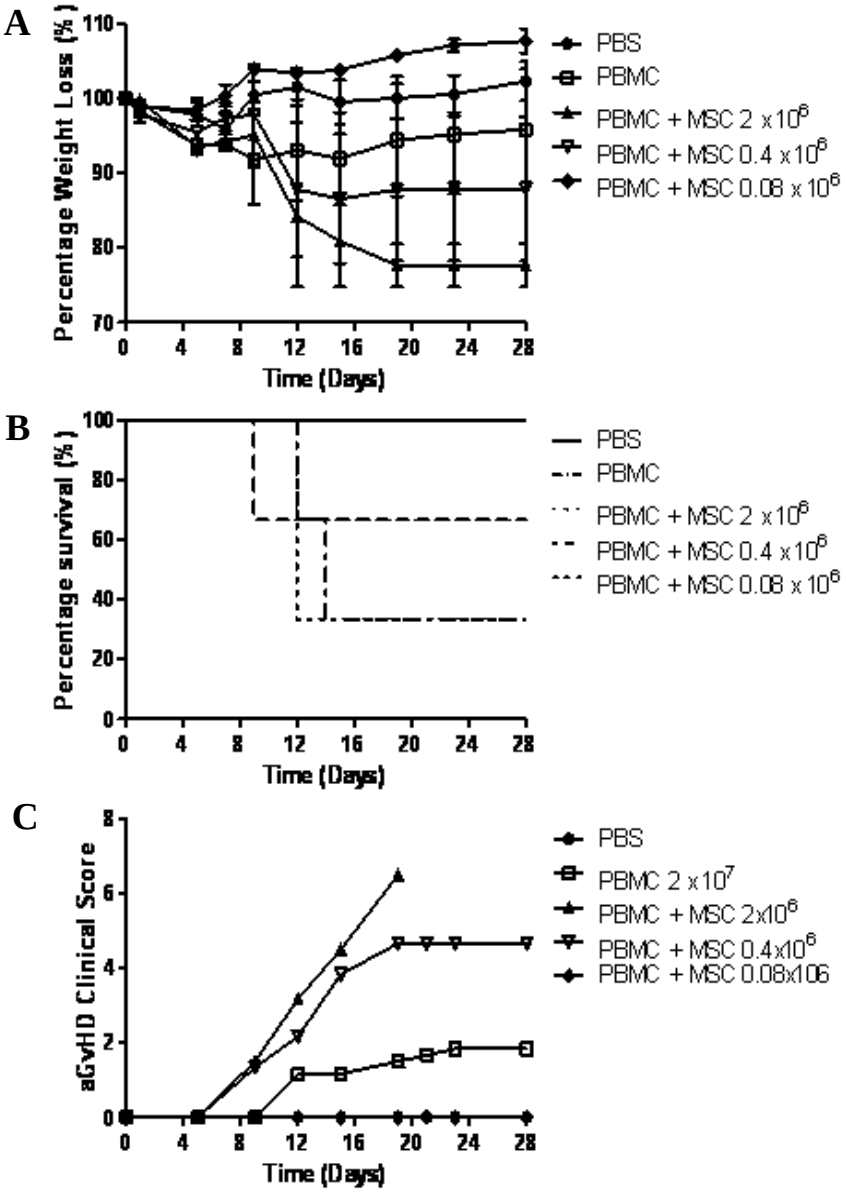

Fig 5.8 Optimisation of MSC dose response-1. NSG mice received 2.4 Gy irradiation. After 4 h, PBMC at 2 x 10^7/mouse were i.v. injected into the tail vein. hMSC were given on day 7 at varying concentrations, 2 x 10^6, 0.4 x 10^6 or 0.08 x 10^6/mouse. (A) Weight loss, (B) survival and (C) aGvHD pathological scores were monitored daily for signs of aGvHD development. hMSC at 2 x 10^6 or 0.4 x 10^6 seemed to contribute to aGvHD development. However, PBMC at 2 x 10^7 proved inconsistent for aGvHD pathology (n = 3 mice per group).

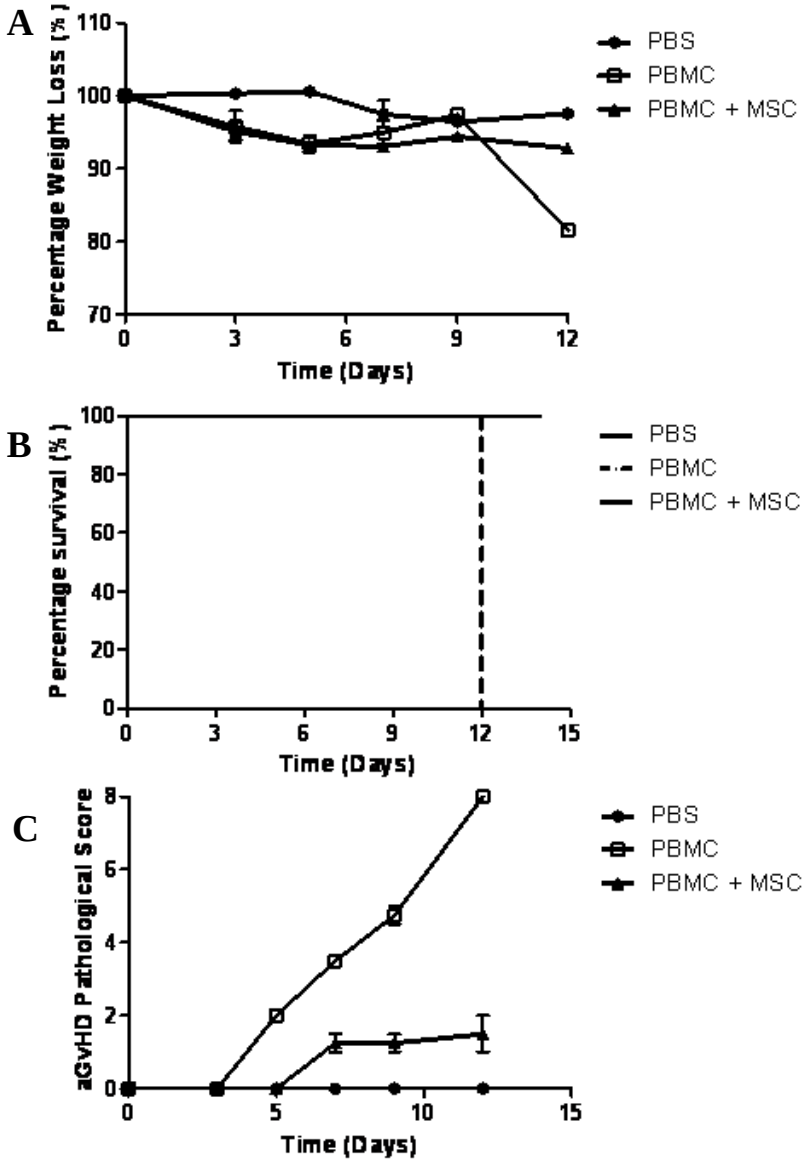

Fig 5.9 Optimisation of MSC dose response-2. NSG mice received 2.4 Gy irradiation. After 4 h, PBMC at 6.3 x 10^5 g^{-1} were i.v. injected into the tail vein. hMSC were given on day 7 at 4.4 x 10^4 g^{-1}. (A) Percentage weight loss, (B) percentage survival and (C) aGvHD pathological scores were monitored daily for signs of aGvHD development. PBMC at 6.3 x 10^5 g^{-1} induced consistent signs of aGvHD (A & C) by day 12. hMSC therapy dampened the signs of aGvHD pathology and prolonged the survival of NSG mice when compared to PBMC alone mice on day 12 (n = 2 mice per group).

5.6 THE EFFICACY OF MSC THERAPY IS DEPENDENT ON TIME OF ADMINISTRATION

The time of administration of cell therapy may be a critical parameter in determining efficacy and clinical application. This was amenable to study in our system. Using the newly optimised protocol for aGvHD development in a humanised mouse model (Fig 5.7), NSG mice were given low dose total body irradiation of 2.4 Gy and freshly isolated PBMC (6.3×10^5 g^{-1}) from healthy donors. hMSC (4.4×10^4 g^{-1}) were given as a therapy on day 0, 7 or 14 (Fig 5.10). Irradiation alone did not induce pathology or affect the wellbeing of the mice, as NSG mice that received PBS alone did not develop aGvHD and had no observed effect from irradiation. However, mice that were irradiated and received PBMC (6.3×10^5 g^{-1}) on day 0, developed significant weight loss, had signs of ruffled fur, reduced activity and hunched posture leading to 100% of mice developing aGvHD by day 15 (Fig 5.10). hMSC therapy delivered concurrent with PBMC had no beneficial effect, as 66% of mice had significant weight loss and developed pathological signs of aGvHD (n=3) (Fig 5.10 C) by day 25 and were sacrificed. However, hMSC given as a treatment on day 7 or day 14, significantly prolonged the survival of mice ($p<0.0001$) (100%) for more than 28 days and mice did not develop any significant pathological signs of aGvHD, when compared to hMSC treatment at day 0 (Fig 5.10 B & C). These data suggested that the timing of hMSC therapy was important for the successful treatment of aGvHD, with hMSC therapy on day 7 post PBMC administration proving to be beneficial. However, due to limited numbers of mice and to preserve animals for further studies on the protective mechanism involved, the numbers of mice used here for this study were limited (n=3).

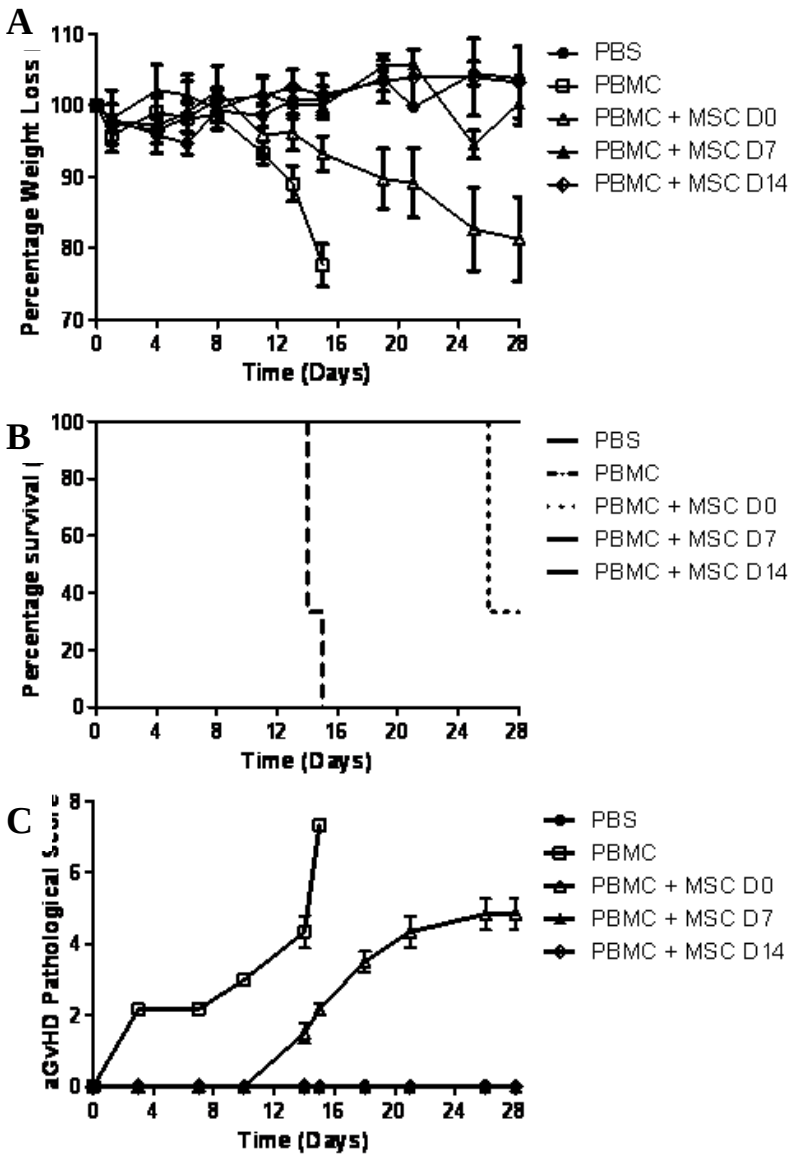

Fig 5.10 MSC cell therapy is time dependent. NSG mice received 2.4 Gy irradiation, 4 h later, PBMC at 6.3 x 10^5 g^{-1} were i.v. injected into the tail vein. hMSC were administered at 4.4 x 10^4 g^{-1} on day 0, concurrent with PBMC or on day 7 or 14 after PBMC treatment. (A) Percentage weight loss (B) Survival and (C) aGvHD pathological symptoms were recorded daily. hMSC administered on day 0 had no significant beneficial effect in preventing (A) weight loss, (B) prolonging survival or (C) reducing aGvHD-like symptoms. However, hMSC administered on day 7 or 14 significantly ($p<0.0001$) increased aGvHD related (B) survival and (C) reduced aGvHD like pathological symptoms (n = 3 mice per group).

5.7 HUMAN MSC PROLONGED THE SURVIVAL OF NSG MICE WITH AGVHD

The series of experiments above meant that it was possible to perform a larger, more informative experiment to determine if hMSC therapy had a beneficial effect on aGvHD development. Freshly isolated PBMC from healthy donors were administered i.v. on day 0 at 6.3 x $10^5 g^{-1}$ to NSG mice after low dose body irradiation. On day 7, hMSC (4.4 x 10^4 g^{-1}) were given i.v. as a cell therapy. NSG mice that received irradiation and PBS alone (n=5) did not develop any signs of aGvHD, such as excessive weight loss, hunched posture, reduced activity or ruffled fur (Fig 5.11). NSG mice that received PBMC on day 0 (n=5), all consistently developed aGvHD (100%) by day 12, indicated by >15% weight loss and development of aGvHD pathology (Fig 5.11 A & C). hMSC treatment on day 7, significantly prolonged the survival ($p<0.0008$) of NSG mice with aGvHD with 20% of mice surviving for more than 30 days (Fig 5.11 B). These data demonstrated that the timing of hMSC administration was important in the use of hMSC as a therapy in aGvHD and that hMSC could significantly reduce the development of aGvHD in this model.

5.8 IFNγ STIMULATION ENHANCED THE IMMUNOSUPPRESSIVE CAPACITY OF MSC *IN VITRO*, BUT TNFα STIMULATION DID NOT

For clinical use, hMSC must remain immunosuppressive in an inflammatory environment. Therefore, the effects of IFNγ and TNFα stimulation on the expression of immunosuppressive properties by hMSC were studied to improve understanding of how hMSC work *in vivo* in the treatment of aGvHD. IFNγ and TNFα are two key proinflammatory cytokines involved in aGvHD pathology. Ryan *et al.* found that IFNγ stimulation on MSC promoted the immunosuppressive capacity of hMSC

(Ryan, 2007). While Polchert *et al.* showed that IFNγ stimulated mMSC were five-fold more beneficial in treating aGvHD in a mouse model, compared to unstimulated mMSC (Polchert, 2008). TNFα on the other hand, can have multiple effects on MSC growth factor secretion, proliferation and survival depending on which TNF receptor is activated (Miettinen, 2011). hMSC were stimulated *in vitro* with IFNγ or TNFα for 48 h and the expression of MHC class I and II were analysed by flow cytometry. Unstimulated hMSC expressed MHC class I and not MHC class II (Fig 5.12 A). However, IFNγ (MSCγ) induced the expression of MHC class II on hMSC (Fig 5.12), whereas, TNFα (MSCα) stimulation did not (Fig 5.12).

The ability of stimulated hMSC to inhibit the proliferation of mitogen driven lymphocytes was analysed. Here, hMSC or hMSC pre-stimulated with IFNγ or TNFα for 48 h, were placed in a proliferation assay in the presence of donor lymphocytes stimulated using the mitogen ConA. As shown in chapter 3.5, hMSC significantly inhibited the proliferation of allogeneic lymphocytes *in vitro.* Pre-stimulation of hMSC with IFNγ or TNFα, did not interfere with the ability of hMSC to suppress lymphocyte proliferation (Fig 5.12 B). These data suggested that in the presence of inflammatory cytokines, hMSC were still capable of immunosuppression. These findings were similar to that found by Polchert *et al.*, therefore, the *in vivo* influence of stimulation by IFNγ on MSC was examined further.

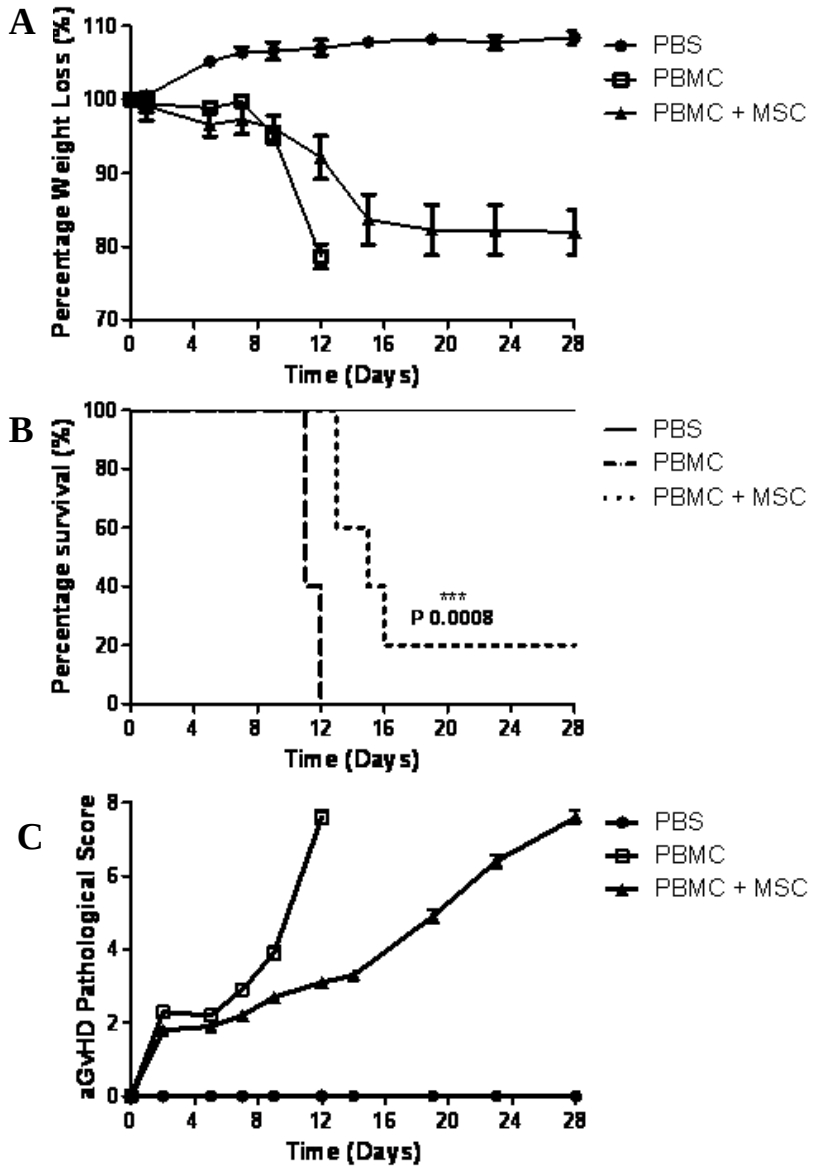

Fig 5.11 MSC cell therapy on day 7 prolonged the survival of NOD Scid IL-2rγ^{null} mice with aGvHD. NSG mice received 2.4 Gy irradiation. After 4 h, PBMC at 6.3 x $10^5 g^{-1}$ were i.v. injected into the tail vein. hMSC were administered at 4.4 x 10^4 g^{-1} on day 7 post PBMC transfusion. (A) Percentage weight loss, (B) percentage survival and (C) pathological signs of aGvHD were recorded daily. hMSC significantly prolonged the survival ($p<0.0008$) of NSG mice with aGvHD, slowing down the rate of weight loss and reducing the clinical signs of aGvHD development (n=5 mice per group). Statistical analysis was carried out using Kaplan Meier survival curves.

A

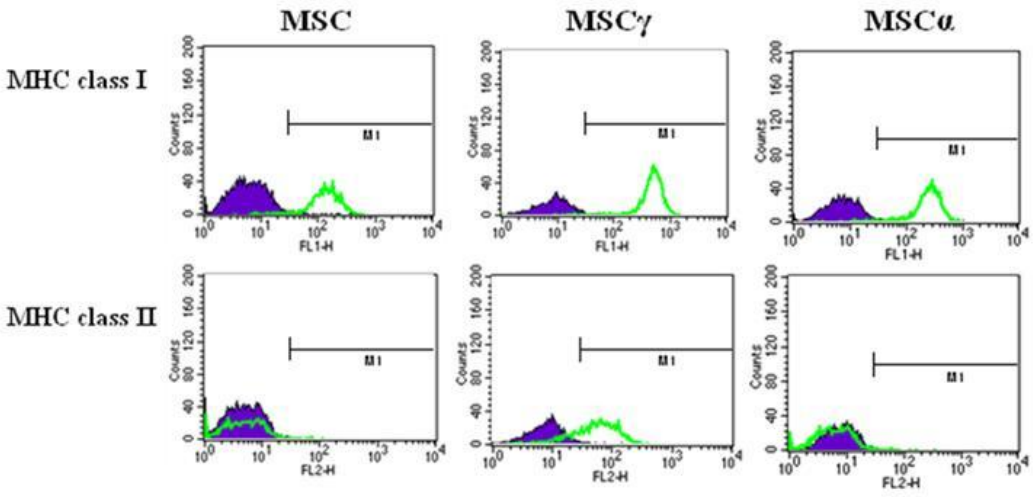

B

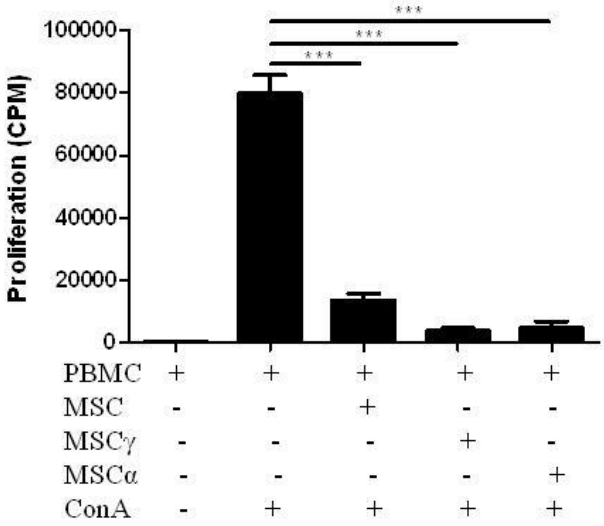

Fig 5.12 IFNγ and TNFα stimulation did not interfere with the immunosuppressive capacity of hMSC. (A) IFNγ stimulation for 48 h upregulated the expression of MSC class II on hMSC, whereas TNFα licensing had no effect on MHC class II expression on hMSC as shown by flow cytometry. (B) hMSC, IFNγ (MSCγ) or TNFα (MSCα) stimulated hMSC were cocultured with PBMC in a mitogen driven proliferation assay. IFNγ or TNFα stimulation did not ablate hMSC inhibition of proliferation (n = 3). Statistical analysis was carried out using the students paired t test.

5.9 IFNγ STIMULATED MSC PROLONGED THE SURVIVAL OF NOD SCID IL-2RγNULL MICE WITH AGVHD WHEN COMPARED TO UNSTIMULATED MSC

The data above suggested a mechanism where hMSC stimulated with IFNγ prior to administration, become activated and somehow are better able to suppress aGvHD. hMSC stimulated by IFNγ showed an increased ability to inhibit proliferation *in vitro* (Fig 5.11). These data suggested the investigation of IFNγ prestimulated hMSC in the treatment of aGvHD in the optimised humanised NSG murine model. The approach here was to prestimulate hMSC with IFNγ (MSCγ) for 48 h prior to their administration to NSG mice on day 0 in conjunction with PBMC. As usual, all mice were irradiated with 2.4 Gy on day 0 and allowed to rest for 4 h before PBMC infusion. Prestimulated MSC (MSCγ) were given concurrent with PBMC on day 0. The symptoms of aGvHD developed by 15, when 100% of mice receiving PBMC alone showed signs of aGvHD (n=5) (Fig 5.13). Treatment with hMSCγ on day 0 significantly prolonged survival ($p<0.0057$) of mice when compared to mice that had not received any hMSC therapy.

These data showed that hMSC prestimulated with IFNγ administered concurrent with PBMC had a beneficial effect on the development of aGvHD. Comparing data from Fig 5.13 with Fig. 5.11, hMSCγ and MSC were equally successful in dampening aGvHD pathology. These data were similar to the findings of Polchert *et al.,* whereby murine MSCγ therapy was found to prevent aGvHD development. However in the model herein, prestimulated hMSC as a therapy prolonged the survival of mice with aGvHD, but did not prevent aGvHD development completely, which was a finding closer to the Osiris Therapeutics phase III clinical trial (Martin, 2010).

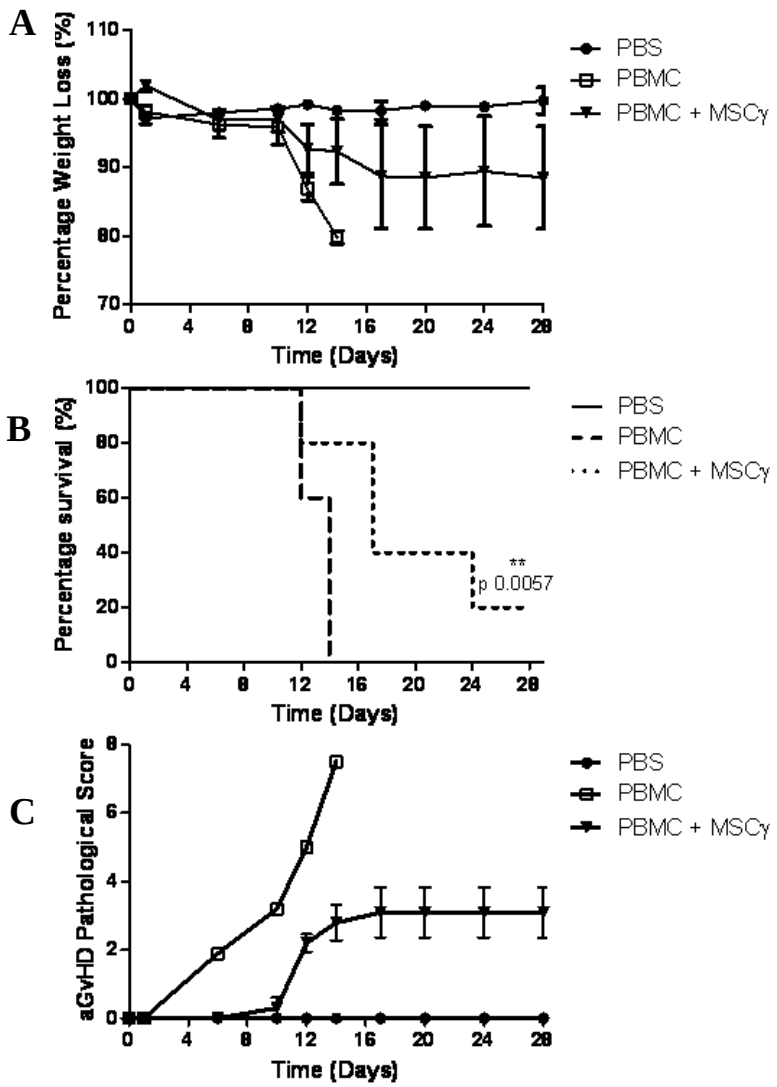

Fig 5.13 Prestimulated MSC significantly prolonged the survival of NOD Scid IL-2rγ^{null} mice with aGvHD. NSG mice received 2.4 Gy irradiation. After 4 h, PBMC at 6.3 x 10^5 g^{-1} were i.v. injected into the tail. IFNγ stimulated MSC (MSCγ) were administered at 4.4 x 10^4 g^{-1} in conjunction with PBMC on day 0. (A) Percentage weight loss, (B) percentage survival and (C) pathology of aGvHD development were recorded daily. MSCγ as a therapy significantly ($p<0.0057$) prolonged the (B) survival of NSG mice with aGvHD, (C) reducing aGvHD symptoms (n = 5 mice per group). Statistical analysis was carried out using Kaplan Meier survival curves.

5.10 HUMAN MSC THERAPY SIGNIFICANTLY REDUCED AGVHD PATHOLOGY

The main target organs involved in aGvHD pathology include the lung, liver and gut. Joo *et al.* found that MSC improved the histological aGvHD score of target organs after transplantation (Joo, 2010). Therefore, in this study histological analysis was carried out on aGvHD target organs after the transplantation of hMSC as a cell therapy. As in the previous experiment, NSG mice were irradiated and received PBMC (6.3×10^5 g^{-1}) on day 0. Unstimulated hMSC (4.4×10^4 g^{-1}) were given on day 7, whereas IFNγ stimulated hMSC were given in conjunction with PBMC on day 0. On the day of significant aGvHD pathology (approximately day 12), the lung, liver and gut were harvested and placed in formalin for histological analysis.

Tissue sections were stained by H&E and the histological aGvHD score was evaluated for each treatment group according to the criteria described in section 2.12.2 and 2.12.3 (Hill, 1997; Grass, 1999; Polchert, 2008). As expected, the livers of NSG mice that received PBS as a control, appeared normal, with no cell infiltration, tissue fibrosis or endothelialitis (Fig 5.14 A) and the histological scoring presented as normal (score of 0) (Fig 5.14 B). After aGvHD development in mice receiving PBMC alone, there was a significant increase in mononuclear cell infiltration and endothelialitis ($p<0.0001$), especially around the hepatic ducts of the liver, when compared to control PBS mice (Fig 5.14 A & B). hMSC treatment on day 7 post PBMC transfusion significantly reduced liver pathology ($p<0.0086$), with a decrease in cell infiltration and reduction in the number of hepatic ducts displaying endothelialitis (Fig 5.14 A & B) on day 12. Therapy with IFNγ stimulated hMSC on day 0, significantly reduced aGvHD pathology of the liver also ($p<0.0163$), with a decrease in cell infiltration and endothelialitis around hepatic ducts (Fig 5.13 A &

B). There was no significant difference in pathology between the hMSC and hMSCγ treated groups (Fig 5.14 B), as both therapies worked equally as well.

Histological analysis of tissue sections taken from the small intestine of the gut found that PBS treated mice appeared normal, with no sloughing of villi or no accumulation of infiltrating cells into the laminar propria. However, NSG mice that received PBMC on day 0 had significant blunting of villi and cell infiltration in the lamina propria of the gut when compared to NSG mice that received the PBS control (Fig 5.15 A & B, $p<0.0001$). NSG mice that received IFNγ prestimulated hMSC ($p<0.0142$) or unstimulated hMSC ($p<0.0249$) had significantly less tissue damage to villi and a decrease in mononuclear cell infiltration (Fig 5.15 A & B). As seen in the liver, there was no significant difference between hMSC treated groups, as both groups equally dampened the pathology of aGvHD in the gut (Fig 5.15 B). Histological analysis of PBS treated NSG mouse lungs appeared normal, comprised of regular air spaces and little or no mononuclear cell infiltration (Fig 5.16 A). However, after PBMC delivery, significant pathology of the lung developed with extensive mononuclear cell infiltration into the lung alveolar spaces compared to the PBS control mice (Fig 5.16, $p<0.0002$). Following treatment with unstimulated hMSC on day 7 or IFNγ prestimulated hMSC on day 0, the lung pathology of mice did not improve when compared to aGvHD mice that received PBMC on day 0 (Fig 5.16 A). MSC treatment did not reduce mononuclear cell infiltration into the lungs, which resulted in no change in aGvHD histological scoring in NSG mice with aGvHD (Fig 5.16 B). These data suggested that while hMSC therapy significantly reduced the PBMC mediated damage of the liver and gut, it had no effect on mouse lung.

A

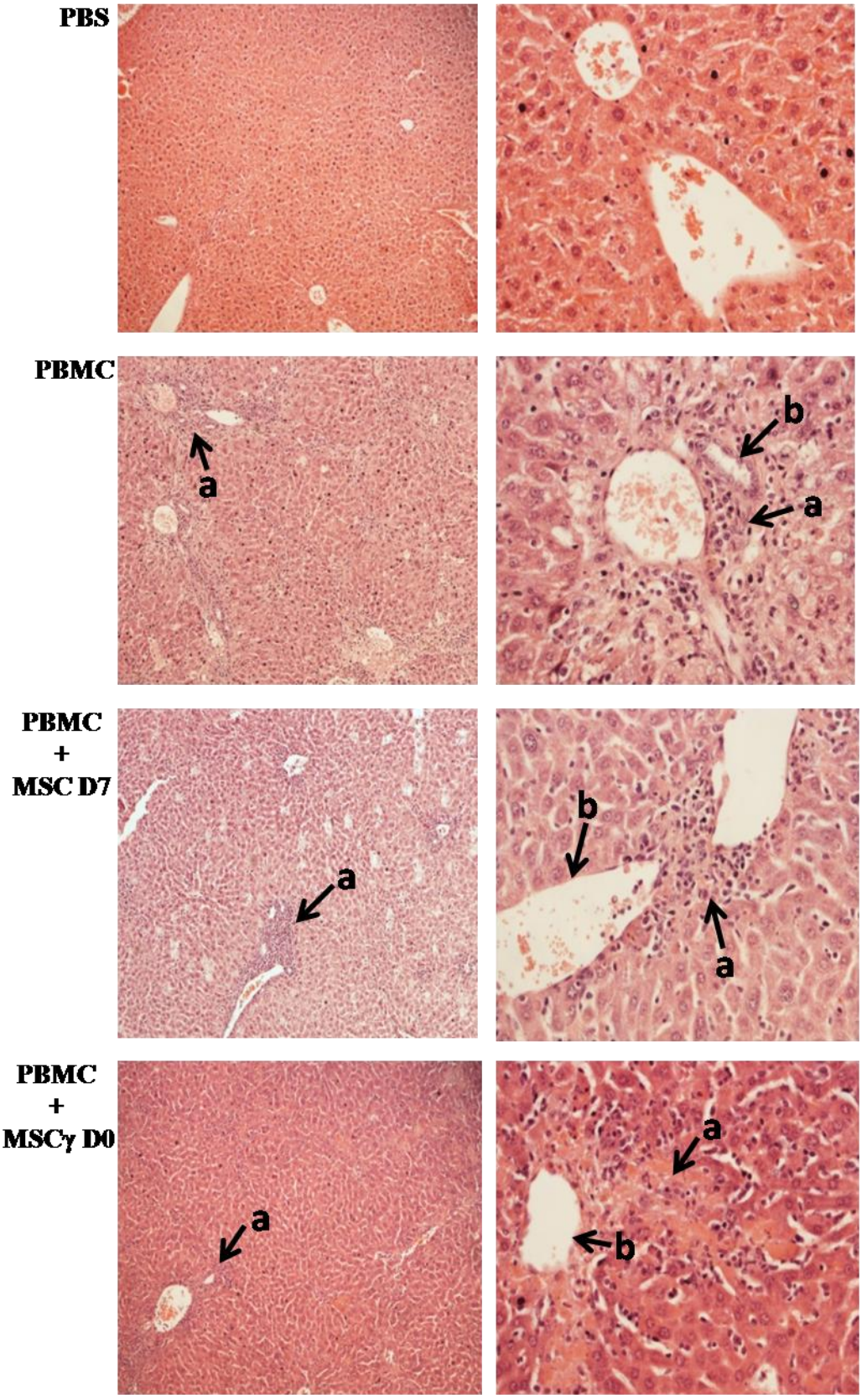

B

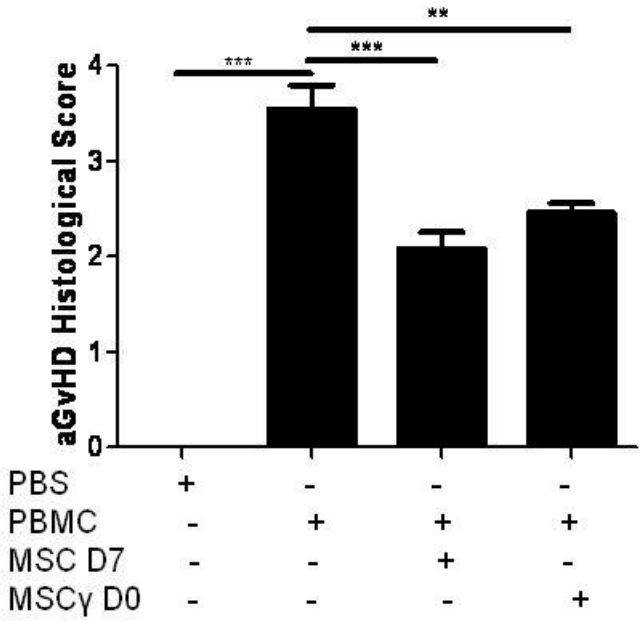

Fig 5.14 Human MSC therapy significantly reduced aGvHD pathology in the liver. NSG mice were given PBMC by i.v. injection on day 0. Mice were treated with unstimulated hMSC on day 7 and IFNγ prestimulated MSC day 0. Following aGvHD development on day 12, livers were harvested from each treatment group and tissue sections were analysed by (A) H&E staining. (B) A well defined aGvHD histological scoring system was used to determine the level of aGvHD development between the groups. (A) Mice that received PBMC on day 0 showed increased mononuclear infiltration (denoted with arrow and letter a) and increased endothelialitis around hepatic ducts (denoted with arrow and letter b). Both unstimulated MSC ($p<0.0086$) and IFNγ prestimulated MSC ($p<0.0163$) significantly improved aGvHD pathology by (A) reducing the collection of mononuclear cells in the hepatic tissue (denoted with arrow and letter a) and reducing the number of vessels displaying endothelialitis (denoted with arrow and letter b). MSC therapy resulted in a reduction in the (B) aGvHD histological score of mice with aGvHD (n = 4 per group). Statistical analysis was carried out using the students paired t test.

A

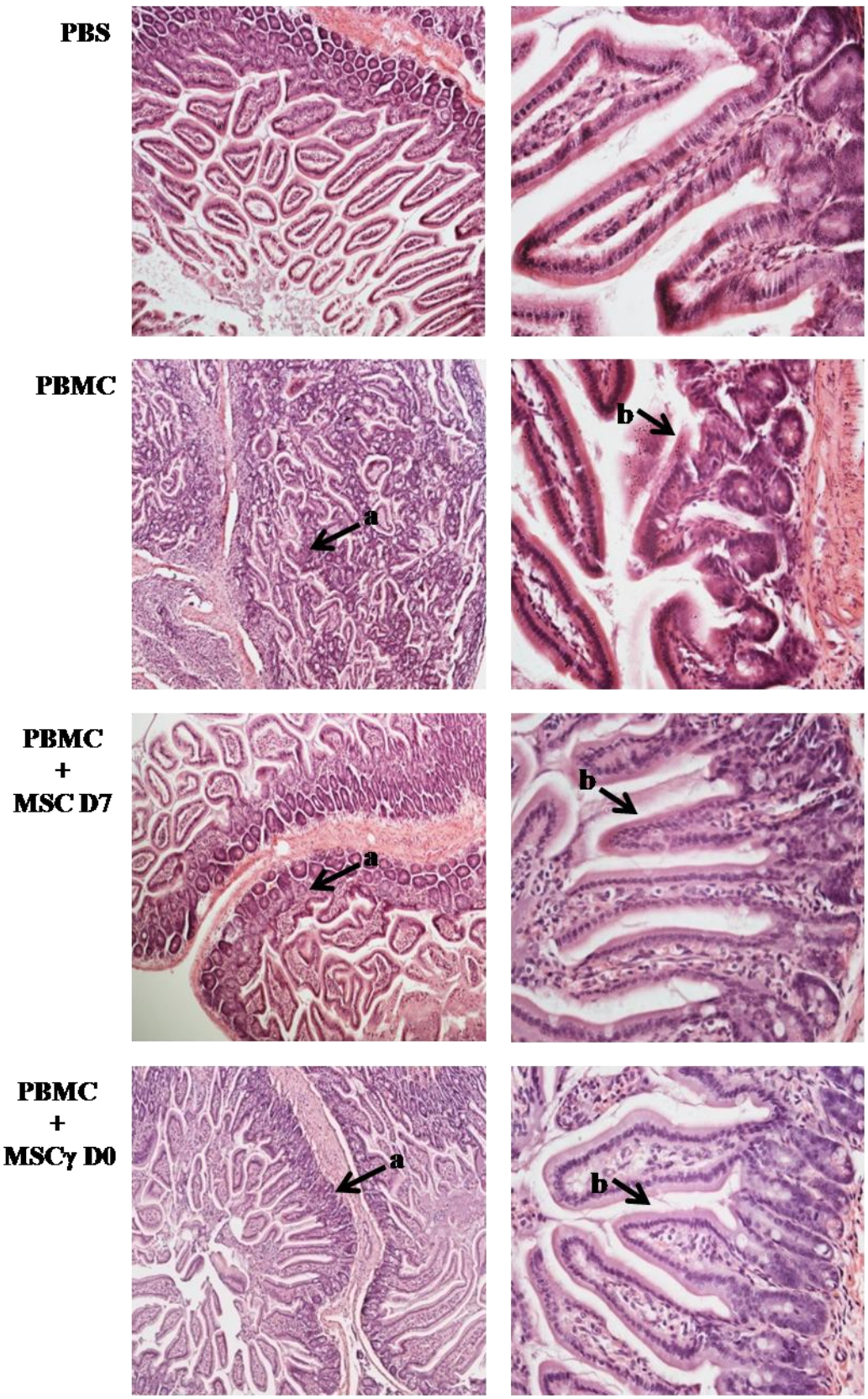

B

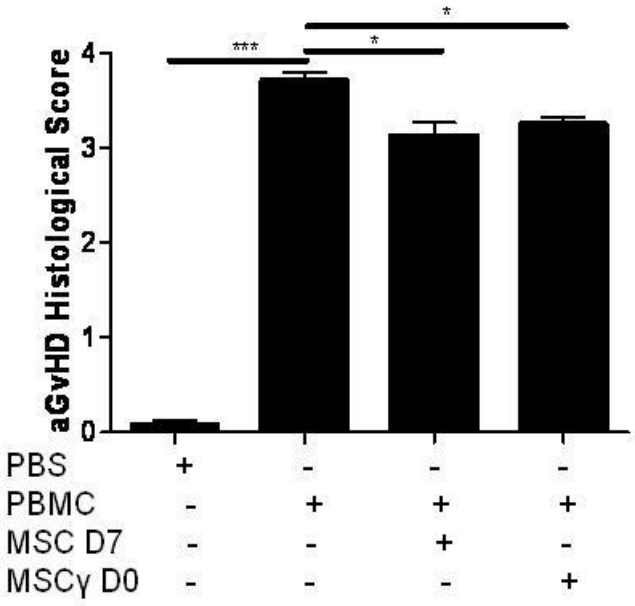

Fig 5.15 Human MSC therapy significantly reduced aGvHD pathology in the gut. NSG mice were given PBMC by i.v. injection on day 0. Mice were treated with unstimulated MSC on day 7 or IFNγ prestimulated MSC day 0. Following aGvHD development on day 12, sections of the gut were harvested from each treatment group and tissue sections were analysed by (A) H&E staining. (B) A well defined aGvHD histological scoring system was used to determine the level of aGvHD development between the groups. (A) Mice that received PBMC on day 0 showed signs of increased cell infiltration (denoted with arrow and letter a) and increased blunting of the villi (denoted with arrow and letter b), indicating a (B) sigificant increase in aGvHD pathology ($p<0.0001$). Both unstimulated MSC ($p<0.0249$) and IFNγ prestimulated MSC ($p<0.0142$) significantly improved aGvHD pathology by (A) reducing cell infiltration (denoted with arrow and letter a) and damage to villi/crypts in lamina propria (denoted with arrow and letter b) and (B) improving the aGvHD histological score of mice with aGvHD (n = 4 per group). Statistical analysis was carried out using the students paired t test.

A

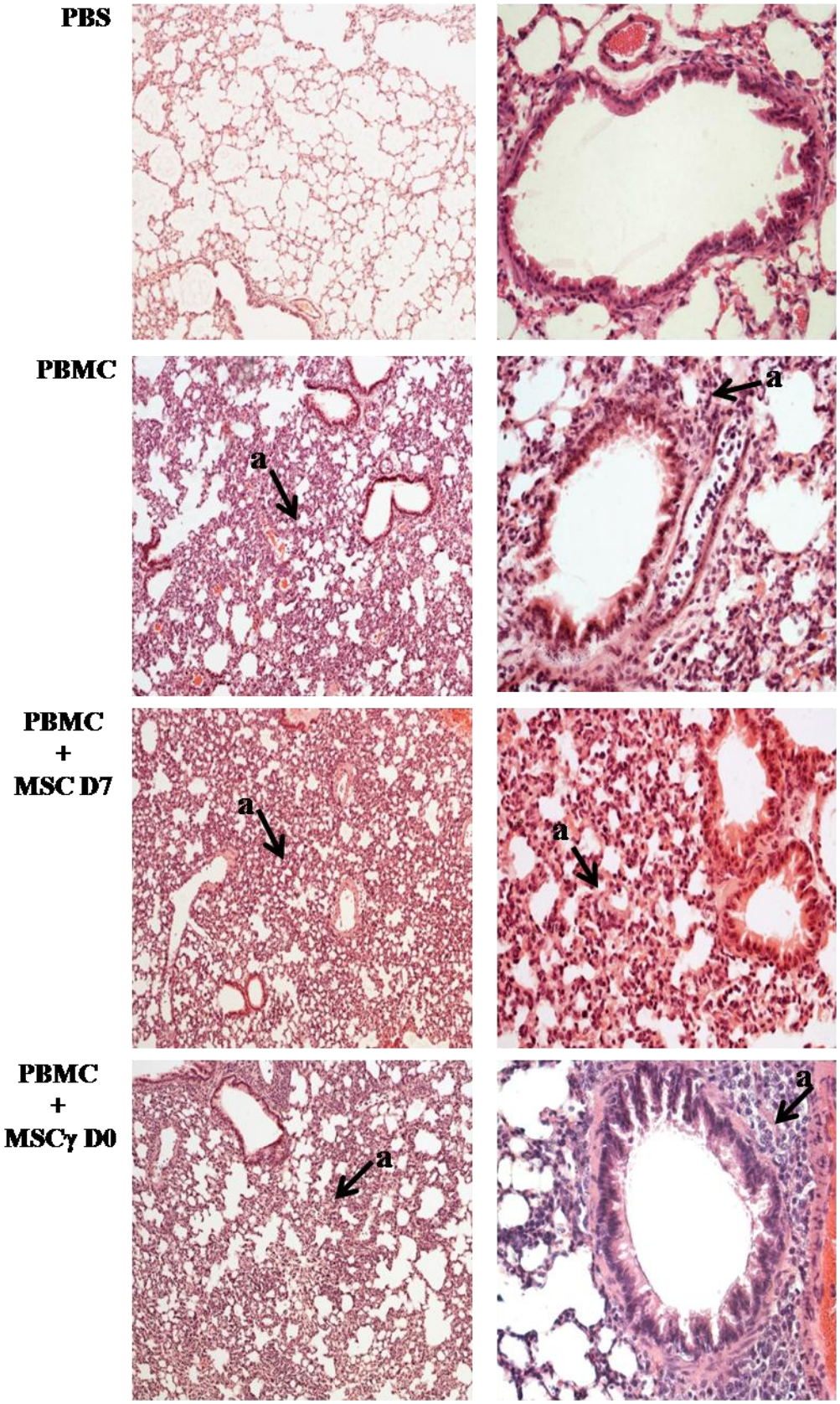

B

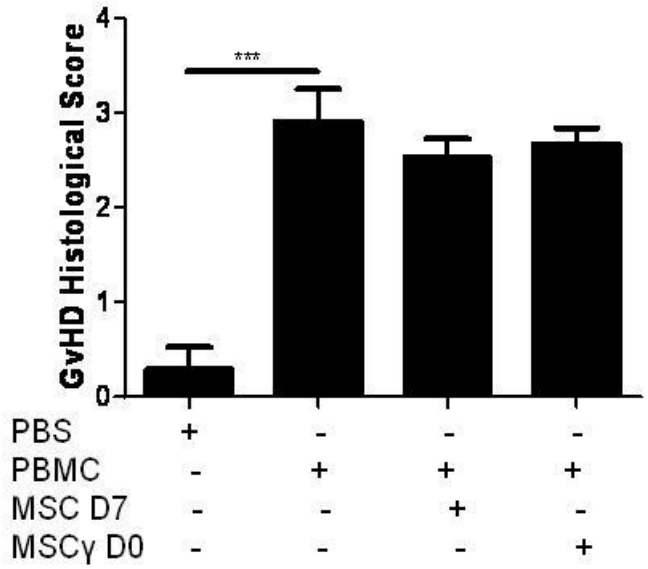

Fig 5.16 Human MSC therapy had no effect on aGvHD pathology in the lung. NSG mice were given PBMC by i.v. injection on day 0. Mice were treated with unstimulated hMSC on day 7 or prestimulated hMSC day 0. Following aGvHD development on day 12, lungs were harvested from each treatment group and tissue sections were analysed by (A) H&E staining. (B) A well-defined aGvHD histological scoring system was used to determine the level of aGvHD development between the groups. (A) Mice that received PBMC on day 0 displayed increased mononuclear infiltration into the alveolar spaces (denoted by arrow and letter a) leading to a (B) significant increase in aGvHD pathology ($p<0.0002$). (A) hMSC therapy did not improve aGvHD pathology as there was no reduction in cell infiltration (denoted by arrow and letter a) following MSC therapy. (B) There was no improvement in aGvHD histological score of mice with aGvHD. (n = 4 per group). Statistical analysis was carried out using the students paired t test.

5.11 IFNγ STIMULATED MSC SIGNIFICANTLY REDUCED TNF-α PRESENT IN THE SERUM OF NOD SCID IL-2Rγ^{NULL} MICE WITH AGVHD

One of the key characteristics of aGvHD is the production of inflammatory cytokines such as IFNγ and TNFα (Ferrara, 2009). In this study, the effect of hMSC cell therapy on the production of IFNγ and TNFα in a humanised model of aGvHD was analysed. Using the optimised protocol for aGvHD development (Fig 5.11 & 5.13), IFNγ prestimulated hMSC were given on day 0 concurrent with PBMC, while unstimulated hMSC were given on day 7 post PBMC injection. On the day of aGvHD development, day 12, serum was taken from all NSG mice (n=6) and analysed for the presence of human TNFα and IFNγ by bead array.

As expected, NSG mice that received PBMC on day 0 had significantly more human TNFα present in the serum after 12 days when compared to NSG mice that received PBS as a control (Fig 5.17 A, $p<0.0027$). Following hMSC cell therapy, NSG mice had significantly less human TNFα present in the serum, as seen after treatment with IFNγ prestimulated MSC (MSCγ) when compared to NSG mice given PBMC alone on day 0 (Fig 5.17 A, $p<0.0197$). Unstimulated MSC given on day 7 had no significant effect on the presence of human TNFα in NSG mice on day 12 (Fig 5.17 A). The presence of human IFNγ in the serum of NSG mice with aGvHD following PBMC administration was significantly more than PBS control NSG mice when compared on day 12 post transfusion (Fig 5.17 B, $p<0.05$). hMSC cell therapy had no significant effect on the presence of human IFNγ in the serum of NSG mice on day 12 (Fig 5.17 B). The data herein suggested that hMSC cell therapy could suppress the production of inflammatory signals involved in the development of aGvHD, in particular TNFα.

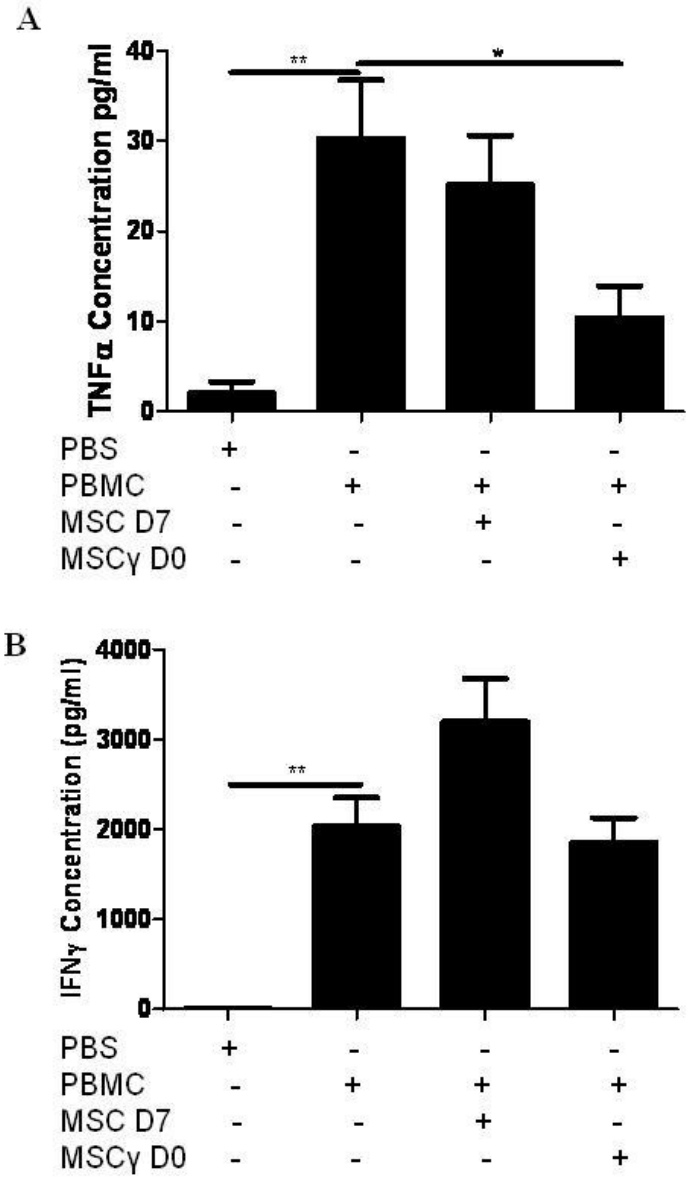

Fig 5.17 MSC cell therapy reduced the production of human TNFα in the serum of NOD scid IL2rγ^{null} mice with aGvHD. NSG mice were given PBMC (6.3 x 10^5 g^{-1}) by i.v injection on day 0. IFNγ prestimulated hMSC (4.4 x 10^4 g^{-1}) were given on day 0 concurrent with PBMC. Unstimulated hMSC (4.4 x 10^4 g^{-1}) were administered on day 7 post PBMC injection. On day 12, the day of aGvHD pathology, serum was taken from NSG mice and analysed for the presence of (A) human TNFα and (B) human IFNγ by bead array. IFNγ prestimulated MSC significantly reduced the production of (A) human TNFα ($p<0.0197$) in the serum of NSG mice with aGvHD. hMSC therapy had no significant effect on (B) human IFNγ production (n=6). Statistical analysis was carried out using the students paired t test.

5.12 SUMMARY

The goals of this chapter were to 1) optimise a humanised mouse model of aGvHD, 2) determine if hMSC were effective as a therapy for aGvHD treatment/prevention and 3) test the hypothesis that MSC require prestimulation for their immunosuppressive abilities to prove beneficial in the setting of aGvHD pathology. Pearson *et al.* designed a protocol for the development of a humanised mouse model of aGvHD in 2008, using the NOD Scid IL-2rγ^{null} mouse (Pearson, 2008). Using this protocol as a guideline and starting point, a more optimised and consistent humanised model of aGvHD was designed in this chapter.

Using an optimised and consistent aGvHD humanised mouse model, hMSC given as a therapy on day 7 post PBMC transplant proved beneficial in prolonging the survival of mice with aGvHD. While IFNγ prestimulated hMSC significantly prolonged the survival of mice with a GvHD when administered concurrent with PBMC on day 0. Following histological analysis of target aGvHD organs, hMSC treatment reduced the pathology of aGvHD in NSG mice. Both unstimulated and stimulated hMSC reduced aGvHD pathology of the liver and the gut. However, in contrast, hMSC treatment had no significant effect in reducing aGvHD pathology in the lung. Following treatment of NSG mice with IFNγ prestimulated MSC, the production of human TNFα was significantly reduced in the serum of NSG mice with aGvHD. Taken together, these data demonstrated a beneficial effect of MSC therapy on aGvHD treatment in a humanised murine model. The next step was to determine how MSC exerted their beneficial role *in vivo*. Identifying the exact mechanisms used by MSC to induce such positive results *in vivo* would allow better design of therapies and clinical studies.

CHAPTER 6

MECHANISMS INVOLVED IN MSC MODULATION OF ACUTE GRAFT VERSUS HOST DISEASE

6.1 INTRODUCTION

The development of a humanised aGvHD model was described in Chapter 5 based on the NOD-Scid IL2rγ^{null} (NSG) mouse. This model provides a very powerful tool for discovering the therapeutic mechanisms exerted by hMSC in a realistic environment. The key observation in Chapter 5 was that hMSC therapy prolonged the survival of NSG mice by delaying the onset of aGvHD. This effect was enhanced when hMSC were pre-stimulated with IFNγ.

In steroid resistant aGvHD, patients are refractory to treatment for the alleviation of symptoms and an alternative treatment modality is required. In some studies, MSC therapy has a beneficial effect (Le Blanc, 2008; Kurtzberg, 2009) however, the exact mechanism of MSC action in these situations remains unclear (Le Blanc, 2004; Augello, 2007). In this Chapter using the optimised humanised mouse model of aGvHD developed in Chapter 5, the beneficial mechanisms evoked by hMSC *in vivo* were investigated.

The aim of the experimental work described herein was to identify possible mechanisms used by hMSC in prolonging the survival of mice with aGvHD. Four possible mechanisms were considered. These included the 1) induction of graft T cell apoptosis by hMSC; 2) induction of graft T cell anergy, as a form of peripheral tolerance *in vivo*, 3) induction of graft T reg cells, similar to those identified *in vitro* or 4) direct inhibition of donor T cell proliferation *in vivo*, which might involve the release of soluble factors by hMSC, such as prostaglandins. These mechanisms were examined using a reductionist approach in the humanised model to determine a how hMSC are of benefit in aGvHD.

6.2 HMSC DID NOT INDUCE APOPTOSIS OF PBMC *IN VITRO* OR *IN VIVO*

One hypothesis for the beneficial effect seen in Chapter 5 could be stated as "hMSC induce apoptosis of donor PBMC" in the aGvHD NSG model. There has been conflicting evidence for MSC induction of T cell apoptosis with Plumas *et al.* suggesting it occurs, whereas Zappia *et al.* put forward the opposite opinion (Plumas, 2005; Zappia, 2005). Therefore, the ability of MSC to induce apoptosis of T cells was investigated, both *in vitro* and *in vivo*.

First, using the hMSC/PBMC coculture model, the induction of PBMC apoptosis *in vitro* by hMSC was examined. A known inducer of PBMC apoptosis, cisplatin (positive control), caused significant apoptosis of PBMC (Fig 6.1 A) as detected by flow cytometry for Annexin V/ Propidium iodide (PI) staining, indicating that apoptosis could be detected using this *in vitro* system. Following this, PBMC were cocultured with or without hMSC for 24 h. PBMC were pulled back from adherent hMSC and the number of apoptotic cells were measured using the flow cytometry method mentioned above. hMSC did not induce apoptosis of PBMC (Fig 6.1 A), but rather hMSC appeared to significantly ($p<0.0002$) protect PBMC from apoptosis. This result is in line with the known supportive role of MSC in lymphopoiesis (Chen, 2006). These data suggested that hMSC were not involved in the induction of PBMC apoptosis *in vitro*. Nevertheless, the capacity for hMSC to induce apoptosis was investigated *in vivo.* As *in vitro* data were not supportive, and as NSG mice were an expensive and scarce resource, this was tested on a small scale. If evidence of enhanced apoptosis was seen *in vivo,* a larger scale experiment would be justified and carried out. However, if no evidence was found for hMSC apoptosis of donor PBMC, then this approach would not be pursued.

Prior to performing this work, it was necessary to validate that *in vivo* apoptosis could be detected *ex vivo.* Therefore, BALB/c mice were lethally irradiated (12 Gy). After 24 h, these mice were injected i.v. with a green fluorescent dye, FLIVO, which binds to activated caspases within apoptotic cells. This technique has been used in other studies to detect apoptosis *in vivo* (Cursio, 2008). The FLIVO dye was allowed to circulate for 1 h, after which the lung, liver and spleen were harvested and the level of FLIVO staining was measured by flow cytometry (Fig 6.1 B). Apoptotic cells were detected in the liver after lethal irradiation, but not found in the lung or spleen (Fig 6.1 B). These data are in line with previous studies suggesting the liver is the main organ responsible for deletion of apoptotic T cells (Reviewed in Park *et al.*, 2002) and showed that the *in vivo* detection of apoptotic cells was possible using this technique.

To investigate whether hMSC therapy functioned through the induction of apoptosis of donor $CD4^+$ T cells *in vivo*, the model above was adapted. NSG mice were sub-lethally irradiated with 2.4 Gy, a conditioning dose as opposed to the positive control dose used above. NSG mice received PBS or PBMC i.v after 4 h. Unstimulated hMSC were given on day 7 post PBMC injection, while IFNγ stimulated hMSC (MSCγ) were given concurrent with PBMC treatment on day 0 (Fig 6.2 B & D). Following the development of aGvHD pathology on day 12, the FLIVO reagent was administered i.v. and allowed to circulate for 1 h. After 1 h, the lung (Fig 6.2 B) and liver (Fig 6.2 D) were harvested and analysed for FLIVO/CD4 by two-colour flow cytometry. No increase in apoptotic $CD4^+$ T cells were detected in the lung or liver following the treatment of aGvHD with hMSC (Fig 6.2 B & D). These data suggested that hMSC did not induce apoptosis of $CD4^+$ T cells *in vivo* and that this was unlikely to be the mechanism involved in the beneficial effect

mediated by hMSC in this model. However, it is always difficult to validate a negative result and it might be argued that apoptotic cells were present at an earlier time point, before day 12. This might be the case for MSCγ delivered on day 0, but more difficult to envisage for hMSC delivered on day 7. MSC would need to a) encounter sufficient PBMC to limit pathology, b) induce significant T cell apoptosis (again at a scale sufficient to limit pathology), c) for these apoptotic cells to be trapped in the liver (the site of lymphocyte deletion) and d) then be completely removed within five days. Nevertheless, a small scale *in vivo* study was carried out. In this case, NSG mice were treated with PBS, PBMC or PBMC and MSCγ therapy on day 0. FLIVO dye was administered i.v. 24 h later (Day 1) and allowed to circulate for 1 h, after which the lung and liver were harvested (Fig 6.2 A & C). As expected, no apoptotic $CD4^+$ T cells were detected in the lung (Fig 6.2 A) or liver (Fig 6.2 C) following hMSC therapy. Taken together with the *in vitro* data and the previous *in vivo* study, these data indicated that the induction of apoptosis could not reasonably account for the beneficial effects seen in Chapter 5.

A

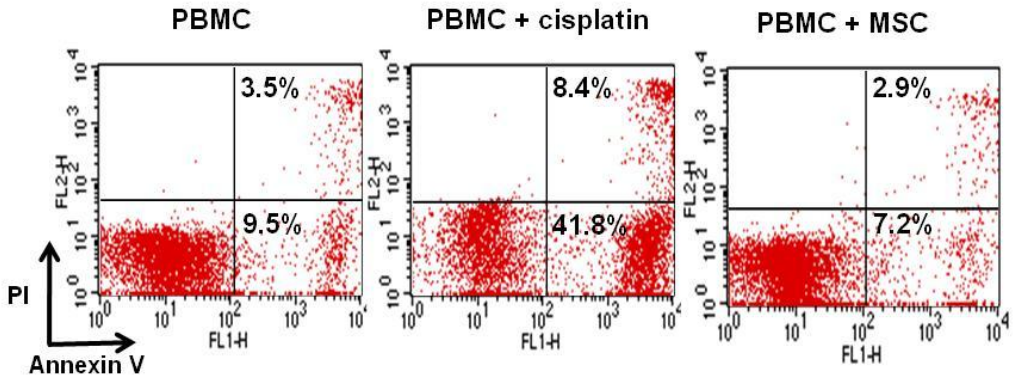

B

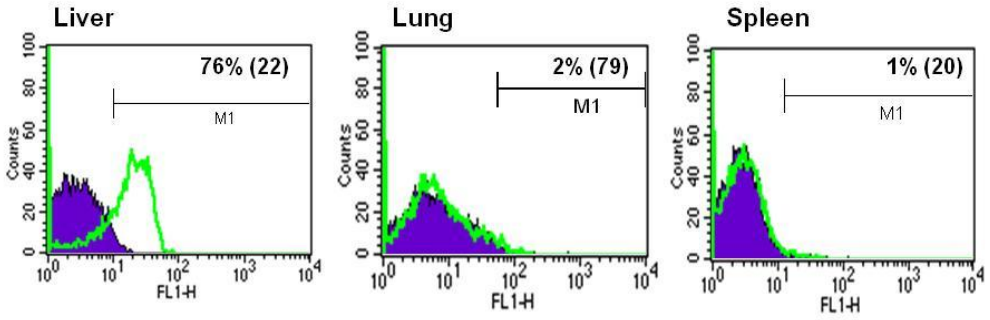

Fig 6.1 hMSC do not induce detectable apoptosis of PBMC *in vitro*. (A) PBMC were cultured in the presence of cisplatin or hMSC for 24 h. PBMC alone or with cisplatin at 250 µg/ml were cultured as controls. The presence of hMSC significantly inhibited apoptosis of PBMC *in vitro* ($p<0.0002$). The percentage of positive cells within the marked region are represented in the upper right quadrant. Data are representative of two studies. (B) Female BALB/c mice were lethally irradiated with 12 Gy to induce apoptosis *in vivo*. After 24 h, FLIVO green dye (8 µg/mouse) was given i.v. via the tail vein and allowed to circulate for 1 h. The lung, liver and spleens of mice were harvested and analysed for FLIVO staining by flow cytometry. Apoptotic cells were detected in the liver of BALB/c mice after lethal irradiation, but not in the lung or spleen. Data are representative of three mice per sample group (n=3). The percentage of positive cells within the marked region and the mean fluorescence intensity (MFI) of those cells are represented in each histogram.

A Lung Day 1

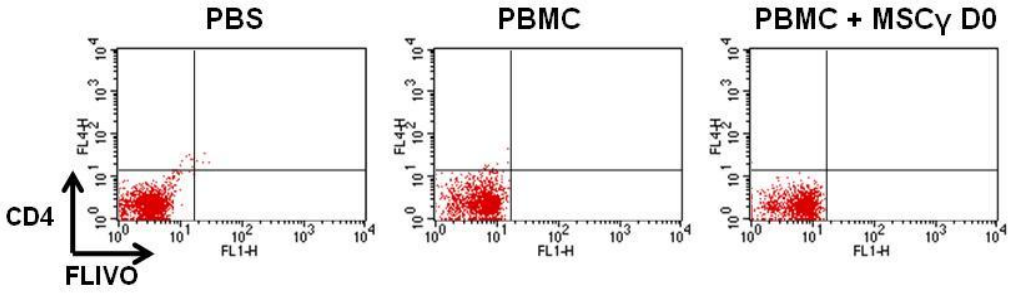

B Lung Day 12

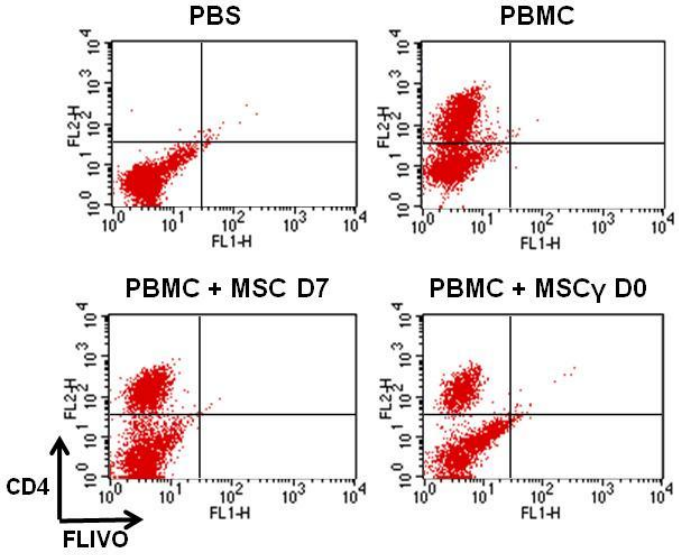

C Liver Day 1

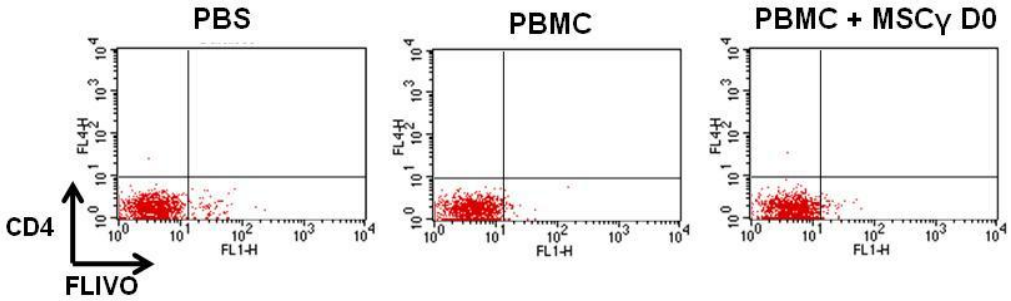

D Liver Day 12

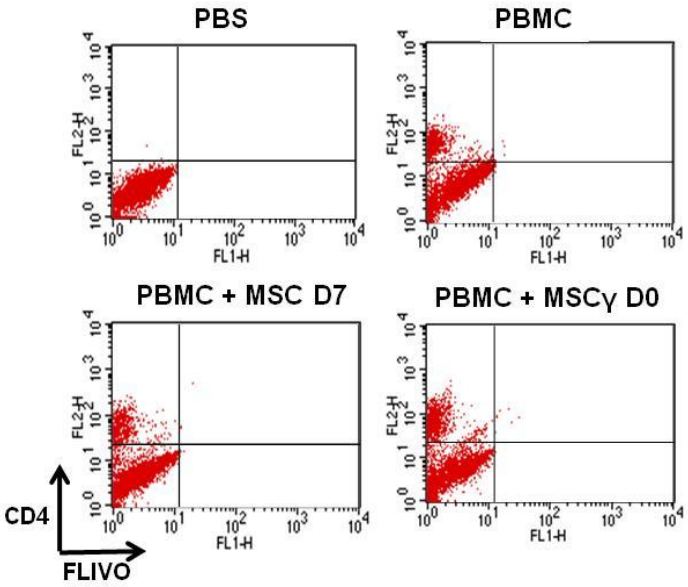

Fig 6.2 hMSC did not induce detectable apoptosis in PBMC *in vivo*. Irradiated NSG mice received PBS or PBMC (6.3 x 10^5 g^{-1}) on day 0. IFNγ stimulated hMSC (MSCγ) (4.4 x 10^4 g^{-1}) were given on day 0 or unstimulated hMSC (4.4 x 10^4 g^{-1}) were given on day 7. On day 1 or 12, FLIVO green dye (8 μg/mouse) was injected i.v and left to circulate for 1 h. The (A & B) lungs and (C & D) liver were harvested from each mouse and analysed for FLIVO staining and human CD4 PE. hMSC cell therapy did not induce CD4 T cell apoptosis *in vivo*. Data are representative of two mice per group (n=2).

6.3 hMSC Did Not Induce T cell Anergy *in vitro*

An alternative hypothesis for the beneficial effect seen in Chapter 5 could be formulated around the induction of T cell anergy by hMSC in the aGvHD NSG model. Krampera *et al.* and Glennie *et al.* have found that murine MSC inhibit T cell proliferation, which appeared to be reversible (Krampera, 2003; Glennie, 2005). These data were similar to that shown by Zappia *et al.*, whereby mMSC cocultured with T cells induced a state of anergy, which was partially reversible through the addition of IL-2 (Zappia, 2005). Combined, these data suggested that MSC were capable of inducing T cell anergy.

The ability of hMSC to induce T cell anergy *in vitro* was examined in this model. To closely mimic *in vivo* circumstances, an *in vitro* two-step proliferation assay was designed. Previous studies found that murine DC alone were insufficient for the stimulation of human $CD4^+$ T cells in an xenogeneic setting *in vitro*. These findings suggested that murine DC required an additional stimulus in order to activate the proliferation of human $CD4^+$ T cells. This led to the design of a two-step proliferation assay. Firstly, murine DC isolated from bone marrow of BALB/c mice were stimulated with polyIC and cocultured with human $CD4^+$ T cells isolated from PBMC for 5 days. To investigate the induction of human $CD4^+$ T cell anergy by MSC, hMSC were added to some coculture treatment groups. Following 5 days of coculture, the proliferation of human $CD4^+$ T cells was analysed through the addition of [3H]-thymidine. Human $CD4^+$ T cells cultured with polyIC stimulated murine DC induced significant T cell proliferation ($p<0.0001$). However, if hMSC were present in the coculture, the induction of T cell proliferation was significantly reduced ($p<0.05$) (Fig 6.3 A). These data showed that hMSC were capable of

inhibiting T cell proliferation in a xenogeneic setting, a setting similar to that found in the aGvHD NSG model.

To examine if the reduction in T cell proliferation by hMSC was due to the induction of T cell anergy, a second proliferation assay was performed. In this case, following coculture with murine DC, polyIC and/or hMSC for 5 days, human $CD4^+$ T cells were repurified from cultures by magnetic bead isolation. $CD4^+$ T cells were allowed to rest overnight after which, these human $CD4^+$ T cells were cultured for a second time with irradiated xenogeneic BALB/c DC stimulated with or without polyIC (Fig 6.3 B). The hypothesis here was that upon restimulation, "anergic" human $CD4^+$ T cells that had previously been cultured in the presence of hMSC would not proliferate and this inhibition would be reversible through the addition of IL-2. However, this was not the case. Following, the second coculture of human $CD4^+$ T cells with irradiated DC and polyIC, an increase in T cell proliferation was observed (Fig 6.3 B). The proliferation of $CD4^+$ T cells that had previously been cultured in the presence of hMSC was similar, suggesting that hMSC did not induce T cell anergy *in vitro* (Fig 6.3 B). The addition of IL-2 did not affect the proliferation of human $CD4^+$ T cells (Fig 6.3 C). These data suggested that although hMSC were capable of inhibiting T cell proliferation *in vitro*, this inhibition of T cell proliferation was not due to induction of T cell anergy. These data are in contrast with Glennie *et al.* and Zappia *et al.*, although one key point to note is that human T cell induced anergy was examined here, whereas others explored MSC induced anergy in a completely murine setting (Glennie, 2005; Zappia, 2005).

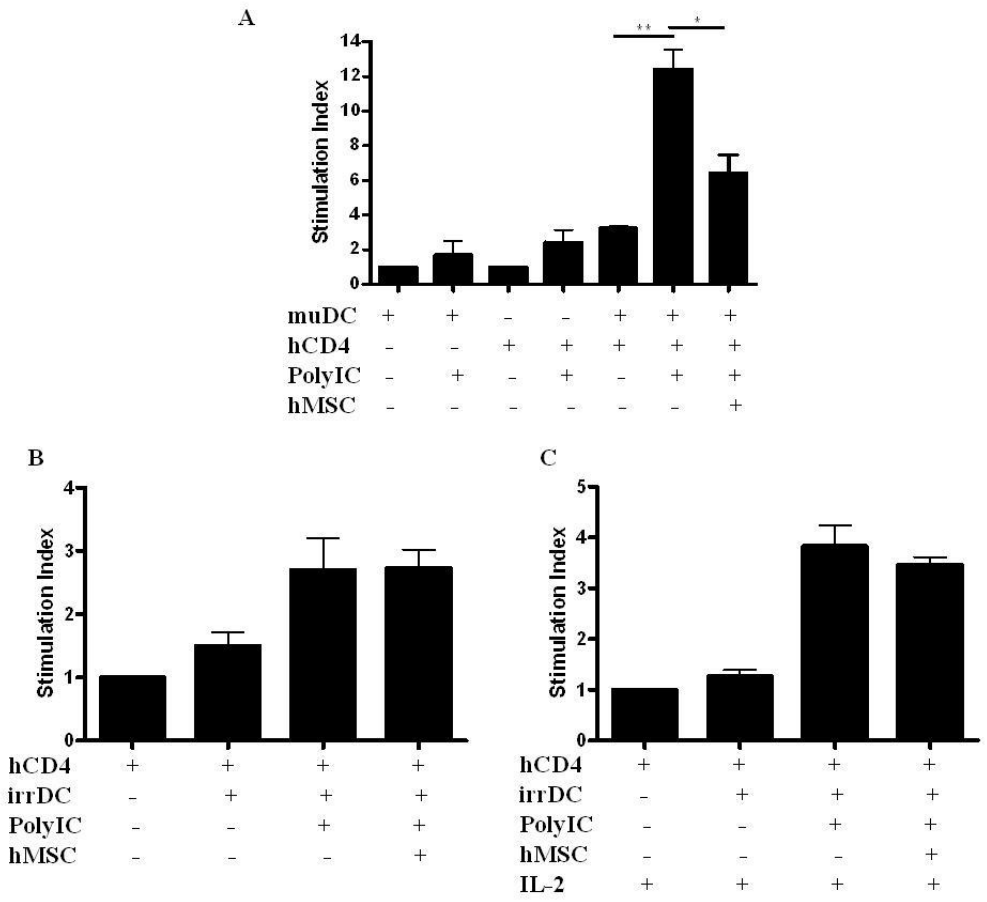

Fig 6.3 hMSC did not induce T cell anergy *in vitro*. (A) Human $CD4^+$ T cells (1 x 10^6/ml) were cocultured in the presence or absence of BALB/c bone marrow derived DC (muDC) (1 x 10^5/ml), polyIC (20 μg/ml) or hMSC (1 x 10^5/ml) in a 96 well plate for 5 days. After 5 days, [^{3}H]-thymidine was added to the well for 6 h and T cell proliferation was analysed. Murine DC stimulated with polyIC induced significant human $CD4^+$ T cell proliferation ($p<0.0001$). In the presence of hMSC, the proliferation of $CD4^+$ T cell proliferation was significantly reduced ($p<0.05$). (B) Following coculture with murine DC, polyIC and/or hMSC, $CD4^+$ T cells were repurified and cocultured with irradiated DC (irrDC) and polyIC for 72 h. After 72 h, T cell proliferation was analysed by [^{3}H]-thymidine incorporation. $CD4^+$ T cells previously cocultured with hMSC proliferated upon restimulation with polyIC. (C) The addition of IL-2 had no effect on T cell proliferation.

6.4 hMSC Induced Regulatory-Like T Cells Expressing FoxP3 *in vitro;* But Failed To Induce Similar Populations *in vivo*

In Chapter 3, it was clearly shown that hMSC were capable of inducing functional regulatory T cells (T reg) *in vitro* (English, 2009). Other studies of cell therapy by the Mahon group have shown that mMSC-induced T reg cells are required for beneficial affects *in vivo* (Kavanagh, 2011). This is supported by work in other models such as Crohn's disease (Ciccocioppo, 2011) and even aGvHD, whereby Cao *et al.* found that *ex vivo* expanded human T reg cells significantly enhanced the survival of NOD-scid mice with aGvHD (Cao, 2009). Therefore, the induction of T reg like cells by hMSC as a possible mechanism involved in the effective treatment of aGvHD in NSG humanised model was examined.

Firstly, hMSC were examined for their ability to induce FoxP3 expressing T reg cells *in vitro* from a population of PBMC isolated from one of the four healthy donors used for the induction of aGvHD *in vivo* (Fig 6.4 A & B). After coculture with hMSC for 72 h *in vitro*, PBMC were harvested by gentle aspiration from adherent hMSC and analysed for the coexpression of CD4, CD25 and intracellular FoxP3 by flow cytometry. hMSC induced a $CD4^+$ T reg like cell population expressing FoxP3 and CD25 *in vitro* (Fig 6.4 A). These data were in line with the findings in Chapter 3. However, hMSC did not to induce a $CD8^+$ $FoxP3^+$ population *in vitro* (Fig 6.4 B) suggesting that unconventional $CD8^+$ T reg like cells were not induced by hMSC.

IFNγ and TNFα are two key cytokines involved in aGvHD pathology. hMSC are likely to encounter high levels of these two cytokines *in vivo*. In Chapter 5, it was shown that hMSC prestimulation had an enhanced beneficial therapeutic effect.

Therefore, the above experiment was repeated where hMSC were pre-stimulated with IFNγ or TNFα for 48 h prior to coculture with PBMC *in vitro*. The expression of the regulatory markers FoxP3 and CD25 was examined on $CD4^+$ T cells by flow cytometry. Stimulation of hMSC with inflammatory mediators did not further increase the number of cells expressing CD25 or FoxP3 on $CD4^+$ or $CD8^+$ T cells *in vitro* (Fig 6.4 A & B). These data implied that although MSC induced $CD4^+$ T reg like cells *in vitro*, pre-stimulation of hMSC with proinflammatory cytokines did not increase the number of regulatory like cells.

The induction of a T reg-like population *in vitro* from PBMC suggested that this could be a potential therapeutic mechanism utilised by hMSC *in vivo*. Therefore, the possibility of T reg induction by MSC in the *in vivo* model of aGvHD was explored. NSG mice were irradiated with 2.4 Gy and received PBS or PBMC after 4 h. MSC treated groups received hMSC on day 7 post PBMC administration or IFNγ stimulated hMSC on day 0 concurrent with PBMC. On day 12, the typical onset day of aGvHD pathology, the lung, liver and spleen were harvested and analysed for the expression of human CD4, CD8, CD25 and Foxp3 by flow cytometry (Fig 6.5) (n=6). Whilst hMSC induction of a T reg population was clearly seen *in vitro* (Fig 6.4 A) and previously detectable *in vivo* in other models used in the Mahon lab (Kavanagh, 2011), there was no evidence of induction or expansion of $CD4^+$ $CD25^+$ $FoxP3^+$ or $CD8^+$ $CD25^+$ $FoxP3^+$ T reg like cell populations *in vivo* (Fig. 6.5). This was the case following treatment with either hMSC on day 7 or IFNγ stimulated hMSC on day 0. No such populations were observed in the lung (Fig 6.5 A), liver (Fig 6.5 B) or spleen (Fig 6.5 C). These data suggested that the hMSC induction of $CD4^+$ or $CD8^+$ $CD25^+$ FoxP3 expressing T reg like cells was

unlikely to be the mechanism involved in hMSC induced prolonged survival of NSG mice with aGvHD.

It is important to be cautious in the interpretation of the above data. The induction/expansion of human $CD4^+$ or $CD8^+$ $FoxP3^+$ T reg cell was analysed here. Firstly, there may be human stromal or third party factors that are absent in this humanised mouse model that prevent human T reg cell expansion, however that does little to explain the therapeutic benefit that had been observed (Chapter 5). Secondly, there are many other recently described T reg populations that do not express FoxP3, CD4, CD8 or CD25, which may be induced *in vivo* but not explored in this study. In addition, T reg cells may have had an effect early and disappeared or be present in non-sampled organs. Once again, it is highly unlikely that T reg cells could have an effect and not be present in the organs sampled, especially when these are the target organs involved in GvHD pathology and displaying improvement with cell therapy. In summary, hMSC did not induce a detectable $CD4^+$ $CD25^+$ $FoxP3^+$ or $CD8^+$ $CD25^+$ $FoxP3^+$ T reg cell population *in vivo* in this model.

A

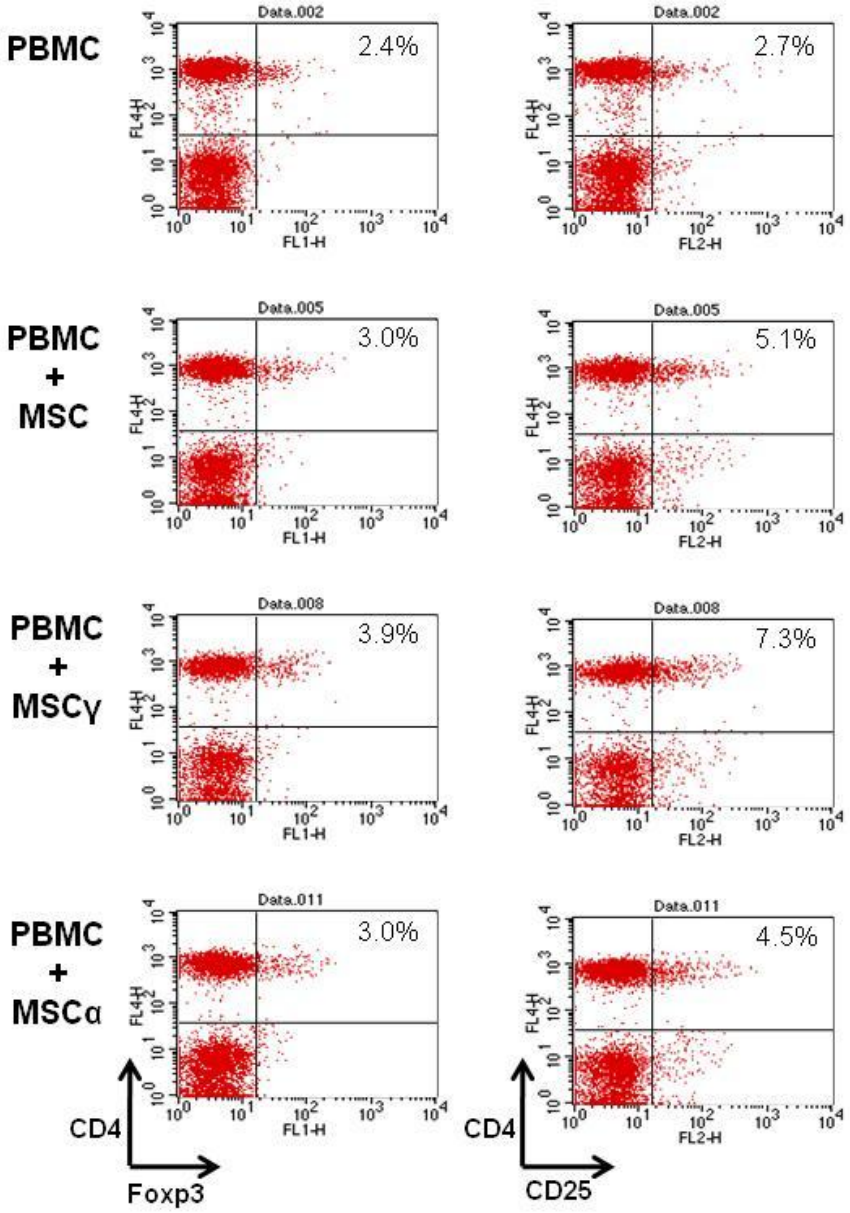
PBMC
Data.002
2.4%
Data.002
2.7%
PBMC + MSC
Data.005
3.0%
Data.005
5.1%
PBMC + MSCγ
Data.008
3.9%
Data.008
7.3%
PBMC + MSCα
Data.011
3.0%
Data.011
4.5%
FL4-H
FL1-H
FL2-H
CD4
Foxp3
CD4
CD25

B

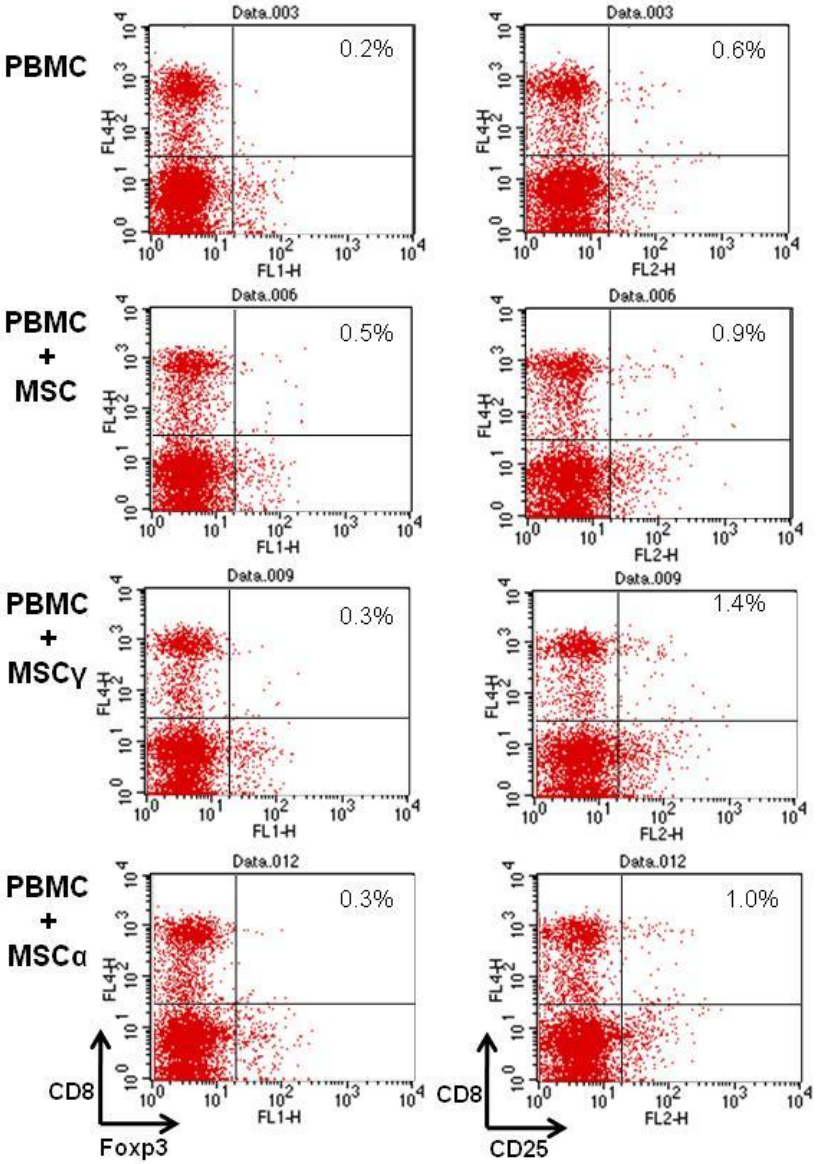

Fig 6.4 hMSC induced CD4$^+$ but not CD8$^+$ T cells expressing FoxP3 and CD25 *in vitro*. PBMC (1 x 10^6/well) were isolated from fresh healthy donor blood and cocultured with hMSC (3 x 10^5/well) or pre-stimulated MSC (MSCγ) (IFNγ (50 ng/ml) or (MSCα) TNFα (50 ng/ml) for 72 h in a 6 well plate. PBMC were examined for the co-expression of (A) CD4 or (B) CD8 with the regulatory markers FoxP3 and CD25 by flow cytometry. The percentage of double positive cells are given in the upper quadrant. Data are representative of three independent experiments.

A Lung

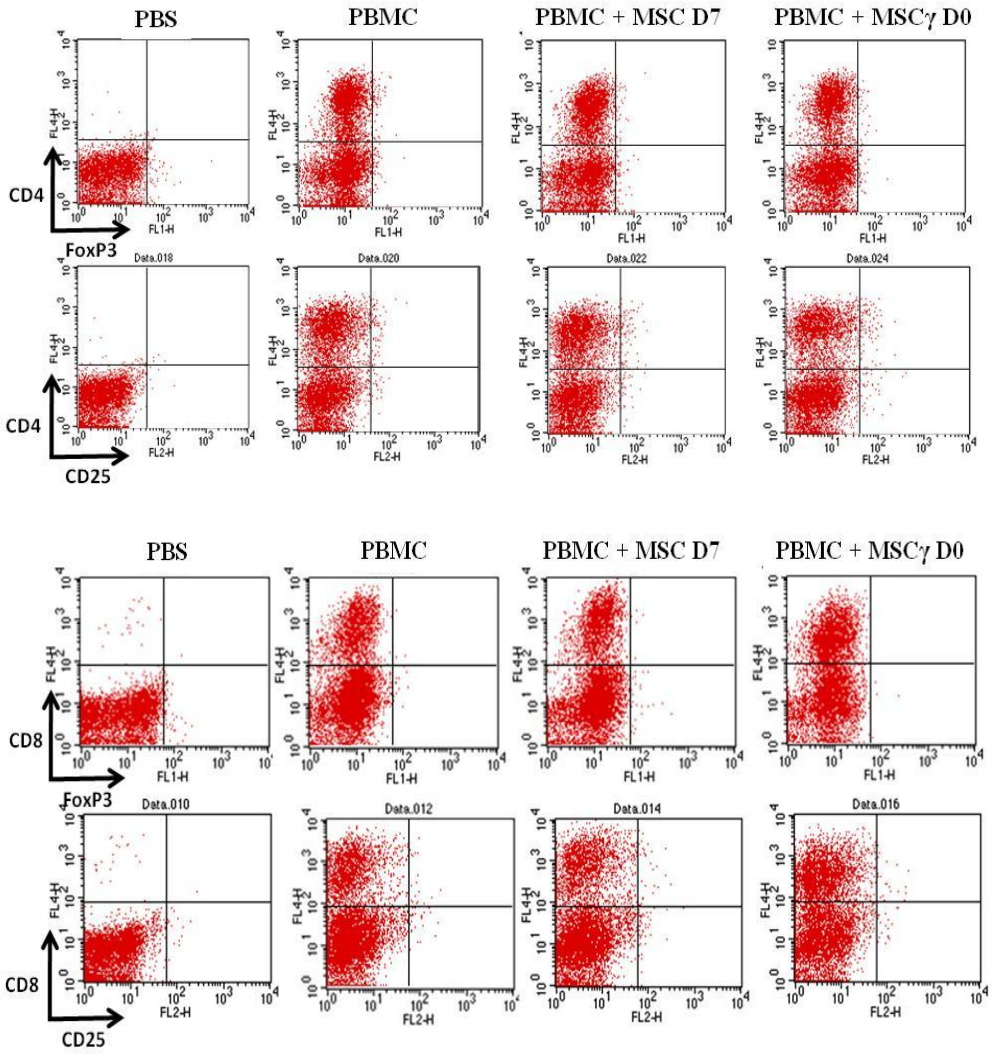
PBS
PBMC
PBMC + MSC D7
PBMC + MSCγ D0
CD4
FoxP3
CD4
CD25
PBS
PBMC
PBMC + MSC D7
PBMC + MSCγ D0
CD8
FoxP3
CD8
CD25

B Liver

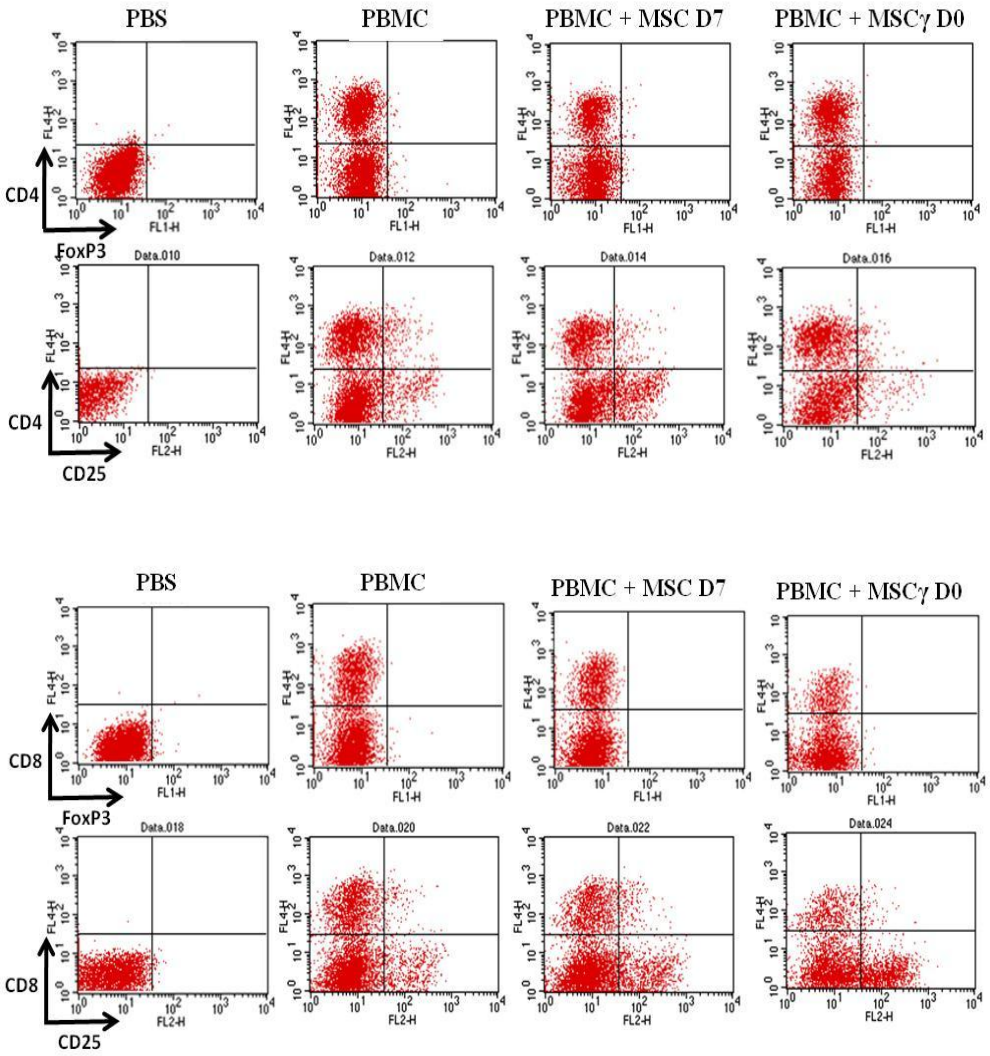
PBS
PBMC
PBMC + MSC D7
PBMC + MSCγ D0
CD4
FoxP3
CD25
CD8
Data.010
Data.012
Data.014
Data.016
Data.018
Data.020
Data.022
Data.024
FL1-H
FL2-H
FL4-H

C Spleen

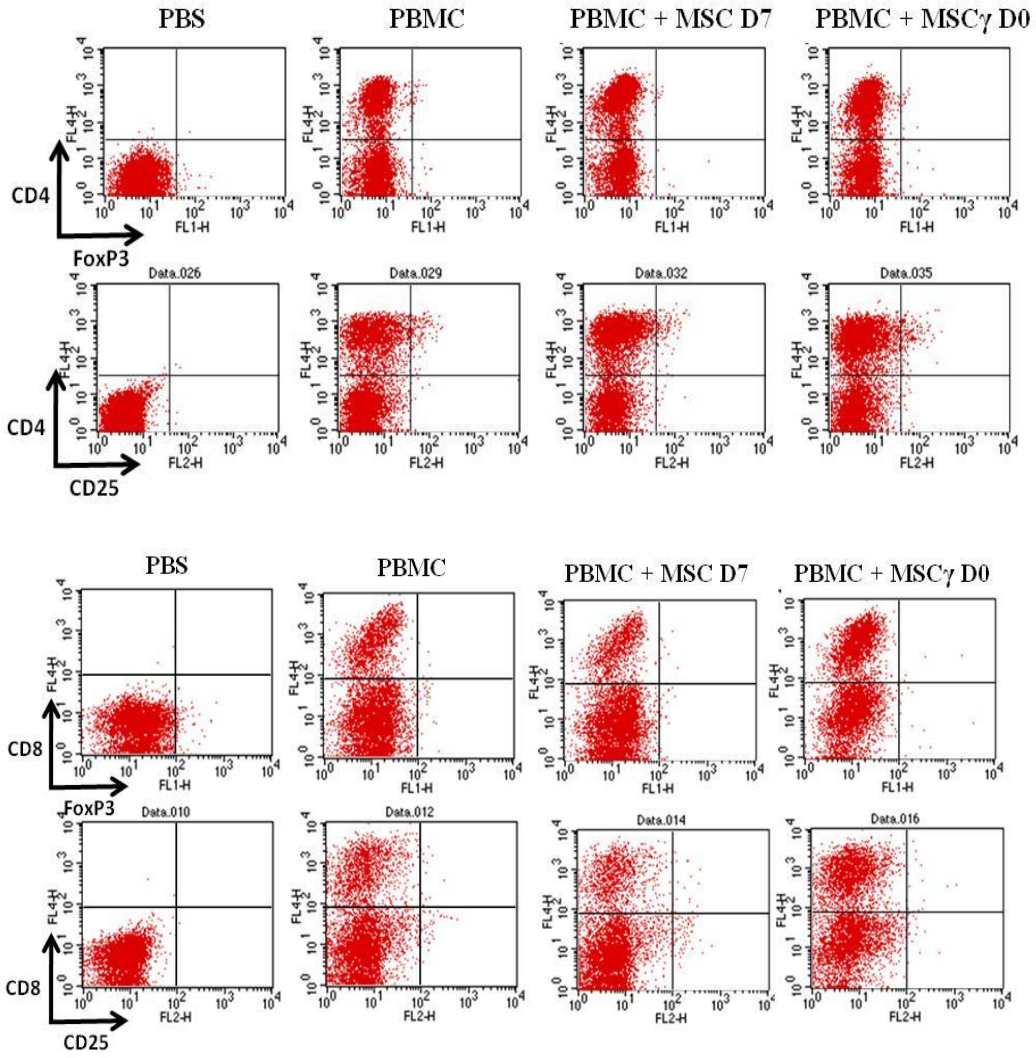

Fig 6.5 hMSC did not induce FoxP3 expressing T regulatory like population *in vivo*. NSG mice received PBS or PBMC (6.3 x 10^5 g^{-1}) on day 0. IFNγ stimulated (MSCγ) or unstimulated MSC (4.4 x 10^4 g^{-1}) were given i.v. on day 0 or 7 respectively. On day 12, the (A) lung, (B) liver and (C) spleen were harvested and analysed for the expression of human CD4, CD8, CD25 and FoxP3 by flow cytometry. $CD4^+$ $FoxP3^+$ or $CD8^+$ $FoxP3^+$ T reg-like cells were not detected *in vivo* following hMSC therapy. Data are representative of six mice per group (n=6).

6.5 hMSC Inhibited the Proliferation of PBMC *in vitro* and *in vivo*

It was demonstrated in Chapters 3 and 4 that both human and mouse MSC can inhibit T cell proliferation induced in an MLR by allogeneic cells or in proliferation assays driven by non-specific mitogens. It was therefore possible that the beneficial influence of hMSC therapy on aGvHD development was a direct anti-proliferative effect on donor T cells. This hypothesis was examined *in vitro* and *in vivo*. First, the hMSC used here were examined to verify the *in vitro* suppression of proliferation of the donor PBMC used for the induction of aGvHD *in vivo.* Donor PBMC were stimulated *in vitro* by either MHC mismatched PBMC (Fig 6.6 A) or a mitogen (PHA) (Fig 6.6 B) for 72 h. hMSC significantly inhibited the proliferation of alloantigen driven and mitogen driven proliferation of donor PBMC (Fig 6.6 A & B) ($p<0.0001$). This inhibition of alloantigen driven proliferation of PBMC by hMSC was associated with a significant decrease in both IFNγ (Fig 6.6 C) ($p<0.0001$) and TNFα (Fig 6.6 E) ($p<0.0201$) present in culture supernatants, as analysed by ELISA. hMSC inhibition of mitogen driven proliferation of PBMC, was associated with a significant decrease in IFN-γ (Fig 6.6 D) ($p<0.0001$) and TNF-α (Fig 6.6 F) ($p<0.0001$) production. This decrease in lymphocyte proliferation attributable to hMSC suggested that hMSC might have a similar effect *in vivo*, mediating the development of aGvHD pathology.

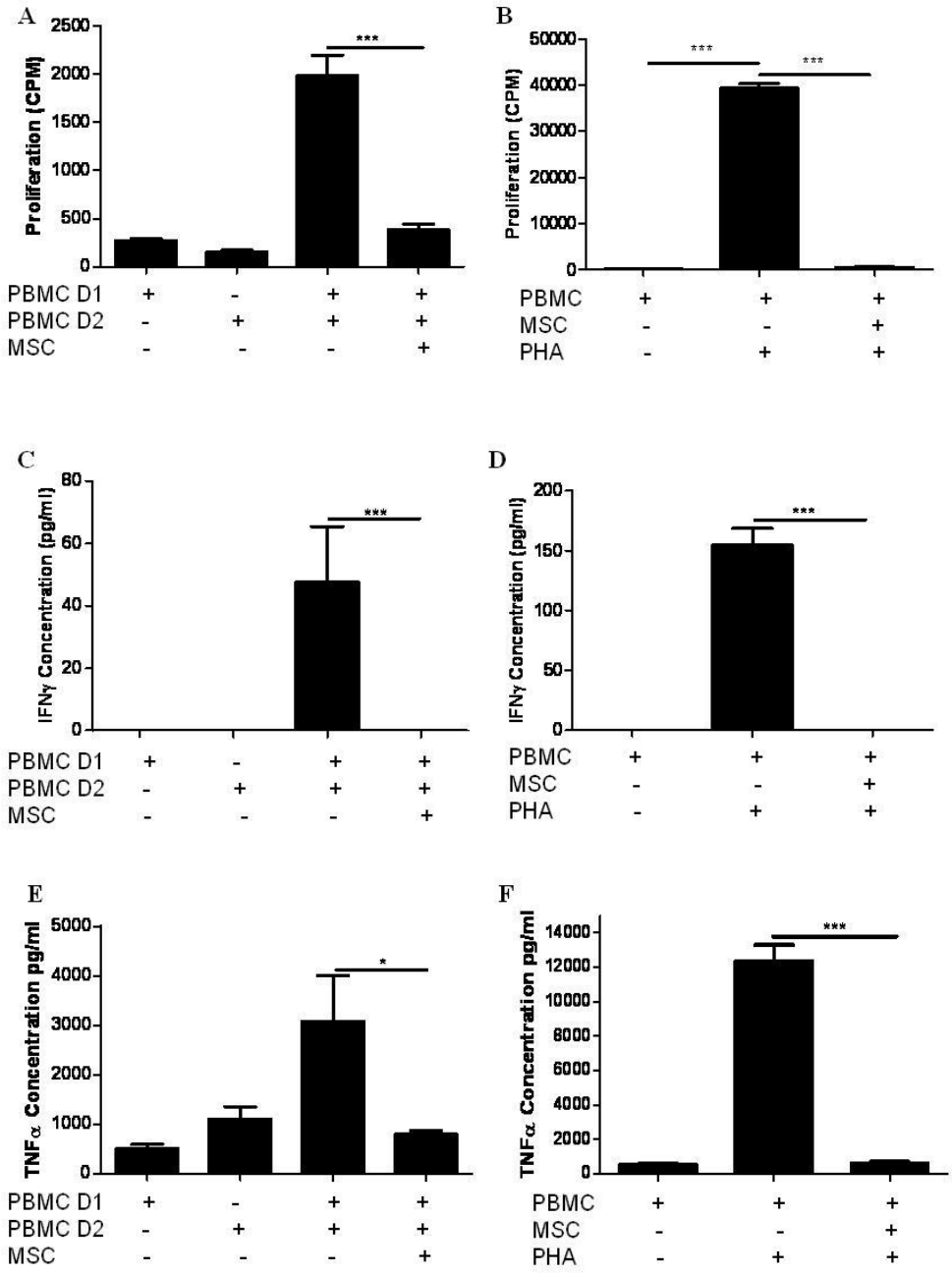

Fig 6.6 hMSC inhibit PBMC proliferation and decrease IFNγ and TNFα production *in vitro.* (A) PBMC (number) from two MHC mismatched donors (D1 or D2) were cultured in the presence or absence of number MSC in MLR. (A) MSC significantly inhibited alloantigen proliferation ($p<0.0001$) and (B) mitogen driven proliferation ($p<0.0001$) *in vitro*. This inhibition of proliferation correlated with a significant decrease in the production of (C & D) IFNγ ($p<0.0001$) and (E & F) TNFα ($p<0.0201$, $p<0.0001$ respectively) as analysed by ELISA. Statistical analysis was carried out using the students paired t test. Data are representative of three experiments, each performed in triplicate.

In order to investigate whether hMSC inhibited the proliferation of donor PBMC *in vivo*, the optimisation of an *in vivo* measure of lymphocyte proliferation was required. Carboxyfluorescein succinimidyl ester (CFSE) is a fluorescent dye, which is progressively and consistently diluted following each consecutive cell division (Lyons, 1994). CFSE was used to label donor PBMC *in vitro* and to look for the proliferation of PBMC in response to rhIL-2 and a mitogen, PHA (Fig 6.7). A number of attempts were made to obtain meaningful data from CFSE experiments, eventually the protocol described in section 2.11.6 was used, representing the approach that yielded interpretable data consistent with other workers. PBMC were labelled with 2.5 µM, 5 µM or 10 µM CFSE and cultured on anti-human CD3 coated tissue culture plates *in vitro*. Cultures were stimulated with rhIL-2 and PHA (Fig 6.7) for 5 days. After 5 days, CFSE labelled PBMC were counter labelled with anti human CD4 and proliferation was analysed using flow cytometry. A decrease in CFSE fluorescence (MFI) was indicative of CD4 T cell division (Fig 6.7). Following the stimulation of CFSE labelled PBMC with rhIL-2 and PHA, the distribution of $CD4^+$ T cell peak fluorescence was altered (Fig 6.7). Each peak corresponded to a successive cell division, approximately half the fluorescence (MFI) of the previous peak. $CD4^+$ T cells labelled with various concentrations of CFSE showed proliferation. Peaks representing three or more rounds of proliferation were clearly seen when $CD4^+$ T cells were labelled with 5 or 10 µM CFSE, compared with PBMC labelled with 2.5 µM CFSE (Fig 6.7), a CFSE concentration of 10 µM was chosen for further experiments. These data showed that the proliferation of $CD4^+$ T cells *in vitro* could be successfully detected using CFSE staining.

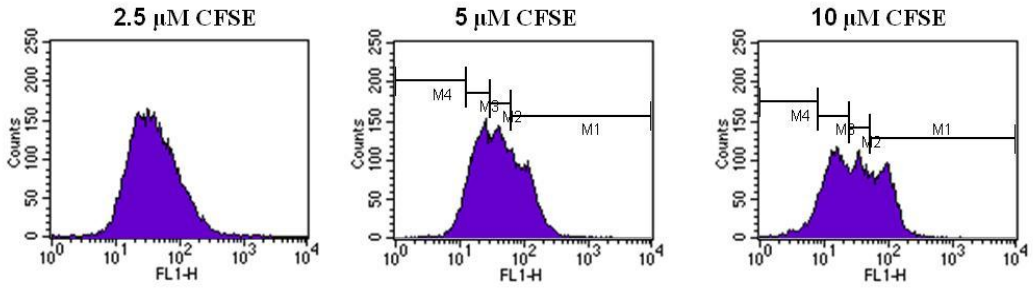

Fig 6.7 CFSE labelled CD4$^+$ T cells proliferate *in vitro*. PBMC were labelled with CFSE at 2.5 µM, 5 µM or 10 µM. CFSE PBMC were cultured on anti-human CD3 (2 µg/ml) coated tissue stimulated with rhIL-2 (100 U/ml) and PHA (10 µg/ml) for 5 days. CFSE PBMC were counterstained with anti-human CD4 and proliferation analysed by flow cytometry. Proliferation of CD4$^+$ T cell was undetectable on cells labelled with 2.5 µM CFSE. CD4$^+$ T cells labelled with 5 µM or 10 µM underwent proliferation. Data representative of two independent studies.

Next, the possibility that hMSC had an effect on the PBMC division *in vitro* was examined. Using a technique derived from the *in vitro* approach above, PBMC were labelled with 10 μM CFSE, but in this case, cocultured in the presence of hMSC and stimulated with rhIL-2 and PHA for 5 days. After 5 days, PBMC were pulled back from coculture by gentle aspiration from adherent hMSC, counter labelled with anti-human CD4 and analysed by flow cytometry (Fig 6.8). Unstimulated $CD4^+$ T cells only had 35 % of cells progress into division, (65 % of $CD4^+$ T cells undergoing no divisions) (Fig 6.8). Upon stimulation with rhIL-2 and PHA, $CD4^+$ T cells in the presence or absence of hMSC underwent division. However, in the presence of hMSC $CD4^+$ T cells underwent fewer divisions (36 % progressing to a second division), when compared to $CD4^+$ T cells in the absence of hMSC (46 %). These findings showed that hMSC inhibited the proliferation of $CD4^+$ T cells *in vitro*, as indicated by CFSE expression.

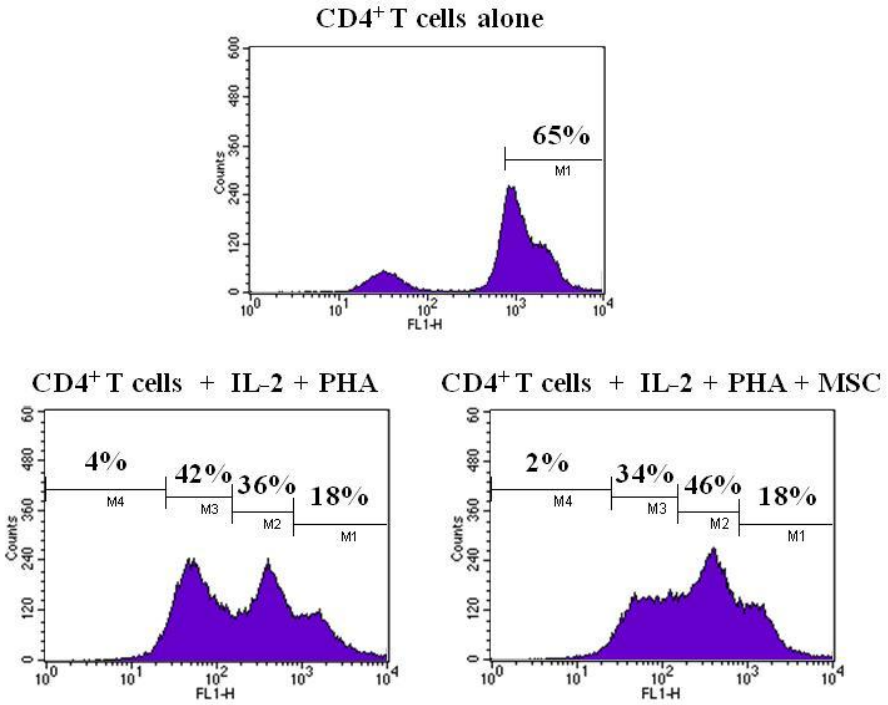

Fig 6.8 hMSC reduced the proliferation of CD4$^+$ T cells *in vitro.* PBMC (1 x 10^6/ml) were labelled with 10 μM CFSE and stimulated with rhIL-2 (100 U/ml) and PHA (10 μg/ml) in the presence or absence of MSC (1 x 10^5/ml) for 5 days. After 5 days, CFSE stained PBMC were labelled with anti-CD4 and cell proliferation was analysed by flow cytometry. CD4$^+$ T cells underwent proliferation in response to rhIL-2/PHA by day 5. In the presence of hMSC, CD4$^+$ T cells displayed reduced proliferation, with the majority of cell proliferations prohibited after one division. Percentage of cells in each division are represented on the histogram. Data are representative of two independent studies.

The hypothesis was therefore formulated that, hMSC therapy directly inhibited PBMC proliferation in the aGvHD humanised mouse model. To test this, an *in vivo* model of the CFSE technique was required. Again, a number of preliminary experiments were performed to permit detection of CFSE labelled PBMC *in vivo*. Ultimately, a concentration of 10 µM was used for labelling. Higher concentrations were found to have a toxic effect on PBMC but lower levels were not detectable *ex vivo*. This was supported by a protocol from Lyons *et al.* (Lyons, 2004).

The *in vivo* approach initially involved labelling PBMC with 10 µM CFSE on day 0, prior to i.v. injection into a sub-lethally irradiated NSG mouse. Like previous studies, IFNγ stimulated MSC were given concurrently on day 0, while unstimulated MSC were given on day 7 post transfusion of PBMC. When NSG mice developed aGvHD on day 12 the lung, liver and spleen were harvested. The level of CFSE staining by $CD4^+$ T cells in these organs was analysed by flow cytometry. However, no CFSE was detected at day 12 in any of the target organs, lung, liver or spleen (Data not shown). Therefore, the protocol was refined and the readout was shifted to day 5 post transfusion of CFSE labelled PBMC. The shift to an earlier time point was not compatible with use of hMSC alone, as in Chapter 5 it was found that hMSC were only effective with delayed administration, primarily given on day 7. Therefore, only IFNγ stimulated hMSC were used for the purpose of this experiment.

Sub-lethally irradiated NSG mice received CFSE labelled PBMC on day 0 and MSCγ treatment was given concurrently. Mice were left for 5 days before analysing the effect of MSCγ treatment on PBMC proliferation. On day 5, the lung, liver and spleen were harvested and the fluorescence of $CFSE^+$ $CD4^+$ labelled T cells

were analysed by flow cytometry (Fig 6.9). CFSE labelled PBMC were detected in the lung of NSG on day 5. MSCγ treated mice had significantly fewer $CD4^+$ T cells progressing to division ($p<0.0041$) when compared to mice that received PBMC alone on day 0 (Fig 6.9 A & B). There was also a significant reduction in the number of human $CD4^+$ T cells divisions when NSG mice were treated with allogeneic MSCγ therapy ($P<0.0037$) (Fig 6.9 A & B). Typically, mice receiving MSCγ had significantly fewer $CD4^+$ T cells that had undergone subsequent divisions. Thus in aGvHD mice not treated with hMSC, 66% of $CD4^+$ T cells had undergone 2 or more divisions whereas in the presence of MSCγ therapy, most (52%) of $CD4^+$ T cells underwent only one or fewer divisions (Fig 6.9). These data also revealed that aGvHD development in this humanised mouse model was primarily a $CD4^+$ T cell driven disease as PBMC not expressing CD4 did not undergo proliferation *in vivo* (Fig 6.9). CFSE labelled PBMC were not detected in the liver or spleen of NSG mice 5 days post transfusion. These data suggested that the majority of PBMC are located in the lung 5 days post administration and this is consistent with the lung pathology evident in this model (Fig 5.16).

A

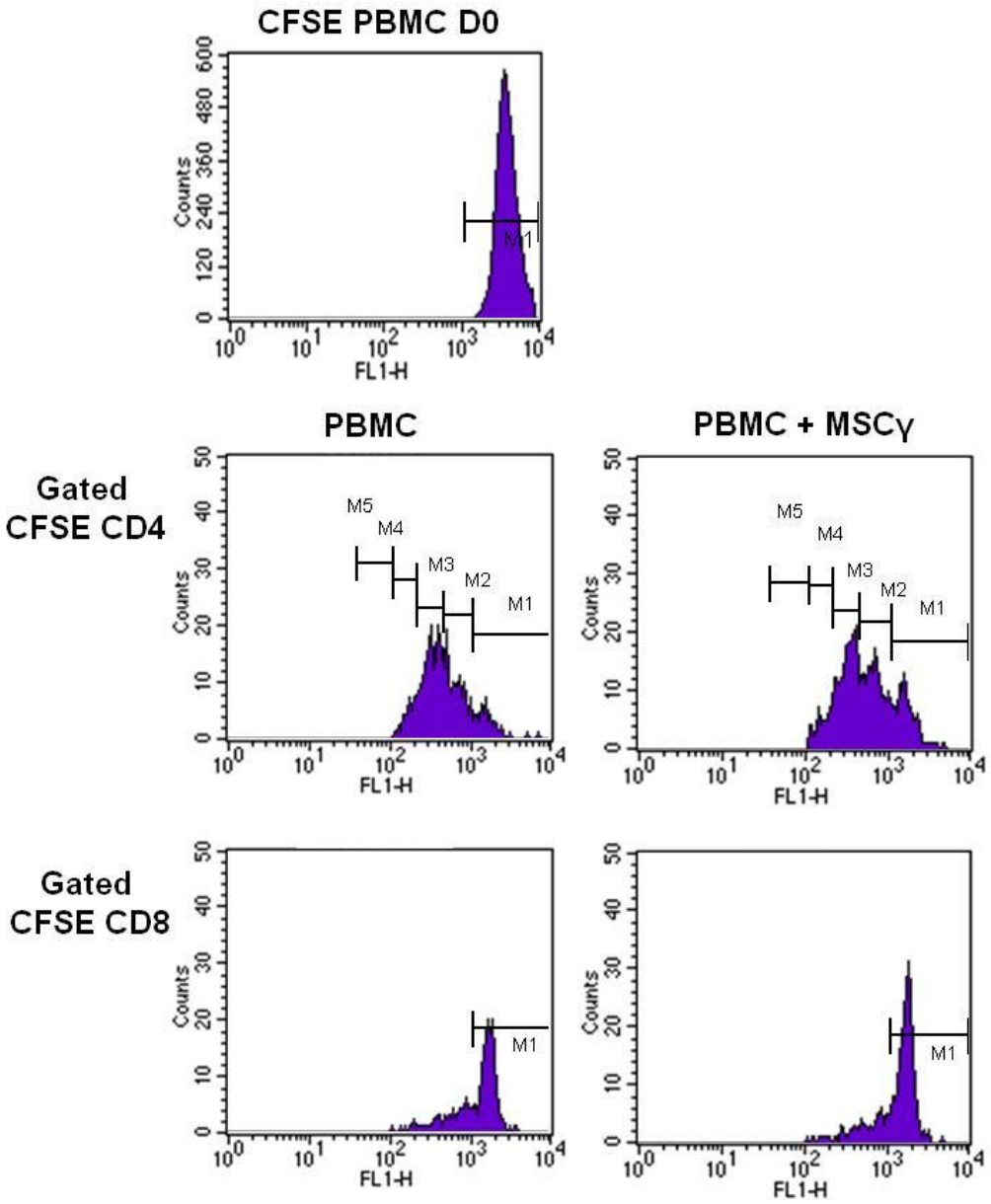
CFSE PBMC D0
Counts
FL1-H
M1
PBMC
PBMC + MSCγ
Gated
CFSE CD4
M5
M4
M3
M2
M1
Gated
CFSE CD8

B

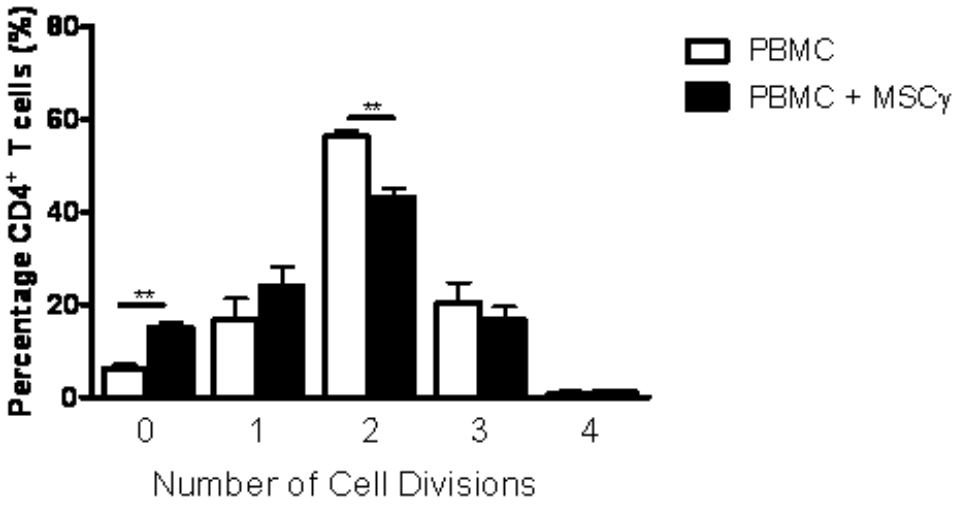

Fig 6.9 MSC reduced the proliferation of CD4 T cells *in vivo*. PBMC labelled with 10 µM CFSE were administered to NOD-Scid IL2rγ^{null} mice that were irradiated with 2.4 Gy with or without MSCγ on day 0. After 5 days, the lung, liver and spleen were harvested. (A) The level of CFSE on CD4$^+$ T cells was analysed by flow cytometry. MSC reduced the proliferation of CD4$^+$ T cells in the lung only after 5 days. CD4$^+$ T cells were not detected in the liver or spleen after 5 days. (B) Percentage of CD4$^+$ cells present in the lung at each division from CFSE labelled PBMC after 5 days *in vivo.* Data are representative of 5 mice per group (n=5).

6.6 PROSTAGLANDIN PRODUCTION BY HMSC IS NOT ESSENTIAL FOR PREVENTING CD4$^+$ T CELL DIVISION *IN VIVO*

MSC immune modulation is multifactorial requiring both cell: cell contact and the release of soluble factors for different aspects of suppression. To investigate if hMSC production of prostaglandins was involved in the inhibition of T cell proliferation, *in vitro* and *in vivo* studies were carried out. Firstly, the production of PGE_2 by hMSC in coculture with PBMC was analysed *in vitro.* PBMC were cocultured with hMSC for 48 h and the production of PGE_2 was analysed by ELISA. Prostaglandin production was also blocked in coculture studies through the addition of indomethacin (Fig 6.10). PBMC alone did not produce PGE_2, however, in the presence of hMSC, the production of PGE_2 was significantly increased ($p<0.0001$) (Fig 6.10) consistent with hMSC production of prostaglandins shown earlier (Chapter 3). Following the addition of indomethacin, the production of PGE_2 by hMSC in the presence of PBMC was significantly reduced ($p<0.0001$) (Fig 6.10 A). The vehicle control for indomethacin (ethanol diluted in medium) had no effect on the production of PGE_2 by hMSC *in vitro*. To investigate if the production of prostaglandins by hMSC were essential for the inhibition of PBMC proliferation *in vitro*, proliferation assays were performed. PBMC were stimulated with a mitogen (PHA) in the presence or absence of hMSC for 72 h. Prostaglandin production was blocked using indomethacin. PBMC stimulated with PHA proliferated significantly more that PBMC alone (Fig 6.10 B). In the presence of hMSC, the proliferation of PBMC was significantly reduced. However, when prostaglandin production was blocked through the addition of indomethacin, hMSC could no longer inhibit the proliferation of PBMC (Fig 6.10 B). These data demonstrated that the hMSC used in this study were capable of PGE_2 production and that PGE_2 was essential for

hMSC inhibition of PBMC proliferation. These data also suggested a possible mechanism by which hMSC reduce T cell proliferation *in vivo*, prolonging the survival of mice with aGvHD.

The possibility that the production of prostaglandins by hMSC was the mechanism by which hMSC prolonged the survival of NSG mice with aGvHD *in vivo* was examined. Indomethacin significantly reduced the production of PGE_2 by MSC and was essential for hMSC inhibition of PBMC proliferation *in vitro* (Fig 6.10). The concentration of indomethacin used *in vivo* was similar to that used by other groups for the blocking of prostaglandin production *in vivo* (Kulkarni, 1981; Bordet, 2000; Cooper, 2010). Irradiated NSG mice received PBS or PBMC on day 0 by i.v injection. Unstimulated hMSC were given on day 7 or prestimulated hMSC (MSCγ) were given on day 0. Mice that received PBMC on day 0 developed aGvHD by day 13, indicated by significant weight loss (Fig 6.11 A) and development of aGvHD pathological signs (ruffled fur, reduced activity, hunched posture and diarrhoea) (Fig 6.11 C). However, mice that received hMSCγ therapy on day 0 or hMSC therapy on day 7 did not develop any significant signs of aGvHD (Fig 6.11 C) and survived, similar to those observed in Chapter 5.

Next, prostaglandin production was blocked *in vivo* through the administration of indomethacin (6 mg/kg) via intraperitoneal (i.p) injection on day 0 and every 3 days thereafter. Blocking prostaglandin production had no effect on the development of aGvHD, as mice that received PBMC along with indomethacin i.p on day 0 has significant weight loss (Fig 6.12 A) and developed pathological signs of aGvHD by day 13 (Fig 6.12 C). Mice that received hMSCγ therapy on day 0 along with indomethacin (i.p) every 3 days did not develop any significant signs of aGvHD development (Fig 6.12 C), when compared to mice that received hMSCγ therapy

without indomethacin (Fig 6.11 C). These data suggested that prostaglandin production by hMSCγ was not essential for the prevention of aGvHD in this model.

The role for prostaglandin production via unstimulated MSC was investigated *in vivo*. In this case, indomethacin therapy did not commence until hMSC administration on day 7. Mice were irradiated on day 0 and received PBS or PBMC by i.v injection. Following hMSC therapy on day 7, indomethacin was given i.p to all groups, including PBS, PBMC and hMSC treated groups on day 7 and every 3 days thereafter (Fig 6.13). Blocking prostaglandin production from day 7 had no effect on the development of aGvHD by day 16 (Fig 6.13). Mice that received MSC therapy on day 7, along with indomethacin did not develop any signs of aGvHD. These data suggested that prostaglandin production by hMSC was not essential for the prevention of aGvHD in this model.

The production of PGE_2 was analysed in the serum of NSG mice with aGvHD following hMSC cell therapy by ELISA (Fig 6.14 A). Low dose irradiated NSG mice that received PBS on day 0 had significantly higher levels of PGE_2 present in the serum on day 13, when compared to NSG mice that received PBMC (Fig 6.14.A). hMSC cell therapy administered on day 7 or IFNγ stimulated MSC administered on day 0 did not result in an increase in PGE_2 in the serum of NSG mice with aGvHD when compared to NSG mice that received PBMC alone on day 0 (Fig 6.14 A). These data supported the findings shown in figure 6.12 and 6.13, which suggested that the production of PGE_2 was not involved in the prolonged survival of NSG mice with aGvHD. The analysis of serum following the administration of indomethacin also confirmed that the addition of indomethacin via intraperitoneal injection (i.p.) every three days was sufficient for a consistent decrease in PGE_2 production *in vivo* (Fig 6.14 B & C). It is important to note that

indomethacin treatment was not specific for MSC produced prostaglandins in this case. However, these data clearly show that prostaglandin production, whether already present *in vivo* or through the presence of MSC therapy was not essential for suppression of aGvHD in this model.

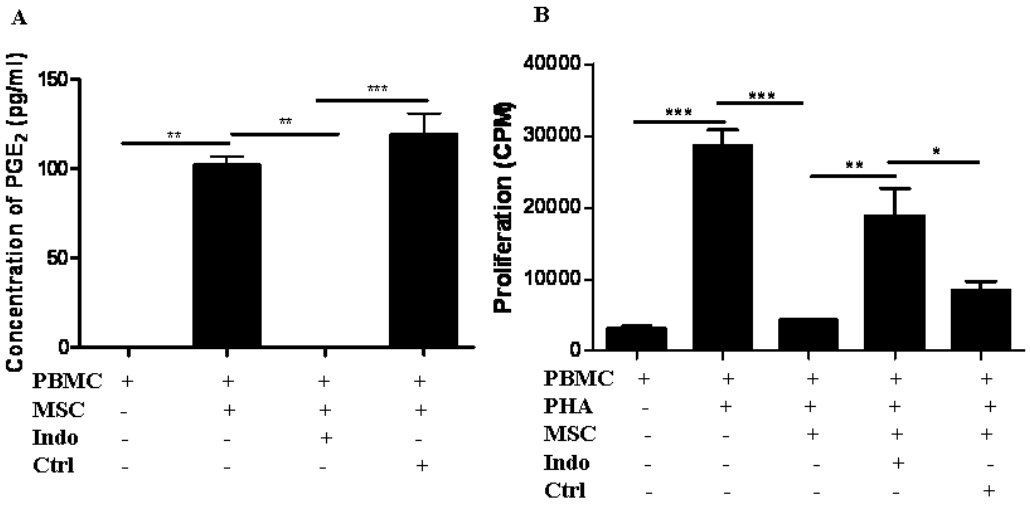

Fig 6.10 Prostaglandins are essential for MSC inhibition of PBMC proliferation *in vitro*. (A) hMSC (3 x 10^5/well) were coculture with PBMC (1 x 10^6/well) in a 6 well plate for 48 h and the production of PGE_2 was analysed by ELISA. PGE_2 production was blocked through the addition of indomethacin (indo) (20 μM). Vehicle control (crtl) (ethanol) for indomethacin was added to control wells. hMSC produced PGE_2 *in vitro* in the presence of $CD4^+$ T cells. (B) hMSC (4 x 10^5/ml) were cocultured with PBMC (4 x 10^6/ml) in a 96 well plate for 72 h in the presence of indomethacin. [3H]-Thymidine at 0.5 μCi was added for the final 6 h of culture. hMSC significantly reduced ($p<0.0001$) the proliferation of PBMC *in vitro* through the secretion of PGE2. Blocking prostaglandin production through the addition of indomethacin significantly increased ($p<0.05$) the proliferation of PBMC in the presence of hMSC. Indomethacin successfully blocked PGE_2 production by hMSC. Statistical analysis was carried out using the students paired t test. Data are representative of three experiments.

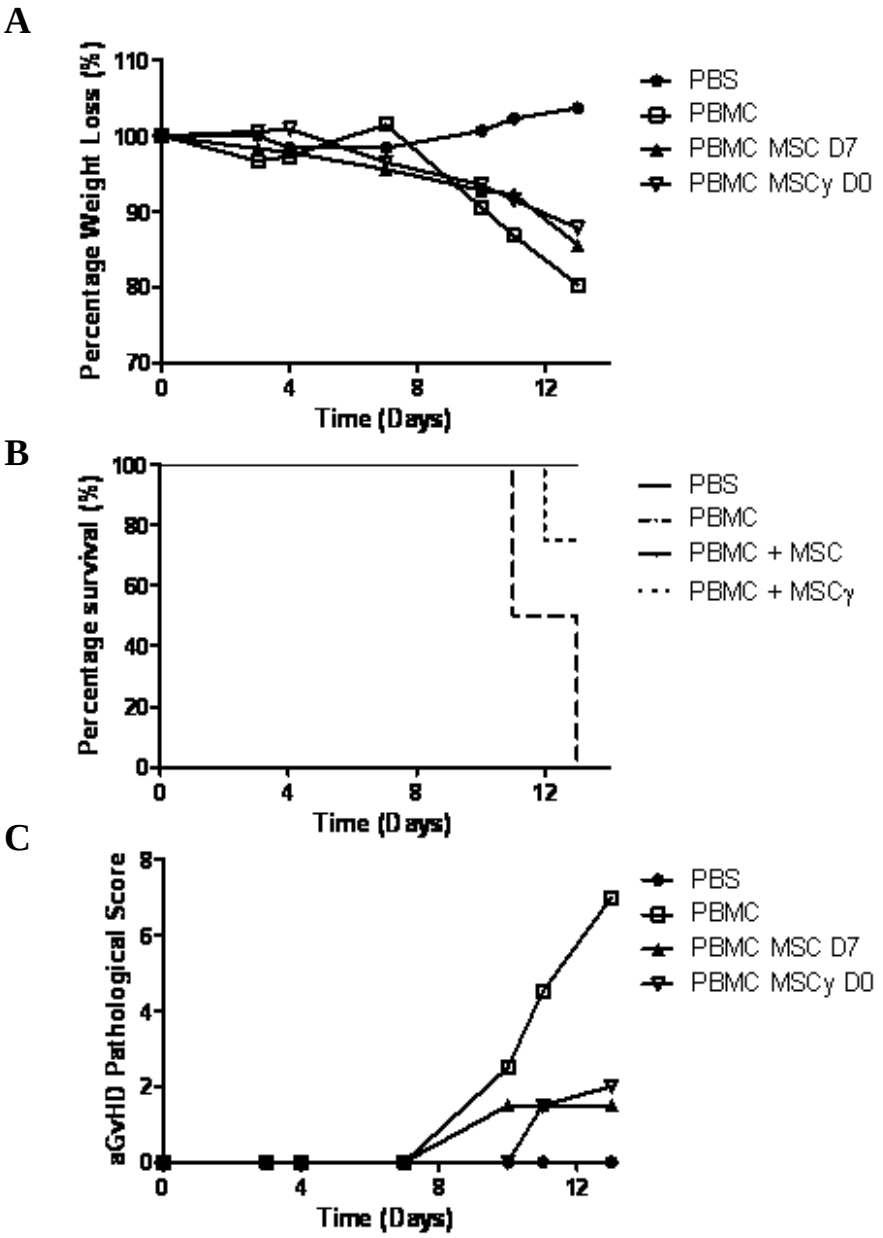

Fig 6.11 MSC cell therapy prolonged the survival of mice with aGvHD. Irradiated mice received PBS or PBMC on day 0. Unstimulated MSC were given on day 7 or prestimulated MSC (MSCγ) were given on day 0. MSC therapy (A) reduced weight loss, (B) increased survival and (C) reduced the development of aGvHD symptoms. Data are representative of 4 mice per group (n=4).

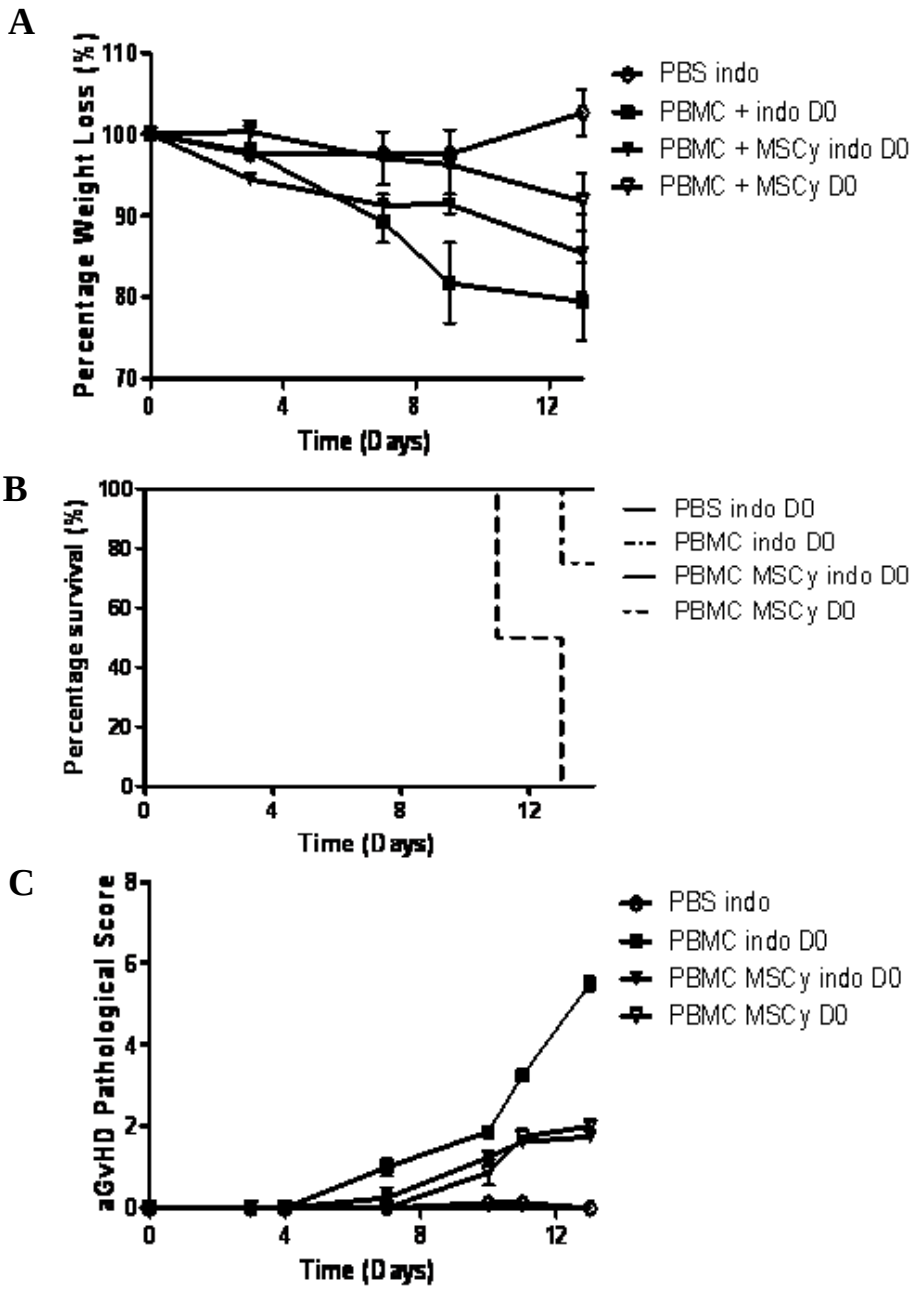

Fig 6.12 Production of prostaglandins by MSCγ were not essential in the beneficial effect seen *in vivo*. Irradiated mice received PBS or PBMC on day 0. Prestimulated MSC (MSCγ) were given concurrent with PBMC on day 0. Indomethacin (6mg/kg) was administered intraperitoneal (i.p) on day 0 and every 3 days thereafter. Blocking prostaglandin production did not interfere with the ability of MSCγ prolonging the survival of mice with aGvHD. Indomethacin treatment did not (A) increase weight loss, (B) decrease survival or (C) increase the symptoms of aGvHD development in mice. Data are representative of 4 mice per group (n=4).

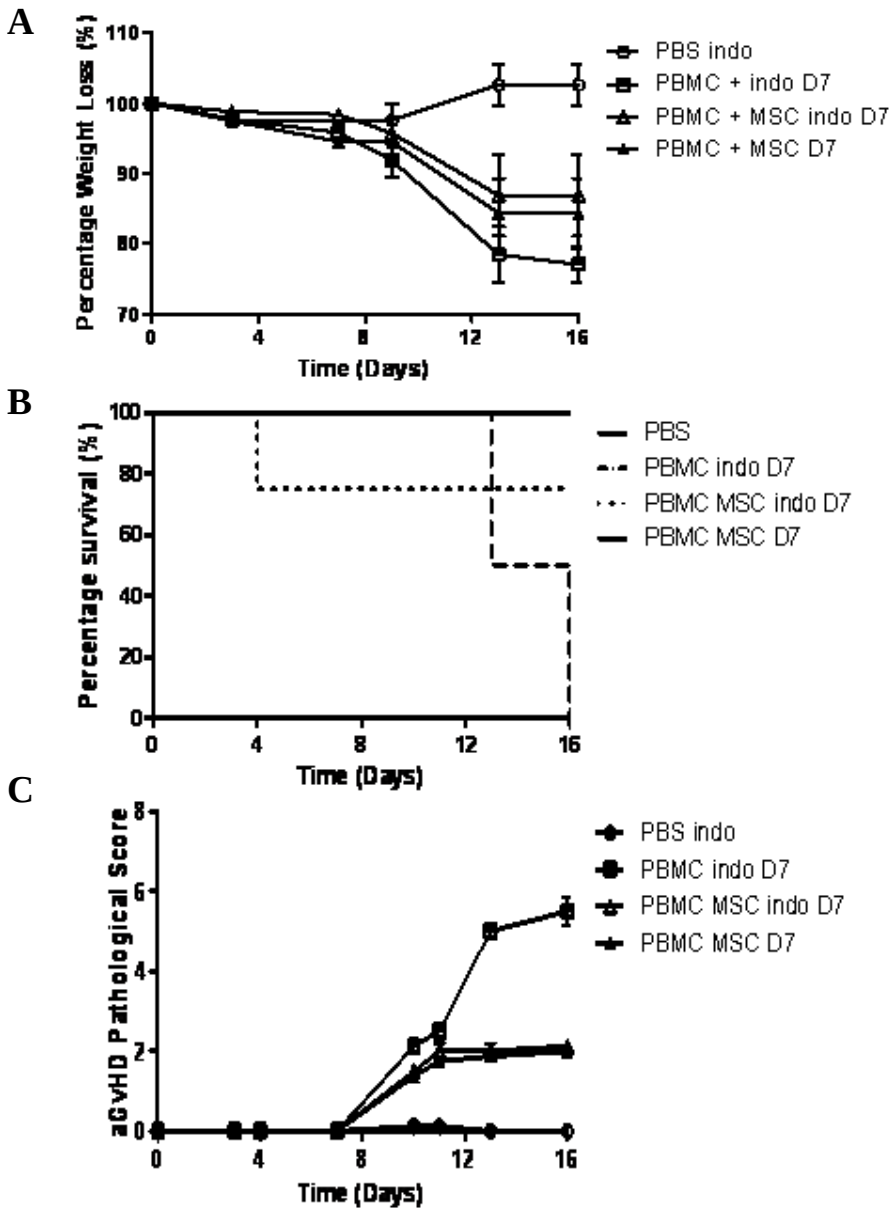

Fig 6.13 Prostaglandins by hMSC were not essential for the beneficial effect seen *in vivo*. Irradiated mice received PBS or PBMC on day 0. Unstimulated MSC were given on day 7. Treatment of mice with indomethacin via i.p injection commenced on day 7 and was given every 3 days thereafter. Blocking prostaglandin production did not interfere with the ability of MSC prolonging the survival of mice with aGvHD. Indomethacin treatment did not (A) increase weight loss, (B) decrease survival or (C) increase the symptoms of aGvHD development in mice. Data are representative of 4 mice per group (n=4).

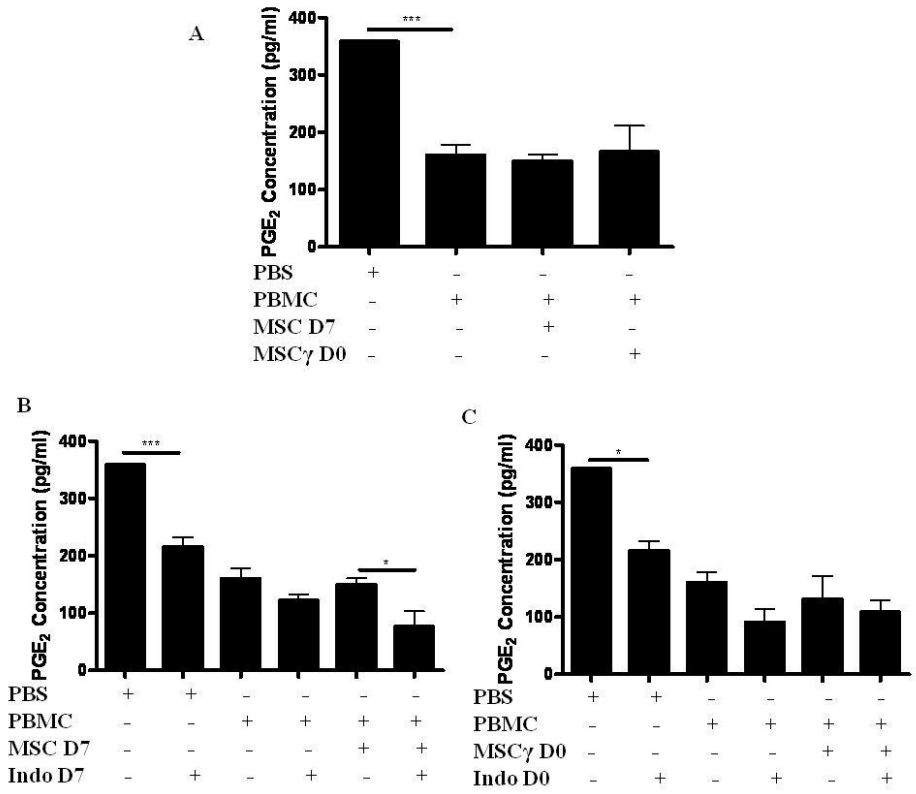

Fig 6.14 hMSC did not increase prostaglandin production in NSG mice with aGvHD. (A) Low dose irradiated NSG mice received PBS or PBMC on day 0. hMSC cell therpay was given on day 7, while IFNγ stimulated MSC (MSCγ) therapy was given concurrent with PBMC on day 0. Following the evelopment of aGvHD on day 13, serum was taken from each mouse and analysed for the production of PGE2 by ELISA. hMSC cell therapy did not increase the production of PGE_2 in NSG mice with aGvHD. Indomethacin (indo) at 6 mg/kg was adminitered by intraperitoneal injection (i.p.) on (B) day 7 with hMSC therapy or on (C) day 3 with hMSCγ therapy and every three days thereafter. Serum was taken from each NSG mouse on day 13 following aGvHD development. The production of PGE_2 was analysed by ELISA. Indomethacin consistently reduced the amount of PGE_2 present in the serum of NSG mice. Data are representative of 4 mice per group (n=4).

6.7 SUMMARY

The aim of this Chapter was to determine the mechanism involved in hMSC modulation of aGvHD development in a humanised mouse model as found in Chapter 5. The literature suggested four possible mechanisms by which MSC cell therapy might be mediating a beneficial effect *in vivo*. These mechanisms included the induction of lymphocyte apoptosis, induction of T cell anergy, the induction of regulatory T cells or the direct inhibition of T cell proliferation.

In vitro and *in vivo* analysis suggested that hMSC did not induce PBMC apoptosis. Although there is contradictory published data, the data presented herein clearly suggested that hMSC did not induce apoptosis and this was not the mechanism used by hMSC in prolonging the survival of mice with aGvHD. hMSC were found not to be involved in the induction of T cell anergy, following *in vitro* analysis. The induction or expansion of T reg populations were suggested to be involved in the regulation and prevention of aGvHD in other models. Although, hMSC induced a T reg-like population *in vitro*, this did not translate to the situation *in vivo* as hMSC did not induce a detectable T reg-like population in NSG mice with aGvHD. Therefore, the therapeutic benefit was unlikely to depend on this mechanism.

hMSC can suppress immune responses through the direct inhibition of T cell proliferation *in vitro*. Following hMSC therapy *in vivo*, donor lymphocytes displayed reduced proliferation in the lung of NSG mice with aGvHD. Possible roles for hMSC derived prostaglandins were examined using the antagonist indomethacin to block the secretion of prostaglandin, PGE_2, by MSC *in vitro* and *in vivo*. However, blocking PGE_2 production had no effect on the ability of hMSC to

prolong the survival of mice with aGvHD. This suggested that, although MSC secrete PGE_2, the mechanism involved in the reduced proliferation of donor T cells *in vivo* by MSC did not require PGE_2 production. This Chapter developed both *in vitro* and *in vivo* models to address the four key hypotheses by which MSC cell therapy could be beneficial in treating aGvHD. These findings contribute to on going research in this area.

CHAPTER 7

DISCUSSION

The induction of tolerance is an important mechanism involved in the regulation of immune responses against self antigens ("self tolerance") or innocuous non-self antigens ("induced tolerance"). Tolerance supports successful organ and hematopoietic stem cell transplantation. The primary utility for MSC therapy was originally thought to be in repair and regeneration of damaged tissues (Caplan, 1991). However, it has since become apparent that MSC can play a therapeutic role in immune modulation. Haynesworth and Caplan first proposed the contribution of MSC derived trophic factors to therapeutic efficacy (Haynesworth, 1996). These findings paved the way for using MSC as cell based modulators of immune mediated diseases rather than purely regeneration-based therapies. MSC have a unique if partial, privilege from allogeneic rejection, meaning that in the absence of complete immune suppression, MSC are not rapidly rejected by an allogeneic host (Bruder, 1998; Le Blanc, 2004; Ryan, 2005). This finding put MSC in a spotlight, where their use as a unique allogeneic cell therapy becomes plausible. Autologous MSC therapy had proved successful (Koc, 2000), however, allogeneic MSC allows for a more "off the shelf" multi-recipient therapy with comparable efficacy to autologous cells. The aims of this thesis were to investigate the ability of MSC to induced regulatory DC and T cell populations *in vitro,* to determine the exact mechanisms of suppression and to extend this to define the regulatory mechanisms used by MSC in the treatment of aGvHD using a humanised mouse model.

In chapter 3, the effect of allogeneic hMSC on human $CD4^+$ T cells was examined in *vitro.* Firstly, the effect of a validated homogenous population of hMSC on whole PBMC proliferation was examined and proliferation shown to be significantly reduced in the presence of hMSC (Fig 3.4). These data were similar to other groups, where MSC exhibited potent anti-inflammatory properties associated

with an inhibitory effect on T cell activation and proliferation (Di Nicola, 2002; English, 2007; Ryan, 2007; Benvenuto, 2007; Ramasamy, 2008; Park, 2011). Following hMSC coculture, the expression of the regulatory markers, FoxP3 and CD25 were increased in purified $CD4^+$ T cells, suggestive of a T reg cell population (Fig 3.6 & 3.7). $CD4^+$ $CD25^+$ $FoxP3^+$ T cells induced by hMSC had suppressive characteristics. Repurifying T cells induced by coculture with hMSC and placing them in a two way MLR demonstrated that such T reg cells were capable of inhibiting allogeneic PBMC responses even after removal of MSC (Fig 3.13). T reg cells have important roles in the induction and maintenance of specific immunological unresponsiveness to foreign alloantigens *in vivo* (reviewed by Wood, 2011). The fact that hMSC were capable of inducing a population of T cells with a regulatory phenotype suggested that MSC might prove beneficial as a cell based therapy for solid organ transplantation, GvHD or autoimmunity.

Through a series of neutralisation studies, the roles of soluble factors, prostaglandins and TGFβ1 production by hMSC were examined in relation to the induction of T reg cells *in vitro*. hMSC constitutively secreted PGE_2 and TGFβ1, key soluble factors involved in mediating MSC immune modulation of T cells (English, 2007; Ryan, 2007). The demonstration of non-redundant roles for soluble factors was similar to data from other groups (Baratelli, 2005; Fu, 2004; Ghannam, 2010; Park, 2011). PGE_2 enhances the *in vitro* inhibitory function of human $CD4^+CD25^+$ T reg cells and significantly up regulates FoxP3 promoter activity, increasing FoxP3 expression (Baratelli, 2005; Ghannam, 2010). While TGFβ signalling is involved in the initiation and maintenance of FoxP3 expression and regulatory function (Fu, 2004). Complimenting the data herein and the work by others, Park *et al.* recently confirmed a role for TGFβ in the induction of $CD4^+$

FoxP3$^+$ T reg cells by mMSC (Park, 2011). The data here and elsewhere identify important roles for both PGE_2 and TGFβ in MSC mediated immune modulation (Baratelli, 2005; Fu, 2004; Ghannam, 2010; Park, 2011). However, these findings were contradicted by Prevosto *et al.* who suggested a role for GITR$^+$/CTLA-4 and CD25$^+$ in the induction of T cells with suppressor activity by MSC, but found no roles for TGFβ1, PGE_2 or IL-10 (Prevosto, 2007). While Selmani *et al.* showed that soluble HLA-G5, secreted by hMSC, was required for the suppression of T lymphocytes present in whole PBMC (Selmani, 2008). The conflicting data relating to the release of various soluble factors by MSC (TGFβ1 vs PGE_2 vs HLA-G5) between studies might be explained by experimental design. The use of a purified CD4$^+$ T cell population here compared to a heterogenous unpurified system by Prevosto and Selmani could be the explanation. This would suggest that in a multi-cell system, the role of individual mediators could possibly be masked by the presence of other cells, as multiple independent pathways can modulate different aspects of MSC mediated suppression (English, 2007; English, 2008). This was supported by the findings here when hMSC were cocultured with unseparated whole PMBC. Under these conditions, cell contact was not required for hMSC induction of FoxP3 expression whereas direct cell contact was required when purified CD4$^+$ T cell populations were used (Fig 3.10). This suggested that cell contact signals were substituted by other factors present in a whole population of PBMC that are not present in a purified two-cell system. The exact cell contact molecule/molecules involved in MSC generation of T reg cells are the subject of study by other members of the Mahon group. Chapter 3 found that hMSC induced a FoxP3$^+$ T reg cell population *in vitro*, which required an unidentified direct cell contact signal between

hMSC and $CD4^+$ T cells and the subsequent release of soluble factors, PGE_2 and TGFβ1.

The induction of T reg cells *in vitro* by hMSC, suggested the involvement of hMSC in the induction of immune tolerance through the generation of regulatory cells. This is a key finding in relation to the induction of tolerance in transplantation, as $CD4^+$ $CD25^+$ $FoxP3^+$ T reg cells have a beneficial role in aGvHD and the maintenance of GvL and GvT *in vivo* (Cohen, 2002; Hoffmann, 2002; Cao, 2009). Interestingly, DC can generate T reg cells in patients with different types of cancers (Steinman, 2008; Hubert, 2007), as the induction of semi-mature/tolerogenic DC are capable of driving the differentiation and proliferation of $FoxP3^+$ T reg cells (Mahnke, 2003; Mahnke, 2007; Wakkach, 2003). Therefore, in chapter 4, the ability of murine bone marrow derived MSC induction of semi-mature/tolerogenic DC was examined *in vitro*.

For the purpose of the work carried out in chapter 4, a switch from human to murine cells was made, as there were limitations regarding the use of human derived DC and the isolation of DC and T cells from the same HLA background was difficult to achieve. Therefore, murine bone marrow derived MSC and DC were used. mMSC modulated three aspects of DC function: maturation, cytokine secretion and antigen presentation (Fig 4.6 & 4.7). mMSC coculture prevented the LPS driven increase of DC MHC class II and CD86 expression, which coincided with a significant decrease in the production of IL-12p70 and significant increase in IL-10. To examine if mMSC interfered with antigen presentation by DC, an antigen specific display system was employed exploiting YAe antibody recognition of the I-Eα peptide bound to $I\text{-}A^b$ MHC class II (Rudensky, 1991). This approach yielded data suggesting that mMSC reduced the antigen presentation ability of DC. These

findings were similar to that found by Jiang *et al.*, where hMSC interfered with DC differentiation from monocytes, decreased IL-12 production and hampered antigen presentation (Jiang, 2005). Collectively, these data suggested that by preventing maturation of DC, mMSC were keeping DC in a "semi-mature" or tolerogenic phenotype. Allowing DC to become more regulatory might contribute to the immunosuppressive capacity carried out by MSC (Lutz, 2002; Jiang, 2005; Aggarwal, 2005; English, 2007). To investigate if the semi-mature DC population induced by mMSC had a functional effect, a well-defined antigen specific T cell proliferation system was used. DC pulsed with OVA peptide supported DO11.10 $CD4^+$ T cell proliferation. In the presence of mMSC, OVA pulsed DC were significantly less able to stimulate DO11.10 T cell proliferation. These data suggested that mMSC induced a semi-mature/tolerogenic DC population, interfered with the antigen presentation of DC, induced a "regulatory" DC, and prevented the proliferation of antigen specific T cells, findings recently confirmed by Chiesa *et al.* (Chiesa, 2011). These data supported the hypothesis proposed in chapter 3, that MSC induction of immune tolerance was due to the generation of regulatory immune cells, including $CD4^+$ T reg cells and tolerogenic DC.

mMSC modulation of DC function involved both soluble and cell contact factors (Beyth, 2005; Jiang, 2005; Nauta, 2006; Djouad, 2007; Li, 2008; Zhang, 2009). Previous work by the Mahon group confirmed the work of Jiang *et al.* (Jiang, 2005) identifying a role for IL-6 in mMSC modulation of DC maturation, with no role identified for TGFβ or HGF (English, personal communication). Through neutralisation studies, the secretion of VEGF and M-CSF by MSC were found to be involved in DC differentiation from precursor cells (Nauta, 2006; Djouad, 2007). Collectively, these data identified a role for MSC derived IL-6, IL-10, VEGF and M-

CSF in the DC differentiation, subsequent maturation and ultimate shaping of T cell function.

At the commencement of this work, published data supported a role for soluble factors in MSC immune modulation of DC, but the need for direct cell contact between MSC and DC was unclear. Using a transwell system, similar to that used in chapter 3, the presence of mMSC had no effect on LPS driven DC maturation if contact was prohibited. These data implied that direct cell contact was required between mMSC and DC in order for MSC to have a modulatory effect on DC maturation and suggested that contact was an upstream event to IL-6 secretion. This work was similar to that published by others whereby cell contact played an important role in MSC: DC modulation (Beyth, 2005; Djouad, 2007; Zhang, 2004).

In chapter 4, a number of possible cell contact candidates were analysed for their involvement in mMSC immune modulation of DC function. The first candidate for analyses were the sialic-acid binding immunoglobulin-like lectins, Siglecs. Siglecs are involved in immune cell: cell interactions. The maturation of DC results in an increase of glycan expression, which allows for increased Siglecs and galactin binding (Bax, 2007). Mature cells of the innate immune system, such as monocytes and dendritic cells express CD33-related Siglecs (Crocker, 2007). CD33 related Siglecs modulate leukocyte behaviour, including the inhibition of cellular proliferation (Vitale, 1999; Balaian, 2003) and cytokine production (Lajanias, 2005). These findings encouraged the investigation of CD33-related Siglec expression by mMSC and drove the hypothesis that mMSC could prevent DC maturation through Siglec: glycan recognition, which would relay an inhibitory signal. However, following mRNA and protein analysis of CD33-related Siglecs expression on mMSC alone or prestimulated mMSC could not be demonstrated (Fig 4.10). There is no

data published to suggest the expression of Siglecs by mMSC. Therefore, a role for CD33-related Siglecs in mMSC modulation of DC maturation was considered improbable. However, the possibility of CD33-related Siglec expression by DC and glycan expression by mMSC was not explored. In this case, the recognition of specific Siglecs on DC may occur through the expression of various glycans by mMSC. However, the differential glycan expression on mMSC following various stimulations was not profiled during this thesis.

The B7 family of ligands play important roles in the regulation of T cell activation and immune tolerance (Greenwald, 2005). The B7 receptors (CD28, CTLA4, ICOS, PD-1) and ligands (LICOS, PDL-1, PDL-2, CD80, CD86) are involved in the activation, regulation and inhibition of T cell responses (Alegre, 2001; Herman, 2004; Latchman, 2001; Nishimura, 2001) with the balance between stimulatory and inhibitory signalling important for the maintenance of tolerance. As MSC were capable of inducing regulatory cell populations the expression of CTLA-4 (CD152), ICOS (CD278), LICOS (CD275), PD-1 (CD279) and PDL-1 (CD274) were analysed on mMSC and DC. mMSC did not express the B7 ligands, LICOS and PDL-1 or the receptors, CTLA-4, ICOS or PD-1. DC expressed receptors, ICOS and PD-1 and ligands, LICOS and PDL-1. However, the binding of ICOS: LICOS stimulates T cell activation, while the binding of PD-1: PDL-1 inhibits T cell activation (Greenwald, 2005). ICOS and PD-1 are expressed on activated T cells and their respective ligands on DC. T reg cells can develop with support through the ICOS: LICOS pathway, for the expression of regulatory molecules, such as IL-10, (Akbari, 2002). PD-1 ligation results in the decrease of DC maturation marker expression and an increase in IL-10 production, inducing a suppressive DC phenotype (Kuipers, 2006). Although the ICOS and PD-1 signalling pathways were

not identified as key cell contact factors between MSC and DC *in vitro*, ICOS and PD-1 signalling pathways are involved in the generation of regulatory cells and the balance of tolerance and immunity (Salomon, 2001; Aramaki, 2004). ICOS signalling between DC and naïve $CD4^+$ T cells is involved in the upregulation of IL-10 and the induction of suppressor T cells (Tuettenberg, 2009; Levings, 2002). ICOS deficient $CD4^+$ T cells are insensitive to the tolerogenic effects of DC, inhibiting the induction of T reg cells and anergic T cells *in vitro* (Tuettenberg, 2009). In relation to PD-1 signalling, there is a feedback loop whereby, T reg cells induce PDL-1 expression on DC, inducing a suppressor phenotype. In turn, these regulatory DC are capable of inducing T reg cells involved in promoting immune suppression (Sharma, 2007; Amarnath, 2010). Although there was no significant role found here for ICOS or PD-1 signalling in mMSC induction of tolerogenic DC, there are published roles for both ICOS and PD-1 signalling between $CD4^+$ T cells: DC and the induction of tolerance. Therefore, it is possible that the induction of tolerogenic DC via MSC could occur through different pathways, not involving ICOS or PD-1 signalling. However, the induction T reg cells via MSC could possibly involve the ICOS or PD-1 pathways, which could indirectly influence the induction of tolerogenic DC by MSC. This hypothesis highlights a multi-relationship system whereby numerous contact signals might be involved in the modulation of immune tolerance, some of which are independent of MSC. This concept is represented in Figure 7.1.

Another candidate for contact dependent suppression was the Notch signalling pathway. Interactions between Notch receptors and ligands play a crucial role in the cross talk between cells of the immune system and their surrounding microenvironment (Radtke, 2004). The expression of Notch receptors and ligands

are important in stem cell maintenance, cell proliferation, differentiation, apoptosis and induction of peripheral tolerance (Hoyne, 2000; Radtke, 2004; Fiuza, 2007). Notch signalling is involved in the regulation of T cell activation (Yvon, 2003; Beyth, 2005; Liotta, 2008) and DC maturation (Weijzen, 2002; Cheng, 2003; Amsen, 2004; Cheng, 2007; Li, 2008; Zhang, 2009). The expression of Notch receptors, Notch 1 & 2, and Notch ligands, Jagged 1 & 2 and Delta like ligand 1, by mMSC and DC were analysed. mMSC expressed both Notch 1 and 2 receptors and the ligands Jagged 1 and Delta like ligand 1. mMSC did not express the ligand Jagged 2. DC on the other hand expressed receptors, Notch 1 and 2 and the ligands, Jagged 1, 2 and Delta like ligand 1. When Notch signalling was blocked in coculture experiments, the induction of a semi-mature DC by mMSC was inhibited. This suggested that when the Notch signalling pathway was blocked, mMSC did not interfere with DC maturation and highlighted the Notch signalling pathway as a required contact signal between mMSC and DC *in vitro*. Therefore, the Notch signalling pathway was examined in more detail. In the presence of GSI, mMSC were unable to interfere with DC antigen presentation and maturation and blocking Notch signalling interfered with the induction of a tolerogenic DC (Fig 4.22). These findings identified a required role for Notch signalling in the induction of a functional tolerogenic DC by mMSC. Unfortunately, the exact Notch receptors or ligands involved were not identified in this study.

Li *et al.* found that Notch signalling was involved in hMSC induction of DC that expressed high levels of IL-10, low levels IL-12, and inhibited T cell proliferation. These hMSC-induced tolerogenic DC also induced a population of T reg cells (Li, 2008). Recently Zhang *et al.* identified a novel Jagged 2 dependent regulatory DC that was generated through cell: cell contact with MSC (Zhang,

2009). These novel Jagged 2 dependent tolerogenic DC secreted high levels of TGFβ and were capable of inhibiting mitogen driven lymphocyte proliferation, while reducing the production of both IFNγ and IL-2 in culture supernatants (Zhang, 2009). Cheng *et al.* demonstrated that the main Notch ligands, Jagged 1 and Delta like ligand 1 had the opposite effects on DC differentiation (Cheng, 2007). Notch signalling through Delta like ligand 1 promoted the generation of fully differentiated DC. However, similar to the hypothesis herein whereby the silencing of Jagged 1 on mMSC was attempted, Cheng *et al.* found that Notch signalling through Jagged 1 resulted in the accumulation of DC precursors, which prevented the full differentiation of DC *in vitro* (Cheng, 2007). This finding was similar to that demonstrated in Chapter 4. Therefore, additional measures are currently underway within the Mahon Lab to development a cell line of bone marrow isolated mMSC that are completely silenced for Jagged 1 ($mMSC^{Jag-/-}$) expression by short hairpin RNA (shRNA). Once developed, the need for Jagged 1 expression by mMSC will be analysed for its role in the induction of a tolerogenic DC and regulatory T cell populations, identifying its significance in the induction of immune tolerance. If the contact signal between MSC and DC involves members of the Notch signalling pathway, this re-emphasises how the modulation of immune tolerance by MSC involves many pathways.

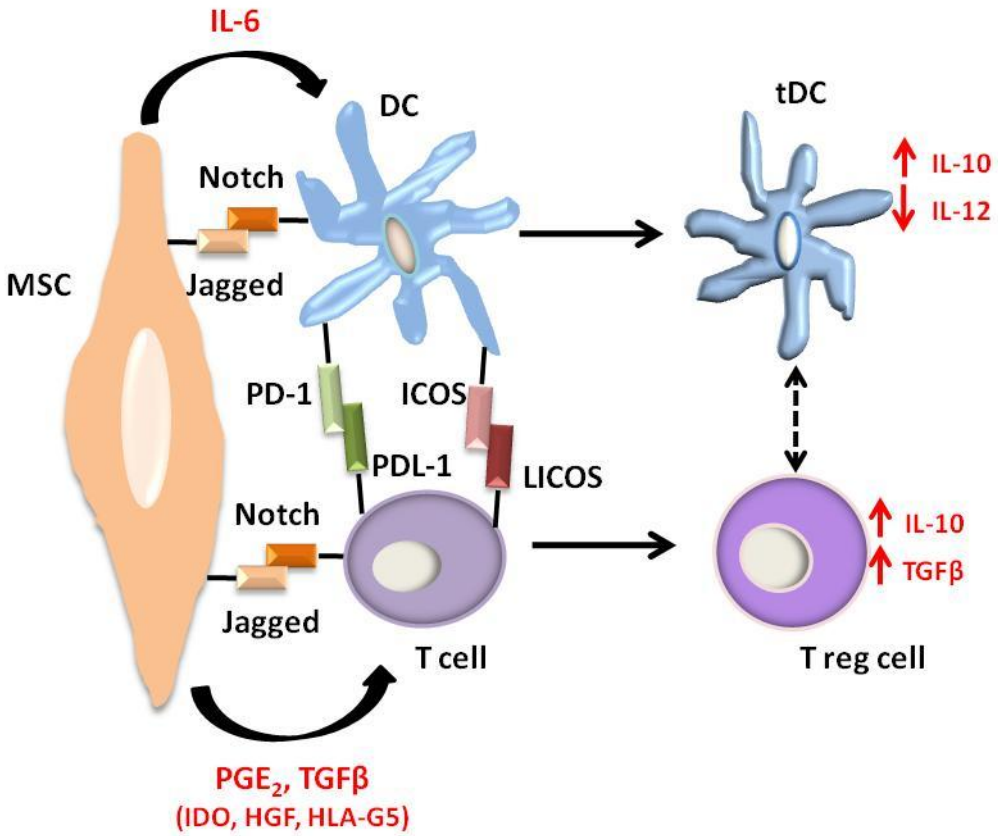

Fig 7.1 A proposed model of the contact signals required for MSC induction of regulatory cells. MSC mediate their immunomodulatory effects by influencing DC and T cell fate. MSC induce tolerogenic DC through direct cell contact involving the Notch signalling pathway and the secretion of IL-6. While the secretion PGE_2, and TGFβ subsequent to direct cell contact via Notch are required for the induction of T reg cells. DC mediation of T cell fate can involve multiple signalling pathways including Notch, ICOS or PD-1 signalling.

Chapter 3 and 4 identified MSC signals capable of influencing immune tolerance, through the induction of both innate and adaptive regulatory cells. This suggested that MSC could act therapeutically to prevent T cell mediated diseases, where the induction of tolerance could be beneficial. Therefore, a model system was chosen to examine the potential of hMSC to be used therapeutically. Allogeneic bone marrow transplantation is used to treat life-threatening haematological, oncological and immunological disorders. The induction of donor specific tolerance following allogeneic bone marrow transplantation is very important for the survival of the allograft (Shlomchik, 2007; Ezzelarab, 2011). In transplantation, T cell mediated immune regulation is involved in the induction of antigen-specific tolerance to deliberately introduced foreign antigens present in the allograft (Wood, 2003; Chinen, 2010). Tolerogenic DC are important in transplantation as they are capable of presenting antigen to antigen specific T cells, which results in the inhibition of T cell activation or proliferation through T cell deletion, unresponsiveness (anergy) or induction of T reg cells (Morelli, 2007). Graft versus Host Disease (GvHD) was chosen as a model disease as it is a donor T cell mediated disease, causing extensive host organ damage. Both regulatory DC and T cells are involved in the prevention of GvHD (Duffner, 2004; Taylor, 2002). Therefore, a humanised mouse model of acute GvHD (aGvHD) was developed and used to examine the effect of hMSC cell therapy on aGvHD development within the model.

Successful MSC cell therapy was first reported in 2004, when Le Blanc *et al.* found that *ex vivo* expanded haplo-identical human MSC were beneficial for treatment of steroid refractory aGvHD of the gut and liver in paediatric patients (Le Blanc, 2004). A follow up non-randomised study for the treatment of steroid refractory aGvHD was carried out in 2008, where both paediatric and adult patients

were successfully treated with haplo-identical or third party (mismatched) hMSC (Le Blanc, 2008). These studies were the first to identify that immunosuppressive characteristics of MSC that were found *in vitro* were in fact beneficial *in vivo* also. However, the exact mechanisms used by MSC *in vivo* still remain unclear. The use of murine models are very important tools to help analyse the role of specific mechanisms used by MSC and allow research groups to gain insight into how MSC exert their beneficial effects *in vivo*.

There are many mouse models of aGvHD (reviewed in Chapter 1.11). However a humanised mouse model generated from the NOD-Scid IL2rγ^{null} mouse (NSG), which readily engrafted human hematolymphoid cells and displayed enhanced function of these human lymphocytes *in vivo* was used here (Shultz, 2007). Previously, the NSG humanised model was used to study human type 1 diabetes and more recently human derived GvHD (Shultz, 2007; King, 2009; Pino, 2010). Using the NSG model, this thesis set out to optimise a humanised model of aGvHD and examine the role of human MSC as a cell therapy for the treatment or prevention of aGvHD *in vivo*. Pearson *et al.* published a protocol for the creation of a humanised mouse GvHD model using the NSG mice first described by Shultz *et al.* (Shultz, 2007; Pearson, 2008). This original protocol suggested that human PBMC isolated from whole buffy coat pack blood at a concentration of 2 x 10^7 per NSG mouse was sufficient for the induction of aGvHD between 10 to 20 days post i.v injection. Although PBMC engrafted into the NSG model and were detected in the spleen 12-16 days post transfusion, initial experiments using PBMC at 2 x 10^7 per mouse proved inconsistent for aGvHD development. Upon further analysis, the realisation of obtaining high numbers of NSG mice, all at the same age and weight proved unrealistic for additional studies. Therefore, taking into consideration previous

preliminary studies, an apparent relationship between disease symptoms, PBMC dose, PBMC source and initial body weight of each NSG mouse began to emerge. From this point on, the dose of PBMC required for consistent aGvHD development in this model was optimised with reference to the initial weight of each NSG mouse, 6.3×10^5 PBMC g^{-1} (2×10^7 PBMC/30g mouse) were required for a more consistent aGvHD model (Fig 5.7). The variation between the protocol created by Pearson *et al.* and the newly optimised protocol in Chapter 5 may have been due to differences in radiation dose, delivery rate and source of PBMC between labs. A switch from buffy coat pack isolated PBMC to freshly isolated PBMC from healthy donors on the day of delivery also aided the development of a more consistent humanised model. Consequently, the source of PBMC remained consistent, with four healthy donors chosen for further studies using the humanised mouse model developed herein.

Using the optimised humanised mouse model of aGvHD, the ability of hMSC to prevent, ameliorate or treat aGvHD was examined. MSC were administered on day 0, 7 or 14 post PBMC transfusion (Fig 5.10). MSC therapy on day 0 had no beneficial effect on the survival of NSG mice with aGvHD. However, hMSC given as a therapy on day 7 or 14 significantly prolonged the survival of NSG mice with aGvHD, reducing pathological signs of aGvHD. Subsequent larger studies found that hMSC given as a cell therapy on day 7 post PBMC transfusion prolonged the survival of NSG mice for more than 30 days, reducing pathology (Fig 5.11). These data suggested that the timing of MSC therapy was important in the treatment of aGvHD. These results were similar to that found by other groups in diverse systems (Polchert, 2008; Joo, 2010; Christensen, 2010). Polchert *et al.* found no significant improvement in GvHD related mortality when murine MSC were given as a therapy on day 0, but treatment with MSC on day 2 or 20 post bone

marrow transplantation prolonged the survival of mice with aGvHD (Polchert, 2008). Collectively, these data indicated that for untreated MSC therapy to be successful, clinical cell therapy should not be concurrent with HSC delivery.

In contrast to the data here, others have found no beneficial role for MSC as a therapy for GvHD (Sudres, 2006; Jeon, 2009). Sudres *et al.* showed that mMSC suppressed alloantigen driven T cell proliferation *in vitro* in a dose dependent manner. However, using a model where C57BL/6 bone marrow cells were injected into lethally irradiated BALB/c mice, mMSC therapy had no beneficial effect on survival (Sudres, 2006). This result was not surprising as Sudres administered mMSC at the same time as bone marrow transplantation. Jeon *et al.* found that hMSC were unable to prevent GvHD development in the same murine model used by Sudres *et al.*. Following hMSC administration on day 0 or at a later time point, day 7, the survival rate of mice with GvHD did not improve, nor were symptoms of GvHD alleviated. In this case, human MSC were unable to suppress xenogenic T cell activation *in vitro* and cytokine mismatch may explain why no beneficial effects against GvHD development were observed following hMSC therapy *in vivo*. Unlike the model used by Jeon *et al.*, the humanised model in this thesis used human donor PBMC for the development of GvHD. This would avoid the problems experience by Jeon *et al.*, as in Chapter 6, hMSC significantly inhibited human PBMC proliferation, both *in vitro* and *in vivo*.

The failure of unstimulated MSC to treat aGvHD when delivered concurrently with T cells is interesting. Donor T cells produce high levels of inflammatory cytokines in response to antigen recognition, such as IFNγ. Normally IFNγ enhances allogenicity (Ryan, 2007) however; MSC stimulated with IFNγ show enhanced immunosuppressive ability, largely a result of increased production of the

enzyme IDO (Meisel, 2004; Ryan, 2007; English, 2007). These data suggested that MSC could be activated or "licensed" to display more potent immunosuppressive abilities and/or greater efficacy (Polchert, 2008). Therefore, this aspect of MSC biology was examined. IFNγ stimulated MSC administered with PBMC effectively delayed the development of aGvHD (Fig 5.13). These data suggested that if MSC were administered concurrent with bone marrow transplantation, prior stimulation by IFNγ would improve efficacy. One explanation for this might be that the systemic inflammation in GvHD mice increases after day 0. On day 0, there is little or no IFNγ available for the activation of hMSC. However, as GvHD develops, the levels of IFNγ increase and by day 2 to 7, there are sufficient levels of IFNγ present within the NSG mouse for the activation of hMSC. Therefore, hMSC administered after the development of a proinflammatory environment *in vivo*, are more successful in prolonging the survival of mice with GvHD. These data clearly state the importance of cell manipulation as well as timing in MSC therapy.

Having identified a significant beneficial role of hMSC therapy for the improved survival of NSG mice with aGvHD, the effect of hMSC therapy on aGvHD target organs and inflammatory cytokines involved in aGvHD development were examined. Both unstimulated and IFNγ stimulated MSC therapy significantly reduced the severity of aGvHD pathology detectable in the small intestine and liver of NSG mice after 12 days (Fig 5.14 & 5.15). hMSC therapy reduced villous blunting and lymphocyte infiltration into the lamina propria of the small intestine, while reducing vascular endothelialitis and lymphocyte infiltration into the parenchyma of the liver. These data were similar to that found by Polchert *et al.* and Joo *et al.*, where mMSC therapy significantly improved the histological score of the intestine and liver of mice with GvHD (Polchert, 2008; Joo, 2010). Unlike Polchert

et al., MSC therapy did not improve the histological analysis of the lung in NSG mice with aGvHD, as there was a significant mononuclear cell infiltration in all treatment groups (Fig 5.16). Importantly, the histological results herein mirrored those of a Phase III clinical trial carried out by Osiris Therapeutics™ (Martin, 2010). This trial set out to examine the effects of a human MSC-like product, Prochymal® in the treatment of patients with steroid refractory aGvHD. In a Phase II trial, Prochymal cell therapy was well tolerated in patients with no adverse effects (Kebriaei, 2009). However, in the Phase III trial, patients who received the placebo treatment fared better than those that received the Prochymal cell therapy. This Phase III clinical trial was therefore deemed unsuccessful. Nevertheless, upon further analysis of the data collected in the trial, patients who had presented with aGvHD manifesting in the liver and the gut, showed significant improvement following treatment with Prochymal. Treatment with Prochymal cell therapy had no beneficial effect on skin manifestations or patient survival. Although histological analysis of the skin was not examined in the humanised model in Chapter 5, these findings suggested that the beneficial effect of MSC-based cell therapies for aGvHD could in fact be target organ dependent. One way to investigate this hypothesis could be to examine the expression of migratory/chemokine receptors on MSC and determine if the absence of key skin related chemokine receptors could be one of the reasons why MSC based-cell therapy are not beneficial for the treatment of aGvHD of the skin. However, overall, the data presented in Chapter 5 suggested that hMSC therapy was involved in reducing the pathology in target GvHD organs, which in turn was contributing to the survival of NSG mice with GvHD.

The inflammatory cytokines, IFNγ and TNFα play important roles in determining the severity of GvHD development (Ferrara, 2009). Therefore, the

analysis of cytokines present in the serum following MSC therapy was carried out. IFNγ stimulated MSC significantly reduced the levels of human TNFα detected in the serum of NSG mice with aGvHD (Fig 5.17 A). Interestingly, these findings were similar to results published by King *et al.* (King, 2009). By blocking TNFα production through the addition of Etanercept (Enbrel®-a soluble TNFα decoy receptor), the pathology of aGvHD was significantly reduced and the survival of NSG mice was significantly increased (King, 2009). Analysis of IFNγ levels in the serum of NSG mice following MSC therapy found that the levels of human IFNγ were not affected by treatment with MSC (Fig 5.17 B). Nonetheless, MSC therapy proved beneficial in prolonging the survival of NSG mice with aGvHD, reducing aGvHD pathology in the liver and gut, while decreasing the amount of TNFα present in the serum suggesting that IFNγ is more a result rather than a cause of pathology. It is not known how MSC prevent TNFα production but this is highly likely to involve suppression of monocytes and possibly DC. Such an influence may have profound influence in the NSG model (Fig 7.3)

The key to improving current cell therapies for aGvHD is an understanding of the mechanisms of cell action. The model developed in Chapter 5 proved a unique tool to test human cell therapies and their mechanisms of action. In particular, the influences of hMSC cell therapy on T cell responses in aGvHD were amenable to study. A number of possible mechanisms were analysed *in vivo* using the NSG aGvHD model. The induction of immune tolerance involves a precise balance between activation and inhibition of T cell responses. Therefore, *in vivo* studies were carried out to determine the precise mechanism of efficacy. Specifically, four hypotheses were tested: 1) that hMSC cell therapy was effective through deletion of donor T cells through apoptosis, 2) that hMSC rendered donor T

cells anergic; 3) that hMSC induced a suppressive T reg cell population or 4) hMSC directly inhibited donor T cell proliferation.

Several studies have given contradictory evidence in relation to the induction of T cell apoptosis by MSC (Plumas, 2005; Zappia, 2005). In this study, hMSC did not induce apoptosis of PBMC *in vitro* (Fig 6.1). In fact, hMSC appeared to protect PBMC from apoptosis, which is in line with the known supportive role for MSC in lymphopoiesis (Chen, 2009). Nevertheless a small-scale experiment was carried out to investigate the role for MSC induced T cell apoptosis *in vivo*. Following hMSC therapy in NSG mice with aGvHD, no apoptotic cells were detected *in vivo* after 24 h or 5 days (Fig 6.2). Contradicting the data herein, Plumas *et al.* found that hMSC inhibited both mitogen and antigen specific driven T cell proliferation *in vitro* through induction of apoptosis of activated T cells, involving the production of IDO (Plumas, 2005). Meisel *at al* identified a role for IDO expression by hMSC in the inhibition of T cell proliferation. In this case, MSC did not induce apoptosis and T cell proliferation was reversible through the addition of IL-2 (Meisel, 2004). The functional effect of IDO is to convert Tryptophan to Kynurenine; the Mahon group clarified the study carried out by Meisel *et al.* and showed that Kynurenine was the suppressive agent (Ryan, 2005). Kynurenine is however toxic *in vitro* at high concentration (Darcy, 2011) and it may well be that the finding of Plumas *et al.* are artefacts of culture systems used (Plumas, 2005). In direct contrast, many other groups have reported that MSC play no role in the induction of T cell apoptosis (Di Nicola, 2002; Zappia, 2005; Corcione, 2006; Krampera, 2006). In spite of the contradictory literature, the data here indicated that the induction of T cell apoptosis by hMSC was unlikely to be the mechanism by which MSC prolonged the survival of NSG mice with aGvHD.

The concept that MSC induce T cell anergy has been controversial (Zappia, 2005; Glennie, 2005). The findings here suggested that hMSC did not induce $CD4^+$ T cell anergy *in vitro*. Although hMSC inhibited the proliferation of human $CD4^+$ T cells following xenogeneic stimulation with murine DC, upon restimulation of the repurified $CD4^+$ T cells with irradiated murine DC in the absence of IL-2 stimulation, antigen specific T cell proliferation occurred (Fig 6.3). This suggested that hMSC did not induce an antigen specific anergic T cell population *in vitro*. These data are contradictory to those found by Glennie *et al.* and Zappia *et al.*. In these studies, bone marrow derived murine MSC inhibited antigen specific T cell proliferation and reduced the production of IFNγ. However, following the removal of mMSC, T cells did not regain their ability to proliferate in response to the cognate antigen, but this was reversible by addition of IL-2 suggesting the induction of T cell anergy (Zappia, 2005; Glennie, 2005). Interestingly, the production of IFNγ was restored purely upon mMSC removal. This suggested that mMSC induced a phenomenon known as split anergy (Zappia, 2005; Glennie, 2005). In other murine and human studies, it was demonstrated that T cell unresponsiveness was transient and completely reversed once MSC were removed from cultures (Krampera, 2003; Di Nicola, 2002). Variations between groups may be due to the use of different stimuli in each study design and differences between the uses of murine or human MSC. The transient T cell unresponsiveness seen by others is possibly not due to the direct action by MSC, but rather due to the effect of anti-inflammatory factors released by MSC into the culture system.

As it was unlikely that hMSC were inducing T cell apoptosis or anergy, the next mechanism to be explored was the hypothesis that MSC were inducing T cell tolerance through the induction of T reg cells. Naturally occurring $CD4^+$ $CD25^+$

FoxP3$^+$ T reg cells play a role in the induction and maintenance of immune tolerance (Roncarolo, 2007). The induction and *ex vivo* expansion of T reg cells have had limited success in the prevention of aGvHD. Many murine studies have identified a correlation between T reg cells and the induction, acceleration and treatment/prevention of aGvHD (Cohen, 2002; Edinger, 2003; Cao, 2009). Chapter 3 identified the induction of FoxP3 expressing T reg cells by MSC from a purified population of CD4$^+$ T cells *in vitro*. Knowing that MSC are capable of inducing T cells with a regulatory phenotype and that T reg cells play a role in preventing aGvHD development, the induction of a FoxP3 expressing T reg cell population as a possible mechanism by which hMSC prolong the survival of NSG mice with aGvHD was examined. Following unstimulated or IFNγ stimulated MSC cell therapy, no increase in FoxP3 expressing T reg cells were detected in the lung, liver or spleen of NSG mice with aGvHD. The absence of a FoxP3 expressing T reg cell population was not due to an insufficient *ex vivo* detection technique as the technique for accurate FoxP3 expression was previously utilised by another member of the Mahon group (Kavanagh, 2010). In this case, Kavanagh *et al.* found that murine MSC prevented allergic airway inflammation, through the induction of a FoxP3 expressing T reg cells, detected through intracellular staining for FoxP3 expression by flow cytometry (Kavanagh, 2010).

Other research groups have suggested a role for T reg cells in aGvHD development and treatment. The deletion of CD4$^+$ CD25$^+$ T reg from the bone marrow graft prior to transplantation dramatically accelerated aGvHD development in other murine models (Cohen, 2002; Taylor, 2002; Cohen, 2006). Additionally, the infusion of *ex vivo* expanded CD4$^+$CD25$^+$FoxP3$^+$ T reg cells prevents aGvHD development, while preserving graft versus leukaemia (GvL) activity (Taylor, 2002;

Hoffmann, 2002; Edinger, 2003; Trenado, 2003; Cao, 2009). This inverse correlation between T reg cells and aGvHD has also been found in patients with aGvHD (Cao, 2009). Patients presenting with grade II to IV aGvHD displayed reduced numbers of T reg cells when compared to normal healthy individuals or patients with mild grade I aGvHD (Cao, 2009). Li *et al.* identified a correlation not only between the number of T reg cells present in patients with aGvHD, but also in the production of TNFα (Li, 2010). Patients with reduced T reg cells had increased levels of TNFα. This environment would be very characteristic of aGvHD, with excessive TNFα resulting from tissue damage and immune cell activation (Li, 2010).

Recently, the induction of FoxP3 by MSC in a mouse model of aGvHD was documented. Following murine MSC therapy on day 1 in a C3H donor cells into irradiated BALB/c mouse model of aGvHD, Joo *et al.* found an increase in FoxP3 mRNA in the mesenteric lymph nodes of mice with aGvHD after 9 days, when compared to mice that did not receive mMSC therapy (Joo, 2010). However, mRNA expression does not always equate to protein levels, it might be the discrepancies between Joo *et al.* and the data here may be attributed to the fact that FoxP3 expression was analysed on an mRNA level (Joo, 2010). However that seems unlikely. The data may reflect a more fundamental issue with NSG mice and a limitation of our model. In NSG mice (even with aGvHD), lymph nodes are vestigial. Therefore, FoxP3 expression in the lymph nodes could not be explored.

The difference above deserves further consideration. The use of a mouse in mouse model by Joo *et al.* and human in mouse model here may also contribute to the differences in T reg cell detection. Using a murine model of GvHD (C57BL/6 donor into BALB/c), Hao *et al.* found that hMSC isolated from umbilical cord blood (hUCBDSC), elevated the numbers of murine $FoxP3^{+}$ $CD4^{+}$ splenocytes (Hao,

2011). The absence of T reg cell induction by hMSC in this model might be explained by the absence of third party (stromal) factors preventing the expansion of human T reg cells in the NSG mouse model of aGvHD or that other T reg populations are involved that do not express the transcription factor FoxP3. Of course it may be that the numbers of $CD4^+$ $CD25^+$ $FoxP3^+$ T cells present in the donor PBMC were too low for their expansion following MSC transfusion *in vivo*. Finally, hMSC therapy prolonged the survival of NSG mice with aGvHD but did not prevent aGvHD development, which would suggest that hMSC therapy had more of a transient effect on aGvHD development, rather than a permanent tolerogenic preventative effect in this model.

In this model, MSC cell therapy did not induce the expansion of conventional T reg cells *in vivo.* Therefore, the ability of MSC to directly inhibit T cell proliferation *in vivo* was examined. MSC inhibition of T cell proliferation *in vitro* is well documented (Glennie, 2005; DiNicola, 2005; Zappia, 2005; English, 2009) but there are contradictory data available for the inhibition of T cell proliferation by MSC *in vivo* (Sudres, 2006; Zappia, 2005). Therefore, an *in vivo* method for the detection of T cell proliferation was applied to the NSG model of aGvHD. IFNγ stimulated MSC therapy resulted in the reduction of $CD4^+$ T cell proliferation in the lungs of NSG mice after 5 days. These data showed that not only are MSC capable of inhibiting T cell proliferation *in vitro*, but this characteristic of MSC immune suppression was also found *in vivo*. Interestingly, only $CD4^+$ T cells proliferated within the NSG aGvHD model as no proliferation of $CD8^+$ T cells were detected *in vivo*. These data highlighted the possibility that MSC cell therapy could prolong the survival of NSG mice with aGvHD through the direct inhibition of human donor T cells. In contrast to the data herein, Sudres *et al.* found that although murine MSC

inhibited the proliferation of T cells *in vitro*, murine MSC therapy administered atthe same time as bone marrow transplant to treat GvHD had no effect on the proliferation of CFSE labelled T cells *in vivo* (Sudres, 2006). However, Christensen *et al.* showed that murine MSC only delayed aGvHD onset but did not prevent aGvHD development; finding that although murine MSC could inhibit T cell proliferation *in vitro*, MSC did not prevent T cell proliferation *in vivo* (Christensen, 2010), given the difficulty we encountered in detecting *in vivo* proliferation and its timing, this was not surprising.

If direct inhibition of T cell proliferation is the mechanism of hMSC efficacy then the mechanism underlying this effect needed to be explored. hMSC derived soluble factors play a role in the ability of MSC to inhibit T cell proliferation (Chapter 6). Prostaglandins secreted by MSC, are known regulators of T cell proliferation. In chapter 6, it was shown that the release of prostaglandin, PGE_2, by hMSC was important for the induction of T reg cells *in vitro* and in Chapter 6 PGE_2 was shown to be required for the cells used *in vivo.* Collectively, these data highlighted the importance of MSC derived prostaglandins in the mediation of T cell mediated responses *in vitro*. It was therefore plausible that the direct T cell inhibition seen *in vivo* was due to hMSC production of prostaglandins. To investigate this, indomethacin was administered to aGvHD mice in conjunction with hMSC therapy. Although indomethacin reduced the production of prostaglandins in each treatment group (Fig 6.14), this decrease did not affect the survival or pathological score of NSG mice with aGvHD. There was no significant difference between hMSC treated mice or hMSC/indomethacin treated mice. This suggested that the production of prostaglandins by hMSC *in vivo* were not involved in the beneficial effect seen following hMSC therapy. There are other possible soluble

factors secreted by MSC that may play a role in the reduction of T cell proliferation *in vivo*, such as IDO, HGF or TGFβ, which were not analysed here.

This thesis explored many aspects of MSC immune modulation both *in vitro* and *in vivo* (Fig 7.2). The use of mouse models has allowed for the progression of research tools and therapies over the past decade. By using the novel model here, the effect of hMSC therapy on aGvHD development was assessed and the exact mechanisms employed were explored. One benefit of the NSG model was that the development of aGvHD was due to the infusion of human cells (PBMC) and the treatment of the disease was carried out using hMSC. This allowed for the research of human aGvHD pathology and how human cell therapies might be deployed. One drawback with this humanised model, which was identified in this thesis was, due to the lack of a functional lymphoid system, the detection of key lymphoid organs such as the lymph nodes or thymus were extremely difficult.

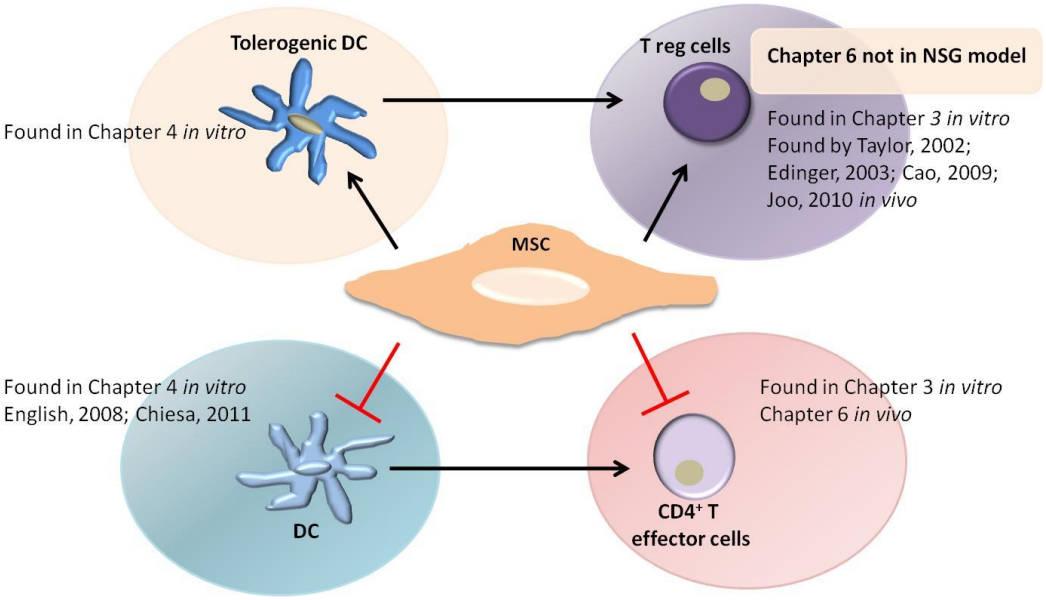

Fig 7.2 A schematic representation of the mechanisms involved in MSC induction of tolerance *in vitro* and *in vivo*. Tolerance induction by MSC involves the generation of tolerogenic DC and T reg cells *in vivo*. MSC therapy can directly reduce donor $CD4^+$ T cell expansion. MSC can also inhibit DC maturation, indirectly interfering with $CD4^+$ T cell proliferation. In aGvHD, donor $CD4^+$ T cells drive pathology leading to destruction of target cells, tissues and organs. This is supported by mature activated DC. MSC prevent $CD4^+$ T cell proliferation. This might be via tolerogenic DC induction as in Chapter 4. In other aGvHD models, MSC induced T reg cells are likely to play a role but this may be less prevalent in the NSG model.

It is therefore appropriate to synthesise the conclusions so far and propose a model of how MSC are beneficial in aGvHD. It is an irony that this thesis focused on adaptive immunity (T reg) and DC, whereas one of the most important aspects was an observation from the animal model on innate responses. Following hMSC cell therapy *in vivo*, the production of human TNFα in the serum of aGvHD mice was significantly reduced. TNFα is the key cytokine involved in the manifestation of aGvHD both in murine models and in patients. The main cells involved in the production of TNFα in the NSG model are donor monocytes, macrophages, DC or the few remaining antigen presenting cells within the NSG mouse. Excessive TNFα can directly or indirectly (Fas/Fas ligand) induce apoptosis of donor and host cells; activate donor DC inducing maturation and enhanced alloantigen presentation; activate donor $CD4^+$ T cells through TNFR 1 or 2; induce target organ damage through the activation of $CD8^+$ CTL and NK cells; and increase the permeability of the endothelium, allowing for the infiltration of donor cells into target organs, resulting in extensive tissue damage. In the NSG model, little $CD8^+$ T cell expansion was seen, however endothelialitis was observed in diseased but not treated mice (Fig 5.14-5.16). It is tempting to speculate that a key aspect of MSC protection here was the prevention of vascular permeability through suppression of monocyte derived TNFα (Fig 7.3). Nevertheless, key aspects of innate and adaptive immunity were shown to be influenced *in vitro* and *in vivo* in this work (Fig 7.2). T reg cell induction was expected to be the key feature of protection, but this was not demonstrated *in vivo* for reasons described above. It is likely that T reg cells have a

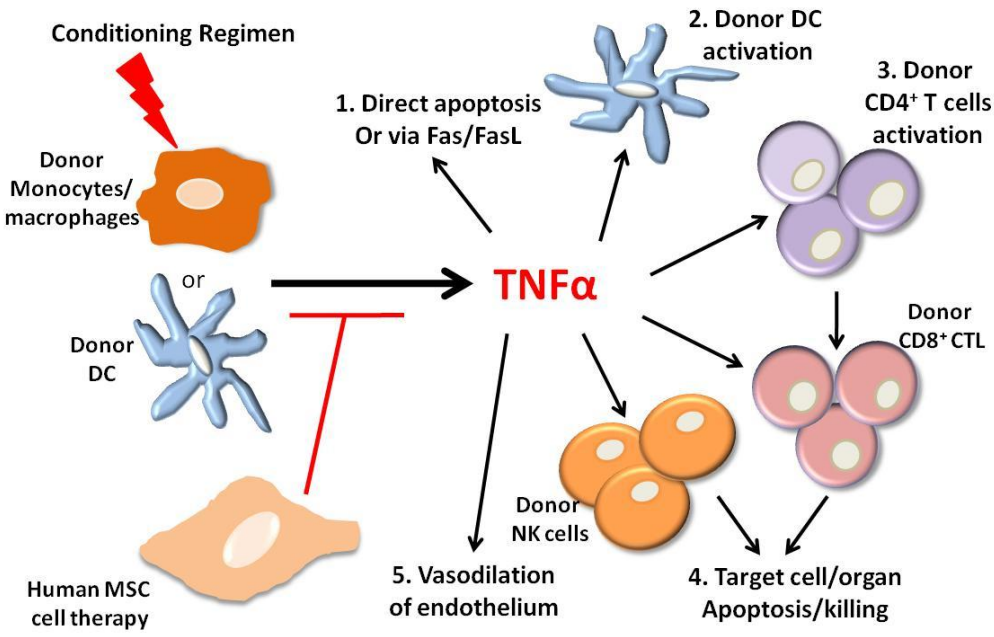

Fig 7.3 The role of MSC in limiting aGvHD pathology. MSC can work in a number of ways; through limiting TNFα production. Donor monocytes, macrophages and DC secrete high levels of TNFα in the humanised aGvHD NSG model. MSC cell therapy significantly reduces TNFα in the serum of NSG mice with aGvHD. Excess TNFα can directly induce host tissue apoptosis or indirectly through the activation of donor cytotoxic T lymphocytes (CTL) and natural killer (NK) cells. TNFα can drive the activation of donor DC and $CD4^+$ T cells increasing donor lymphocyte proliferation. As a stimulator of the acute phase reaction, TNFα can increase the permeability of the endothelium, allowing the infiltration of donor lymphocytes and other effector molecules into target organs.

role in other models and indeed in human disease/therapy and the absence of this here is a reflection of the model. Nevertheless, allogeneic MSC do suppress (xenoantigen driven) $CD4^+$ T cell proliferation *in vivo*; as aGvHD pathology is driven by T cell expansion. This is a significant finding. However, the mechanism does not involve anergy or apoptosis induction of donor T cells, but rather a more direct suppression. PGE_2 was speculated to be the mediator involved (from data in Chapter 3), but this did not appear to be the case. In chapter 4, a role for MSC induced DC suppression was explored, which highlighted this as a future area for *in vivo* study. Recently mMSC were shown to affect the ability of DC to prime T cells *in vivo*; (Chiesa, 2011). It might be that the reduction of donor T cell proliferation observed *in vivo* following hMSC therapy could be due to MSC-induced tolerogenic DC (Fig 7.2 & 7.3) consistent with the *in vitro* data from chapter 4.

To conclude, the use of autologous MSC are beneficial in treating autoimmune diseases and pathologies, but are limited by the time it takes to isolate, standardise, regulate, quality assure and expand these MSC prior to patient treatment. The cost model for bespoke therapy is also prohibitive. Therefore, the concept of using standardised, regulatory compliant, allogeneic MSC as a beneficial cell therapy is very exciting. Knowing the exact mechanisms by which MSC mediate their immunosuppressive characteristics *in vivo* is important for the progression of MSC as a valuable cell therapy. Identifying these exact mechanisms will contribute to current knowledge in MSC biology and help translate these remarkable stem cells into reliable therapies. This thesis has progressed our understanding of MSC biology and delivered the models to make such translation possible.

CHAPTER 8

REFERENCES

Abbas, A. K. 2003. The control of T cell activation vs. tolerance. *Autoimmun Rev* 2:115-118.

Aggarwal, S., and M. F. Pittenger. 2005. Human mesenchymal stem cells modulate allogeneic immune cell responses. *Blood* 105:1815-1822.

Akbari, O., G. J. Freeman, E. H. Meyer, E. A. Greenfield, T. T. Chang, A. H. Sharpe, G. Berry, R. H. DeKruyff, and D. T. Umetsu. 2002. Antigen-specific regulatory T cells develop via the ICOS-ICOS-ligand pathway and inhibit allergen-induced airway hyperreactivity. *Nat Med* 8:1024-1032.

Aldinucci, A., L. Rizzetto, L. Pieri, D. Nosi, P. Romagnoli, T. Biagioli, B. Mazzanti, R. Saccardi, L. Beltrame, L. Massacesi, D. Cavalieri, and C. Ballerini. Inhibition of immune synapse by altered dendritic cell actin distribution: a new pathway of mesenchymal stem cell immune regulation. *J Immunol* 185:5102-5110.

Alegre, M. L., K. A. Frauwirth, and C. B. Thompson. 2001. T-cell regulation by CD28 and CTLA-4. *Nat Rev Immunol* 1:220-228.

Allison, J. P., C. Chambers, A. Hurwitz, T. Sullivan, B. Boitel, S. Fournier, M. Brunner, and M. Krummel. 1998. A role for CTLA-4-mediated inhibitory signals in peripheral T cell tolerance? *Novartis Found Symp* 215:92-98; discussion 98-102, 186-190.

Allison, M. 2009. Genzyme backs Osiris, despite Prochymal flop. *Nat Biotechnol* 27:966-967.

Amarnath, S., C. M. Costanzo, J. Mariotti, J. L. Ullman, W. G. Telford, V. Kapoor, J. L. Riley, B. L. Levine, C. H. June, T. Fong, N. L. Warner, and D. H. Fowler. 2010. Regulatory T cells and human myeloid dendritic cells promote tolerance via programmed death ligand-1. *PLoS Biol* 8:e1000302.

Amsen, D., J. M. Blander, G. R. Lee, K. Tanigaki, T. Honjo, and R. A. Flavell. 2004. Instruction of distinct CD4 T helper cell fates by different notch ligands on antigen-presenting cells. *Cell* 117:515-526.

Anderson, D., Billingham, R. E., Lampkin, G. H. & P. B. Medawar, P. B. 1951. The use of skin grafting to distinguish between monozygotic and dizygotic twins in cattle. Heredity. 6 : 319-397.

Anderson, M. S., E. S. Venanzi, Z. Chen, S. P. Berzins, C. Benoist, and D. Mathis. 2005. The cellular mechanism of Aire control of T cell tolerance. *Immunity* 23:227-239.

Aramaki, O., N. Shirasugi, T. Takayama, M. Shimazu, M. Kitajima, Y. Ikeda, M. Azuma, K. Okumura, H. Yagita, and M. Niimi. 2004. Programmed death-1-programmed death-L1 interaction is essential for induction of regulatory cells by intratracheal delivery of alloantigen. *Transplantation* 77:6-12.

Artavanis-Tsakonas, S., M. D. Rand, and R. J. Lake. 1999. Notch signaling: cell fate control and signal integration in development. *Science* 284:770-776.

Augello, A., R. Tasso, S. M. Negrini, A. Amateis, F. Indiveri, R. Cancedda, and G. Pennesi. 2005. Bone marrow mesenchymal progenitor cells inhibit lymphocyte proliferation by activation of the programmed death 1 pathway. *Eur J Immunol* 35:1482-1490.

Augello, A., R. Tasso, S. M. Negrini, R. Cancedda, and G. Pennesi. 2007. Cell therapy using allogeneic bone marrow mesenchymal stem cells prevents tissue damage in collagen-induced arthritis. *Arthritis Rheum* 56:1175-1186.

Balaian, L., R. K. Zhong, and E. D. Ball. 2003. The inhibitory effect of anti-CD33 monoclonal antibodies on AML cell growth correlates with Syk and/or ZAP-70 expression. *Exp Hematol* 31:363-371.

Baldwin, W. M., 3rd, S. K. Pruitt, R. B. Brauer, M. R. Daha, and F. Sanfilippo. 1995. Complement in organ transplantation. Contributions to inflammation, injury, and rejection. *Transplantation* 59:797-808.

Banchereau, J., and R. M. Steinman. 1998. Dendritic cells and the control of immunity. *Nature* 392:245-252.

Baratelli, F., Y. Lin, L. Zhu, S. C. Yang, N. Heuze-Vourc'h, G. Zeng, K. Reckamp, M. Dohadwala, S. Sharma, and S. M. Dubinett. 2005. Prostaglandin E2 induces

FOXP3 gene expression and T regulatory cell function in human CD4+ T cells. *J Immunol* 175:1483-1490.

Baron, M., H. Aslam, M. Flasza, M. Fostier, J. E. Higgs, S. L. Mazaleyrat, and M. B. Wilkin. 2002. Multiple levels of Notch signal regulation (review). *Mol Membr Biol* 19:27-38.

Barry, F. P. 2003. Mesenchymal stem cell therapy in joint disease. *Novartis Found Symp* 249:86-96; discussion 96-102, 170-104, 239-141.

Barry, F. P., and J. M. Murphy. 2004. Mesenchymal stem cells: clinical applications and biological characterization. *Int J Biochem Cell Biol* 36:568-584.

Barry, F. P., J. M. Murphy, K. English, and B. P. Mahon. 2005. Immunogenicity of adult mesenchymal stem cells: lessons from the fetal allograft. *Stem Cells Dev* 14:252-265.

Bartholomew, A., C. Sturgeon, M. Siatskas, K. Ferrer, K. McIntosh, S. Patil, W. Hardy, S. Devine, D. Ucker, R. Deans, A. Moseley, and R. Hoffman. 2002. Mesenchymal stem cells suppress lymphocyte proliferation in vitro and prolong skin graft survival in vivo. *Exp Hematol* 30:42-48.

Bax, M., J. J. Garcia-Vallejo, J. Jang-Lee, S. J. North, T. J. Gilmartin, G. Hernandez, P. R. Crocker, H. Leffler, S. R. Head, S. M. Haslam, A. Dell, and Y. van Kooyk. 2007. Dendritic cell maturation results in pronounced changes in glycan expression affecting recognition by siglecs and galectins. *J Immunol* 179:8216-8224.

Baxter, A. G., and A. Cooke. 1993. Complement lytic activity has no role in the pathogenesis of autoimmune diabetes in NOD mice. *Diabetes* 42:1574-1578.

Bellinghausen, I., U. Brand, K. Steinbrink, A. H. Enk, J. Knop, and J. Saloga. 2001. Inhibition of human allergic T-cell responses by IL-10-treated dendritic cells: differences from hydrocortisone-treated dendritic cells. *J Allergy Clin Immunol* 108:242-249.

Benvenuto, F., S. Ferrari, E. Gerdoni, F. Gualandi, F. Frassoni, V. Pistoia, G. Mancardi, and A. Uccelli. 2007. Human mesenchymal stem cells promote survival of T cells in a quiescent state. *Stem Cells* 25:1753-1760.

Betterle, C., N. A. Greggio, and M. Volpato. 1998. Clinical review 93: Autoimmune polyglandular syndrome type 1. *J Clin Endocrinol Metab* 83:1049-1055.

Beyth, S., Z. Borovsky, D. Mevorach, M. Liebergall, Z. Gazit, H. Aslan, E. Galun, and J. Rachmilewitz. 2005. Human mesenchymal stem cells alter antigen-presenting cell maturation and induce T-cell unresponsiveness. *Blood* 105:2214-2219.

Billingham, R. E. 1966. The biology of graft-versus-host reactions. *Harvey Lect* 62:21-78.

Billingham, R. E., and J. Reynolds. 1952. Transplantation studies on sheets of pure epidermal epithelium and on epidermal cell suspensions. *Br J Plast Surg* 5:25-36.

Billingham, R. E., L. Brent, and P. B. Medawar. 1953. Actively acquired tolerance of foreign cells. *Nature* 172:603-606.

Blazar, B. R., S. F. Carroll, and D. A. Vallera. 1991. Prevention of murine graft-versus-host disease and bone marrow alloengraftment across the major histocompatibility barrier after donor graft preincubation with anti-LFA1 immunotoxin. *Blood* 78:3093-3102.

Bordet, R., D. Deplanque, P. Maboudou, F. Puisieux, Q. Pu, E. Robin, A. Martin, M. Bastide, D. Leys, M. Lhermitte, and B. Dupuis. 2000. Increase in endogenous brain superoxide dismutase as a potential mechanism of lipopolysaccharide-induced brain ischemic tolerance. *J Cereb Blood Flow Metab* 20:1190-1196.

Bosma, G. C., M. Fried, R. P. Custer, A. Carroll, D. M. Gibson, and M. J. Bosma. 1988. Evidence of functional lymphocytes in some (leaky) scid mice. *J Exp Med* 167:1016-1033.

Bosma, G. C., R. P. Custer, and M. J. Bosma. 1983. A severe combined immunodeficiency mutation in the mouse. *Nature* 301:527-530.

Bruder, S. P., A. A. Kurth, M. Shea, W. C. Hayes, N. Jaiswal, and S. Kadiyala. 1998. Bone regeneration by implantation of purified, culture-expanded human mesenchymal stem cells. *J Orthop Res* 16:155-162.

Buhl, A. M., D. Nemazee, J. C. Cambier, R. Rickert, and M. Hertz. 2000. B-cell antigen receptor competence regulates B-lymphocyte selection and survival. *Immunol Rev* 176:141-153.

Cantor, H., and I. Weissman. 1976. Development and function of subpopulations of thymocytes and T lymphocytes. *Prog Allergy* 20:1-64.

Cao, T., A. Soto, W. Zhou, W. Wang, S. Eck, M. Walker, G. Harriman, and L. Li. 2009. Ex vivo expanded human CD4+CD25+Foxp3+ regulatory T cells prevent lethal xenogenic graft versus host disease (GVHD). *Cell Immunol* 258:65-71.

Caplan, A. I. 1991. Mesenchymal stem cells. *J Orthop Res* 9:641-650.

Caplan, A. I., and J. E. Dennis. 2006. Mesenchymal stem cells as trophic mediators. *J Cell Biochem* 98:1076-1084.

Carpenter, P. A., F. R. Appelbaum, L. Corey, H. J. Deeg, K. Doney, T. Gooley, J. Krueger, P. Martin, S. Pavlovic, J. Sanders, J. Slattery, D. Levitt, R. Storb, A. Woolfrey, and C. Anasetti. 2002. A humanized non-FcR-binding anti-CD3 antibody, visilizumab, for treatment of steroid-refractory acute graft-versus-host disease. *Blood* 99:2712-2719.

Carreno, B. M., and M. Collins. 2002. The B7 family of ligands and its receptors: new pathways for costimulation and inhibition of immune responses. *Annu Rev Immunol* 20:29-53.

Casiraghi, F., N. Azzollini, P. Cassis, B. Imberti, M. Morigi, D. Cugini, R. A. Cavinato, M. Todeschini, S. Solini, A. Sonzogni, N. Perico, G. Remuzzi, and M. Noris. 2008. Pretransplant infusion of mesenchymal stem cells prolongs the survival of a semiallogeneic heart transplant through the generation of regulatory T cells. *J Immunol* 181:3933-3946.

Cederbom, L., H. Hall, and F. Ivars. 2000. CD4+CD25+ regulatory T cells down-regulate co-stimulatory molecules on antigen-presenting cells. *Eur J Immunol* 30:1538-1543.

Chabannes, D., M. Hill, E. Merieau, J. Rossignol, R. Brion, J. P. Soulillou, I. Anegon, and M. C. Cuturi. 2007. A role for heme oxygenase-1 in the

immunosuppressive effect of adult rat and human mesenchymal stem cells. *Blood* 110:3691-3694.

Chalandon, Y., E. Roosnek, B. Mermillod, L. Waelchli, C. Helg, and B. Chapuis. 2006. Can only partial T-cell depletion of the graft before hematopoietic stem cell transplantation mitigate graft-versus-host disease while preserving a graft-versus-leukemia reaction? A prospective phase II study. *Biol Blood Marrow Transplant* 12:102-110.

Chen, X., M. A. Armstrong, and G. Li. 2006. Mesenchymal stem cells in immunoregulation. *Immunol Cell Biol* 84:413-421.

Cheng, P., Y. Nefedova, C. A. Corzo, and D. I. Gabrilovich. 2007. Regulation of dendritic-cell differentiation by bone marrow stroma via different Notch ligands. *Blood* 109:507-515.

Cheng, P., Y. Nefedova, L. Miele, B. A. Osborne, and D. Gabrilovich. 2003. Notch signaling is necessary but not sufficient for differentiation of dendritic cells. *Blood* 102:3980-3988.

Chiesa, S., S. Morbelli, S. Morando, M. Massollo, C. Marini, A. Bertoni, F. Frassoni, S. T. Bartolome, G. Sambuceti, E. Traggiai, and A. Uccelli. Mesenchymal stem cells impair in vivo T-cell priming by dendritic cells. *Proc Natl Acad Sci U S A* 108:17384-17389.

Chinen, J., and R. H. Buckley. Transplantation immunology: solid organ and bone marrow. *J Allergy Clin Immunol* 125:S324-335.

Christensen, M. E., Turner, B. E., Sinfield, L. J., Koller, K., Cullup, H., Waterhouse, N. J., Hart, D. N. J., Atkinson, K., Rice, A. M. 2010. Mesenchymal stem cells transiently alter the inflammatory milieu post transplant to delay graft versus host disease. Haematologca. 95 (12): 2102-2110.

Christianson, S. W., D. L. Greiner, I. B. Schweitzer, B. Gott, G. L. Beamer, P. A. Schweitzer, R. M. Hesselton, and L. D. Shultz. 1996. Role of natural killer cells on engraftment of human lymphoid cells and on metastasis of human T-lymphoblastoid leukemia cells in C57BL/6J-scid mice and in C57BL/6J-scid bg mice. *Cell Immunol* 171:186-199.

Christianson, S. W., D. L. Greiner, R. A. Hesselton, J. H. Leif, E. J. Wagar, I. B. Schweitzer, T. V. Rajan, B. Gott, D. C. Roopenian, and L. D. Shultz. 1997. Enhanced human CD4+ T cell engraftment in beta2-microglobulin-deficient NOD-scid mice. *J Immunol* 158:3578-3586.

Ciccocioppo, R., M. E. Bernardo, A. Sgarella, R. Maccario, M. A. Avanzini, C. Ubezio, A. Minelli, C. Alvisi, A. Vanoli, F. Calliada, P. Dionigi, C. Perotti, F. Locatelli, and G. R. Corazza. Autologous bone marrow-derived mesenchymal stromal cells in the treatment of fistulising Crohn's disease. *Gut* 60:788-798.

Cobbold, S. P., E. Adams, C. A. Farquhar, K. F. Nolan, D. Howie, K. O. Lui, P. J. Fairchild, A. L. Mellor, D. Ron, and H. Waldmann. 2009. Infectious tolerance via the consumption of essential amino acids and mTOR signaling. *Proc Natl Acad Sci U S A* 106:12055-12060.

Cohen, J. L., A. Trenado, D. Vasey, D. Klatzmann, and B. L. Salomon. 2002. CD4(+)CD25(+) immunoregulatory T Cells: new therapeutics for graft-versus-host disease. *J Exp Med* 196:401-406.

Cohen, J. L., and O. Boyer. 2006. The role of CD4+CD25hi regulatory T cells in the physiopathogeny of graft-versus-host disease. *Curr Opin Immunol* 18:580-585.

Cole, M. S., K. E. Stellrecht, J. D. Shi, M. Homola, D. H. Hsu, C. Anasetti, M. Vasquez, and J. Y. Tso. 1999. HuM291, a humanized anti-CD3 antibody, is immunosuppressive to T cells while exhibiting reduced mitogenicity in vitro. *Transplantation* 68:563-571.

Collins, M., V. Ling, and B. M. Carreno. 2005. The B7 family of immune-regulatory ligands. *Genome Biol* 6:223.

Cooper, M. D., R. D. Peterson, and R. A. Good. 1965. DELINEATION OF THE THYMIC AND BURSAL LYMPHOID SYSTEMS IN THE CHICKEN. *Nature* 205:143-146.

Cooper, P. R., A. C. Mesaros, J. Zhang, P. Christmas, C. M. Stark, K. Douaidy, M. A. Mittelman, R. J. Soberman, I. A. Blair, and R. A. Panettieri. 20-HETE mediates ozone-induced, neutrophil-independent airway hyper-responsiveness in mice. *PLoS One* 5:e10235.

Corcione, A., F. Benvenuto, E. Ferretti, D. Giunti, V. Cappiello, F. Cazzanti, M. Risso, F. Gualandi, G. L. Mancardi, V. Pistoia, and A. Uccelli. 2006. Human mesenchymal stem cells modulate B-cell functions. *Blood* 107:367-372.

Cragg, L., B. R. Blazar, T. Defor, N. Kolatker, W. Miller, J. Kersey, M. Ramsay, P. McGlave, A. Filipovich, and D. Weisdorf. 2000. A randomized trial comparing prednisone with antithymocyte globulin/prednisone as an initial systemic therapy for moderately severe acute graft-versus-host disease. *Biol Blood Marrow Transplant* 6:441-447.

Crisan, M., S. Yap, L. Casteilla, C. W. Chen, M. Corselli, T. S. Park, G. Andriolo, B. Sun, B. Zheng, L. Zhang, C. Norotte, P. N. Teng, J. Traas, R. Schugar, B. M. Deasy, S. Badylak, H. J. Buhring, J. P. Giacobino, L. Lazzari, J. Huard, and B. Peault. 2008. A perivascular origin for mesenchymal stem cells in multiple human organs. *Cell Stem Cell* 3:301-313.

Crocker, P. R. 2005. Siglecs in innate immunity. *Curr Opin Pharmacol* 5:431-437.

Crocker, P. R., J. C. Paulson, and A. Varki. 2007. Siglecs and their roles in the immune system. *Nat Rev Immunol* 7:255-266.

Cursio, R., P. Colosetti, P. Auberger, and J. Gugenheim. 2008. Liver apoptosis following normothermic ischemia-reperfusion: in vivo evaluation of caspase activity by FLIVO assay in rats. *Transplant Proc* 40:2038-2041.

da Silva Meirelles, L., P. C. Chagastelles, and N. B. Nardi. 2006. Mesenchymal stem cells reside in virtually all post-natal organs and tissues. *J Cell Sci* 119:2204-2213.

Darcy, C. J., J. S. Davis, T. Woodberry, Y. R. McNeil, D. P. Stephens, T. W. Yeo, and N. M. Anstey. 2011. An observational cohort study of the kynurenine to tryptophan ratio in sepsis: association with impaired immune and microvascular function. *PLoS One* 6:e21185.

Darrasse-Jeze, G., S. Deroubaix, H. Mouquet, G. D. Victora, T. Eisenreich, K. H. Yao, R. F. Masilamani, M. L. Dustin, A. Rudensky, K. Liu, and M. C. Nussenzweig. 2009. Feedback control of regulatory T cell homeostasis by dendritic cells in vivo. *J Exp Med* 206:1853-1862.

Daussett, J. 1958. Iso-leuco-anticorps. Acta Haematol. 20: 156-166.

Deeg, H. J. 2007. How I treat refractory acute GVHD. *Blood* 109:4119-4126.

Delgado, J., K. Thomson, N. Russell, J. Ewing, W. Stewart, G. Cook, S. Devereux, R. Lovell, R. Chopra, D. I. Marks, S. Mackinnon, and D. W. Milligan. 2006. Results of alemtuzumab-based reduced-intensity allogeneic transplantation for chronic lymphocytic leukemia: a British Society of Blood and Marrow Transplantation Study. *Blood* 107:1724-1730.

Di Nicola, M., C. Carlo-Stella, M. Magni, M. Milanesi, P. D. Longoni, P. Matteucci, S. Grisanti, and A. M. Gianni. 2002. Human bone marrow stromal cells suppress T-lymphocyte proliferation induced by cellular or nonspecific mitogenic stimuli. *Blood* 99:3838-3843.

Djouad, F., L. M. Charbonnier, C. Bouffi, P. Louis-Plence, C. Bony, F. Apparailly, C. Cantos, C. Jorgensen, and D. Noel. 2007. Mesenchymal stem cells inhibit the differentiation of dendritic cells through an interleukin-6-dependent mechanism. *Stem Cells* 25:2025-2032.

Djouad, F., P. Plence, C. Bony, P. Tropel, F. Apparailly, J. Sany, D. Noel, and C. Jorgensen. 2003. Immunosuppressive effect of mesenchymal stem cells favors tumor growth in allogeneic animals. *Blood* 102:3837-3844.

Dominici, M., K. Le Blanc, I. Mueller, I. Slaper-Cortenbach, F. Marini, D. Krause, R. Deans, A. Keating, D. Prockop, and E. Horwitz. 2006. Minimal criteria for defining multipotent mesenchymal stromal cells. The International Society for Cellular Therapy position statement. *Cytotherapy* 8:315-317.

Doney, K., P. Martin, R. Storb, J. Whitehead, A. Smith, J. A. Hansen, F. Appelbaum, C. D. Buckner, and E. D. Thomas. 1985. A randomized trial of antihuman thymocyte globulin versus murine monoclonal antihuman T-cell antibodies as immunosuppressive therapy for aplastic anemia. *Exp Hematol* 13:520-524.

Duffner, U. A., Y. Maeda, K. R. Cooke, P. Reddy, R. Ordemann, C. Liu, J. L. Ferrara, and T. Teshima. 2004. Host dendritic cells alone are sufficient to initiate acute graft-versus-host disease. *J Immunol* 172:7393-7398.

Edinger, M., P. Hoffmann, J. Ermann, K. Drago, C. G. Fathman, S. Strober, and R. S. Negrin. 2003. CD4+CD25+ regulatory T cells preserve graft-versus-tumor activity while inhibiting graft-versus-host disease after bone marrow transplantation. *Nat Med* 9:1144-1150.

Egerton, M., R. Scollay, and K. Shortman. 1990. Kinetics of mature T-cell development in the thymus. *Proc Natl Acad Sci U S A* 87:2579-2582.

Ehlers, S. 2005. Tumor necrosis factor and its blockade in granulomatous infections: differential modes of action of infliximab and etanercept? *Clin Infect Dis* 41 Suppl 3:S199-203.

Ehlich, A., V. Martin, W. Muller, and K. Rajewsky. 1994. Analysis of the B-cell progenitor compartment at the level of single cells. *Curr Biol* 4:573-583.

English, K., A. French, and K. J. Wood. Mesenchymal stromal cells: facilitators of successful transplantation? *Cell Stem Cell* 7:431-442.

English, K., F. P. Barry, and B. P. Mahon. 2008. Murine mesenchymal stem cells suppress dendritic cell migration, maturation and antigen presentation. *Immunol Lett* 115:50-58.

English, K., F. P. Barry, C. P. Field-Corbett, and B. P. Mahon. 2007. IFN-gamma and TNF-alpha differentially regulate immunomodulation by murine mesenchymal stem cells. *Immunol Lett* 110:91-100.

English, K., J. M. Ryan, L. Tobin, M. J. Murphy, F. P. Barry, and B. P. Mahon. 2009. Cell contact, prostaglandin E(2) and transforming growth factor beta 1 play non-redundant roles in human mesenchymal stem cell induction of CD4+CD25(High) forkhead box P3+ regulatory T cells. *Clin Exp Immunol* 156:149-160.

Ezzelarab, M., and A. W. Thomson. Tolerogenic dendritic cells and their role in transplantation. *Semin Immunol* 23:252-263.

Falco, M., R. Biassoni, C. Bottino, M. Vitale, S. Sivori, R. Augugliaro, L. Moretta, and A. Moretta. 1999. Identification and molecular cloning of p75/AIRM1, a novel

member of the sialoadhesin family that functions as an inhibitory receptor in human natural killer cells. *J Exp Med* 190:793-802.

Ferrara, J. L., and G. Yanik. 2005. Acute graft versus host disease: pathophysiology, risk factors, and prevention strategies. *Clin Adv Hematol Oncol* 3:415-419, 428.

Ferrara, J. L., J. E. Levine, P. Reddy, and E. Holler. 2009. Graft-versus-host disease. *Lancet* 373:1550-1561.

Fife, B. T., and J. A. Bluestone. 2008. Control of peripheral T-cell tolerance and autoimmunity via the CTLA-4 and PD-1 pathways. *Immunol Rev* 224:166-182.

Fiuza, U. M., and A. M. Arias. 2007. Cell and molecular biology of Notch. *J Endocrinol* 194:459-474.

Fowler, D. H., J. Breglio, G. Nagel, M. A. Eckhaus, and R. E. Gress. 1996. Allospecific CD8+ Tc1 and Tc2 populations in graft-versus-leukemia effect and graft-versus-host disease. *J Immunol* 157:4811-4821.

Francisco, L. M., P. T. Sage, and A. H. Sharpe. 2010. The PD-1 pathway in tolerance and autoimmunity. *Immunol Rev* 236:219-242.

Francisco, L. M., V. H. Salinas, K. E. Brown, V. K. Vanguri, G. J. Freeman, V. K. Kuchroo, and A. H. Sharpe. 2009. PD-L1 regulates the development, maintenance, and function of induced regulatory T cells. *J Exp Med* 206:3015-3029.

Freeman, G. J., A. J. Long, Y. Iwai, K. Bourque, T. Chernova, H. Nishimura, L. J. Fitz, N. Malenkovich, T. Okazaki, M. C. Byrne, H. F. Horton, L. Fouser, L. Carter, V. Ling, M. R. Bowman, B. M. Carreno, M. Collins, C. R. Wood, and T. Honjo. 2000. Engagement of the PD-1 immunoinhibitory receptor by a novel B7 family member leads to negative regulation of lymphocyte activation. *J Exp Med* 192:1027-1034.

Friedenstein, A. J., R. K. Chailakhyan, N. V. Latsinik, A. F. Panasyuk, and I. V. Keiliss-Borok. 1974. Stromal cells responsible for transferring the microenvironment of the hemopoietic tissues. Cloning in vitro and retransplantation in vivo. *Transplantation* 17:331-340.

Friedenstein, A. J., S. Piatetzky, II, and K. V. Petrakova. 1966. Osteogenesis in transplants of bone marrow cells. *J Embryol Exp Morphol* 16:381-390.

Fu, S., N. Zhang, A. C. Yopp, D. Chen, M. Mao, H. Zhang, Y. Ding, and J. S. Bromberg. 2004. TGF-beta induces Foxp3 + T-regulatory cells from CD4 + CD25 - precursors. *Am J Transplant* 4:1614-1627.

Gay, D., T. Saunders, S. Camper, and M. Weigert. 1993. Receptor editing: an approach by autoreactive B cells to escape tolerance. *J Exp Med* 177:999-1008.

Ge, W., J. Jiang, J. Arp, W. Liu, B. Garcia, and H. Wang. Regulatory T-cell generation and kidney allograft tolerance induced by mesenchymal stem cells associated with indoleamine 2,3-dioxygenase expression. *Transplantation* 90:1312-1320.

Ghannam, S., J. Pene, G. Torcy-Moquet, C. Jorgensen, and H. Yssel. 2010. Mesenchymal stem cells inhibit human Th17 cell differentiation and function and induce a T regulatory cell phenotype. *J Immunol* 185:302-312.

Gibson, T. J., C. Ramu, C. Gemund, and R. Aasland. 1998. The APECED polyglandular autoimmune syndrome protein, AIRE-1, contains the SAND domain and is probably a transcription factor. *Trends Biochem Sci* 23:242-244.

Glennie, S., I. Soeiro, P. J. Dyson, E. W. Lam, and F. Dazzi. 2005. Bone marrow mesenchymal stem cells induce division arrest anergy of activated T cells. *Blood* 105:2821-2827.

Goldrath, A. W., and M. J. Bevan. 1999. Selecting and maintaining a diverse T-cell repertoire. *Nature* 402:255-262.

Gorer, PA, Lyman, S, Snell, GD. 1948. Studies on the genetic and antigenic basis of tumour transplantation. Linkage between a histocompatibility gene and "fused" in mice. Proceedings of the Royal Society of London - Series B: Biological Sciences. 135:499-505

Gorer, PA. 1936. The detection of antigenic differences in mouse erythrocytes by the employment of immune sera. Br J Exp Biol 17:42-6.

Grass, J. A., T. Wafa, A. Reames, D. Wages, L. Corash, J. L. Ferrara, and L. Lin. 1999. Prevention of transfusion-associated graft-versus-host disease by photochemical treatment. *Blood* 93:3140-3147.

Graziani, F., M. T. Van Lint, A. Dominietto, A. M. Raiola, C. Di Grazia, T. Lamparelli, F. Gualandi, S. Bregante, M. Fiorone, B. Bruno, and A. Bacigalupo. 2002. Treatment of acute graft versus host disease with low dose-alternate day anti-thymocyte globulin. *Haematologica* 87:973-978.

Greenwald, R. J., G. J. Freeman, and A. H. Sharpe. 2005. The B7 family revisited. *Annu Rev Immunol* 23:515-548.

Greiner, D. L., R. A. Hesselton, and L. D. Shultz. 1998. SCID mouse models of human stem cell engraftment. *Stem Cells* 16:166-177.

Griffin, M. D., T. Ritter, and B. P. Mahon. Immunological aspects of allogeneic mesenchymal stem cell therapies. *Hum Gene Ther* 21:1641-1655.

Griffith, T. S., T. Brunner, S. M. Fletcher, D. R. Green, and T. A. Ferguson. 1995. Fas ligand-induced apoptosis as a mechanism of immune privilege. *Science* 270:1189-1192.

Groh, M. E., B. Maitra, E. Szekely, and O. N. Koc. 2005. Human mesenchymal stem cells require monocyte-mediated activation to suppress alloreactive T cells. *Exp Hematol* 33:928-934.

Grohmann, U., C. Orabona, F. Fallarino, C. Vacca, F. Calcinaro, A. Falorni, P. Candeloro, M. L. Belladonna, R. Bianchi, M. C. Fioretti, and P. Puccetti. 2002. CTLA-4-Ig regulates tryptophan catabolism in vivo. *Nat Immunol* 3:1097-1101.

Hao, L., L. Gao, X. H. Chen, Z. M. Zou, X. Zhang, P. Y. Kong, C. Zhang, X. G. Peng, A. H. Sun, and Q. Y. Wang. Human umbilical cord blood-derived stromal cells prevent graft-versus-host disease in mice following haplo-identical stem cell transplantation. *Cytotherapy* 13:83-91.

Hardy, R. R., and K. Hayakawa. 2001. B cell development pathways. *Annu Rev Immunol* 19:595-621.

Haynesworth, S. E., M. A. Baber, and A. I. Caplan. 1996. Cytokine expression by human marrow-derived mesenchymal progenitor cells in vitro: effects of dexamethasone and IL-1 alpha. *J Cell Physiol* 166:585-592.

Heino, M., P. Peterson, J. Kudoh, K. Nagamine, A. Lagerstedt, V. Ovod, A. Ranki, I. Rantala, M. Nieminen, J. Tuukkanen, H. S. Scott, S. E. Antonarakis, N. Shimizu, and K. Krohn. 1999. Autoimmune regulator is expressed in the cells regulating immune tolerance in thymus medulla. *Biochem Biophys Res Commun* 257:821-825.

Heng, T. S., J. A. Dudakov, D. M. Khong, A. P. Chidgey, and R. L. Boyd. 2009. Stem cells--meet immunity. *J Mol Med* 87:1061-1069.

Herman, A. E., G. J. Freeman, D. Mathis, and C. Benoist. 2004. CD4+CD25+ T regulatory cells dependent on ICOS promote regulation of effector cells in the prediabetic lesion. *J Exp Med* 199:1479-1489.

Hesselton, R. M., D. L. Greiner, J. P. Mordes, T. V. Rajan, J. L. Sullivan, and L. D. Shultz. 1995. High levels of human peripheral blood mononuclear cell engraftment and enhanced susceptibility to human immunodeficiency virus type 1 infection in NOD/LtSz-scid/scid mice. *J Infect Dis* 172:974-982.

Hill, G. R., J. M. Crawford, K. R. Cooke, Y. S. Brinson, L. Pan, and J. L. Ferrara. 1997. Total body irradiation and acute graft-versus-host disease: the role of gastrointestinal damage and inflammatory cytokines. *Blood* 90:3204-3213.

Ho, V. T., H. T. Kim, S. Li, E. P. Hochberg, C. Cutler, S. J. Lee, D. C. Fisher, E. Milford, G. Kao, H. Daley, J. Levin, A. Ng, P. Mauch, E. P. Alyea, J. H. Antin, and R. J. Soiffer. 2004. Partial CD8+ T-cell depletion of allogeneic peripheral blood stem cell transplantation is insufficient to prevent graft-versus-host disease. *Bone Marrow Transplant* 34:987-994.

Hoffmann, J. A., F. C. Kafatos, C. A. Janeway, and R. A. Ezekowitz. 1999. Phylogenetic perspectives in innate immunity. *Science* 284:1313-1318.

Hoffmann, P., J. Ermann, M. Edinger, C. G. Fathman, and S. Strober. 2002. Donor-type CD4(+)CD25(+) regulatory T cells suppress lethal acute graft-versus-host disease after allogeneic bone marrow transplantation. *J Exp Med* 196:389-399.

Holler, E., H. J. Kolb, A. Moller, J. Kempeni, S. Liesenfeld, H. Pechumer, W. Lehmacher, G. Ruckdeschel, B. Gleixner, C. Riedner, and et al.. 1990. Increased serum levels of tumor necrosis factor alpha precede major complications of bone marrow transplantation. *Blood* 75:1011-1016.

Holt, P. G., M. A. Schon-Hegrad, J. Oliver, B. J. Holt, and P. G. McMenamin. 1990. A contiguous network of dendritic antigen-presenting cells within the respiratory epithelium. *Int Arch Allergy Appl Immunol* 91:155-159.

Horowitz, M. M., R. P. Gale, P. M. Sondel, J. M. Goldman, J. Kersey, H. J. Kolb, A. A. Rimm, O. Ringden, C. Rozman, B. Speck, and et al.. 1990. Graft-versus-leukemia reactions after bone marrow transplantation. *Blood* 75:555-562.

Horwitz, E. M., K. Le Blanc, M. Dominici, I. Mueller, I. Slaper-Cortenbach, F. C. Marini, R. J. Deans, D. S. Krause, and A. Keating. 2005. Clarification of the nomenclature for MSC: The International Society for Cellular Therapy position statement. *Cytotherapy* 7:393-395.

Hoyne, G. F., I. Le Roux, M. Corsin-Jimenez, K. Tan, J. Dunne, L. M. Forsyth, M. J. Dallman, M. J. Owen, D. Ish-Horowicz, and J. R. Lamb. 2000. Serrate1-induced notch signalling regulates the decision between immunity and tolerance made by peripheral CD4(+) T cells. *Int Immunol* 12:177-185.

Hozumi, N., and S. Tonegawa. 1976. Evidence for somatic rearrangement of immunoglobulin genes coding for variable and constant regions. *Proc Natl Acad Sci U S A* 73:3628-3632.

Hubert, P., N. Jacobs, J. H. Caberg, J. Boniver, and P. Delvenne. 2007. The cross-talk between dendritic and regulatory T cells: good or evil? *J Leukoc Biol* 82:781-794.

Janeway, C. A., Jr. 1989. Approaching the asymptote? Evolution and revolution in immunology. *Cold Spring Harb Symp Quant Biol* 54 Pt 1:1-13.

Jeon, M. S., H. J. Lim, T. G. Yi, M. W. Im, H. S. Yoo, J. H. Choi, E. Y. Choi, and S. U. Song. 2009. Xenoreactivity of human clonal mesenchymal stem cells in a major histocompatibility complex-matched allogeneic graft-versus-host disease mouse model. *Cell Immunol* 261:57-63.

Jiang, X. X., Y. Zhang, B. Liu, S. X. Zhang, Y. Wu, X. D. Yu, and N. Mao. 2005. Human mesenchymal stem cells inhibit differentiation and function of monocyte-derived dendritic cells. *Blood* 105:4120-4126.

Jonuleit, H., E. Schmitt, G. Schuler, J. Knop, and A. H. Enk. 2000. Induction of interleukin 10-producing, nonproliferating CD4(+) T cells with regulatory properties by repetitive stimulation with allogeneic immature human dendritic cells. *J Exp Med* 192:1213-1222.

Jonuleit, H., E. Schmitt, H. Kakirman, M. Stassen, J. Knop, and A. H. Enk. 2002. Infectious tolerance: human CD25(+) regulatory T cells convey suppressor activity to conventional CD4(+) T helper cells. *J Exp Med* 196:255-260.

Jonuleit, H., E. Schmitt, K. Steinbrink, and A. H. Enk. 2001. Dendritic cells as a tool to induce anergic and regulatory T cells. *Trends Immunol* 22:394-400.

Joo, S. Y., K. A. Cho, Y. J. Jung, H. S. Kim, S. Y. Park, Y. B. Choi, K. M. Hong, S. Y. Woo, J. Y. Seoh, S. J. Cho, and K. H. Ryu. 2010. Mesenchymal stromal cells inhibit graft-versus-host disease of mice in a dose-dependent manner. *Cytotherapy* 12:361-370.

Jung, Y. J., S. Y. Ju, E. S. Yoo, S. J. Cho, K. A. Cho, S. Y. Woo, J. Y. Seoh, J. W. Park, H. S. Han, and K. H. Ryu. 2007. MSC-DC interactions: MSC inhibit maturation and migration of BM-derived DC. *Cytotherapy* 9:451-458.

Kataoka, S., J. Satoh, H. Fujiya, T. Toyota, R. Suzuki, K. Itoh, and K. Kumagai. 1983. Immunologic aspects of the nonobese diabetic (NOD) mouse. Abnormalities of cellular immunity. *Diabetes* 32:247-253.

Kavanagh, H., and B. P. Mahon. 2010. Allogeneic mesenchymal stem cells prevent allergic airway inflammation by inducing murine regulatory T cells. *Allergy* 66:523-531.

Kebriaei, P., L. Isola, E. Bahceci, K. Holland, S. Rowley, J. McGuirk, M. Devetten, J. Jansen, R. Herzig, M. Schuster, R. Monroy, and J. Uberti. 2009. Adult human mesenchymal stem cells added to corticosteroid therapy for the treatment of acute graft-versus-host disease. *Biol Blood Marrow Transplant* 15:804-811.

Kendal, A. R., Y. Chen, F. S. Regateiro, J. Ma, E. Adams, S. P. Cobbold, S. Hori, and H. Waldmann. 2011. Sustained suppression by Foxp3+ regulatory T cells is vital for infectious transplantation tolerance. *J Exp Med* 208:2043-2053.

King, M., T. Pearson, A. A. Rossini, L. D. Shultz, and D. L. Greiner. 2008. Humanized mice for the study of type 1 diabetes and beta cell function. *Ann N Y Acad Sci* 1150:46-53.

Kishimoto, H., and J. Sprent. 1997. Negative selection in the thymus includes semimature T cells. *J Exp Med* 185:263-271.

Kitko, C. L., S. Paczesny, G. Yanik, T. Braun, D. Jones, J. Whitfield, S. W. Choi, R. J. Hutchinson, J. L. Ferrara, and J. E. Levine. 2008. Plasma elevations of tumor necrosis factor-receptor-1 at day 7 postallogeneic transplant correlate with graft-versus-host disease severity and overall survival in pediatric patients. *Biol Blood Marrow Transplant* 14:759-765.

Klein, L., and B. Kyewski. 2000. Self-antigen presentation by thymic stromal cells: a subtle division of labor. *Curr Opin Immunol* 12:179-186.

Koc, O. N., S. L. Gerson, B. W. Cooper, S. M. Dyhouse, S. E. Haynesworth, A. I. Caplan, and H. M. Lazarus. 2000. Rapid hematopoietic recovery after coinfusion of autologous-blood stem cells and culture-expanded marrow mesenchymal stem cells in advanced breast cancer patients receiving high-dose chemotherapy. *J Clin Oncol* 18:307-316.

Korngold, R., and J. Sprent. 1978. Lethal graft-versus-host disease after bone marrow transplantation across minor histocompatibility barriers in mice. Prevention by removing mature T cells from marrow. *J Exp Med* 148:1687-1698.

Kovanen, P. E., and W. J. Leonard. 2004. Cytokines and immunodeficiency diseases: critical roles of the gamma(c)-dependent cytokines interleukins 2, 4, 7, 9, 15, and 21, and their signaling pathways. *Immunol Rev* 202:67-83.

Krampera, M., S. Glennie, J. Dyson, D. Scott, R. Laylor, E. Simpson, and F. Dazzi. 2003. Bone marrow mesenchymal stem cells inhibit the response of naive and memory antigen-specific T cells to their cognate peptide. *Blood* 101:3722-3729.

Kroger, N., T. Zabelina, W. Kruger, H. Renges, N. Stute, J. Rischewski, S. Sonnenberg, F. Ayuk, F. Togel, U. Schade, H. Fiegel, R. Erttmann, C. Loliger, and A. R. Zander. 2002. In vivo T cell depletion with pretransplant anti-thymocyte globulin reduces graft-versus-host disease without increasing relapse in good risk myeloid leukemia patients after stem cell transplantation from matched related donors. *Bone Marrow Transplant* 29:683-689.

Kuipers, H., F. Muskens, M. Willart, D. Hijdra, F. B. van Assema, A. J. Coyle, H. C. Hoogsteden, and B. N. Lambrecht. 2006. Contribution of the PD-1 ligands/PD-1 signaling pathway to dendritic cell-mediated CD4+ T cell activation. *Eur J Immunol* 36:2472-2482.

Kulkarni, P. S., and B. D. Srinivasan. 1981. Effect of topical and intraperitoneal indomethacin on the generation of PGE2-like activity in rabbit conjunctiva and iris-ciliary body. *Exp Eye Res* 33:121-129.

Kuroda, N., T. Mitani, N. Takeda, N. Ishimaru, R. Arakaki, Y. Hayashi, Y. Bando, K. Izumi, T. Takahashi, T. Nomura, S. Sakaguchi, T. Ueno, Y. Takahama, D. Uchida, S. Sun, F. Kajiura, Y. Mouri, H. Han, A. Matsushima, G. Yamada, and M. Matsumoto. 2005. Development of autoimmunity against transcriptionally unrepressed target antigen in the thymus of Aire-deficient mice. *J Immunol* 174:1862-1870.

Kurtzberg, J. 2009. Update on umbilical cord blood transplantation. *Curr Opin Pediatr* 21:22-29.

Lajaunias, F., J. M. Dayer, and C. Chizzolini. 2005. Constitutive repressor activity of CD33 on human monocytes requires sialic acid recognition and phosphoinositide 3-kinase-mediated intracellular signaling. *Eur J Immunol* 35:243-251.

Landsteiner, K. 1900. Zur Kenntnis der antifermentativen, lytischen und agglutinierenden Wirkungen des Blutserums und der Lymphe. Zentralblatt Bakteriologie. 27: 357–62.

Lanier, L. L., S. O'Fallon, C. Somoza, J. H. Phillips, P. S. Linsley, K. Okumura, D. Ito, and M. Azuma. 1995. CD80 (B7) and CD86 (B70) provide similar costimulatory

signals for T cell proliferation, cytokine production, and generation of CTL. *J Immunol* 154:97-105.

Larmonier, N., M. Marron, Y. Zeng, J. Cantrell, A. Romanoski, M. Sepassi, S. Thompson, X. Chen, S. Andreansky, and E. Katsanis. 2007. Tumor-derived CD4(+)CD25(+) regulatory T cell suppression of dendritic cell function involves TGF-beta and IL-10. *Cancer Immunol Immunother* 56:48-59.

Latchman, Y., C. R. Wood, T. Chernova, D. Chaudhary, M. Borde, I. Chernova, Y. Iwai, A. J. Long, J. A. Brown, R. Nunes, E. A. Greenfield, K. Bourque, V. A. Boussiotis, L. L. Carter, B. M. Carreno, N. Malenkovich, H. Nishimura, T. Okazaki, T. Honjo, A. H. Sharpe, and G. J. Freeman. 2001. PD-L2 is a second ligand for PD-1 and inhibits T cell activation. *Nat Immunol* 2:261-268.

Lazarus, H. M., S. E. Haynesworth, S. L. Gerson, N. S. Rosenthal, and A. I. Caplan. 1995. Ex vivo expansion and subsequent infusion of human bone marrow-derived stromal progenitor cells (mesenchymal progenitor cells): implications for therapeutic use. *Bone Marrow Transplant* 16:557-564.

Le Blanc, K., F. Frassoni, L. Ball, F. Locatelli, H. Roelofs, I. Lewis, E. Lanino, B. Sundberg, M. E. Bernardo, M. Remberger, G. Dini, R. M. Egeler, A. Bacigalupo, W. Fibbe, and O. Ringden. 2008. Mesenchymal stem cells for treatment of steroid-resistant, severe, acute graft-versus-host disease: a phase II study. *Lancet* 371:1579-1586.

Le Blanc, K., H. Samuelsson, B. Gustafsson, M. Remberger, B. Sundberg, J. Arvidson, P. Ljungman, H. Lonnies, S. Nava, and O. Ringden. 2007. Transplantation of mesenchymal stem cells to enhance engraftment of hematopoietic stem cells. *Leukemia* 21:1733-1738.

Le Blanc, K., I. Rasmusson, B. Sundberg, C. Gotherstrom, M. Hassan, M. Uzunel, and O. Ringden. 2004. Treatment of severe acute graft-versus-host disease with third party haploidentical mesenchymal stem cells. *Lancet* 363:1439-1441.

Leonard, M. F. 1946. Chronic idiopathic hypoparathyroidism with superimposed Addison's disease in a child. *J Clin Endocrinol Metab* 6:493-506.

Levine, J. E., J. P. Uberti, L. Ayash, C. Reynolds, J. L. Ferrara, S. M. Silver, T. Braun, G. Yanik, R. Hutchinson, and V. Ratanatharathorn. 2003. Lowered-intensity preparative regimen for allogeneic stem cell transplantation delays acute graft-versus-host disease but does not improve outcome for advanced hematologic malignancy. *Biol Blood Marrow Transplant* 9:189-197.

Levine, J. E., S. Paczesny, S. Mineishi, T. Braun, S. W. Choi, R. J. Hutchinson, D. Jones, Y. Khaled, C. L. Kitko, D. Bickley, O. Krijanovski, P. Reddy, G. Yanik, and J. L. Ferrara. 2008. Etanercept plus methylprednisolone as initial therapy for acute graft-versus-host disease. *Blood* 111:2470-2475.

Levings, M. K., R. Bacchetta, U. Schulz, and M. G. Roncarolo. 2002. The role of IL-10 and TGF-beta in the differentiation and effector function of T regulatory cells. *Int Arch Allergy Immunol* 129:263-276.

Li, Q., Z. Zhai, X. Xu, Y. Shen, A. Zhang, Z. Sun, H. Liu, L. Geng, and Y. Wang. 2010. Decrease of CD4(+)CD25(+) regulatory T cells and TGF-beta at early immune reconstitution is associated to the onset and severity of graft-versus-host disease following allogeneic haematogenesis stem cell transplantation. *Leuk Res* 34:1158-1168.

Li, Y. P., S. Paczesny, E. Lauret, S. Poirault, P. Bordigoni, F. Mekhloufi, O. Hequet, Y. Bertrand, J. P. Ou-Yang, J. F. Stoltz, P. Miossec, and A. Eljaafari. 2008. Human mesenchymal stem cells license adult CD34+ hemopoietic progenitor cells to differentiate into regulatory dendritic cells through activation of the Notch pathway. *J Immunol* 180:1598-1608.

Lieber, M. R., J. E. Hesse, S. Lewis, G. C. Bosma, N. Rosenberg, K. Mizuuchi, M. J. Bosma, and M. Gellert. 1988. The defect in murine severe combined immune deficiency: joining of signal sequences but not coding segments in V(D)J recombination. *Cell* 55:7-16.

Liotta, F., R. Angeli, L. Cosmi, L. Fili, C. Manuelli, F. Frosali, B. Mazzinghi, L. Maggi, A. Pasini, V. Lisi, V. Santarlasci, L. Consoloni, M. L. Angelotti, P. Romagnani, P. Parronchi, M. Krampera, E. Maggi, S. Romagnani, and F. Annunziato. 2008. Toll-like receptors 3 and 4 are expressed by human bone marrow-

derived mesenchymal stem cells and can inhibit their T-cell modulatory activity by impairing Notch signaling. *Stem Cells* 26:279-289.

Lohmann, T., R. D. Leslie, and M. Londei. 1996. T cell clones to epitopes of glutamic acid decarboxylase 65 raised from normal subjects and patients with insulin-dependent diabetes. *J Autoimmun* 9:385-389.

Loiseau, P., M. Busson, M. L. Balere, A. Dormoy, J. D. Bignon, K. Gagne, L. Gebuhrer, V. Dubois, I. Jollet, M. Bois, P. Perrier, D. Masson, A. Moine, L. Absi, D. Reviron, V. Lepage, R. Tamouza, A. Toubert, E. Marry, Z. Chir, J. P. Jouet, D. Blaise, D. Charron, and C. Raffoux. 2007. HLA Association with hematopoietic stem cell transplantation outcome: the number of mismatches at HLA-A, -B, -C, -DRB1, or -DQB1 is strongly associated with overall survival. *Biol Blood Marrow Transplant* 13:965-974.

Lutz, M. B., and G. Schuler. 2002. Immature, semi-mature and fully mature dendritic cells: which signals induce tolerance or immunity? *Trends Immunol* 23:445-449.

Lyons, A. B., and C. R. Parish. 1994. Determination of lymphocyte division by flow cytometry. *J Immunol Methods* 171:131-137.

Lyons, A. B., and K. V. Doherty. 2004. Flow cytometric analysis of cell division by dye dilution. *Curr Protoc Cytom* Chapter 9:Unit 9 11.

MacMillan, M. L., D. J. Weisdorf, J. E. Wagner, T. E. DeFor, L. J. Burns, N. K. Ramsay, S. M. Davies, and B. R. Blazar. 2002. Response of 443 patients to steroids as primary therapy for acute graft-versus-host disease: comparison of grading systems. *Biol Blood Marrow Transplant* 8:387-394.

Mahnke, K., E. Schmitt, L. Bonifaz, A. H. Enk, and H. Jonuleit. 2002. Immature, but not inactive: the tolerogenic function of immature dendritic cells. *Immunol Cell Biol* 80:477-483.

Mahnke, K., T. S. Johnson, S. Ring, and A. H. Enk. 2007. Tolerogenic dendritic cells and regulatory T cells: a two-way relationship. *J Dermatol Sci* 46:159-167.

Mahnke, K., Y. Qian, J. Knop, and A. H. Enk. 2003. Induction of CD4+/CD25+ regulatory T cells by targeting of antigens to immature dendritic cells. *Blood* 101:4862-4869.

Maldonado, R. A., and U. H. von Andrian. How tolerogenic dendritic cells induce regulatory T cells. *Adv Immunol* 108:111-165.

Martin, B. J. Uberti, J. P. Soiffer, R. J. Klingemann, H. Waller, E. K. Daly, A. S. Herrmann, R. P. Visani, G. Bernardo, M. E. Schwerdtfeger, R., Kebriaei, P. 2010. Prochymal imporoves response rates in patients with steroid-refractory acute graft versus host disease involving the liver and gut: results of a randomised placebo controlled multicentre phase III trial in GvHD. Orlando: American Society of Bone Marrow Transplantation.

Martin, P. J., G. Schoch, L. Fisher, V. Byers, C. Anasetti, F. R. Appelbaum, P. G. Beatty, K. Doney, G. B. McDonald, J. E. Sanders, and et al.. 1990. A retrospective analysis of therapy for acute graft-versus-host disease: initial treatment. *Blood* 76:1464-1472.

Masteller, E. L., M. R. Warner, Q. Tang, K. V. Tarbell, H. McDevitt, and J. A. Bluestone. 2005. Expansion of functional endogenous antigen-specific CD4+CD25+ regulatory T cells from nonobese diabetic mice. *J Immunol* 175:3053-3059.

McAdam, A. J., T. T. Chang, A. E. Lumelsky, E. A. Greenfield, V. A. Boussiotis, J. S. Duke-Cohan, T. Chernova, N. Malenkovich, C. Jabs, V. K. Kuchroo, V. Ling, M. Collins, A. H. Sharpe, and G. J. Freeman. 2000. Mouse inducible costimulatory molecule (ICOS) expression is enhanced by CD28 costimulation and regulates differentiation of CD4+ T cells. *J Immunol* 165:5035-5040.

McDonald, G. B. 2006. Review article: management of hepatic disease following haematopoietic cell transplant. *Aliment Pharmacol Ther* 24:441-452.

McMillan, S. J., and P. R. Crocker. 2008. CD33-related sialic-acid-binding immunoglobulin-like lectins in health and disease. *Carbohydr Res* 343:2050-2056.

Meisel, R., A. Zibert, M. Laryea, U. Gobel, W. Daubener, and D. Dilloo. 2004. Human bone marrow stromal cells inhibit allogeneic T-cell responses by

indoleamine 2,3-dioxygenase-mediated tryptophan degradation. *Blood* 103:4619-4621.

Messina, C., M. Faraci, V. de Fazio, G. Dini, M. P. Calo, and E. Calore. 2008. Prevention and treatment of acute GvHD. *Bone Marrow Transplant* 41 Suppl 2:S65-70.

Miettinen, J. A., M. Pietila, R. J. Salonen, S. Ohlmeier, K. Ylitalo, H. V. Huikuri, and P. Lehenkari. Tumor necrosis factor alpha promotes the expression of immunosuppressive proteins and enhances the cell growth in a human bone marrow-derived stem cell culture. *Exp Cell Res* 317:791-801.

Miller, J. F. 1961. Immunological function of the thymus. *Lancet* 2:748-749.

Mills, K. H. 2004. Regulatory T cells: friend or foe in immunity to infection? *Nat Rev Immunol* 4:841-855.

Morelli, A. E., and A. W. Thomson. 2007. Tolerogenic dendritic cells and the quest for transplant tolerance. *Nat Rev Immunol* 7:610-621.

Mosier, D. E., R. J. Gulizia, S. M. Baird, and D. B. Wilson. 1988. Transfer of a functional human immune system to mice with severe combined immunodeficiency. *Nature* 335:256-259.

Mosmann, T. R., H. Cherwinski, M. W. Bond, M. A. Giedlin, and R. L. Coffman. 1986. Two types of murine helper T cell clone. I. Definition according to profiles of lymphokine activities and secreted proteins. *J Immunol* 136:2348-2357.

Munn, D. H., and A. L. Mellor. 2007. Indoleamine 2,3-dioxygenase and tumor-induced tolerance. *J Clin Invest* 117:1147-1154.

Nagamine, K., P. Peterson, H. S. Scott, J. Kudoh, S. Minoshima, M. Heino, K. J. Krohn, M. D. Lalioti, P. E. Mullis, S. E. Antonarakis, K. Kawasaki, S. Asakawa, F. Ito, and N. Shimizu. 1997. Positional cloning of the APECED gene. *Nat Genet* 17:393-398.

Nauta, A. J., A. B. Kruisselbrink, E. Lurvink, R. Willemze, and W. E. Fibbe. 2006. Mesenchymal stem cells inhibit generation and function of both CD34+-derived and monocyte-derived dendritic cells. *J Immunol* 177:2080-2087.

Nishimura, H., and T. Honjo. 2001. PD-1: an inhibitory immunoreceptor involved in peripheral tolerance. *Trends Immunol* 22:265-268.

Nishimura, H., Y. Agata, A. Kawasaki, M. Sato, S. Imamura, N. Minato, H. Yagita, T. Nakano, and T. Honjo. 1996. Developmentally regulated expression of the PD-1 protein on the surface of double-negative (CD4-CD8-) thymocytes. *Int Immunol* 8:773-780.

O'Shea, J. J., A. Ma, and P. Lipsky. 2002. Cytokines and autoimmunity. *Nat Rev Immunol* 2:37-45.

Owen, R. D. 1945. IMMUNOGENETIC CONSEQUENCES OF VASCULAR ANASTOMOSES BETWEEN BOVINE TWINS. *Science* 102:400-401.

Park, M. J., H. S. Park, M. L. Cho, H. J. Oh, Y. G. Cho, S. Y. Min, B. H. Chung, J. W. Lee, H. Y. Kim, and S. G. Cho. Transforming growth factor beta-transduced mesenchymal stem cells ameliorate experimental autoimmune arthritis through reciprocal regulation of Treg/Th17 cells and osteoclastogenesis. *Arthritis Rheum* 63:1668-1680.

Park, M. J., J. S. Shin, Y. H. Kim, S. H. Hong, S. H. Yang, J. Y. Shin, S. Y. Kim, B. Kim, J. S. Kim, and C. G. Park. Murine mesenchymal stem cells suppress T lymphocyte activation through IL-2 receptor alpha (CD25) cleavage by producing matrix metalloproteinases. *Stem Cell Rev* 7:381-393.

Park, S., D. Murray, B. John, and I. N. Crispe. 2002. Biology and significance of T-cell apoptosis in the liver. *Immunol Cell Biol* 80:74-83.

Parker, D. C. 1993. The functions of antigen recognition in T cell-dependent B cell activation. *Semin Immunol* 5:413-420.

Pearson, T., D. L. Greiner, and L. D. Shultz. 2008. Creation of "humanized" mice to study human immunity. *Curr Protoc Immunol* Chapter 15:Unit 15 21.

Peister, A., J. A. Mellad, B. L. Larson, B. M. Hall, L. F. Gibson, and D. J. Prockop. 2004. Adult stem cells from bone marrow (MSCs) isolated from different strains of inbred mice vary in surface epitopes, rates of proliferation, and differentiation potential. *Blood* 103:1662-1668.

Perez-Simon, J. A., M. Diez-Campelo, R. Martino, S. Brunet, A. Urbano, M. D. Caballero, A. de Leon, D. Valcarcel, E. Carreras, M. C. del Canizo, J. Lopez-Fidalgo, J. Sierra, and J. F. San Miguel. 2005. Influence of the intensity of the conditioning regimen on the characteristics of acute and chronic graft-versus-host disease after allogeneic transplantation. *Br J Haematol* 130:394-403.

Perez-Simon, J. A., P. D. Kottaridis, R. Martino, C. Craddock, D. Caballero, R. Chopra, J. Garcia-Conde, D. W. Milligan, S. Schey, A. Urbano-Ispizua, A. Parker, A. Leon, K. Yong, A. Sureda, A. Hunter, J. Sierra, A. H. Goldstone, D. C. Linch, J. F. San Miguel, and S. Mackinnon. 2002. Nonmyeloablative transplantation with or without alemtuzumab: comparison between 2 prospective studies in patients with lymphoproliferative disorders. *Blood* 100:3121-3127.

Pino, S., M. A. Brehm, L. Covassin-Barberis, M. King, B. Gott, T. H. Chase, J. Wagner, L. Burzenski, O. Foreman, D. L. Greiner, and L. D. Shultz. 2010. Development of novel major histocompatibility complex class I and class II-deficient NOD-SCID IL2R gamma chain knockout mice for modeling human xenogeneic graft-versus-host disease. *Methods Mol Biol* 602:105-117.

Pittenger, M. F., A. M. Mackay, S. C. Beck, R. K. Jaiswal, R. Douglas, J. D. Mosca, M. A. Moorman, D. W. Simonetti, S. Craig, and D. R. Marshak. 1999. Multilineage potential of adult human mesenchymal stem cells. *Science* 284:143-147.

Plumas, J., L. Chaperot, M. J. Richard, J. P. Molens, J. C. Bensa, and M. C. Favrot. 2005. Mesenchymal stem cells induce apoptosis of activated T cells. *Leukemia* 19:1597-1604.

Polchert, D., J. Sobinsky, G. Douglas, M. Kidd, A. Moadsiri, E. Reina, K. Genrich, S. Mehrotra, S. Setty, B. Smith, and A. Bartholomew. 2008. IFN-gamma activation of mesenchymal stem cells for treatment and prevention of graft versus host disease. *Eur J Immunol* 38:1745-1755.

Ponec, R. J., R. C. Hackman, and G. B. McDonald. 1999. Endoscopic and histologic diagnosis of intestinal graft-versus-host disease after marrow transplantation. *Gastrointest Endosc* 49:612-621.

Prevosto, C., M. Zancolli, P. Canevali, M. R. Zocchi, and A. Poggi. 2007. Generation of CD4+ or CD8+ regulatory T cells upon mesenchymal stem cell-lymphocyte interaction. *Haematologica* 92:881-888.

Prockop, D. J. 2009. Repair of tissues by adult stem/progenitor cells (MSCs): controversies, myths, and changing paradigms. *Mol Ther* 17:939-946.

Qin, S., S. P. Cobbold, H. Pope, J. Elliott, D. Kioussis, J. Davies, and H. Waldmann. 1993. "Infectious" transplantation tolerance. *Science* 259:974-977.

Radic, M. Z., J. Erikson, S. Litwin, and M. Weigert. 1993. B lymphocytes may escape tolerance by revising their antigen receptors. *J Exp Med* 177:1165-1173.

Radtke, F., A. Wilson, S. J. Mancini, and H. R. MacDonald. 2004. Notch regulation of lymphocyte development and function. *Nat Immunol* 5:247-253.

Ramasamy, R., C. K. Tong, H. F. Seow, S. Vidyadaran, and F. Dazzi. 2008. The immunosuppressive effects of human bone marrow-derived mesenchymal stem cells target T cell proliferation but not its effector function. *Cell Immunol* 251:131-136.

Ramasamy, R., H. Fazekasova, E. W. Lam, I. Soeiro, G. Lombardi, and F. Dazzi. 2007. Mesenchymal stem cells inhibit dendritic cell differentiation and function by preventing entry into the cell cycle. *Transplantation* 83:71-76.

Rameshwar, P. 2008. IFNgamma and B7-H1 in the immunology of mesenchymal stem cells. *Cell Res* 18:805-806.

Rao, P. E., A. L. Petrone, and P. D. Ponath. 2005. Differentiation and expansion of T cells with regulatory function from human peripheral lymphocytes by stimulation in the presence of TGF-{beta}. *J Immunol* 174:1446-1455.

Reddy, P. 2003. Pathophysiology of acute graft-versus-host disease. *Hematol Oncol* 21:149-161.

Reddy, P., and J. L. Ferrara. 2003. Immunobiology of acute graft-versus-host disease. *Blood Rev* 17:187-194.

Roncarolo, M. G., and M. Battaglia. 2007. Regulatory T-cell immunotherapy for tolerance to self antigens and alloantigens in humans. *Nat Rev Immunol* 7:585-598.

Roths, J. B., E. D. Murphy, and E. M. Eicher. 1984. A new mutation, gld, that produces lymphoproliferation and autoimmunity in C3H/HeJ mice. *J Exp Med* 159:1-20.

Rudensky, A., S. Rath, P. Preston-Hurlburt, D. B. Murphy, and C. A. Janeway, Jr. 1991. On the complexity of self. *Nature* 353:660-662.

Rutz, S., B. Mordmuller, S. Sakano, and A. Scheffold. 2005. Notch ligands Delta-like1, Delta-like4 and Jagged1 differentially regulate activation of peripheral T helper cells. *Eur J Immunol* 35:2443-2451.

Ryan, J. M., F. Barry, J. M. Murphy, and B. P. Mahon. 2007. Interferon-gamma does not break, but promotes the immunosuppressive capacity of adult human mesenchymal stem cells. *Clin Exp Immunol* 149:353-363.

Ryan, J. M., F. P. Barry, J. M. Murphy, and B. P. Mahon. 2005. Mesenchymal stem cells avoid allogeneic rejection. *J Inflamm (Lond)* 2:8.

Saas, P., P. R. Walker, M. Hahne, A. L. Quiquerez, V. Schnuriger, G. Perrin, L. French, E. G. Van Meir, N. de Tribolet, J. Tschopp, and P. Y. Dietrich. 1997. Fas ligand expression by astrocytoma in vivo: maintaining immune privilege in the brain? *J Clin Invest* 99:1173-1178.

Salomon, B., and J. A. Bluestone. 2001. Complexities of CD28/B7: CTLA-4 costimulatory pathways in autoimmunity and transplantation. *Annu Rev Immunol* 19:225-252.

Samon, J. B., A. Champhekar, L. M. Minter, J. C. Telfer, L. Miele, A. Fauq, P. Das, T. E. Golde, and B. A. Osborne. 2008. Notch1 and TGFbeta1 cooperatively regulate Foxp3 expression and the maintenance of peripheral regulatory T cells. *Blood* 112:1813-1821.

Sato, K., K. Ozaki, I. Oh, A. Meguro, K. Hatanaka, T. Nagai, K. Muroi, and K. Ozawa. 2007. Nitric oxide plays a critical role in suppression of T-cell proliferation by mesenchymal stem cells. *Blood* 109:228-234.

Sato, K., N. Yamashita, M. Baba, and T. Matsuyama. 2003. Regulatory dendritic cells protect mice from murine acute graft-versus-host disease and leukemia relapse. *Immunity* 18:367-379.

Schena, F., C. Gambini, A. Gregorio, M. Mosconi, D. Reverberi, M. Gattorno, S. Casazza, A. Uccelli, L. Moretta, A. Martini, and E. Traggiai. 2010. Interferon-gamma-dependent inhibition of B cell activation by bone marrow-derived mesenchymal stem cells in a murine model of systemic lupus erythematosus. *Arthritis Rheum* 62:2776-2786.

Schroeder, M. A., and J. F. DiPersio. 2011. Mouse models of graft-versus-host disease: advances and limitations. *Dis Model Mech* 4:318-333.

Schuler, G., and R. M. Steinman. 1985. Murine epidermal Langerhans cells mature into potent immunostimulatory dendritic cells in vitro. *J Exp Med* 161:526-546.

Scollay, R. G., E. C. Butcher, and I. L. Weissman. 1980. Thymus cell migration. Quantitative aspects of cellular traffic from the thymus to the periphery in mice. *Eur J Immunol* 10:210-218.

Selmani, Z., A. Naji, I. Zidi, B. Favier, E. Gaiffe, L. Obert, C. Borg, P. Saas, P. Tiberghien, N. Rouas-Freiss, E. D. Carosella, and F. Deschaseaux. 2008. Human leukocyte antigen-G5 secretion by human mesenchymal stem cells is required to suppress T lymphocyte and natural killer function and to induce CD4+CD25highFOXP3+ regulatory T cells. *Stem Cells* 26:212-222.

Serreze, D. V., J. W. Gaedeke, and E. H. Leiter. 1993. Hematopoietic stem-cell defects underlying abnormal macrophage development and maturation in NOD/Lt mice: defective regulation of cytokine receptors and protein kinase C. *Proc Natl Acad Sci U S A* 90:9625-9629.

Sharma, M. D., B. Baban, P. Chandler, D. Y. Hou, N. Singh, H. Yagita, M. Azuma, B. R. Blazar, A. L. Mellor, and D. H. Munn. 2007. Plasmacytoid dendritic cells from mouse tumor-draining lymph nodes directly activate mature Tregs via indoleamine 2,3-dioxygenase. *J Clin Invest* 117:2570-2582.

Shlomchik, W. D. 2007. Graft-versus-host disease. *Nat Rev Immunol* 7:340-352.

Shultz, L. D., P. A. Lang, S. W. Christianson, B. Gott, B. Lyons, S. Umeda, E. Leiter, R. Hesselton, E. J. Wagar, J. H. Leif, O. Kollet, T. Lapidot, and D. L. Greiner. 2000. NOD/LtSz-Rag1null mice: an immunodeficient and radioresistant model for engraftment of human hematolymphoid cells, HIV infection, and adoptive transfer of NOD mouse diabetogenic T cells. *J Immunol* 164:2496-2507.

Shultz, L. D., P. A. Schweitzer, S. W. Christianson, B. Gott, I. B. Schweitzer, B. Tennent, S. McKenna, L. Mobraaten, T. V. Rajan, D. L. Greiner, and et al.. 1995. Multiple defects in innate and adaptive immunologic function in NOD/LtSz-scid mice. *J Immunol* 154:180-191.

Shultz, L. D., T. Pearson, M. King, L. Giassi, L. Carney, B. Gott, B. Lyons, A. A. Rossini, and D. L. Greiner. 2007. Humanized NOD/LtSz-scid IL2 receptor common gamma chain knockout mice in diabetes research. *Ann N Y Acad Sci* 1103:77-89.

Snell, GD & Higgins, GF. 1951. Alleles at the histocompatibility-*2* locus in the mouse as determined by tumor transplantation. Genetics. 36:306-310.

Snell, GD. 1948. Methods for the study of histocompatibility genes. J Genet. 49:87-108.

Snell,GD. 1951. A fifth allele at the histocompatibility-2 locus of the mouse as determined by tumor transplantation. J. Natl. Cancer Inst. 11:1299-305.

Spaggiari, G. M., A. Capobianco, S. Becchetti, M. C. Mingari, and L. Moretta. 2006. Mesenchymal stem cell-natural killer cell interactions: evidence that activated NK cells are capable of killing MSCs, whereas MSCs can inhibit IL-2-induced NK-cell proliferation. *Blood* 107:1484-1490.

Sprent, J., M. Schaefer, D. Lo, and R. Korngold. 1986. Properties of purified T cell subsets. II. In vivo responses to class I vs. class II H-2 differences. *J Exp Med* 163:998-1011.

Steinman, R. M., D. S. Lustig, and Z. A. Cohn. 1974. Identification of a novel cell type in peripheral lymphoid organs of mice. 3. Functional properties in vivo. *J Exp Med* 139:1431-1445.

Steinman, R. M., S. Turley, I. Mellman, and K. Inaba. 2000. The induction of tolerance by dendritic cells that have captured apoptotic cells. *J Exp Med* 191:411-416.

Steinman, R. M. 2008. Dendritic cells in vivo: a key target for a new vaccine science. *Immunity* 29:319-324.

Sudres, M., F. Norol, A. Trenado, S. Gregoire, F. Charlotte, B. Levacher, J. J. Lataillade, P. Bourin, X. Holy, J. P. Vernant, D. Klatzmann, and J. L. Cohen. 2006. Bone marrow mesenchymal stem cells suppress lymphocyte proliferation in vitro but fail to prevent graft-versus-host disease in mice. *J Immunol* 176:7761-7767.

Sugamura, K., H. Asao, M. Kondo, N. Tanaka, N. Ishii, K. Ohbo, M. Nakamura, and T. Takeshita. 1996. The interleukin-2 receptor gamma chain: its role in the multiple cytokine receptor complexes and T cell development in XSCID. *Annu Rev Immunol* 14:179-205.

Sullivan, K. M., E. Agura, C. Anasetti, F. Appelbaum, C. Badger, S. Bearman, K. Erickson, M. Flowers, J. Hansen, T. Loughran, and et al.. 1991. Chronic graft-versus-host disease and other late complications of bone marrow transplantation. *Semin Hematol* 28:250-259.

Suzuki, H., Y. W. Zhou, M. Kato, T. W. Mak, and I. Nakashima. 1999. Normal regulatory alpha/beta T cells effectively eliminate abnormally activated T cells lacking the interleukin 2 receptor beta in vivo. *J Exp Med* 190:1561-1572.

Tang, Q., and J. A. Bluestone. 2008. The Foxp3+ regulatory T cell: a jack of all trades, master of regulation. *Nat Immunol* 9:239-244.

Tang, Q., E. K. Boden, K. J. Henriksen, H. Bour-Jordan, M. Bi, and J. A. Bluestone. 2004. Distinct roles of CTLA-4 and TGF-beta in CD4+CD25+ regulatory T cell function. *Eur J Immunol* 34:2996-3005.

Tarbell, K. V., L. Petit, X. Zuo, P. Toy, X. Luo, A. Mqadmi, H. Yang, M. Suthanthiran, S. Mojsov, and R. M. Steinman. 2007. Dendritic cell-expanded, islet-specific CD4+ CD25+ CD62L+ regulatory T cells restore normoglycemia in diabetic NOD mice. *J Exp Med* 204:191-201.

Taylor, P. A., C. J. Lees, and B. R. Blazar. 2002. The infusion of ex vivo activated and expanded CD4(+)CD25(+) immune regulatory cells inhibits graft-versus-host disease lethality. *Blood* 99:3493-3499.

Thornton, A. M., and E. M. Shevach. 2000. Suppressor effector function of CD4+CD25+ immunoregulatory T cells is antigen nonspecific. *J Immunol* 164:183-190.

Tiegs, S. L., D. M. Russell, and D. Nemazee. 1993. Receptor editing in self-reactive bone marrow B cells. *J Exp Med* 177:1009-1020.

Tolar, J., P. Villeneuve, and A. Keating. Mesenchymal stromal cells for graft-versus-host disease. *Hum Gene Ther* 22:257-262.

Trenado, A., F. Charlotte, S. Fisson, M. Yagello, D. Klatzmann, B. L. Salomon, and J. L. Cohen. 2003. Recipient-type specific CD4+CD25+ regulatory T cells favor immune reconstitution and control graft-versus-host disease while maintaining graft-versus-leukemia. *J Clin Invest* 112:1688-1696.

Tse, W. T., J. D. Pendleton, W. M. Beyer, M. C. Egalka, and E. C. Guinan. 2003. Suppression of allogeneic T-cell proliferation by human marrow stromal cells: implications in transplantation. *Transplantation* 75:389-397.

Tu, Z., Q. Li, H. Bu, and F. Lin. Mesenchymal stem cells inhibit complement activation by secreting factor H. *Stem Cells Dev* 19:1803-1809.

Tuettenberg, A., E. Huter, M. Hubo, J. Horn, J. Knop, B. Grimbacher, R. A. Kroczek, S. Stoll, and H. Jonuleit. 2009. The role of ICOS in directing T cell responses: ICOS-dependent induction of T cell anergy by tolerogenic dendritic cells. *J Immunol* 182:3349-3356.

Uccelli, A., L. Moretta, and V. Pistoia. 2008. Mesenchymal stem cells in health and disease. *Nat Rev Immunol* 8:726-736.

van Leeuwen, L., A. Guiffre, K. Atkinson, S. P. Rainer, and W. A. Sewell. 2002. A two-phase pathogenesis of graft-versus-host disease in mice. *Bone Marrow Transplant* 29:151-158.

Van Lint, M. T., C. Uderzo, A. Locasciulli, I. Majolino, R. Scime, F. Locatelli, G. Giorgiani, W. Arcese, A. P. Iori, M. Falda, A. Bosi, R. Miniero, P. Alessandrino, G. Dini, B. Rotoli, and A. Bacigalupo. 1998. Early treatment of acute graft-versus-host disease with high- or low-dose 6-methylprednisolone: a multicenter randomized trial from the Italian Group for Bone Marrow Transplantation. *Blood* 92:2288-2293.

Van Lint, M. T., G. Milone, S. Leotta, C. Uderzo, R. Scime, S. Dallorso, A. Locasciulli, S. Guidi, N. Mordini, S. Sica, L. Cudillo, F. Fagioli, C. Selleri, B. Bruno, W. Arcese, and A. Bacigalupo. 2006. Treatment of acute graft-versus-host disease with prednisolone: significant survival advantage for day +5 responders and no advantage for nonresponders receiving anti-thymocyte globulin. *Blood* 107:4177-4181.

van Noort, J. M., A. van Sechel, J. Boon, W. J. Boersma, C. H. Polman, and C. J. Lucas. 1993. Minor myelin proteins can be major targets for peripheral blood T cells from both multiple sclerosis patients and healthy subjects. *J Neuroimmunol* 46:67-72.

Vitale, C., C. Romagnani, M. Falco, M. Ponte, M. Vitale, A. Moretta, A. Bacigalupo, L. Moretta, and M. C. Mingari. 1999. Engagement of p75/AIRM1 or CD33 inhibits the proliferation of normal or leukemic myeloid cells. *Proc Natl Acad Sci U S A* 96:15091-15096.

Vujovic, S., S. R. Henderson, A. M. Flanagan, and M. O. Clements. 2007. Inhibition of gamma-secretases alters both proliferation and differentiation of mesenchymal stem cells. *Cell Prolif* 40:185-195.

Wakkach, A., N. Fournier, V. Brun, J. P. Breittmayer, F. Cottrez, and H. Groux. 2003. Characterization of dendritic cells that induce tolerance and T regulatory 1 cell differentiation in vivo. *Immunity* 18:605-617.

Weijzen, S., M. P. Velders, A. G. Elmishad, P. E. Bacon, J. R. Panella, B. J. Nickoloff, L. Miele, and W. M. Kast. 2002. The Notch ligand Jagged-1 is able to induce maturation of monocyte-derived human dendritic cells. *J Immunol* 169:4273-4278.

Wing, K., Y. Onishi, P. Prieto-Martin, T. Yamaguchi, M. Miyara, Z. Fehervari, T. Nomura, and S. Sakaguchi. 2008. CTLA-4 control over Foxp3+ regulatory T cell function. *Science* 322:271-275.

Wood, K. J. Regulatory T cells in transplantation. 2011. *Transplant Proc* 43:2135-2136.

Wood, K. J., and S. Sakaguchi. 2003. Regulatory T cells in transplantation tolerance. *Nat Rev Immunol* 3:199-210.

Yamazaki, S., M. Patel, A. Harper, A. Bonito, H. Fukuyama, M. Pack, K. V. Tarbell, M. Talmor, J. V. Ravetch, K. Inaba, and R. M. Steinman. 2006. Effective expansion of alloantigen-specific Foxp3+ CD25+ CD4+ regulatory T cells by dendritic cells during the mixed leukocyte reaction. *Proc Natl Acad Sci U S A* 103:2758-2763.

Yamazaki, S., T. Iyoda, K. Tarbell, K. Olson, K. Velinzon, K. Inaba, and R. M. Steinman. 2003. Direct expansion of functional CD25+ CD4+ regulatory T cells by antigen-processing dendritic cells. *J Exp Med* 198:235-247.

Yao, S., S. Wang, Y. Zhu, L. Luo, G. Zhu, S. Flies, H. Xu, W. Ruff, M. Broadwater, I. H. Choi, K. Tamada, and L. Chen. 2009. PD-1 on dendritic cells impedes innate immunity against bacterial infection. *Blood* 113:5811-5818.

Yu, W., H. Nagaoka, M. Jankovic, Z. Misulovin, H. Suh, A. Rolink, F. Melchers, E. Meffre, and M. C. Nussenzweig. 1999. Continued RAG expression in late stages of B cell development and no apparent re-induction after immunization. *Nature* 400:682-687.

Yvon, E. S., S. Vigouroux, R. F. Rousseau, E. Biagi, P. Amrolia, G. Dotti, H. J. Wagner, and M. K. Brenner. 2003. Overexpression of the Notch ligand, Jagged-1, induces alloantigen-specific human regulatory T cells. *Blood* 102:3815-3821.

Zappia, E., S. Casazza, E. Pedemonte, F. Benvenuto, I. Bonanni, E. Gerdoni, D. Giunti, A. Ceravolo, F. Cazzanti, F. Frassoni, G. Mancardi, and A. Uccelli. 2005. Mesenchymal stem cells ameliorate experimental autoimmune encephalomyelitis inducing T-cell anergy. *Blood* 106:1755-1761.

Zhang, B., R. Liu, D. Shi, X. Liu, Y. Chen, X. Dou, X. Zhu, C. Lu, W. Liang, L. Liao, M. Zenke, and R. C. Zhao. 2009. Mesenchymal stem cells induce mature dendritic cells into a novel Jagged-2-dependent regulatory dendritic cell population. *Blood* 113:46-57.

Zhang, M., H. Tang, Z. Guo, H. An, X. Zhu, W. Song, J. Guo, X. Huang, T. Chen, J. Wang, and X. Cao. 2004. Splenic stroma drives mature dendritic cells to differentiate into regulatory dendritic cells. *Nat Immunol* 5:1124-1133.